

School of Medicine and School of Science

PhD program in Translational and Molecular Medicine (DIMET)  
XXXII Cycle

# **Novel Insights into the Immunobiology of Leukemia Relapse after Allogeneic Hematopoietic Cell Transplantation**

Coordinator: Prof. Andrea Biondi  
Tutor: Prof. Andrea Biondi  
Co-Tutors: Dr. Raffaella Di Micco  
Dr. Luca Aldo Edoardo Vago

Dr. Valentina GAMBACORTA

Matr. No. 823407

**Academic year 2018-2019**



*To my family*





## Table of contents

1. General introduction and Scope of the thesis .....	7
1.1 General introduction .....	7
1.2 Scope of the thesis.....	10
2. Quantitative PCR-based chimerism in bone marrow or peripheral blood to predict acute myeloid leukemia relapse in high-risk patients: results from the KIM-PB prospective study.....	17
3. NK cell recovery after haploidentical HSCT with post-transplant cyclophosphamide: dynamics and clinical implications .....	33
4. Bone marrow central memory and memory stem T-cell exhaustion in AML patients relapsing after HSCT .....	71
5. Immune signature drives leukemia escape and relapse after hematopoietic cell transplantation .....	95
6. Mechanisms of Leukemia Immune Evasion and Their Role in Relapse after Haploidentical Hematopoietic Cell transplantation .....	133
7. Integrated Epigenetic Profiling Identifies EZH2 as a Therapeutic Target to Re-Establish Immune Recognition of Leukemia Relapses with Loss of HLA Class II Expression .....	169
8. Epigenetic Therapies for Acute Myeloid Leukemia and Their Immune-Related Effects .....	201
9. Summary, Conclusions and Future perspectives .....	221
9.1. Summary.....	221
9.2. Conclusions and Future Perspectives .....	223



## **Chapter 1. General Introduction and Scope of the Thesis**

### **1.1 General introduction**

The term allogeneic hematopoietic cell transplantation (allo-HCT) defines a medical procedure in which patients receive hematopoietic stem cells harvested from a healthy donor, chosen between relatives or volunteers from international registries (matched or mismatched unrelated donors). Prior to the infusion of hematopoietic stem cells, patients receive the conditioning regimen, which is a combination of chemo- and radio-therapy that can be partially or totally myeloablative. The aim of this pre-transplant treatment is to create space in the bone marrow to accommodate donor-derived progenitor cells, to suppress the host immune system, reduce the risk of rejection, and (when allo-HCT is performed to treat cancer) to further reduce the bulk of residual malignant disease.

The rationale of employing allo-HCT to treat cancer mainly lies in its immunotherapeutic potential. Indeed, the donor immune system, reconstituting from hematopoietic stem cells or directly transferred as part of the graft, can react against tumor and patient antigens, mediating the so-called graft versus tumor (GvT) effect. The most potent targets of this response are the HLA molecules themselves, capable of eliciting responses of several orders of magnitude more intense than any peptidic antigen. The main mediators of the GvT effect are the donor T cells, which are also responsible for the other, dark face of the allo-HCT coin: graft versus host disease (GvHD), that

contributes to a significant proportion of the morbidity and mortality observed after allo-HCT.

Starting from the early 1990, several investigators worked relentlessly on improving allo-HCT, developing new strategies to reduce the risk of GvHD without affecting immune reconstitution, to decrease the toxicity of the pre-transplant conditioning regimens and to diminish the frequency and severity of opportunistic infections.

All these improvements allowed clinicians to overcome the HLA barrier and to enlarge the donor pool, to utilize more graft sources beside the original bone marrow and to expand the indication to allo-HCT also to patients that were not considered fit, including elderly individuals and patients with comorbidities. As a result, the number of allo-HCT performed worldwide every year has been continuously growing, to date reaching more than 30,000 procedures<sup>1</sup> performed every year for a wide range of indications, amongst which acute myeloid leukemia (AML) represents the most frequent.

However, most of these improvements have been strictly related to the reduction of transplant-related mortality (TRM), exposing the issue of post-transplantation disease relapse. Relapse, defined as the reappearance of the original malignancy after a period of apparent remission, occurs in up to 50% of patients receiving allo-HCT for AML. Not only the incidence of relapse has not decreased over the last few decades, but, when it occurs, relapse remains just as invariably lethal as it was 20 years ago.

It is becoming increasingly recognized that the two key aspects to be tackled to reduce the incidence and improve the outcome of post-

transplantation relapses are i) understanding its biology and ii) improving its early detection to enact preemptive treatments; works presented in this thesis will be related to both of these crucial topics. Regarding the first point, evidence is growing on the fact that relapse may occur through the clonal selection of immune resistant variants able to evade control from the donor immune system<sup>2</sup>.

As mentioned above, HLA molecules represent a major target of T cell mediated alloreaactions, and recent studies have shown that genomic<sup>3</sup> and non-genomic<sup>4</sup> alterations in the antigen processing and presentation machinery can be detected in the majority of post-transplantation relapses. Another way that leukemia enacts to escape elimination is to thwart immune recognition, as by the overexpression of immune-checkpoint molecules<sup>3</sup>.

Additionally, the functional dysregulation of the main effectors of post-allo-HCT immune surveillance can also lead to relapse, such as by the activation of an exhaustion program in T cells<sup>5</sup> and/or by the dysfunction or late recovery of NK cells<sup>6</sup>.

Unfortunately, most of the strategies that are currently available to treat leukemia relapse display limited or poor efficacy when enacted against overt disease. Hence the first step to improve results in AML post-transplantation relapses is to intervene earlier. Efforts should thus be aimed at identifying the precise risk profile for each patient and to perform tight monitoring for the prevention of relapse onset.

## **1.2 Scope of the thesis**

The main goal of my research activity is to study the immunobiology of allo-HCT, with particular interest in understanding the mechanisms governing post-transplantation AML immune evasion and relapse, and the final objective to develop new targeted treatment options.

The first step to combat relapse is to intervene before overt disease reappearance. Detection of increasing host hematopoietic chimerism after a myeloablative conditioning can represent a valid surrogate marker of impending relapse in patients lacking other molecular markers of minimal residual disease. To understand whether novel, more sensitive, chimerism detection technologies could improve the clinical utility of this method, I took part to a study aiming at prospectively compare qPCR-based chimerism monitoring on peripheral blood or bone marrow samples in patients who received transplantation for high-risk AML. This work will be described and discussed in **Chapter 2**.

### **Chapter 2:**

#### **Quantitative PCR-based chimerism in bone marrow or peripheral blood to predict acute myeloid leukemia relapse in high-risk patients: results from the KIM-PB prospective study**

Gambacorta V, Parolini R, Xue E, Greco R, Bouwmans EE, Toffalori C, Giglio F, Assanelli A, Lupo Stanghellini MT, Ambrosi A, Mazzi B, Mulder W, Corti C, Peccatori J, Ciceri F\*, Vago L\*

*Under second revision in Haematologica*

Immune reconstitution after allo-HCT represents a unique and highly informative setting to study the dynamics of the immune system and how they can be influenced by therapies. **Chapter 3** of this thesis will present the study on the effect of post-transplant cyclophosphamide on NK cell recovery and alloreactivity.

**Chapter 3:**

**NK cell recovery after haploidentical HSCT with post-transplant cyclophosphamide: dynamics and clinical implications**

Russo A, Oliveira G, Berglund S, Greco R, Gambacorta V, Cieri N, Toffalori C, Zito L, Lorentino F, Piemontese S, Morelli M, Giglio F, Assanelli A, Lupo Stanghellini MT, Bonini C, Peccatori J, Ciceri F, Luznik L\*, Vago L\*

*Published in Blood (2018)*

Moreover, longitudinal monitoring of patients after transplantation can also reveal why in some individuals the donor immune system fails at controlling AML disease recurrence, and identify immune-related biomarkers to predict post-transplantation relapse. This will be the aim of **Chapter 4**, which reports on a study aimed at investigating whether T cell exhaustion is involved in the development of AML post-transplantation relapse.

#### **Chapter 4:**

##### **Bone marrow central memory and memory stem T-cell exhaustion in AML patients relapsing after HSCT**

Noviello M, Manfredi F, Ruggiero E, Perini T, Oliveira G, Cortesi F, De Simone P, Toffalori C, Gambacorta V, Greco R, Peccatori J, Casucci M, Casorati G, Dellabona P, Onozawa M, Teshima T, Griffioen M, Halkes CJM, Falkenburg JHF, Stölzel F, Altmann H, Bornhäuser M, Waterhouse M, Zeiser R, Finke J, Cieri N, Bondanza A, Vago L\*, Ciceri F\*, Bonini C\*

*Published in Nature Communications (2019)*

Besides the description of how the immune system reconstitutes and reshaped upon allo-HCT, to understand and treat relapse is necessary to study how tumor cells interact with the different immune subsets in each patient and transplantation setting. This is the focus of the work reported in **Chapters 5**, and comprehensively reviewed in **Chapter 6**.

#### **Chapter 5:**

##### **Immune signature drives leukemia escape and relapse after hematopoietic cell transplantation**

Toffalori C, Zito L\*, Gambacorta V\*, Riba M\*, Oliveira G, Bucci G, Barcella M, Spinelli O, Greco R, Crucitti L, Cieri N, Noviello M, Manfredi F, Montaldo E, Ostuni R, Naldini MM, Gentner B, Waterhouse M, Zeiser R, Finke J, Hanoun M, Beelen D, Gojo I, Luznik L, Onozawa M, Teshima T, Devillier R, Blaise D, Halkes CJM, Griffioen



M, Carrabba MG, Bernardi M, Peccatori J, Barlassina C, Stupka E, Lazarevic D., Tonon G, Rambaldi A, Cittaro D, Bonini C, Fleischhauer K, Ciceri F\*, Vago L\*

Published in Nature Medicine (2019)

#### **Chapter 6:**

#### **Mechanisms of Leukemia Immune Evasion and Their Role in Relapse after Haploidentical Hematopoietic Cell transplantation**

Rovatti PE\*, Gambacorta V\*, Lorentino F\*, Ciceri F and Vago L

Under second revision in Frontiers in Immunology

Identification of patterns of immune evasion and relapse can in turn lead to new research questions and rationales for treatment: in **Chapter 7** I will present my main and unpublished thesis project, aimed at understanding the epigenetic mechanisms of AML relapses with downregulation of HLA class II expression and **Chapter 8** provides a review on the epigenetic treatments for AML and their immune-related effects.

#### **Chapter 7:**

#### **Integrated Epigenetic Profiling Identifies EZH2 as a Therapeutic Target to Re-Establish Immune Recognition of Leukemia Relapses with Loss of HLA Class II Expression**

Gambacorta V, Gnani D, Zito L, Beretta S, Zanotti L, Oliveira G, Cittaro D, Merelli I, Ciceri F, Di Micco R\* and Vago L\*

In preparation

**Chapter 8:**

**Epigenetic Therapies for Acute Myeloid Leukemia and Their  
Immune-Related Effects**

Gambacorta V, Gnani D, Vago L, Di Micco R

*Published in Frontiers in Cell and Developmental Biology (2019)*

## **References**

1. Gratwohl, A. *et al.* One million haemopoietic stem-cell transplants: a retrospective observational study. *Lancet Haematol* **2**, e91-100 (2015).
2. Khong, H. T. & Restifo, N. P. Natural selection of tumor variants in the generation of “tumor escape” phenotypes. *Nat Immunol* **3**, 999–1005 (2002).
3. Toffalori, C. *et al.* Immune signature drives leukemia escape and relapse after hematopoietic cell transplantation. *Nat. Med.* **25**, 603–611 (2019).
4. Christopher, M. J. *et al.* Immune Escape of Relapsed AML Cells after Allogeneic Transplantation. *N. Engl. J. Med.* **379**, 2330–2341 (2018).
5. Noviello, M. *et al.* Bone marrow central memory and memory stem T-cell exhaustion in AML patients relapsing after HSCT. *Nat Commun* **10**, 1065 (2019).
6. Russo, A. *et al.* NK cell recovery after haploidentical HSCT with posttransplant cyclophosphamide: dynamics and clinical implications. *Blood* **131**, 247–262 (2018).



## **Chapter 2.**

### **Quantitative PCR-based chimerism in bone marrow or peripheral blood to predict acute myeloid leukemia relapse in high-risk patients: results from the KIM-PB prospective study**

Gambacorta V, Parolini R, Xue E, Greco R, Bouwmans EE, Toffalori C, Giglio F, Assanelli A, Lupo Stanghellini MT, Ambrosi A, Mazzi B, Mulder W, Corti C, Peccatori J, Ciceri F\*, Vago L\*

*Under second revision in Haematologica*

ARTICLE SUMMARY: This study prospectively addresses qPCR-based chimerism monitoring on peripheral blood or bone marrow samples for prediction of post-transplantation relapse in patients with high-risk AML. Using this high sensitivity technique peripheral blood proved superior to bone marrow in detecting impending relapse, allowing tighter monitoring due to its lower invasiveness.

Haematologica  
HAEMATOL/2019/238543  
Version 1

Quantitative PCR-based chimerism in bone marrow or peripheral blood to predict acute myeloid leukemia relapse in high-risk patients: results from the KIM-PB prospective study

Valentina Gambacorta, Riccardo Parolini, Elisabetta Xue, Raffaella Greco, Evelien Bouwmans, Cristina Toffalori, Fabio Giglio, Andrea Assanelli, Marta Teresa Lupo Stanghellini, Alessandro Ambrosi, Benedetta Mazzi, Wietse Mulder, Consuelo Corti, Jacopo Pecatori, Fabio Ciceri, and Luca Vago

Disclosures: LV received research support from GenDx and Moderna Therapeutics. None of the other authors has any relevant conflicts of interest to disclose.

Contributions: FC and LV designed the study. VG, RP and EX performed and analyzed the experiments. EB, CT, BM and WM provided advice on chimerism experiments and data interpretation. EX, RG, FG, AAs, MTLs, CC, JP, FC and LV contributed to patient clinical care and data collection. AAm supervised statistical analyses. VG, FC, and LV wrote the manuscript.

## LETTER TO THE EDITOR

### **Quantitative PCR-based chimerism in bone marrow or peripheral blood to predict acute myeloid leukemia relapse in high-risk patients: results from the KIM-PB prospective study**

Valentina Gambacorta<sup>1</sup>, Riccardo Parolini<sup>1</sup>, Elisabetta Xue<sup>1,2</sup>, Raffaella Greco<sup>2</sup>, Evelien E. Bouwmans<sup>3</sup>, Cristina Toffalori<sup>1</sup>, Fabio Giglio<sup>2</sup>, Andrea Assanelli<sup>2</sup>, Maria Teresa Lupo Stanghellini<sup>2</sup>, Alessandro Ambrosi<sup>4</sup>, Benedetta Mazzi<sup>5</sup>, Wietse Mulder<sup>3</sup>, Consuelo Corti<sup>2</sup>, Jacopo Peccatori<sup>2</sup>, Fabio Ciceri<sup>2,4,\*</sup>, Luca Vago<sup>1,2,\*</sup>

<sup>1</sup>Unit of Immunogenetics, Leukemia Genomics and Immunobiology, IRCCS San Raffaele Scientific Institute, Milano, Italy; <sup>2</sup>Hematology and Bone Marrow Transplantation Unit, IRCCS San Raffaele Scientific Institute, Milano, Italy; <sup>3</sup>GenDx, Utrecht, Netherlands; <sup>4</sup>Vita-Salute San Raffaele University, Milano, Italy <sup>5</sup>HLA and Chimerism Laboratory, IRCCS San Raffaele Scientific Institute, Milano, Italy.

\* indicates equal contribution from these Authors

TEXT WORD COUNT: 1472

FIGURES/TABLES/REFERENCES: 1/1/15

RUNNING HEAD: PB or BM chimerism for relapse prediction

ARTICLE SUMMARY: This study prospectively addresses qPCR-based chimerism monitoring on peripheral blood or bone marrow samples for prediction of post-transplantation relapse in patients with high-risk AML. Using this high sensitivity technique peripheral blood proved superior to bone marrow in detecting impending relapse, allowing tighter monitoring due to its lower invasiveness.

**Corresponding Author:** Dr. Luca Vago, Unit of Immunogenetics, Leukemia Genomics and Immunobiology, IRCCS San Raffaele Scientific Institute, via Olgettina 60, Milano, Italy; e-mail: vago.luca@hsr.it

Allogeneic hematopoietic stem cell transplantation (allo-HSCT) represents the best curative option available for many patients suffering from high-risk acute myeloid leukemia (AML). Nevertheless, especially in patients with high or very high disease risk index (DRI), relapses are extremely frequent<sup>1,2</sup>. Although salvage treatments are expectedly more effective when enacted before overt hematological recurrence, in such high-risk patients it is extremely difficult to identify this clinically-relevant time window, due to the rapid growth kinetics of the disease and to the fact that relapses occur very early after allo-HSCT. The issue is made even more complicated by the genetic heterogeneity and clonal plasticity of AML, hampering the identification of reliable and stable-over-time genetic markers to monitor minimal residual disease (MRD)<sup>3</sup>.

After myeloablative allo-HSCT, reappearance of host-specific hematopoietic chimerism has been strongly associated with relapse<sup>4</sup>, therefore representing a practical and nearly universal surrogate marker of MRD. The development of quantitative-PCR based assays for chimerism monitoring has increased dramatically the sensitivity of this approach<sup>5</sup>, and a number of studies have reported the clinical utility of qPCR-based chimerism monitoring for relapse prediction<sup>6-9</sup>. However, most of these studies were performed retrospectively and in highly heterogeneous patient cohorts, and it is yet largely unaddressed whether the increased sensitivity of this approach might allow to monitor disease reappearance from peripheral blood samples and in very high risk AML patients.

To answer these questions we designed a prospective, non-interventional, single-center study to compare chimerism monitoring in peripheral blood (PB) or bone marrow (BM) in patients undergoing myeloablative allo-HSCT for high-risk AML ("KIM-PB" study, approved by the San Raffaele Ethic Committee on September 1<sup>st</sup>, 2014). Primary endpoint of the study was prediction of relapse. In the initial design, the study group comprised 30 AML patients with DRI high or very high, and the control group 15 patients with Hodgkin or non-Hodgkin lymphomas without BM disease involvement. Conditioning regimens and graft versus host disease prophylaxis were similar in both the study and the control group, and mainly based on treosulfan plus fludarabine and sirolimus plus mycophenolate, respectively. Between September 2014 and March 2016, 29 patients



were enrolled to the study group (one patient was dropped out because his donor refused to participate to the study), but only 20 were evaluable for the study endpoint, since 4 were excluded because of the early non relapse mortality (NRM), 2 for disease persistence at first hematological evaluation, 2 for randomization to a non-myeloablative conditioning regimen, and 1 for graft rejection (**Figure 1B**). We enrolled to the control group 8 patients, excluded one for early NRM, and upon a planned ad interim analysis considered the 7 evaluable patients sufficient to perform the relevant comparisons. Patient and transplant characteristics for evaluable patients from both groups are summarized in **Table 1**. Chimerism was monitored using commercially available qPCR-based assays (KMRtype and KMRtrack, GenDx, Utrecht) (*see Online Methods for supplementary information*). BM evaluations were performed at day 30, 60, 90, 180, 270 and 360 after allo-HSCT, according to the practice of our center (6 total BM time points per patient). PB evaluations were performed at day 3, 7 and 15, every 15 days during the first 4 months after allo-HSCT, and monthly during the subsequent period, until one year after allo-HSCT. Sampling schedule for the study is summarized in **Figure 1A**.

Out of the 20 patients belonging to the study group that were evaluable for study endpoint, 7 subsequently relapsed (median time to relapse: 73 days; range, 61-93), 11 were alive and in complete remission at the end of the one-year follow-up (FU) and 2 died in remission before the end of the FU (at day 58 and 112 after allo-HSCT, respectively, **Figure 1B**). In the control group, out of the 7 patients evaluable for chimerism monitoring, 5 were alive at the end-of-study time-point and 2 died before that (at day 25 and 116), with no patient developing BM involvement throughout the study. Altogether, we collected and analyzed 409 samples (PB, n=310; BM, n=99). When we compared the values of host-specific chimerism obtained from paired PB and BM samples (n=97) we detected a significantly higher host signal in BM compared to PB, especially at late time-points (**Figure 1C**) and moderate correlation between the two measurements ( $R^2=0.7$ ;  $p<0.0001$ ) (**Figure 1D**). Amongst several models tested, the best results in term of relapse prediction were achieved for both PB and BM considering as of interest only samples with

increasing mixed chimerism (IMC) as compared to the previous determination. Using this model, we conducted a receiver operating characteristic (ROC) curve analysis to compare the predictive value of PB and BM in relapse prediction and select thresholds of significance (**Figure 1E**). Area under the ROC curve was 0.881 (95% CI =0.7846-0.9782) for PB and 0.7000 (95% CI=0.4276-0.9724) for BM, with superior performance for PB at all possible thresholds. ROC curve analysis indicated that the best cut-offs to predict relapse were 0.13% for PB (representing also the maximal reproducible sensitivity of the method, yielding 87.5% sensitivity and 84.6% specificity in relapse prediction) and 0.24 for BM (yielding 100% sensitivity and 55% specificity in relapse prediction).

When we translated this model and thresholds to the analysis of patients enrolled to our study we could document that PB chimerism predicted 4/7 relapses (57%, **Figure 1F**) and gave false positive results in 4/13 patients from the study group who did not relapse (31%, **Figure 1G**) and in 1/7 patients from the control group (14%, **Figure 1H**). All these false positive results were detected in the first four months after allo-HSCT. Results using PB compared favorably with those obtained by BM monitoring, that allowed relapse prediction in 2/7 patients from the study group (29%, **Figure 1I**) and provided false positive results in 6/13 non-relapsing patients from the study group (46%, **Figure 1J**) and in 1/7 patients from the control series (14%, **Figure 1K**). Of notice, BM false positive results spanned over the entire observation follow-up, including some documented at very late time-points. Finally, we compared median time from IMC detection to relapse in the two sites of sampling, which was 17 days for PB (range: 8-44) and 33 days for BM (range: 30-59), indicating that in most cases relapse was anticipated by a single over-threshold IMC.

This study is the first, to our knowledge, to prospectively address the clinical utility of qPCR-based chimerism monitoring in DRI high or very-high AML patients undergoing allo-HSCT. This particular subset of patients represents a significant clinical challenge since, due to the aggressiveness and intrinsic chemoresistance of their disease, even if they achieve remission, this is often short-lived. This prompts the search for approaches to anticipate the detection of leukemia recurrence and to rationally allocate pre-emptive therapies.

Despite a number of recent studies documented encouraging results obtained by qPCR chimerism monitoring<sup>6,7,9</sup>, very few properly compared qPCR with semiquantitative analysis of short tandem repeat polymorphisms<sup>8,10</sup>, and for this reason the latter remains to date the standard for chimerism monitoring. Our study was designed on the rationale that the higher sensitivity of qPCR could be a perfect fit for PB monitoring, and that in turn this could allow tighter follow-up of high-risk patients. Indeed, our results proved us right, evidencing clear superiority of PB monitoring over BM. This was not only due to the more frequent sampling, allowing to capture IMC before overt relapse, but also to higher specificity of positive signals, since BM analysis by qPCR detected significant "background noise" at all time-points, possibly explained by aspiration and highly sensitive detection of host BM stromal cells. Despite being superior to the ones obtained with BM monitoring, results obtained from PB monitoring are far from perfect, and evidently inferior to those obtained in similar studies by tracking specific mutations<sup>11,12</sup>. However, it should be considered that in our study cohort only 4/20 (20%) patients carried nucleophosmin-1 mutations, and that the value of monitoring most other molecular abnormalities remains matter of debate<sup>3</sup>. One of the main issues evidenced from our study is that in high-risk patients the median time to relapse is exceptionally short. This renders the value of early determinations crucial, especially to understand whether a positive chimerism at these time-points is the sign of a still active clearance of patient hematopoiesis or the first sign of disease reappearance. Again, tighter monitoring may be key to address this issue, but also the use of techniques with higher accuracy than qPCR, such as droplet digital PCR<sup>13-15</sup>, may more precisely quantify changes in chimerism and further improve on this crucial hurdle.

Taken together, our data show that the limited invasiveness, rapid analytical turnaround and nearly universal applicability of PB qPCR-based monitoring render it a valuable tool to complement the still too limited armamentarium that is available for the follow-up of patients transplanted for high-risk AML. Further multicenter studies should be aimed to confirm these results, and to address the crucial issue of standardization of this method across different laboratories.

## **ACKNOWLEDGEMENTS**

Reagents for this study were generously provided by GenDx. The study was supported by the Italian Ministry of Health (RF-2011-02351998 to FC and LV, RF-2011-02348034 to LV and TRANSCAN HLALOSS to LV), by the Associazione Italiana per la Ricerca sul Cancro (Start-Up Grant #14162 to LV) and by the DKMS Mechtild Harf Foundation (DKMS Mechtild Harf Research Grant 2015 to LV).

## **AUTHORSHIP**

FC and LV designed the study. VG, RP and EX performed and analyzed the experiments. EB, CT, BM and WM provided advice on chimerism experiments and data interpretation. EX, RG, FG, AAs, MTLs, CC, JP, FC and LV contributed to patient clinical care and data collection. AAm supervised statistical analyses. VG, FC, and LV wrote the manuscript.

## **DISCLOSURES**

LV received research support from GenDx and Moderna Therapeutics. None of the other authors has any relevant conflicts of interest to disclose.

## **REFERENCES**

1. Horowitz M, Schreiber H, Elder A, et al. Epidemiology and biology of relapse after stem cell transplantation. *Bone Marrow Transplant* [Epub ahead of print].
2. Armand P, Gibson CJ, Cutler C, et al. A disease risk index for patients undergoing allogeneic stem cell transplantation. *Blood* 2012;120(4):905–913.
3. Ball B, Stein EM. Which are the most promising targets for minimal residual disease-directed therapy in acute myeloid leukemia prior to allogeneic stem cell transplant? *Haematologica* 2019;104(8):1521–1531.

4. Bader P, Kreyenberg H, Hoelle W, et al. Increasing mixed chimerism defines a high-risk group of childhood acute myelogenous leukemia patients after allogeneic stem cell transplantation where pre-emptive immunotherapy may be effective. *Bone Marrow Transplant* 2004;33(8):815–821.
5. Alizadeh M, Bernard M, Danic B, et al. Quantitative assessment of hematopoietic chimerism after bone marrow transplantation by real-time quantitative polymerase chain reaction. *Blood* 2002;99(12):4618–4625.
6. Qin X-Y, Li G-X, Qin Y-Z, et al. Quantitative chimerism: an independent acute leukemia prognosis indicator following allogeneic hematopoietic SCT. *Bone Marrow Transplant* 2014;49(10):1269–1277.
7. Jacque N, Nguyen S, Golmard J-L, et al. Chimerism analysis in peripheral blood using indel quantitative real-time PCR is a useful tool to predict post-transplant relapse in acute leukemia. *Bone Marrow Transplant* 2015;50(2):259–265.
8. Ahci M, Stempelmann K, Buttkeireit U, et al. Clinical Utility of Quantitative PCR for Chimerism and Engraftment Monitoring after Allogeneic Stem Cell Transplantation for Hematologic Malignancies. *Biol Blood Marrow Transplant* 2017;23(10):1658–1668.
9. Sellmann L, Rabe K, Bünting I, et al. Diagnostic value of highly-sensitive chimerism analysis after allogeneic stem cell transplantation. *Bone Marrow Transplantation* 2018;53(11):1457–1465.
10. Bader P, Niethammer D, Willasch A, Kreyenberg H, Klingebiel T. How and when should we monitor chimerism after allogeneic stem cell transplantation? *Bone Marrow Transplant* 2005;35(2):107–119.
11. Xue E, Tresoldi C, Sala E, et al. Longitudinal qPCR monitoring of nucleophosmin 1 mutations after allogeneic hematopoietic stem cell transplantation to predict AML relapse. *Bone Marrow Transplantation* 2016;51(3):466–469.
12. Brambati C, Galbiati S, Xue E, et al. Droplet digital polymerase chain reaction for DNMT3A

and IDH1/2 mutations to improve early detection of acute myeloid leukemia relapse after allogeneic hematopoietic stem cell transplantation. *Haematologica* 2016;101(4):e157-161.

13. Valero-Garcia J, González-Espinosa M del C, Barrios M, et al. Earlier relapse detection after allogeneic haematopoietic stem cell transplantation by chimerism assays: Digital PCR versus quantitative real-time PCR of insertion/deletion polymorphisms. *PLOS ONE* 2019;14(2):e0212708.
14. Waterhouse M, Pfeifer D, Duque-Afonso J, et al. Droplet digital PCR for the simultaneous analysis of minimal residual disease and hematopoietic chimerism after allogeneic cell transplantation. *Clinical Chemistry and Laboratory Medicine (CCLM)* 2019;57(5):641–647.
15. Stahl T, Böhme MU, Kröger N, Fehse B. Digital PCR to assess hematopoietic chimerism after allogeneic stem cell transplantation. *Exp Hematol* 2015;43(6):462-468.e1.

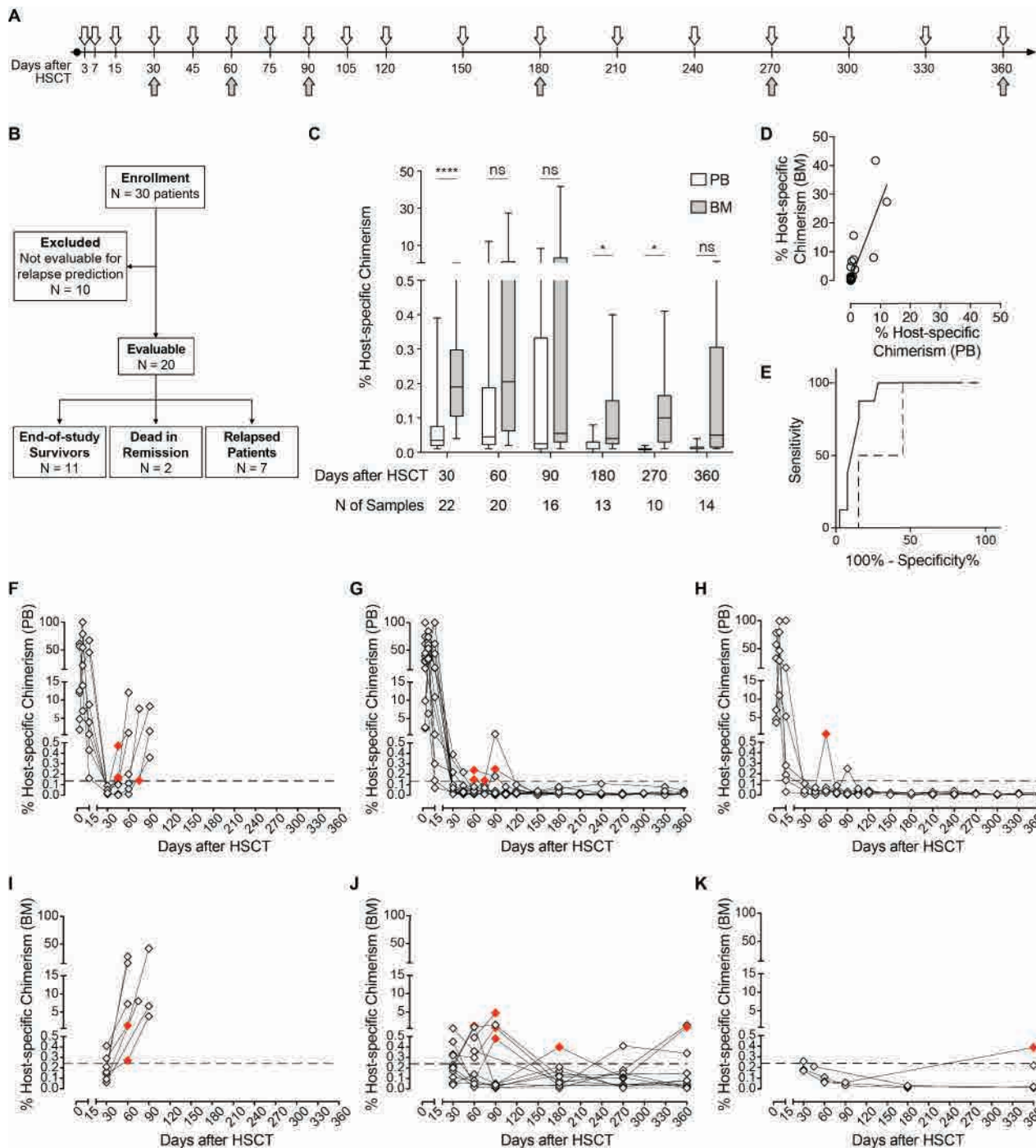
**Table 1. Patient and transplant characteristics**

	Study Group (n=20) <i>Number (%)</i>	Control Group (n=7) <i>Number (%)</i>
<b>Median age, years (range)</b>	54 (29-72)	30 (19-36)
<b>Sex</b>		
Male	13 (65.0)	2 (28.6)
Female	7 (35.0)	5 (71.4)
<b>Disease</b>		
AML	20 (100)	-
HL	-	3 (42.9)
NHL	-	4 (57.1)
<b>Disease status at HSCT</b>		
Complete Remission	9 (45.0)	4 (57.1)
Active Disease	11 (55.0)	3 (42.8)
<b>Disease Risk Index (DRI)</b>		
Low	0	1 (14.2)
Intermediate	0	3 (42.9)
High	17 (85.0)	3 (42.9)
Very high	3 (15.0)	0
<b>Donor type</b>		
Matched related	1 (5.0)	1 (14.3)
Matched unrelated	5 (25.0)	3 (42.9)
Haploidentical	14 (70.0)	3 (42.9)
<b>Median follow up after HSCT, days (range)</b>	351 (56-375)	372 (26-385)
<b>Median time to engraftment, days (range)</b>	20 (13-31)	18 (3-25)
<b>Relapse</b>	7 (35.0)	0
Median time to relapse, days (range)	72 (60-91)	
<b>Transplant related mortality</b>	2 (10.0)	2 (28.6)
Median time to TRM, days (range)	84 (56-112)	70 (26-114)
<b>End-of-study survivors</b>	11 (55.0)	5 (71.4)

## FIGURE LEGEND

**Figure 1. Outline and results of the KIM-PB prospective study.** **A**, Study sampling schedule. White arrows indicate PB samplings, gray arrow BM samplings. **B**, Diagram summarizing enrollment and outcome of patients belonging to the study group. **C**, Percentage of host-specific chimerism detected in 97 paired PB (white box-and-whiskers plots) and BM (gray box-and-whiskers plots) samples collected during the post-transplantation follow-up. Boxes display median and interquartile range, whiskers minimum and maximum values. For all comparisons, paired t test where used (ns = not significant; \*Pvalue < 0.05; \*\*\*\*Pvalue < 0.0001); **D**, Correlation analysis between the host-specific chimerism values detected in PB (x axis) and BM (y axis) in the same 97 sample pairs displayed in panel **C**. Shown are results of two-sided Pearson correlation analysis, with linear regression line and 95% confidential interval. **E**, ROC curves, showing sensitivity (Y-axis) and 1-specificity (X-axis) obtained by taking into account 310 PB samples (full line) and 99 BM samples (dashed line) with IMC as compared to the immediately previous determination. **F-K**, Kinetics of host-specific chimerism during the post-transplantation follow-up measured in the PB (panels **F-H**) and BM (panels **I-K**) of patients from the study group who experienced relapse (leftmost panels), of patients from the study group who remained in remission throughout the observation period (center panels) and of patients from the control group (rightmost panels). The dashed line indicates the threshold values of 0.13% for PB and 0.24% for BM, selected on the basis of ROC curve analysis. Red diamonds indicate samples with IMC and exceeding the threshold values, defined in the text as “true positives” if they were observed in study group patients who relapsed, or “false positives” if they were observed in study group patients who did not relapse or in control group patients.





## **SUPPLEMENTARY METHODS**

### **Sample collection and preparation**

Peripheral blood and bone marrow samples were collected at the pre-specified study time-points illustrated in **Figure 1A**, in concomitance to routine diagnostic procedures and upon specific written informed consent. Samples were centrifuged for seven minutes at 1500 revolutions per minute and the cell-enriched interphase was collected and stored at -80°C for subsequent use. Upon sample thawing, genomic DNA was extracted using the Qiamp Blood Minikit (QIAGEN, Venlo, The Netherlands) according to the manufacturer's instructions, checked for quality and concentration using a Nanodrop spectrophotometer (Thermo Scientific, Franklin, MA, USA), and stored at -20°C.

### **Hematopoietic chimerism analysis**

Hematopoietic chimerism was analysed using a commercial qPCR-based system (KMRtype and KMRtrack assays, GenDx, Utrecht, The Netherlands) according to the manufacturer's instructions. Briefly, host-specific polymorphisms for subsequent chimerism monitoring were selected using the KMRtype genotyping assay, which probes for 29 insertion-deletion polymorphisms spread over 18 different chromosomes by 10 independent multiplexed TaqMan qPCR reactions. For each well, 10 ng of genomic DNA from the individual of interest were used in a final test volume of 20 µl.

For each donor-recipient pair, two markers positive in the patient and negative in the donor were selected as informative using the KMREngine software and employed in parallel for post-transplantation monitoring. Quantification of these informative patient-specific markers at each study time-point was performed using the KMRtrack qPCR assays. Each assay consists in a singleplex Taqman reaction probing an indel polymorphism. Comparators for each reaction consisted in a pre-transplant sample from the patient and in a reference reaction, amplifying the invariant *RPPHI* gene. Percentage of host-specific chimerism was calculated according to the to the

$\Delta\Delta CT$  formula:  $2^{-\Delta\Delta CT} \times 100\%$ , in which  $\Delta\Delta CT$  equals to: (CT (marker post-transplant sample) - CT (reference gene post-transplant sample)) - (CT (marker patient pre-transplant sample) - CT (reference gene patient pre-transplant sample)). All reactions were performed in duplicate, testing 50 ng of genomic DNA per well in a final test volume of 20  $\mu$ l. All qPCR reactions were amplified and analysed using an Applied Biosystems 7500 Thermocycler, using the cycling conditions suggested by the assay manufacturers.

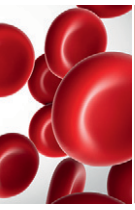


### **Chapter 3.**

#### **NK cell recovery after haploidentical HSCT with post-transplant cyclophosphamide: dynamics and clinical implications**

Russo A, Oliveira G, Berglund S, Greco R, Gambacorta V, Cieri N, Toffalori C, Zito L, Lorentino F, Piemontese S, Morelli M, Giglio F, Assanelli A, Lupo Stanghellini MT, Bonini C, Peccatori J, Ciceri F, Luznik L\*, Vago L\*

*Published in Blood (2018)*



TRANSPLANTATION

# NK cell recovery after haploidentical HSCT with posttransplant cyclophosphamide: dynamics and clinical implications

Antonio Russo,<sup>1,2,\*</sup> Giacomo Oliveira,<sup>1,3,\*</sup> Sofia Berglund,<sup>4</sup> Raffaella Greco,<sup>2</sup> Valentina Gambacorta,<sup>1</sup> Nicoletta Cieri,<sup>3</sup> Cristina Toffalori,<sup>1</sup> Laura Zito,<sup>1</sup> Francesca Lorentino,<sup>2</sup> Simona Piemontese,<sup>2</sup> Mara Morelli,<sup>2</sup> Fabio Giglio,<sup>2</sup> Andrea Assanelli,<sup>2</sup> Maria Teresa Lupo Stanghellini,<sup>2</sup> Chiara Bonini,<sup>3,5</sup> Jacopo Peccatori,<sup>2</sup> Fabio Ciceri,<sup>2,5</sup> Leo Luznik,<sup>4,†</sup> and Luca Vago<sup>1,2,†</sup>

<sup>1</sup>Unit of Immunogenetics, Leukemia Genomics and Immunobiology, <sup>2</sup>Hematology and Bone Marrow Transplantation Unit, and <sup>3</sup>Experimental Hematology Unit, Istituto di Ricovero e Cura a Carattere Scientifico San Raffaele Scientific Institute, Milan, Italy; <sup>4</sup>Sidney Kimmel Comprehensive Cancer Center, Johns Hopkins University School of Medicine, Baltimore, MD; and <sup>5</sup>Vita-Salute San Raffaele University, Milan, Italy

KEY POINTS

- Posttransplantation cyclophosphamide eliminates most mature donor NK cells infused with the graft, including alloreactive NK cells.
- High levels of serum interleukin-15 early after HSCT provide a favorable environment for adoptive infusion of mature donor NK cells.

**The use of posttransplant cyclophosphamide (PT-Cy) as graft-versus-host disease (GVHD) prophylaxis has revolutionized haploidentical hematopoietic stem cell transplantation (HSCT), allowing safe infusion of unmanipulated T cell-replete grafts. PT-Cy selectively eliminates proliferating alloreactive T cells, but whether and how it affects natural killer (NK) cells and their alloreactivity is largely unknown. Here we characterized NK cell dynamics in 17 patients who received unmanipulated haploidentical grafts, containing high numbers of mature NK cells, according to PT-Cy-based protocols in 2 independent centers. In both series, we documented robust proliferation of donor-derived NK cells immediately after HSCT. After infusion of Cy, a marked reduction of proliferating NK cells was evident, suggesting selective purging of dividing cells. Supporting this hypothesis, proliferating NK cells did not express aldehyde dehydrogenase and were killed by Cy in vitro. After ablation of mature NK cells, starting from day 15 after HSCT and favored by the high levels of interleukin-15 present in patients' sera, immature NK cells (CD62L<sup>+</sup>NKG2A<sup>+</sup>KIR<sup>-</sup>) became highly prevalent, possibly directly stemming from infused hematopoietic stem cells. Importantly, also putatively alloreactive single KIR<sup>+</sup> NK cells were eliminated by PT-Cy and were thus decreased in numbers and antileukemic potential at day 30 after HSCT. As a consequence, in an extended series of 99 haplo-HSCT with PT-Cy, we found no significant difference in progression-free survival between patients with or without predicted NK alloreactivity (42% vs 52% at 1 year,  $P = NS$ ). Our data suggest that the majority of mature NK cells infused with unmanipulated grafts are lost upon PT-Cy administration, blunting NK cell alloreactivity in this transplantation setting. (*Blood*. 2018;131(2):247-262)**

## Introduction

Conceiving strategies to render allogeneic hematopoietic stem cell (HSC) transplantation (HSCT) from HLA-haploidentical family donors safe and feasible has been one of the most challenging efforts faced by the HSCT community over the past several decades. Besides having cured numerous patients that lacked a suitable donor, haploidentical HSCT provided fascinating scientific insights into how the immune system operate upon transfer into an allogeneic environment.<sup>1,2</sup>

One the most remarkable discoveries that originated from early trials of haploidentical HSCT was the description of the principles according to which natural killer (NK) cell alloreactivity ensues, and the observation that, when unleashed, it is accompanied by beneficial effects on HSCT outcome, including protection from relapse.<sup>3-5</sup>

In more recent years, another game-changing discovery stemming from haploidentical HSCT has been the demonstration that high-dose posttransplant cyclophosphamide (PT-Cy) can selectively eliminate the most alloreactive donor T-cell clones in vivo.<sup>6-8</sup> This fostered a true revolution in the field, and haploidentical HSCT platforms based on PT-Cy are increasingly being used worldwide,<sup>9,10</sup> not only because of the impressive abatement of graft-versus-host disease (GVHD) incidence they can convey, but also of their very limited requirements in terms of graft processing and specific expertise from the transplant team. It is largely unknown, however, whether the models that were developed in T cell-depleted haploidentical HSCT still hold true in this setting.

The aim of this study is to trace the dynamics of posttransplantation NK cell recovery in 2 independent series of patients who received

**Table 1. Characteristics of patients analyzed longitudinally during the posttransplantation follow-up**

UPN	Sex	Age (y)	Diagnosis	Refined DFI*	Conditioning regimen†	GVHD prophylaxis‡	Predicted NK alloreactivity§	Graft source	CD3+ cells infused/kg × 10 <sup>6</sup>	NK cells infused/kg × 10 <sup>6</sup>
OSR 1	M	33	sAML	Low	Thio-Treo-Flu	PT-Cy-sirolimus-MMF	Yes (C1)	PB	135.28	19.9
OSR 2	M	69	sAML	High	Thio-Treo-Flu	PT-Cy-sirolimus-MMF	No	PB	250	17.32
OSR 3	F	24	HL	High	Thio-Treo-Flu	PT-Cy-sirolimus-MMF	No	PB	194.3	9.18
OSR 4	F	62	AML	High	Thio-Treo-Flu	PT-Cy-sirolimus-MMF	Yes (C1)	PB	267.89	17.13
OSR 5	M	57	sAML	Intermediate	Thio-Treo-Flu	PT-Cy-sirolimus-MMF	Yes (C1)	PB	174.91	21.09
OSR 6	F	45	AML	High	Thio-Treo-Flu	PT-Cy-sirolimus-MMF	No	BM	31.55	1.66
OSR 7	M	34	NHL	Very high	Thio-Treo-Flu	PT-Cy-sirolimus-MMF	No	PB	81.9	13.09
OSR 8	F	76	MDS	High	Thio-Treo-Flu	PT-Cy-sirolimus-MMF	No	PB	326.4	17.2
OSR 9	M	63	AML	High	Thio-Treo-Flu	PT-Cy-sirolimus-MMF	Yes (Bw4)	PB	98.57	8.02
OSR 10	F	65	AML	High	Thio-Treo-Flu	PT-Cy-sirolimus-MMF	Yes (C2)	PB	98.86	16.58
JHU 1	M	27	AML	High	Flu-CTX-TBI 2 Gy	PT-Cy-tacrolimus-MMF	Yes (C2)	BM	85.5	8.2
JHU 2	M	67	CML	High	Flu-CTX-TBI 2 Gy	PT-Cy-tacrolimus-MMF	No	BM	157.6	5.3
JHU 3	M	56	NHL	Very high	Flu-CTX-TBI 2 Gy	PT-Cy-tacrolimus-MMF	No	BM	73.3	6.3
JHU 4	M	58	sAML	Very high	Flu-CTX-TBI 2 Gy	PT-Cy-tacrolimus-MMF	Yes (C1)	BM	199.2	26.2
JHU 5	M	69	AML	Very high	Flu-CTX-TBI 2 Gy	PT-Cy-tacrolimus-MMF	Yes (C2)	BM	42.5	2.95
JHU 6	M	33	ALL	High	Flu-CTX-TBI 2 Gy	PT-Cy-sirolimus-MMF	No	BM	41.9	5.50
JHU 7	M	65	AML	High	Flu-CTX-TBI 2 Gy	PT-Cy-tacrolimus-MMF	Yes (Bw4)	BM	72.0	6.83

ALL, acute lymphoid leukemia; AML, acute myeloid leukemia; Bw4, HLA-Bw4; C1, HLA-C group 1; C2, HLA-C group 2; CML, chronic myeloid leukemia; DRI, Disease Risk Index; F, female; HL, Hodgkin lymphoma; M, male; MDS, myelodysplastic syndrome; NHL, non-Hodgkin lymphoma; sAML, secondary acute myeloid leukemia.

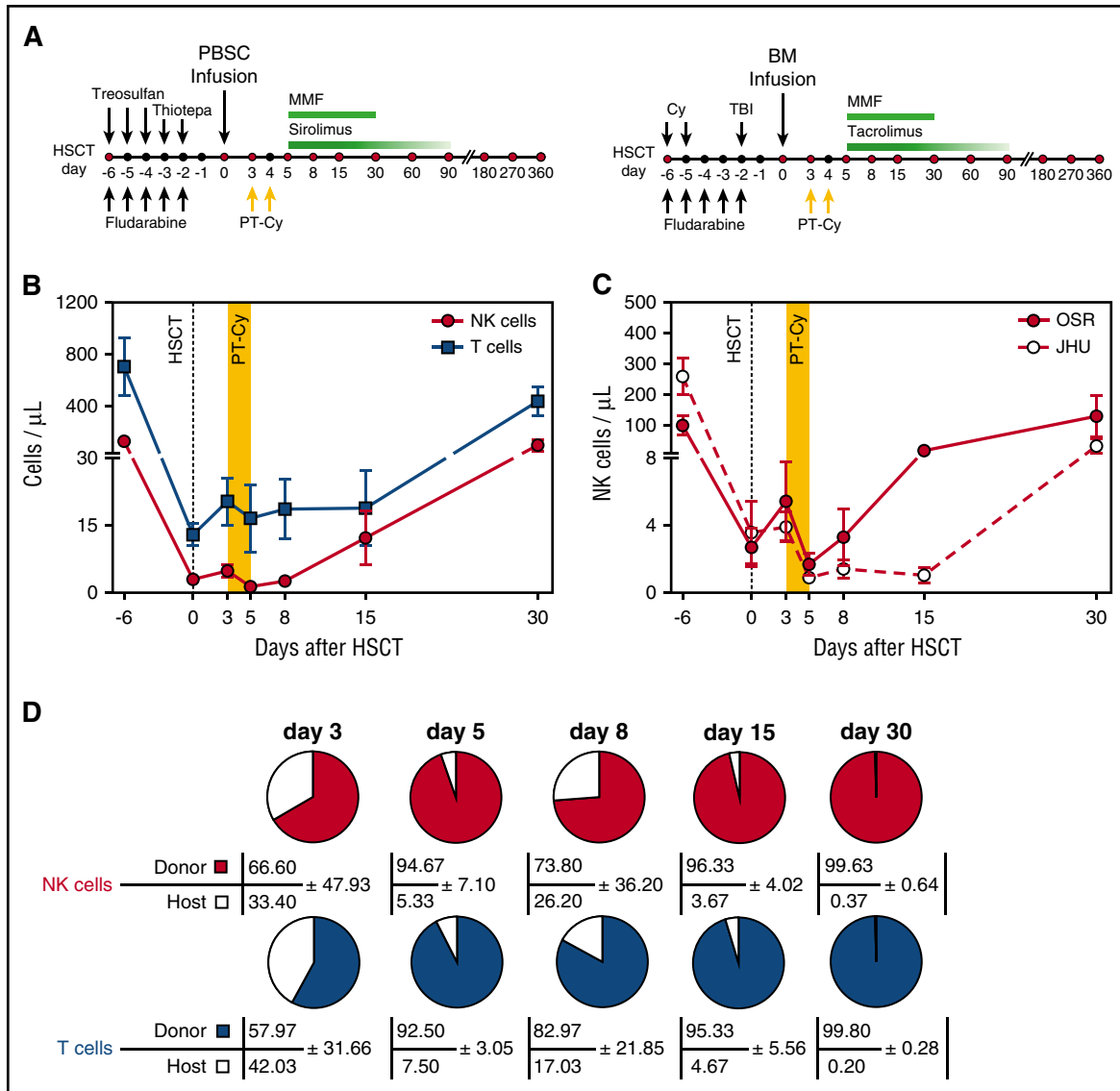
\*DFI calculated according to Armand et al.<sup>49</sup>

†Conditioning regimens: Flu-CTX-TBI 2 Gy, fludarabine (30 mg/m<sup>2</sup>/d on days -6 to -2), cyclophosphamide (14.5 mg/kg/d on days -6 and -5), and 200 cGy of TBI on day -1; Thio-Treo-Flu, thiotepa (5 mg/kg/d on days -3 and -2), treosulfan (14 g/m<sup>2</sup>/d on days -6 to -4), and fludarabine (30 mg/m<sup>2</sup>/d on days -6 to -2).

‡GVHD prophylaxis: PT-Cy-sirolimus-MMF, cyclophosphamide (50 mg/kg) on days +3 and +4, sirolimus (monitored to maintain a target therapeutic plasma level of 5-15 ng/mL) from day +5, mycophenolate mofetil (10 mg/kg 3 times daily) from day 5; PT-Cy-tacrolimus-MMF, cyclophosphamide (50 mg/kg) on days +3 and +4, tacrolimus (monitored to maintain a target therapeutic plasma level of 5-15 ng/mL) from day +5, and mycophenolate mofetil (15 mg/kg, twice daily) from day 5.

§Predicted NK alloreactivity: exclusively in the graft-versus-leukemia reaction, calculated according to the Perugia algorithm as the absence in the patient of killer cell immunoglobulin-like receptor ligands (either Bw4, C1, or C2) present in the donor.

||These patients received a reduced dose of thiotepa (3 mg/kg) and treosulfan (12 gram/m<sup>2</sup>) because of old age.



**Figure 1. NK cell counts and chimerism early after haploidentical HSCT and PT-Cy.** (A) Outline of the haploidentical HSCT platforms used at OSR (left) and at JHU (right). (B) Absolute counts of NK cells (red circles) and T cells (blue squares) circulating in the PB of patients ( $n = 17$ ) receiving haploidentical HSCT followed by PT-Cy (days of Cy administration are shaded in yellow). Data are displayed as mean values  $\pm$  standard error of the mean (SEM). (C) Absolute counts of PB NK cells in patients treated in the 2 transplantation centers (OSR, red circles:  $n = 10$ ; JHU, white circles:  $n = 7$ ). Data are displayed as mean values with SEM. (D) Chimerism within T- and NK-cell compartment after HSCT. HLA-A\*02 mismatches allowed to discriminate by multiparametric flow cytometry donor-derived cells (colored) and residual host lymphocytes (white). Pies depict NK cell (upper line) and T cell (bottom lines) chimerism measured at different time points after HSCT in 3 donor-recipient pairs. Numbers indicate mean values with standard deviation (SD). MMF, mycophenolate mofetil; PBSC, peripheral blood cell transplantation; TBI, total body irradiation.

haploidentical HSCT with a GVHD prophylaxis based on PT-Cy, and to investigate whether NK cell alloreactivity is preserved in this innovative and increasingly used transplant modality.

## Materials and methods

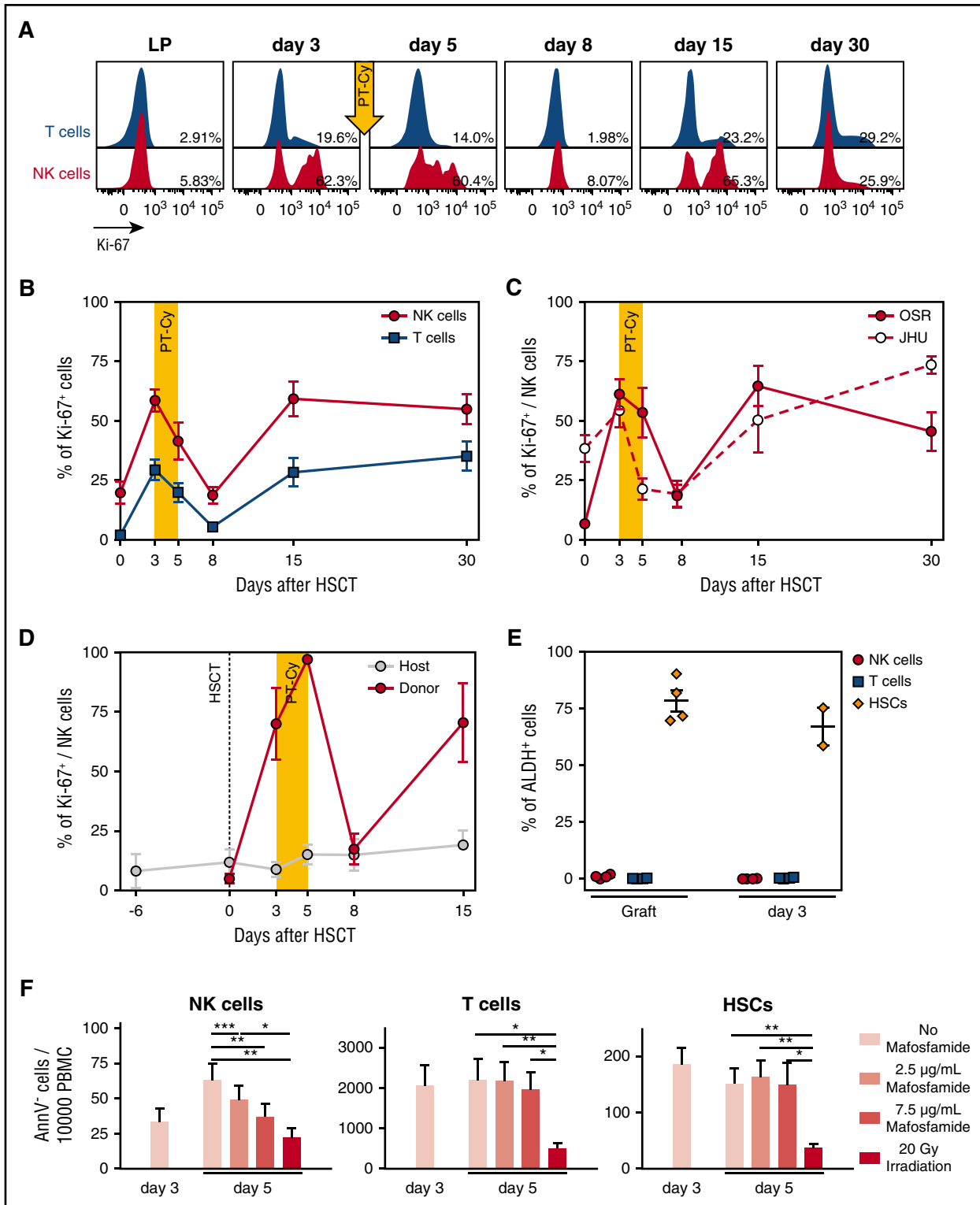
### Multiparametric flow cytometry

Absolute quantification of NK ( $\text{CD}3^- \text{CD}56^+$ ) and T ( $\text{CD}3^+$ ) cells was performed in fresh whole blood samples as previously described.<sup>11</sup>

For extended phenotypic analyses, mononuclear cells were isolated from peripheral blood (PB) or bone marrow (BM) by density gradient separation (Lymphoprep; Fresenius). Details on antibodies and panel assembly are provided in the supplemental

Methods on the *Blood* Web site. Acquisition was performed on an LSR Fortessa and an LSR II instrument (both from BD Biosciences). Analysis was performed using FlowJo (TreeStar) and visualized as heatmaps using the pheatmap function in R. Data were further analyzed using the Barnes-Hut stochastic neighbor embedding (bh-SNE) algorithm (using the CYT tool and the MatLab software as described previously<sup>12</sup>). The input dataset was resampled to obtain an equal number of NK cell events for all of the samples analyzed; the bidimensional maps obtained from this analysis were then processed with FlowJo software to highlight the spatial distribution of NK cells at each time point. Upon bh-SNE analysis,<sup>12</sup> the k-means algorithm was used for unsupervised clustering of data to identify and quantify in an unbiased manner memory-like NK cells in patient and healthy donor samples.





**Figure 2. Cyclophosphamide administration induces killing of proliferating NK cells.** (A) Flow cytometry histograms depicting Ki-67 expression measured on T (blue) and NK cells (red) from the leukapheresis (LP) graft and in the PB of a representative patient (OSR #1) at different time points after HSCT, as indicated. Percentages indicate frequencies of Ki-67–positive cells. (B) Ki-67 positivity in NK (red circles) and T (blue squares) cells from the graft (day 0), or circulating in the PB of patients after HSCT with PT-Cy (n = 17). (C) Ki-67 positivity in NK cells from the graft (day 0) or in the PB of patient transplanted at OSR (red circles; n = 10) or JHU (white circles; n = 7). (D) Level of proliferation of donor-derived NK cells (red circles) and residual host NK cells (gray circles) measured with Ki-67 intracellular staining in 3 representative patients. Donor- or host-derived NK cells were discriminated by immunophenotypic analysis using differential expression of the mismatched HLA-A\*02 allele. (E) Scatter plot depicting the mean percentage of ALDH+ cells detected by flow cytometry among NK (red circles), T (blue squares), and stem (orange diamonds) cells present within the infused graft, or in the patient PB 3 days after transplant, in 4 representative patients. Note that for 2 of 4 patients, CD34+ stem cells were no more detectable in the patient PB at day 3. (F) In vitro assay of mafosfamide-induced cell death. The LP product of 6 patients was stimulated with IL-15 at day 0 and treated with different doses of mafosfamide at day 3. The graphs report the number of viable (AnnexinV–) NK cells, T cells, and HSCs detected by flow cytometry before the treatment (day 3) and after administration of different doses of the drug (day 5; light pink bars: untreated; dark pink bars: 2.5 µg/mL; light red bars: 7.5 µg/mL) and after irradiation as positive control (day 5, red bars). Unless otherwise specified, shown in all panels are average values ± SEM.

### Mafofamide-sensitivity assay

An in vitro assay to test the effect of mafosfamide on NK cells was adapted from a published protocol.<sup>13</sup> Briefly, cryopreserved PB mononuclear cells obtained from a donor's graft were thawed, marked with Cell Trace Violet (CTV, Life Technologies), and cultured in Iscove modified Dulbecco medium (Lonza) supplemented with 10% human serum (Euroclone), 1% penicillin streptomycin, 1% glutamine (Lonza), and 5 µg/mL interleukin-15 (IL-15, Miltenyi). Mafosfamide L-lysine salt (Niomech) was diluted in distilled water and added to the culture after 3 days. After 1 hour of incubation, cells were centrifuged twice and then plated in fresh medium supplemented with IL-15. CTV dilution and quantification of live nonapoptotic cells (Annexin V<sup>-</sup>) were assessed by flow cytometry, before (day 3) and 2 days after (day 5) adding mafosfamide. The same experiment was performed in the absence of CTV labeling to analyze proliferation using Ki-67 intracellular staining.

### Cytotoxicity assay

Cryopreserved PB mononuclear cells obtained from HSC donors before granulocyte colony-stimulating factor mobilization, from patients at day 30 after HSCT, and from healthy subjects, were thawed and plated in Iscove modified Dulbecco medium supplemented with 10% human serum in the presence of 20 IU/mL of recombinant human IL-2 (Novartis). After overnight incubation, NK cells were isolated by negative selection with anti-CD3, anti-CD14, and anti-CD19 magnetic beads (Miltenyi), labeled with CTV and plated in a 50:1, 10:1, or 1:1 effector:target ratio in the presence of the following targets: K562 cell line, OCI/AML3 cell line, and primary AML blasts collected from a patient at diagnosis (90% purity). After a 6-hour incubation, apoptosis of CTV-negative target cells was analyzed by assessing Annexin V (Biolegend) expression by flow cytometry.

### Statistical analyses

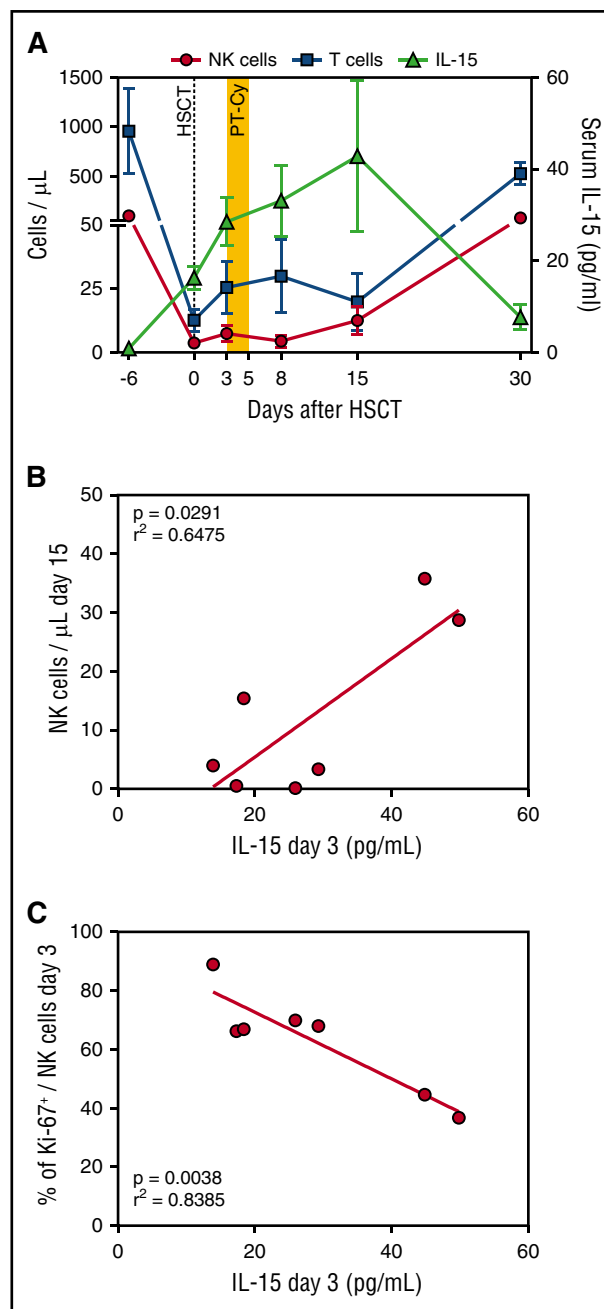
A detailed description of statistical analyses performed to compare experimental data and patient outcome is provided in the supplemental Methods.

## Results

### NK cell recovery displays similar metrics in different PT-Cy-based haploidentical HSCT protocols

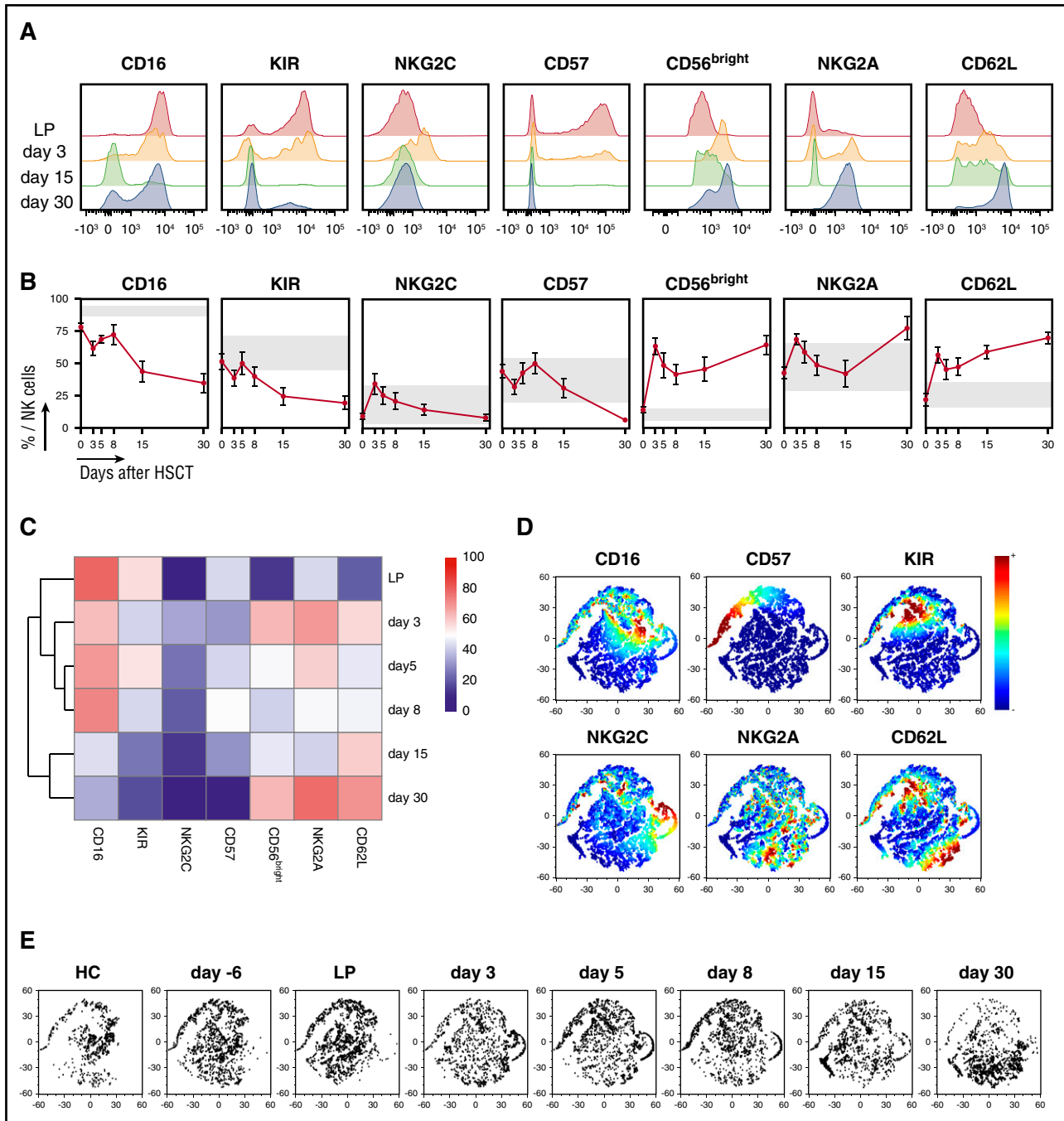
To assess NK cell dynamics after haploidentical T cell-replete HSCT with PT-Cy, we analyzed PB and BM samples collected longitudinally in time from 17 patients treated over the same period in 2 transplantation centers (Ospedale San Raffaele, Milano, Italy [OSR]; John Hopkins University, Baltimore, MD [JHU]). Patient and transplant characteristics are provided in the supplemental Methods and summarized in Table 1; HSCT platforms are outlined in Figure 1A.

After infusion of the graft, which for all patients included an elevated content of mature donor NK cells (median,  $9.18 \times 10^6$ /kg; range,  $1.66$ - $26.2 \times 10^6$ /kg), absolute T-cell and NK cell counts were measured in PB before (day 3) and after (days 5, 8, 15, and 30) cyclophosphamide administration (Figure 1A-B). As previously reported,<sup>14-16</sup> T and NK cells were detectable at very low levels even immediately after graft infusion. PT-Cy treatment resulted in a further decrease of cell counts, with residual NK



**Figure 3. IL-15 serum levels sharply increase after HSCT and cyclophosphamide administration and correlate with NK cell dynamics.** (A) IL-15 concentration (green triangles) measured in the sera of 7 patients before and after HSCT with PT-Cy is shown with the number of NK cells (red circles) and T cells (blue squares) in the PB of the same patients. Mean values with SEM are shown. (B) Correlation between IL-15 serum concentration at 3 days after HSCT (x-axis) and NK cell counts at day 15 after HSCT (y-axis). The red line denotes the best-fit line of the linear regression analysis. (C) Correlation between IL-15 serum concentration at 3 days after HSCT (x-axis) and the percentage of NK cells proliferating at the same time point, measured by Ki-67 intracellular staining (y-axis). The red line denotes the best-fit line of the linear regression analysis.

cells barely detectable at day 5. After that, T and NK cells progressively increased at days 15 and 30 after HSCT. Patients treated in the 2 transplant centers displayed similar in vivo dynamics, with a slight delay in recovery in JHU patients (Figure 1C). To assess the origin of the circulating NK cells, we analyzed lymphocyte chimerism in 3 donor-recipient pairs mismatched for

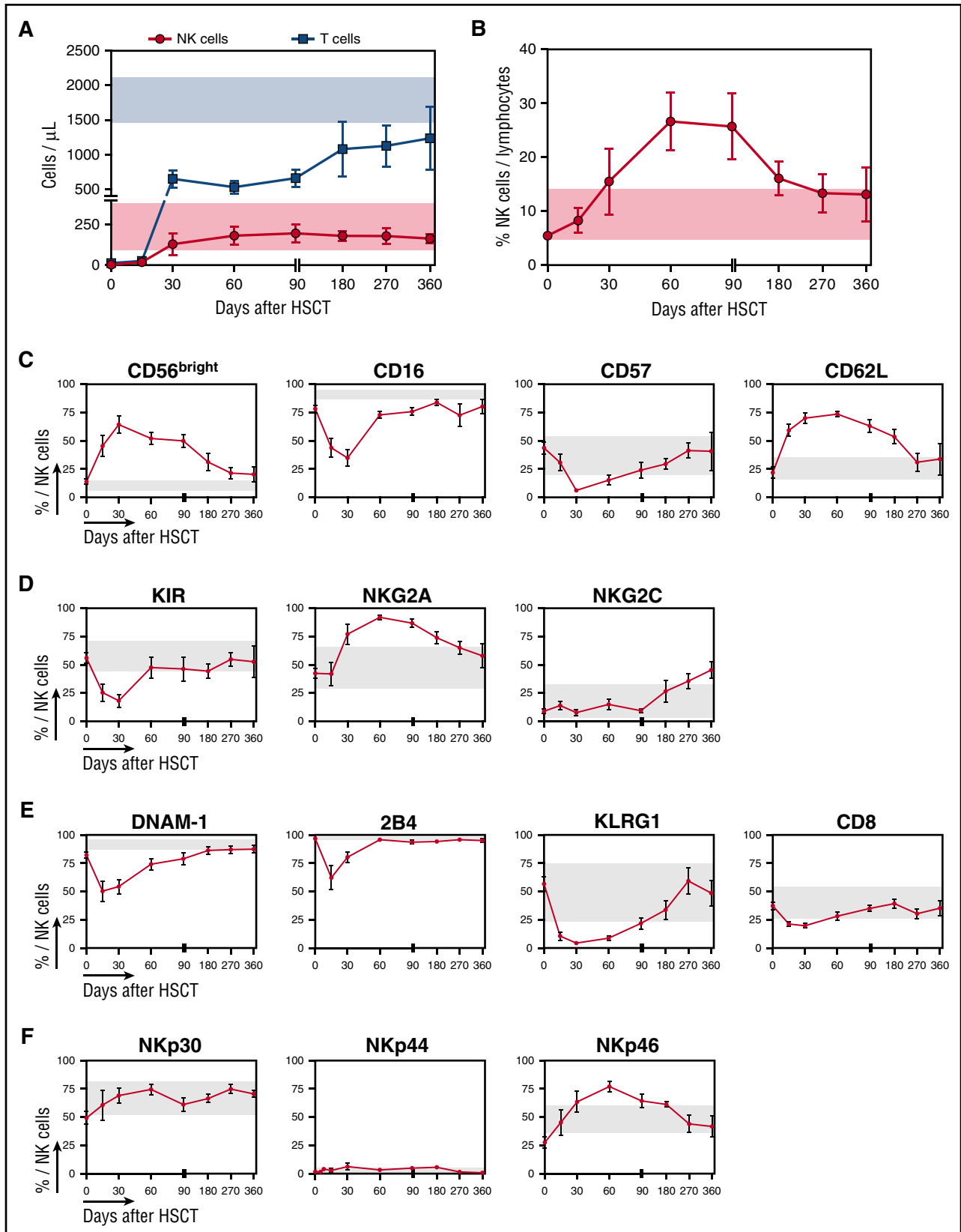


**Figure 4. The second wave of NK cells that appear after PT-Cy displays an immature phenotype.** (A) Flow cytometry histograms depicting expression of indicated maturation markers on CD56<sup>+</sup> CD3<sup>-</sup> NK cells from a representative patient (OSR #1) at the indicated time points (LP: red; day 3: orange; day 15: green; day 30: blue). (B) The expression of the described maturation markers measured by flow cytometry in NK cells from the graft (day 0) and from patients longitudinally sampled after HSCT with PT-Cy (n = 10). For each marker, a normal reference interval (mean ± SD) measured in NK cells from 5 healthy subjects is displayed (gray box). (C) Heat map of the average NK cell maturation marker expression at different time points, with unsupervised hierarchical clustering, for 10 OSR patients analyzed by multiparametric flow cytometry at the indicated time points. (D-E) Multidimensional single-cell analysis of the maturation status of NK cells harvested from 5 healthy controls (HC), from leukaphereses (LP, n = 10) and from 10 patients at different time points after HSCT. The panel D bidimensional maps were obtained from flow cytometric data using the bh-SNE algorithm show all analyzed NK cell events, with coloring denoting the expression of each maturation marker, as indicated. The same data are depicted in panel E, where NK cells from a selected time point are displayed separately.

HLA-A\*02. In both the T- and NK-cell compartments, donor-derived lymphocytes accounted for the majority of cells even at early time points (Figure 1D); host-derived lymphocytes became undetectable by day 30. A minor deflection of chimerism was observed at day 8, suggesting a preferential sensitivity of donor-derived cells to PT-Cy administration.

### PT-Cy eliminates proliferating donor-derived NK cells in vitro and in vivo

Cyclophosphamide is an alkylating agent known to be particularly active on dividing immune cells.<sup>7,17</sup> We thus used Ki-67 staining to investigate the effects of PT-Cy on NK cell proliferation. At day 3 after transplantation, NK cells robustly proliferated, even



**Figure 5. Despite early recovery of NK cell counts after PT-Cy-based HSCT, NK cell phenotype normalization occurs only several months after transplantation.** (A) Absolute counts of NK cells (red circles) and T cells (blue squares) detected in the PB of 10 patients followed long-term after HSCT with PT-Cy (from days 30 to 360). A reference physiological cell count interval (mean  $\pm$  SD) obtained from 5 healthy controls is shown for NK cells (light red box) and T cells (light blue box). (B) The proportion of NK cells out of total lymphocytes in the infused donor graft (day 0) and longitudinally after HSCT is displayed for 10 OSR patients. (C-F) Flow cytometry histograms depicting the expression of selected markers on CD56<sup>+</sup> CD3<sup>-</sup> NK cells in the donor graft (day 0) or from patient PB obtained longitudinally after transplant in

to a higher extent than T cells (Figure 2A-B). As previously described for T lymphocytes,<sup>14,15</sup> we found that NK cell proliferation was completely abrogated by day 8, suggesting selective elimination of cycling NK cells. Importantly, similar NK cell proliferation kinetics were observed in patients from the 2 centers (Figure 2C), suggesting that this dynamic is minimally influenced by differences in graft source, conditioning intensity, and subsequent pharmacological GVHD prophylaxis. Interestingly, in patients in which the donor or host origin of circulating NK cells could be assessed through the expression of mismatched HLA-A\*02, we found that the *in vivo* proliferation was largely restricted to donor-derived NK cells (Figure 2D).

These observations suggested that actively proliferating donor-derived NK cells were selectively eliminated upon cyclophosphamide administration. In line with this hypothesis, we failed to record any activity of ALDH, an enzyme known to confer intrinsic resistance to Cy,<sup>13,18,19</sup> in NK cells contained within the graft or in PB samples collected at day 3 after infusion (Figure 2E).

To directly demonstrate that proliferating NK cells are selectively eliminated by Cy, we mimicked *in vitro* the transplantation protocol by prompting the proliferation of NK cells with recombinant human IL-15 and challenging them after 3 days with mafosfamide, a Cy analog suitable for *in vitro* use. After 2 additional days, proliferating NK cells had been eliminated by mafosfamide in a dose-dependent manner, as demonstrated by a progressive decrease in the counts of viable cells (Figure 2F) and in the abrogation of proliferation (supplemental Figure 1A-C). Conversely, T cells and CD34<sup>+</sup> stem cells from the graft did not proliferate in these experimental conditions and were consequently not eliminated by *in vitro* administration of the drug. Overall, these data demonstrate that NK cells contained in the graft proliferate robustly upon infusion into patients, and that the proliferation state and lack of ALDH of these NK cells jointly cause them to be purged *in vivo* by PT-Cy.

### IL-15 serum levels peak after PT-Cy administration and correlate with the kinetics of NK cell recovery

IL-15 is a “4  $\alpha$ -helix bundle” cytokine primarily produced by monocytes, macrophages, and dendritic cells, and is known to play a pivotal role in lymphocyte homeostasis and especially in NK cell development, maturation, and proliferation.<sup>20</sup> In a lymphodepleted environment, such as the one established in patients after conditioning, elevated IL-15 levels can affect the fate and the function of the infused donor NK cells.<sup>21,22</sup> We thus measured the serum concentration of IL-15 longitudinally during the first months after haploidentical HSCT with PT-Cy (details provided in supplemental Methods).

Systemic levels of IL-15 rose immediately after conditioning (Figure 3A), possibly favoring the donor NK cell proliferation seen early after graft infusion (Figure 2B). Interestingly, the high levels of IL-15 documented at day 3 displayed a direct correlation with the number of NK cells reconstituting thereafter (Figure 3B) and an inverse correlation with the frequency of NK cells proliferating at the same time point (Figure 3C). A potential

explanation is that higher early proliferation of NK cells consumes IL-15, leading to lower measurable levels in these patients. Starting from day 15, a second wave of highly proliferating donor NK cells appeared in the PB of patients, followed by a drop in IL-15 levels at day 30, suggesting again consumption of the cytokine by reconstituting lymphocytes.

Although much remains to be discovered about the factors that regulate NK cell dynamics in the early posttransplantation phase, these findings highlight that the cytokine milieu early after haploidentical HSCT with PT-Cy include high levels of IL-15, and that these are significantly correlated with the metrics of NK cell recovery.

### Second wave of reconstituting NK cells appears 2 weeks after HSCT with PT-Cy and predominantly consists of cells with an immature phenotype

Our analysis of absolute counts (Figure 1B-C) and proliferation kinetics (Figure 2B-C) of NK cells after haploidentical HSCT and PT-Cy demonstrated that a sizeable population of highly proliferating NK cells becomes evident around day 15 after HSCT. To evaluate the ability of these cells to provide an effective protection against pathogens and disease recurrence, we assessed their phenotypical features and maturation status. The expression of maturation markers was assessed through multiparametric flow cytometry on NK cells contained within the donor leukapheresis (shown as day 0 in Figure 4B), and on patient PB NK cells immediately after HSCT (day 3) and after PT-Cy (days 5, 8, 15, and 30). The results for OSR patients are shown in Figure 4A-B; JHU patient results appear in supplemental Figure 2A-B.

As expected, NK cells in the donor graft exhibited high expression of markers associated with a mature phenotype (CD16, KIR, NKG2C, and CD57) and low expression of markers of immature NK cells (NKG2A and CD62L). Although the phenotype of NK cells circulating in the PB of patients immediately after HSCT (day 3, Figure 4A-B) resembled that of infused NK cells, the NK cell phenotype seen after PT-Cy administration was significantly different. By day 8, in fact, expression of maturation markers on NK cells became low or absent, whereas the percentage of CD56<sup>bright</sup> NK cells and the overall expression of NKG2A and CD62L increased. Unsupervised clustering of fluorescence-activated cell sorter data demonstrated clear differences between NK cells found in the graft and in patients immediately after transplant compared with patient NK cells at days 15 and 30, both in OSR and in JHU patients (Figure 4C; supplemental Figure 2A-C).

To validate these findings, the same flow cytometry data were analyzed using the bh-SNE algorithm for unbiased high-dimensional analysis.<sup>12</sup> NK cell events from all samples were plotted together on a bidimensional map based on the similarities of expression of maturation markers (Figure 4D). NK cells harvested from healthy subjects, grafts, patients pretransplant, and at the early time points after HSCT (from days 3 to 8) clustered in the upper portion of the multidimensional map (Figure 4E), characterized

**Figure 5 (continued)** 10 OSR patients. For all panels, gray boxes show reference values (mean  $\pm$  SD) obtained analyzing 5 healthy controls. (C) Expression of maturation markers. (D) Expression of KIRs and lectin-type receptors. (E) Expression of markers of exhaustion or activation. (F) Expression of natural cytotoxicity receptors. Unless otherwise specified, data are shown as mean  $\pm$  SEM.

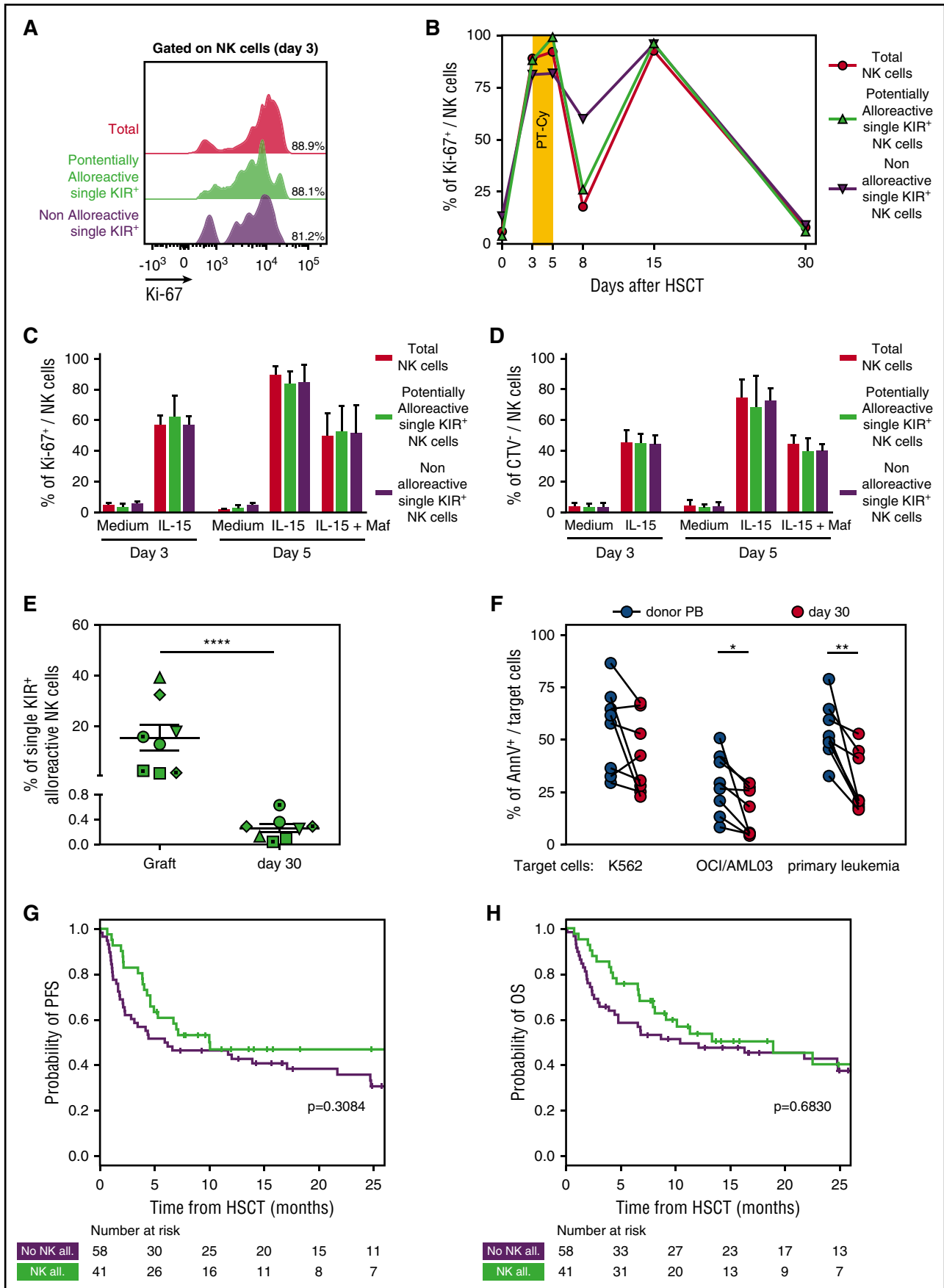


Figure 6.



by high positivity for CD16, CD57, and KIR molecules and by intermediate expression of NKG2C. Conversely, NK cells harvested from patients at days 15 and 30 after HSCT grouped in the opposite part of the map, denoting high expression of NKG2A and CD62L molecules (Figure 4D-E). Overall, these data suggest that after the rapid purging of mature proliferating lymphocytes operated by PT-Cy, the subsequent NK cell recovery occurs principally through maturation from graft progenitors rather than by homeostatic expansion of mature graft NK cells.

### After haploidentical HSCT with PT-Cy, the reconstitution of a mature NK cell compartment can take up to 1 year

To address whether, and if so at what time, a mature and functional NK cell repertoire is restored, we longitudinally traced the phenotype of circulating NK cells during the first year after transplant in OSR patients. Consistent with previous reports,<sup>23</sup> we documented stable physiological absolute counts of circulating NK cells from 1 month after HSCT onwards (Figure 5A). Because of the relatively low number of circulating T cells in PB during the first 3 months after transplant, NK cells were the most abundant lymphocyte subset during this time (Figure 5B). Many features linked to immaturity, such as increased proportions of the CD56<sup>bright</sup> subset and of CD62L<sup>+</sup> NK cells, decreased over time and regained normal levels after 9 to 12 months post-transplant (Figure 5C). An opposite trend, but with different kinetics, was observed for the expression levels of the maturation markers CD16 and CD57. The expression of KIRs returned to normal levels by day 60 (Figure 5D), but, as previously reported in other HSCT settings,<sup>24,25</sup> the levels of the inhibitory receptor NKG2A diminished only 6 months after HSCT, suggesting that the ability of circulating NK cells to use target recognition through HLA class I-KIR interactions is not fully recovered before this time point. Of notice, we documented higher than normal expression of the activating receptors NKG2C in reconstituting NK cells from our patients, and acquisition of this receptor was even faster in patients who developed cytomegalovirus (CMV) reactivations during their posttransplant follow-up, in line with previous reports<sup>26,27</sup> (data not shown).

As observed for maturation markers, the expression of DNAM-1, 2B4, KLRG-1, and CD8 also rapidly decreased early after transplant and normalized 2 to 6 months after HSCT (Figure 5E). Finally, in line with other HSCT settings,<sup>24</sup> we did not detect any significant deviations from normal reference values in natural cytotoxicity receptor (NKp30, NKp44, and NKp46) expression in PT-Cy-based haploidentical transplant recipients (Figure 5F). Of

note, throughout the entire follow-up period, the receptor repertoire appeared nearly identical between NK cells circulating in the PB and those harvested at the same time point from the BM (supplemental Figure 3). Overall, these data indicate that the phenotypic recovery of the NK cell repertoire is a long process, taking up to 1 year after haploidentical HSCT with PT-Cy, similarly to what has been reported in other HSCT settings.<sup>24,25</sup>

### PT-Cy dampens NK cell-mediated alloreactivity, and the graft-versus-leukemia effect correlates with residual mature NK cells

In the context of T cell-depleted haploidentical HSCT, numerous studies demonstrated that donor-recipient KIR ligand mismatches can unleash reconstituting donor NK cells against residual tumor cells.<sup>2-5</sup> NK cell-mediated alloreactivity is, according to this model, mediated by "single-KIR<sup>+</sup>" donor NK cells, expressing on their surface a sole inhibitory receptor that can bind ligands present in the donor and absent in the recipient.<sup>24,28,29</sup> We thus chose to explore this specific NK cell subset to address the effect of PT-Cy on NK cell-mediated alloreactivity.

Using multiparametric flow cytometry, we compared the dynamics of potentially alloreactive single-KIR<sup>+</sup> NK cells with their nonalloreactive counterparts and with total NK cells. We found similarly high levels of proliferation in all 3 groups of NK cells at day 3 after graft infusion (Figure 6A) and an analogous behavior in response to PT-Cy (Figure 6B). These *ex vivo* observations, limited by the low number of NK cells circulating early after HSCT, were supported by *in vitro* experiments, in which alloreactive and nonalloreactive NK cells from PBSC grafts proliferated in a comparable manner upon exposure to IL-15, and were equally susceptible to mafosfamide (Figure 6C-D).

Indeed, we documented that single-KIR<sup>+</sup> NK cells present in the graft became almost completely undetectable in the PB of patients at day 30 ( $0.26 \pm 0.19\%$  of total NK cells,  $P < .0001$ , Figure 6E).

To investigate the functional consequences of this marked reduction of single KIR<sup>+</sup> after PT-Cy, we compared the antileukemic potential of NK cells purified from 8 patients at day 30 after transplant. Compared with their counterparts from the corresponding donor PB, patient NK cells displayed impaired killing of the OCI/AML03 cell line and of primary AML blasts ( $P = .026$  and  $P = .004$ , respectively), whereas the ability to kill the HLA class I-negative K562 cell line was less affected (Figure 6F; supplemental Figure 4).

**Figure 6. PT-Cy eliminates single-KIR<sup>+</sup> NK cells and thus dampens NK cell-mediated alloreactivity.** (A) Flow cytometry histogram depicting proliferation measured by Ki-67 expression in total NK cells (red), in single KIR<sup>+</sup> NK cells predicted to be alloreactive (green), and in single-KIR<sup>+</sup> NK cells predicted to be nonalloreactive (purple) in a representative patient (OSR #10) immediately before PT-Cy administration (day 3 after HSCT). (B) Time course of Ki-67 positivity in total NK cells (red circles), single-KIR<sup>+</sup> NK cells predicted to be alloreactive (green triangles), or single-KIR<sup>+</sup> NK cells predicted not to be alloreactive (purple triangles) from the graft (day 0) or circulating in the PB from a representative patient (OSR #10) after HSCT. (C) Percentage of Ki-67 positivity in total NK cells from 3 PBSC grafts (red), in the subset of single-KIR<sup>+</sup> NK cells predicted to be alloreactive (green), or in the subset of single-KIR<sup>+</sup> NK cells predicted not to be alloreactive (purple) upon 3 days of exposure to IL-15, and after subsequent addition of mafosfamide to the culture medium. (D) Percentage of proliferating cells, measured through CTV dilution, among total NK cells from 3 PBSC grafts (red), among the subset of single-KIR<sup>+</sup> NK cells predicted to be alloreactive (green), and among the subset of single-KIR<sup>+</sup> NK cells predicted not to be alloreactive (purple) upon 3 days of exposure to IL-15 and after subsequent addition of mafosfamide to the culture medium. (E) Frequency of predictably alloreactive single-KIR<sup>+</sup> NK cells within the graft and in PB NK cells in patients 30 days after HSCT, measured in 8 donor-recipient pairs with KIR-ligand mismatches. (F) Target cell death, expressed as Annexin V positivity (AnnV<sup>+</sup>), measured on K562 cells, OCI/AML cells, or primary leukemic cells after incubation at a 10:1 effector:target ratio with NK cells purified from patient PB day 30 after HSCT with PT-Cy ( $n = 8$ , red dots) or from their respective donors PB ( $n = 8$ , black dots). (G-H) Progression-free survival (G) and overall survival (H) in patients who received PT-Cy-based haploidentical HSCT from donor with (green line,  $n = 41$ ) or without (purple line,  $n = 58$ ) predicted NK cell alloreactivity. Tick marks represent censoring for live patients. Unless otherwise specified, data are shown in all panels as mean values  $\pm$  SEM.

**Table 2. Characteristics of patients analyzed for the impact of NK alloreactivity on HSCT outcome**

Characteristics	Patients with predicted NK alloreactivity (n = 41)	Patients without predicted NK alloreactivity (n = 58)	P
Median follow-up, mo (range)	15.5 (5.2-38.6)	27.4 (3.5-44.3)	.13
Median age, y (range)	53 (21-77)	49.5 (21-76)	.54
<b>Patient sex, n</b>			.39
M	29	36	
F	12	22	
<b>Disease, n</b>			.66
AML	27	32	
ALL	2	6	
MPN	1	2	
MDS	1	5	
NHL	2	5	
HL	7	7	
MM	1	0	
Median Sorror HCT-CI (range)*	2 (0-6)	3 (0-8)	.14
<b>Refined DRI, n†</b>			.28
Low	3	4	
Intermediate	9	9	
High	13	19	
Very high	4	15	
Previous allogeneic HSCT	12	11	
<b>Conditioning regimen, n‡</b>			.36
Treo-Flu-Mel	25	34	
Thio-Treo-Flu	13	12	
Thio-Bu-Flu	0	3	
Treo-Flu	1	5	
Other	2	4	
<b>Source of stem cells, n</b>			.26
PB	41	55	
BM	0	3	
<b>Graft composition</b>			
CD34 <sup>+</sup> cells × 10 <sup>6</sup> /kg, median (range)	5.6 (4-10.3)	5.4 (1.6-6.7)	.69
CD3 <sup>+</sup> cells × 10 <sup>7</sup> /kg, median (range)	156 (5-400)	196 (4-729)	.02
<b>GVHD prophylaxis, n</b>			NA
PT-Cy, sirolimus, MMF	41 (100%)	58 (100%)	

HCT-CI, hematopoietic cell transplantation-comorbidity index; MM, multiple myeloma; MPN, myeloproliferative neoplasm; NA, not available.

\*HCT-CI calculated according to Sorror et al.<sup>50</sup>

†DRI calculated according to Armand et al.<sup>49</sup>

‡Conditioning regimens: Thio-Bu-Flu, thiotepa (5 mg/kg/d on days -7 and -6), busulfan (3.2 mg/kg/d on days -5 to -3), and fludarabine (50 mg/m<sup>2</sup>/d on days -5 to -3); Treo-Flu, treosulfan (14 g/m<sup>2</sup>/d on days -6 to -4) and fludarabine (30 mg/m<sup>2</sup>/d on days -6 to -2); Treo-Flu-Mel, treosulfan (14 g/m<sup>2</sup>/d on days -6 to -4), fludarabine (30 mg/m<sup>2</sup>/d on days -6 to -2), and melphalan (70 mg/m<sup>2</sup>/d on days -2 and -1).

Although these in vitro data suggest that NK cells reconstituting early after haploidentical HSCT with PT-Cy display an impaired antileukemic potential compared with their mature donor counterparts, this small but significant difference might still be overruled by other factors in vivo. To provide more insights into this relevant issue, we analyzed the clinical impact of predicted NK alloreactivity in a cohort of 99 consecutive patients who received haploidentical HSCT at OSR. All patients received a myeloablative chemotherapy-based conditioning and a GVHD prophylaxis based on PT-Cy. KIR ligand mismatches were

present in 41 of 99 patients (Table 2). In line with our expectations, and contrary to what has been consistently documented in T cell-depleted haploidentical transplants,<sup>2-4</sup> predicted NK cell alloreactivity did not significantly affect any of the major HSCT end points (including GVHD, relapse incidence, and survival) either in the entire cohort (Figure 6G-H; supplemental Figure 5) or in subgroup analysis (supplemental Table 2). These data suggest that by eliminating the majority of mature alloreactive NK cells transferred as part of the graft, PT-Cy dampens the impact of KIR ligand mismatches on HSCT outcome.



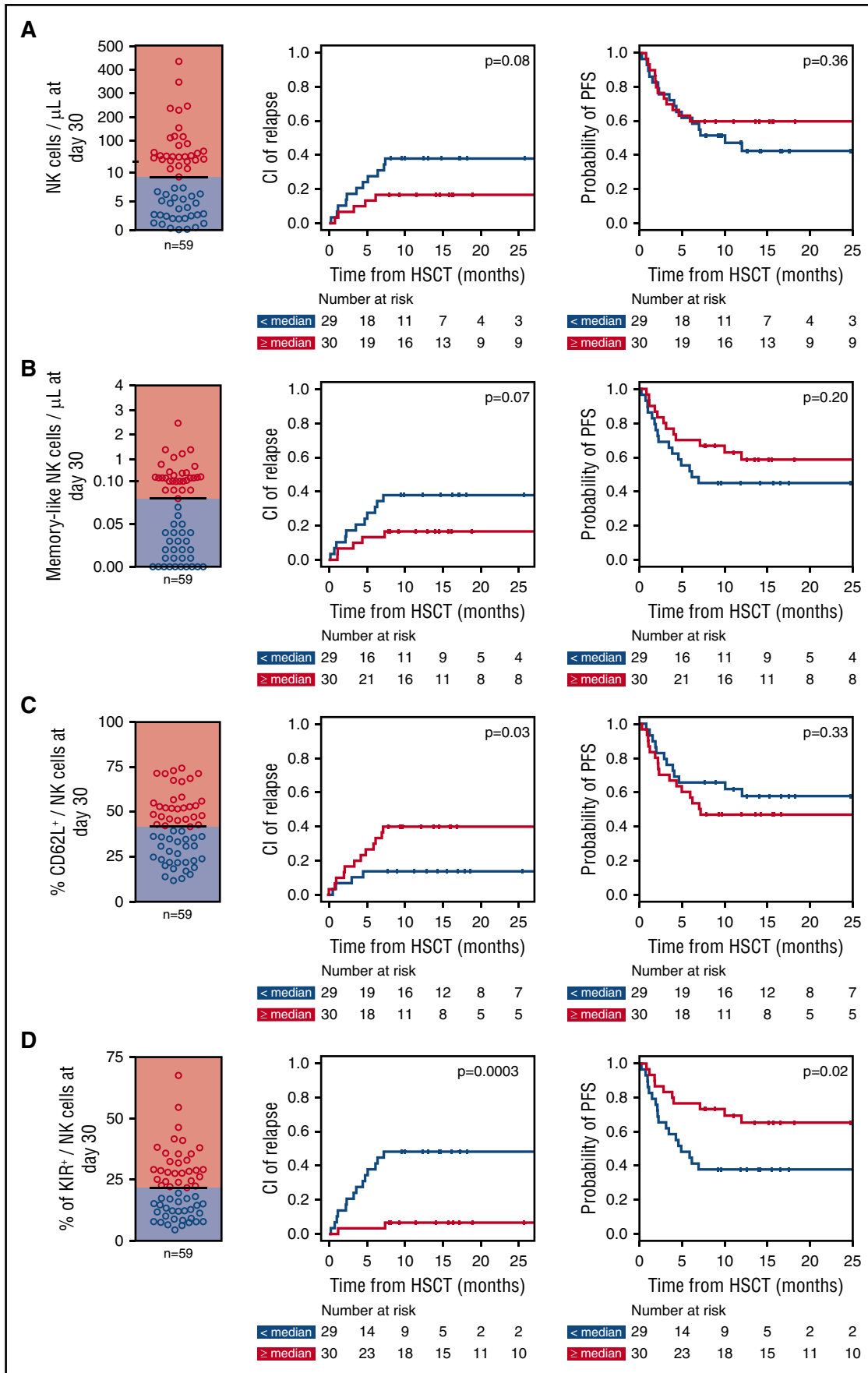


Figure 7.

Finally, to verify whether the proportion of mature NK cells spared by PT-Cy might have a clinically relevant role in determining HSCT outcome, we analyzed the maturation phenotype of NK cells circulating at day 30 after HSCT in 59 OSR patients who underwent haploidentical HSCT with PT-Cy and linked it to disease-related clinical end points. Beside the analysis of single maturation markers, we also enumerated CD57<sup>+</sup>CD16<sup>+</sup>KIR<sup>+</sup>NKG2C<sup>+</sup> mature memory-like NK cells, based on unsupervised data clustering of bh-SNE data using the k-means algorithm (supplemental Figure 6). In univariate analysis, low expression of CD62L and high expression of KIRs on NK cells at day 30 after HSCT were significantly correlated with lower relapse incidence ( $P = .03$  and  $P = .0003$ , respectively), and high absolute counts of total and memory-like NK cells displayed a trend toward significance for the same end point ( $P = .08$  and  $P = .07$ ), in line with previous reports.<sup>30</sup> Moreover, high expression of KIRs on NK cells at day 30 displayed a significant correlation with higher progression-free survival ( $P = .02$ , Figure 7A-D; supplemental Table 3). Despite the relatively small size of our patient series, the significant correlation between KIR expression on NK cells at day 30 and lower relapse incidence held true in multivariate analysis ( $P = .012$ ; supplemental Table 4), suggesting that KIR expression might represent a clinically relevant proxy for the functional competence of reconstituting NK cells in preventing recurrence.

## Discussion

By counterposing the immune systems of 2 individuals with disparate HLA and KIR assets, haploidentical HSCT represents a unique model to investigate the biological determinants of NK cell tolerance and alloreactivity and has provided convincing *in vivo* evidence of the immunotherapeutic potential endowed in this cell subset.<sup>2,5,22,31</sup> However, with the ongoing development of strategies to render HLA-mismatched transplant more feasible, it is becoming increasingly evident that the complex dynamics of NK cell recovery are dramatically affected by changes in the conditioning regimen and GVHD prophylaxis: for this reason, immunogenetic models to predict NK cell-mediated effects have to be validated in each HSCT platform.

In the present study, we integrated immunogenetic, functional, and clinical data to analyze the metrics and correlates of NK cell repertoire reconstitution in patients who received haploidentical HSCT according to 2 different PT-Cy platforms. We undertook this to address whether the models formulated in T cell-depleted haploidentical HSCT also hold true in this more recent and increasingly common transplantation modality.

We showed that the high numbers of mature NK cells infused as part of the graft in this HSCT setting immediately encounter high levels of homeostatic cytokines released as a consequence of the conditioning regimen-mediated lymphodepletion. As a result, we observed that infused NK cells are prompted to

proliferate to an even higher extent than their T cell counterparts, and showed *in vitro* and *in vivo* that such proliferation confers NK cell sensitivity to Cy-mediated killing.

After the purging of the majority of mature donor NK cells from the graft by PT-Cy, we observed the appearance of a second wave of donor-derived NK cells. These cells, however, displayed phenotypic and functional features of immaturity for several months after HSCT, strongly suggesting that they might stem directly from HSCs contained in the graft rather than from the mature NK cells infused alongside them.

Although it is extremely difficult to track their complex dynamics during the early posttransplant phase because of their very low numbers, single-KIR<sup>+</sup> NK cells, considered to include potentially alloreactive NK cells, appeared to behave similarly to all other mature NK cells and were thus almost completely eliminated by PT-Cy. As a consequence, the most widely accepted algorithm used to predict beneficial NK alloreactivity in T cell-depleted transplants<sup>3</sup> failed to predict clinical outcome in our patient series. Conversely, and consistently with the role we described for PT-Cy in this setting, the absolute counts and relative proportion of mature NK cells at day 30 after HSCT appeared to be a more reliable predictor of an effective NK cell-mediated immunosurveillance against relapse in this HSCT platform.

Our results have several other practical implications: whereas, for instance, it is becoming widely accepted that transplantation from HLA-mismatched relatives represents a viable alternative for patients who lack a conventional matched donor,<sup>9,10</sup> the question of which donor to select among several possible family members is still debated.<sup>32,33</sup> Here we found that the “classical” KIR ligand mismatch model of NK cell alloreactivity did not correlate with any of the major HSCT end points in PT-Cy-based haploidentical HSCTs, indicating that, in this context, priority should be given to other donor selection criteria, including CMV serostatus, gender mismatch, and presence of donor-specific anti-HLA antibodies in the recipient. It should be considered, however, that different NK cell alloreactivity models, also taking into account the donor-recipient KIR genotype, might be needed to predict NK-mediated effects in this context, as widely accepted for HLA-matched donor HSCT,<sup>34,35</sup> and already proposed by other studies for the haploidentical context.<sup>36,37</sup>

A second observation relates to the finding of a relatively long time window in which most of the circulating NK cells display phenotypic features of immaturity. Previous reports have highlighted that, despite the relatively rapid recovery of CD8 T-cell counts, PT-Cy transplantation is often accompanied by frequent viral reactivations, including those from CMV, polyomaviruses, and human herpes virus 6.<sup>38</sup> We can speculate that at least part of this susceptibility might be due to the ineffective protection conferred by the immature donor-derived NK cells, and future studies should verify whether the dynamics of recovery of memory

**Figure 7. Mature KIR<sup>+</sup> NK cells that are spared by PT-Cy can protect against posttransplantation disease relapse.** (A) Absolute counts of circulating NK cells, (B) absolute counts of CD57<sup>+</sup>CD16<sup>+</sup>KIR<sup>+</sup>NKG2C<sup>+</sup> memory-like NK cells, (C) percentage of CD62L<sup>+</sup> NK cells, and (D) percentage of KIR<sup>+</sup> NK cells were determined in samples collected at day 30 after HSCT from 59 patients who received haploidentical HSCT followed by PT-Cy at OSR. For each of these parameters, dot plots to the left of the figure display the distribution in the patient cohort, discriminating between patients with values above (red dots and background) or below (blue dots and background) the median. Curves display the cumulative incidence of disease relapse (center panels) and PFS (right panels) in each subgroup. *P* values reported in each panel corner are relative to univariate comparisons performed using Gray's test (for cumulative incidence of relapse) or log-rank test (for PFS).

NK cells could predict antiviral immune competence more effectively than currently used biomarkers.

Besides pointing out these limitations in NK cell defense intrinsic to PT-Cy-based haploidentical HSCTs, our study provides a framework to integrate new strategies to better exploit the immunotherapeutic potential of NK cells for this transplant platform.

For instance, the marked increase in IL-15 levels in the time window that immediately follows PT-Cy administration, reaching levels not commonly detected in physiological conditions, suggests that there is a temporal window here with a very favorable cytokine milieu for the *in vivo* expansion of alloreactive NK cells and provides the rationale for adoptive infusion of mature donor NK cells in this time frame. Of notice, several investigational trials of PT-Cy-based haploidentical HSCT followed by infusion of donor NK cells have recently been initiated and already reported promising results.<sup>39-41</sup>

In addition, several new agents developed to improve NK cell-mediated antileukemic responses might be integrated into PT-Cy-based haploidentical HSCTs. For instance, the recently developed anti-CD16/anti-CD33/IL-15 TriKe constructs<sup>42</sup> might be of benefit during the intermediate phase of recovery, when CD16 expression has been recovered but the KIR/NKG2A system has not yet reached its final equilibrium and IL-15 serum concentration has dropped to levels that might be insufficient to sustain the *in vivo* expansion and persistence of adoptively transferred NK cells.

An additional ground for improvement relates to the pharmacological GVHD prophylaxis used after PT-Cy administration. In accordance with the majority of current protocols for T cell-replete haploidentical HSCT, both regimens used in our study included mycophenolate mofetil during the first month after transplant: a number of studies have shown that this drug can negatively affect NK cell function<sup>43,44</sup>; thus, together with the *in vivo* purging of mature alloreactive NK cells, it might further reduce the antileukemic potential of early reconstituting NK cells. Importantly, the observed effects may also relate to other pharmacological agents and GVHD prophylaxis, an issue to be addressed in more detail in future studies.

In conclusion, our study strongly supports the notion that the complex and not yet fully elucidated dynamics of NK cell recovery after haploidentical HSCT are heavily affected by competition with other immune subsets and by the drugs used in the transplantation protocol. Whereas models of predicted NK cell alloreactivity developed in the original T cell-depleted setting held true in transplants performed with selective depletion of T-cell receptor  $\alpha\beta$  positive T cells from the graft,<sup>45</sup> or with confusion of donor-derived regulatory and conventional T cells,<sup>46,47</sup> the same algorithms were

unable to predict outcome in the context of GIAC protocols<sup>48</sup> or, as shown in this report, in PT-Cy-based transplants.<sup>36,37</sup> In the dawning era of “personalized” haploidentical transplants, it is necessary to adapt tools to predict outcome to an informed analysis of the dynamics of immune recovery in each HSCT setting and to leverage this knowledge to develop appropriate adjunctive strategies to improve HSCT outcome.

## Acknowledgments

Work at Ospedale San Raffaele was supported by grants from the Italian Ministry of Health (RF-2011-02351998, RF-2011-02348034, and TRANSCAN HLALOSS), the Associazione Italiana per la Ricerca sul Cancro (Start-Up Grant #14162), the ASCO Conquer Cancer Foundation (2014 Young Investigator Award), and the DKMS Mechthild Harf Foundation. G.O. was supported by a Fondazione Matarelli fellowship from the Associazione Italiana Leucemie and by a Fondazione Umberto Veronesi fellowship. Work at Johns Hopkins University was supported by the National Institutes of Health National Heart, Lung, and Blood Institute (grant R01HL110907) (L.L.) and by Wenner-Gren Foundation fellowship (S.B.).

## Authorship

Contribution: A.R., G.O., F.C., L.L., and L.V. designed the study. A.R., G.O., S.B., V.G., N.C., C.T., and L.Z. performed experiments. R.G., S.P., M.M., F.G., A.A., M.T.L.S., J.P., L.L., and F.C. collected and analyzed patient clinical data. A.R., F.L. and S.P. performed statistical analyses, C.B. provided scientific counseling, A.R., G.O., F.C., L.L., and L.V. wrote the paper. All authors read and approved the final version of the manuscript.

Conflict-of-interest disclosure: The authors declare no competing financial interests.

The current affiliation for N.C. is the University of Milan, Milan, Italy.

Correspondence: Fabio Ciceri, Hematology and Bone Marrow Transplantation Unit, San Raffaele Scientific Institute, via Olgettina 60, Milano, Italy; e-mail: ciceri.fabio@hsr.it.

## Footnotes

Submitted 8 May 2017; accepted 30 September 2017. Prepublished online as *Blood* First Edition paper, 6 October 2017; DOI 10.1182/blood-2017-05-780668.

\*A.R. and G.O. contributed equally to this study.

†L.L. and L.V. contributed equally to this study.

The online version of this article contains a data supplement

There is a *Blood* Commentary on this article in this issue.

The publication costs of this article were defrayed in part by page charge payment. Therefore, and solely to indicate this fact, this article is hereby marked “advertisement” in accordance with 18 USC section 1734.

## REFERENCES

1. Kanakry CG, Fuchs EJ, Luznik L. Modern approaches to HLA-haploidentical blood or marrow transplantation. *Nat Rev Clin Oncol*. 2016;13(1):10-24.
2. Mancusi A, Ruggeri L, Velardi A. Haploidentical hematopoietic transplantation for the cure of leukemia: from its biology to clinical translation. *Blood*. 2016;128(23):2616-2623.
3. Ruggeri L, Capanni M, Urbani E, et al. Effectiveness of donor natural killer cell alloreactivity in mismatched hematopoietic transplants. *Science*. 2002;295(5562):2097-2100.
4. Ruggeri L, Mancusi A, Capanni M, et al. Donor natural killer cell allorecognition of missing self in haploidentical hematopoietic transplantation for acute myeloid leukemia: challenging its predictive value. *Blood*. 2007;110(1):433-440.
5. Locatelli F, Pende D, Mingari MC, et al. Cellular and molecular basis of haploidentical hematopoietic stem cell transplantation in the successful treatment of high-risk leukemias: role of alloreactive NK cells. *Front Immunol*. 2013;4:15.
6. Luznik L, O'Donnell PV, Symons HJ, et al. HLA-haploidentical bone marrow transplantation for hematologic malignancies using non-myeloablative conditioning and high-dose, posttransplantation cyclophosphamide. *Biol*

- Blood Marrow Transplant.* 2008;14(6):641-650.
7. Luznik L, O'Donnell PV, Fuchs EJ. Post-transplantation cyclophosphamide for tolerance induction in HLA-haploidentical bone marrow transplantation. *Semin Oncol.* 2012;39(6):683-693.
  8. Robinson TM, O'Donnell PV, Fuchs EJ, Luznik L. Haploidentical bone marrow and stem cell transplantation: experience with post-transplantation cyclophosphamide. *Hematol.* 2016;53(2):90-97.
  9. Passweg JR, Baldomero H, Bader P, et al. Use of haploidentical stem cell transplantation continues to increase: the 2015 European Society for Blood and Marrow Transplant activity survey report. *Bone Marrow Transplant.* 2017;52(6):811-817.
  10. Apperley J, Niederwieser D, Huang X-J, et al. Haploidentical hematopoietic stem cell transplantation: a global overview comparing Asia, the European Union, and the United States. *Biol Blood Marrow Transplant.* 2016;22(1):23-26.
  11. Oliveira G, Ruggiero E, Stanghellini MTL, et al. Tracking genetically engineered lymphocytes long-term reveals the dynamics of T cell immunological memory [published correction appears in *Sci Transl Med.* 2015;7(319):319e9]. *Sci Transl Med.* 2015;7(317):317ra198.
  12. Amir AD, Davis KL, Tadmor MD, et al. viSNE enables visualization of high dimensional single-cell data and reveals phenotypic heterogeneity of leukemia. *Nat Biotechnol.* 2013;31(6):545-552.
  13. Kanakry CG, Ganguly S, Zahurak M, et al. Aldehyde dehydrogenase expression drives human regulatory T cell resistance to post-transplantation cyclophosphamide. *Sci Transl Med.* 2013;5(211):211ra157.
  14. Cieri N, Oliveira G, Greco R, et al. Generation of human memory stem T cells after haploidentical T-replete hematopoietic stem cell transplantation. *Blood.* 2015;125(18):2865-2874.
  15. Roberto A, Castagna L, Zanon V, et al. Role of naive-derived T memory stem cells in T-cell reconstitution following allogeneic transplantation. *Blood.* 2015;125(18):2855-2864.
  16. Kanakry CG, Coffey DG, Towler AMH, et al. Origin and evolution of the T cell repertoire after posttransplantation cyclophosphamide. *JCI Insight.* 2016;1(5):e86252.
  17. Winkelstein A. Mechanisms of immunosuppression: effects of cyclophosphamide on cellular immunity. *Blood.* 1973;41(2):273-284.
  18. Kastan MB, Schläffer E, Russo JE, Colvin OM, Civin CI, Hilton J. Direct demonstration of elevated aldehyde dehydrogenase in human hematopoietic progenitor cells. *Blood.* 1990;75(10):1947-1950.
  19. Jones RJ, Barber JP, Vala MS, et al. Assessment of aldehyde dehydrogenase in viable cells. *Blood.* 1995;85(10):2742-2746.
  20. Mishra A, Sullivan L, Caligiuri MA. Molecular pathways: interleukin-15 signaling in health and in cancer. *Clin Cancer Res.* 2014;20(8):2044-2050.
  21. Dudley ME, Yang JC, Sherry R, et al. Adoptive cell therapy for patients with metastatic melanoma: evaluation of intensive myeloablative chemoradiation preparative regimens. *J Clin Oncol.* 2008;26(32):5233-5239.
  22. Miller JS, Soignier Y, Panoskaltis-Mortari A, et al. Successful adoptive transfer and in vivo expansion of human haploidentical NK cells in patients with cancer. *Blood.* 2005;105(8):3051-3057.
  23. Cieri N, Greco R, Crucitti L, et al. Post-transplantation cyclophosphamide and sirolimus after haploidentical hematopoietic stem cell transplantation using a treosulfan-based myeloablative conditioning and peripheral blood stem cells. *Biol Blood Marrow Transplant.* 2015;21(8):1506-1514.
  24. Vago L, Forno B, Sormani MP, et al. Temporal, quantitative, and functional characteristics of single-KIR-positive alloreactive natural killer cell recovery account for impaired graft-versus-leukemia activity after haploidentical hematopoietic stem cell transplantation. *Blood.* 2008;112(8):3488-3499.
  25. Shilling HG, McQueen KL, Cheng NW, Shizuru JA, Negrin RS, Parham P. Reconstitution of NK cell receptor repertoire following HLA-matched hematopoietic cell transplantation. *Blood.* 2003;101(9):3730-3740.
  26. Della Chiesa M, Muccio L, Moretta A. CMV induces rapid NK cell maturation in HSCT recipients. *Immunol Lett.* 2013;155(1-2):11-13.
  27. Foley B, Cooley S, Verneris MR, et al. Cytomegalovirus reactivation after allogeneic transplantation promotes a lasting increase in educated NKG2C+ natural killer cells with potent function. *Blood.* 2012;119(11):2665-2674.
  28. Anfossi N, André P, Guia S, et al. Human NK cell education by inhibitory receptors for MHC class I. *Immunity.* 2006;25(2):331-342.
  29. Pende D, Marcenaro S, Falco M, et al. Anti-leukemia activity of alloreactive NK cells in KIR ligand-mismatched haploidentical HSCT for pediatric patients: evaluation of the functional role of activating KIR and redefinition of inhibitory KIR specificity. *Blood.* 2009;113(13):3119-3129.
  30. Cichocki F, Cooley S, Davis Z, et al. CD56dimCD57+NKG2C+ NK cell expansion is associated with reduced leukemia relapse after reduced intensity HCT. *Leukemia.* 2016;30(2):456-463.
  31. Rubnitz JE, Inaba H, Ribeiro RC, et al. NKAML: a pilot study to determine the safety and feasibility of haploidentical natural killer cell transplantation in childhood acute myeloid leukemia. *J Clin Oncol.* 2010;28(6):955-959.
  32. McCurdy SR, Fuchs EJ. Selecting the best haploidentical donor. *Semin Hematol.* 2016;53(4):246-251.
  33. Chang Y-J, Luznik L, Fuchs EJ, Huang X-J. How do we choose the best donor for T-cell-replete, HLA-haploidentical transplantation? *J Hematol Oncol.* 2016;9(1):35.
  34. Venstrom JM, Pittari G, Gooley TA, et al. HLA-C-dependent prevention of leukemia relapse by donor activating KIR2DS1. *N Engl J Med.* 2012;367(9):805-816.
  35. Cooley S, Weisdorf DJ, Guethlein LA, et al. Donor selection for natural killer cell receptor genes leads to superior survival after unrelated transplantation for acute myelogenous leukemia. *Blood.* 2010;116(14):2411-2419.
  36. Symons HJ, Leffell MS, Rossiter ND, Zahurak M, Jones RJ, Fuchs EJ. Improved survival with inhibitory killer immunoglobulin receptor (KIR) gene mismatches and KIR haplotype B donors after nonmyeloablative, HLA-haploidentical bone marrow transplantation. *Biol Blood Marrow Transplant.* 2010;16(4):533-542.
  37. Bastos-Oreiro M, Anguita J, Martínez-Laperche C, et al. Inhibitory killer cell immunoglobulin-like receptor (IKIR) mismatches improve survival after T-cell-repleted haploidentical transplantation. *Eur J Haematol.* 2016;96(5):483-491.
  38. Crocchiolo R, Bramanti S, Vai A, et al. Infections after T-replete haploidentical transplantation and high-dose cyclophosphamide as graft-versus-host disease prophylaxis. *Transpl Infect Dis.* 2015;17(2):242-249.
  39. Jaiswal SR, Zaman S, Nedunchezian M, et al. CD56-enriched donor cell infusion after post-transplantation cyclophosphamide for haploidentical transplantation of advanced myeloid malignancies is associated with prompt reconstitution of mature natural killer cells and regulatory T cells with reduced incidence of acute graft versus host disease: A pilot study. *Cytotherapy.* 2017;19(4):531-542.
  40. Thakar M, Hari P, Maloney DG, et al. Prophylactic natural killer cell immunotherapy following HLA-haploidentical hematopoietic cell transplantation prevents relapse and improves survival in patients with high-risk hematological malignancies [abstract]. *Blood.* 2016;128:1161.
  41. Ciurea SO, Schafer JR, Bassett R, et al. Phase 1 clinical trial using mBIL21 ex-vivo expanded donor-derived NK cells after haploidentical transplantation. *Blood.* 2017;blood-2017-05-785659.
  42. Vallera DA, Felices M, McElmurry R, et al. IL15 trispecific killer engagers (TriKE) make natural killer cells specific to CD33+ targets while also inducing persistence, in vivo expansion, and enhanced function. *Clin Cancer Res.* 2016;22(14):3440-3450.
  43. Dermame S, Perazzo J, Lee F, et al. Differential effects of mycophenolate mofetil and cyclosporine A on peripheral blood and cord blood natural killer cells activated with interleukin-2. *Cytotherapy.* 2014;16(10):1409-1418.
  44. Ohata K, Espinoza JL, Lu X, Kondo Y, Nakao S. Mycophenolic acid inhibits natural killer cell proliferation and cytotoxic function: a possible disadvantage of including mycophenolate mofetil in the graft-versus-host disease prophylaxis regimen. *Biol Blood Marrow Transplant.* 2011;17(2):205-213.
  45. Locatelli F, Bauquet A, Palumbo G, Moretta F, Bertina A. Negative depletion of  $\alpha\beta$  + T cells and of CD19+ B lymphocytes: a novel frontier to optimize the effect of innate immunity in HLA-mismatched hematopoietic stem cell transplantation. *Immunol Lett.* 2013;155(1-2):21-23.

46. Di Ianni M, Falzetti F, Carotti A, et al. Tregs prevent GVHD and promote immune reconstitution in HLA-haploidentical transplantation. *Blood*. 2011;117(14):3921-3928.
47. Martelli MF, Di Ianni M, Ruggeri L, et al. HLA-haploidentical transplantation with regulatory and conventional T-cell adoptive immunotherapy prevents acute leukemia relapse. *Blood*. 2014;124(4):638-644.
48. Huang X-J, Zhao X-Y, Liu D-H, Liu K-Y, Xu L-P. Deleterious effects of KIR ligand incompatibility on clinical outcomes in haploidentical hematopoietic stem cell transplantation without in vitro T-cell depletion. *Leukemia*. 2007;21(4):848-851.
49. Armand P, Kim HT, Logan BR, et al. Validation and refinement of the Disease Risk Index for allogeneic stem cell transplantation. *Blood*. 2014;123(23):3664-3671.
50. Sorror ML, Sandmaier BM, Storer BE, et al. Comorbidity and disease status based risk stratification of outcomes among patients with acute myeloid leukemia or myelodysplasia receiving allogeneic hematopoietic cell transplantation. *J Clin Oncol*. 2007;25(27):4246-4254.



**blood**<sup>®</sup>

2018 131: 247-262  
doi:10.1182/blood-2017-05-780668 originally published  
online October 6, 2017

## **NK cell recovery after haploidentical HSCT with posttransplant cyclophosphamide: dynamics and clinical implications**

Antonio Russo, Giacomo Oliveira, Sofia Berglund, Raffaella Greco, Valentina Gambacorta, Nicoletta Cieri, Cristina Toffalori, Laura Zito, Francesca Lorentino, Simona Piemontese, Mara Morelli, Fabio Giglio, Andrea Assanelli, Maria Teresa Lupo Stanghellini, Chiara Bonini, Jacopo Peccatori, Fabio Ciceri, Leo Luznik and Luca Vago

---

Updated information and services can be found at:  
<http://www.bloodjournal.org/content/131/2/247.full.html>

Articles on similar topics can be found in the following Blood collections  
[Immunobiology and Immunotherapy](#) (5589 articles)  
[Transplantation](#) (2296 articles)

---

Information about reproducing this article in parts or in its entirety may be found online at:  
[http://www.bloodjournal.org/site/misc/rights.xhtml#repub\\_requests](http://www.bloodjournal.org/site/misc/rights.xhtml#repub_requests)

Information about ordering reprints may be found online at:  
<http://www.bloodjournal.org/site/misc/rights.xhtml#reprints>

Information about subscriptions and ASH membership may be found online at:  
<http://www.bloodjournal.org/site/subscriptions/index.xhtml>

## **SUPPLEMENTARY METHODS**

### **Patients and Transplantation Procedures**

NK cell reconstitution dynamics were studied in a total of seventeen adult patients transplanted from HLA-haploidentical related donors for high-risk hematologic malignancies. Patient and donor's characteristics are summarized in Table 1. Ten patients were treated at San Raffaele Hospital (OSR) in Milan, Italy, and seven at Johns Hopkins University (JHU) in Baltimore, USA. OSR patients received a myeloablative conditioning based on Thiotepa (5 mg/kg/day on day -3 and -2), Treosulfan (14 g/m<sup>2</sup>/day on day -6 to -4) and Fludarabine (30 mg/m<sup>2</sup>/day on day -6 to -2) followed by the infusion of an unmanipulated G-CSF mobilized peripheral blood stem cell (PBSC) graft (with the exception of patient OSR#6, who received an unmanipulated bone marrow (BM) graft); JHU patients received the "standard" Baltimore non-myeloablative conditioning<sup>1</sup> followed by infusion of unmanipulated BM. Both OSR and JHU patients received a GvHD prophylaxis based on infusion of high doses of Cyclophosphamide (Cy) at day 3 and 4 after HSCT (50mg/kg/day). Starting from day 5, OSR patients were treated with mycophenolate mofetil (10 mg/kg 3 times a day) for 30 days, and sirolimus (target through level: 7-14 ng/ mL) for 3 months.<sup>2</sup> JHU patients received mycophenolate mofetil (15 mg/kg 3 times a day) for 30 days, and tacrolimus (target through level: 5-15 ng/ mL) for 90 days. The two transplantation protocols and the timepoints of sampling in our study are summarized in Fig 1 A.

The role of predicted NK cell alloreactivity on HSCT outcome was assessed according to the original Perugia algorithm<sup>3</sup> in an extended series of 99 consecutive patients who received haploidentical HSCT at OSR from November 2012 to June 2016. Patient characteristics for this series are summarized in Table 2. For 59 of these patients, selected based on the availability of biological samples, immunological features at day 30 after HSCT were analyzed in detail by immunophenotypic analysis, and linked to patient clinical outcome.



All samples and data from patients and healthy subjects were collected after written informed consent, and with approval from the OSR and JHU institutional ethical committees, in accordance with the Declaration of Helsinki.

### **Multiparametric Flow Cytometry**

To analyze NK-cell phenotype after HSCT, 5 different panels were implemented. Each panel analyzed a different aspect of NK cell functions: proliferation, maturation, activation, KIR expression and exhaustion. Due to the extremely low counts of circulating lymphocytes, the phenotypic characterization of NK cells early after HSCT (Day 0, 3, 5, 8) was restricted to markers of NK cell proliferation and maturation. Data obtained from the analysis of the maturation status were subsequently used for bhSNE analysis.

Antibodies used in the Maturation Panel were: anti-human CD3 (clone OKT3) conjugated with Brilliant Violet 510 fluorochrome; anti-human CD56 (clone HCD56) conjugated with Brilliant Violet 605 fluorochrome; anti-human CD16 (clone 3G8) conjugated with APC-Cy-7 fluorochrome; anti-human CD57 (clone HCD57) conjugated with FITC fluorochrome; CD62L (clone DRFG56) conjugated with PerCP Cy5.5 fluorochrome; anti-human HLA A\*02 (clone BB7.2) conjugated with APC fluorochrome; (Biolegend); anti-human KIR2D (clone NKVS1) conjugated with PE fluorochrome; anti-human KIR3DL1/3DL2 (clone 5133) conjugated with PE fluorochrome (Miltenyi); anti-human NKG2A (clone Z199, conjugated) with PE-Cy-7 fluorochrome (Beckman Coulter); anti-human NKG2C (clone 134591) conjugated with Alexa 700 fluorochrome (R&D).

Phenotypic characterization of NK cells present within the graft or circulating in patients at late time-points was completed with the following antibodies: anti-human KIR2DL1 (clone 143211) conjugated with FITC fluorochrome (R&D); anti-human KIR2DL2/2DL3 (clone DX27) conjugated with PerCP Cy5.5 fluorochrome; anti-human KIR3DL1 (clone DX9) conjugated with Alexa 700 fluorochrome; anti-human NKp30 (clone P30-15, conjugated with APC fluorochrome); anti-human



NKp44 (clone P44-8) conjugated with PE fluorochrome; anti-human NKp46 (clone 9E2) conjugated with Pacific Blue fluorochrome; anti-human CD8 (clone SK1) conjugated with APC-Cy-7 fluorochrome; anti-human 2B4 (clone C1.7) conjugated with PerCP Cy5.5 fluorochrome; anti-human Ki-67 (clone Ki-67) conjugated with Alexa 488 fluorochrome; anti-human HLA A\*02 (clone BB7.2) conjugated with PE fluorochrome (Biolegend); anti-human DNAM-1 (clone DX11) conjugated with FITC fluorochrome (BD Bioscience); anti-human KLRG1 (clone REA261) conjugated with APC fluorochrome; anti-human KIR3DL1 (clone DX9) conjugated with VioBlue fluorochrome (Miltenyi); anti-human KIR2DL1/2DS1 (clone EB6B) conjugated with APC fluorochrome; anti-human KIR2DL2/2DL3/2SD2 (clone GL183) conjugated with PE-Cy5.5 fluorochrome (Beckman Coulter). Finally, for in vitro experiments, Annexin V, conjugated with APC or PE fluorochromes and anti-human CD34 (clone 581) conjugated with APC fluorochrome (Biolegend) were used together with anti-human CD3 and CD56 antibodies.

For absolute quantification of T and NK cell subsets in fresh whole blood samples we employed the Flow-Count technology (Beckman Coulter) after staining with anti-human CD3-PE-Cy7, CD56 Pacific Blue, HLA A\*02 PE antibodies.<sup>4,5</sup>

For Ki-67 intracellular staining, cells were stained with appropriate surface antibodies, washed, and then fixed and permeabilized with FOXP3 Fix/Perm Buffer Set (Biolegend) at OSR, and Intracellular Fixation & Permeabilization Buffer Set (eBiosciences) at JHU, following manufacturer instructions.

Each acquisition was calibrated using Rainbow Calibration Particles (Spherotech) to correct for day-to-day variation.

#### **Aldefluor Assay to determine ALDH activity**

The Aldefluor kit (Stem Cell Technologies) was used to identify cell populations with high ALDH enzymatic activity, as previously reported.<sup>6</sup> Briefly, cells harvested from donor graft or from

patients' PB were incubated with Aldefluor substrate for 30 min at 37°C, with and without the ALDH inhibitor, diethylaminobenzaldehyde (DEAB), according to manufacturer's instructions. Subsequently, cells were stained with the appropriate fluorochrome-conjugated antibodies to determine ALDH activity within different cell lineages by flow cytometry. Aldefluor was detected in the green fluorescence channel, and samples treated with the inhibitor DEAB were used as negative controls to set the gates defining the ALDH<sup>+</sup> region.

### **Quantification of Serum Cytokines**

IL-15 serum concentration was quantified by Bio-Plex Pro Human Cytokine 4-plex array (Bio-Rad), as described previously.<sup>5</sup> Samples were analyzed in duplicate and compared with a high-sensitivity standard curve prepared by serial dilutions of recombinant IL-15. Data were analyzed using Bio-Plex Manager version 6.1 (Bio-Rad).

### **Statistical Analyses**

Statistical analyses of experimental data were performed using Prism 5 (GraphPad Software). Data are shown as mean ± S.E.M., unless otherwise specified. For comparison of the expression of NK cell receptors, percentages were converted into their logodds to obtain continuous variables and then compared through independent sample t test ( $\alpha = 0.05$ ). For all comparisons, two-sided p values were used, and  $p < 0.05$  was considered statistically significant (where indicated: \*  $p < 0.05$ ; \*\*  $p < 0.01$ ; \*\*\*  $p < 0.001$ ; \*\*\*\*  $p < 0.0001$ ). For linear regression analysis, the best-fit values of the slopes were reported with goodness-of-fit value ( $r^2$ ) and the p value of the slope (F test).

For the analysis of clinical endpoints, statistics were performed with R (R Development Core Team, Vienna, Austria) software package. Outcomes of patients are reported at the censoring date of 30<sup>th</sup> July 2016. The Fisher's exact test was performed to determine differences in the frequencies of categorical variables between the two groups defined by predicted NK alloreactivity. The Mann-

Whitney U test was used to determine differences in the median of continuous variables between the two groups. Cumulative incidences were estimated for acute and chronic GvHD, TRM and relapse to accommodate competing risks.<sup>7</sup> Relapse or progression was a competing risk for TRM, death from any cause was a competing risk for relapse. Relapse/progression and death from any causes were competing risks for GvHD.

Overall survival (OS) was defined as the interval from HSCT to death whatever the cause, and patients were censored at the date of last contact if alive. Progression-free survival (PFS) was defined as the interval from HSCT to either relapse or progression or death in remission (whichever came first). The composite endpoint of GvHD-free/relapse-free survival was defined as survival free of grades 3-4 aGvHD, cGvHD requiring systemic treatment, relapse/progression or death.

The probabilities of OS, PFS and GRFS were estimated using the Kaplan-Meier estimator.<sup>8</sup> Log-rank test was used for univariate comparisons of survival curves,<sup>9</sup> while Gray's test was conducted to compare cumulative incidences of competing-risks endpoints.<sup>10</sup>

Multivariate Cox proportional hazard models<sup>11</sup> were built for relapse and PFS to adjust for potentially confounding clinical factors in the subpopulation of patients for whom we performed extended phenotypic analysis of NK and T cells. Covariates included in each model were: patient age (categorical, based on median value), underlying disease diagnosis (acute myeloid leukemia vs others), disease status at transplantation (complete remission vs active disease), Sorror comorbidity index score<sup>12</sup> (median), absolute counts of T cells (median), absolute counts of NK cells at day 30 after HSCT (median), absolute counts of memory-like NK cells at day 30 after HSCT (median), percentage of CD62L positivity on total NK cells at day 30 after HSCT (median), percentage of KIR positivity on NK cells at day 30 after HSCT (median). Interactions between percentage of KIR positivity on NK cells and percentage of CD62L positivity on NK cells and between absolute counts of T cells and NK cells at day 30 after HSCT were tested and were not significant.

Affirmation of the proportional hazard assumption was met for all variables. All tests were two-sided. The type I error rate was fixed at 0.05 for determination of factors associated with outcome. A p-value of 0.05 was considered significant for determination of factors associated with time to event.

## SUPPLEMENTARY REFERENCES

1. Luznik L, O'Donnell PV, Symons HJ, et al. HLA-haploidentical bone marrow transplantation for hematologic malignancies using nonmyeloablative conditioning and high-dose, posttransplantation cyclophosphamide. *Biol. Blood Marrow Transplant.* 2008;14(6):641–650.
2. Peccatori J, Forcina A, Clerici D, et al. Sirolimus-based graft-versus-host disease prophylaxis promotes the in vivo expansion of regulatory T cells and permits peripheral blood stem cell transplantation from haploidentical donors. *Leukemia.* 2015;29(2):396–405.
3. Ruggeri L, Capanni M, Urbani E, et al. Effectiveness of donor natural killer cell alloreactivity in mismatched hematopoietic transplants. *Science.* 2002;295(5562):2097–2100.
4. Oliveira G, Ruggiero E, Stanghellini MTL, et al. Tracking genetically engineered lymphocytes long-term reveals the dynamics of T cell immunological memory. *Sci Transl Med.* 2015;7(317):317ra198.
5. Cieri N, Oliveira G, Greco R, et al. Generation of human memory stem T cells after haploidentical T-replete hematopoietic stem cell transplantation. *Blood.* 2015;125(18):2865–2874.
6. Kanakry CG, Ganguly S, Zahurak M, et al. Aldehyde dehydrogenase expression drives human regulatory T cell resistance to posttransplantation cyclophosphamide. *Sci Transl Med.* 2013;5(211):211ra157.
7. Gooley TA, Leisenring W, Crowley J, Storer BE. Estimation of failure probabilities in the presence of competing risks: new representations of old estimators. *Stat Med.* 1999;18(6):695–706.
8. Kaplan EL, Meier P. Nonparametric Estimation from Incomplete Observations. *J Am Stat Assoc.* 1958;53:457–481.

9. Mantel N. Evaluation of survival data and two new rank order statistics arising in its consideration. *Cancer Chemother Rep.* 1966;50(3):163–170.
10. Gray RJ. A class of K-sample tests for comparing the cumulative incidence of a competing risk. *Ann Stat.* 1988;16:1141–1154.
11. Cox DR. Regression Models and Life-Tables. *Journal of the Royal Statistical Society. Series B (Methodological).* 1972;34(2):187–220.
12. Sorrow ML, Sandmaier BM, Storer BE, et al. Comorbidity and disease status based risk stratification of outcomes among patients with acute myeloid leukemia or myelodysplasia receiving allogeneic hematopoietic cell transplantation. *J. Clin. Oncol.* 2007;25(27):4246–4254.
13. Armand P, Kim HT, Logan BR, et al. Validation and refinement of the Disease Risk Index for allogeneic stem cell transplantation. *Blood.* 2014;123(23):3664–3671.
14. Holtan SG, DeFor TE, Lazaryan A, et al. Composite end point of graft-versus-host disease-free, relapse-free survival after allogeneic hematopoietic cell transplantation. *Blood.* 2015;125(8):1333–1338.

**Supplementary Table 1. Characteristics of AML patient subgroups.**

Characteristic	Acute Myeloid Leukemia		AML in Complete Remission	
	Pts with predicted NK Alloreactivity	Pts without predicted NK Alloreactivity	Pts with predicted NK Alloreactivity	Pts without predicted NK Alloreactivity
<b>No. of patients</b>	27	32	8	10
<b>Age, median (range), yr</b>	62 (29-77)	52 (29-73)	58 (29-74)	54 (29-73)
<b>Gender</b>				
Male	18	22	6	7
Female	9	10	2	3
<b>Refined Disease Risk Index<sup>^</sup></b>				
Low	0	1	0	1
Intermediate	5	5	5	4
High	15	12	2	5
Very High	5	12	0	0
Previous allogeneic HSCT	2	2	1	0
<b>Conditioning Regimen<sup>†</sup></b>				
Treo-Flu-Mel	16	19	4	5
Thio-Treo-Flu	10	8	4	3
Thio-Bu-Flu	0	1	0	1
Treo-Flu	0	3	0	0
Other conditioning	1	1	0	1
<b>Graft composition</b>				
CD34+ cells x 10 <sup>6</sup> /kg, median (range)	5.32 (4.07-10.29)	5.3 (1.64-8.02)	5.04 (4.35-6.49)	5.33 (1.64-8.02)
CD3+ cells x10 <sup>6</sup> /kg, median (range)	105.61 (9.04-400)	169.17 (3.94-729)	149.86 (14.9-327.54)	173.58 (3.94-339.8)
<b>acute GvHD</b>				
grade 2-4	9	13	3	3
grade 3-4	6	7	2	1

^ Disease Risk Index calculated according to Armand et al. *Blood*, 2014<sup>13</sup>

† Conditioning Regimens: Treo-Flu-Mel: Treosulfan (14 g/m<sup>2</sup>/day on day -6 to -4), Fludarabine (30 mg/m<sup>2</sup>/day on day -6 to -2) and Melphalan (70 mg/m<sup>2</sup>/day on day -2 and -1); Thio-Treo-Flu: Thiotepa (5 mg/kg/day on day -3 and -2), Treosulfan (14 g/m<sup>2</sup>/day on day -6 to -4) and Fludarabine (30 mg/m<sup>2</sup>/day on day -6 to -2); Thio-Bu-Flu: Thiotepa (5 mg/kg/day on day -7 and -6), Busulfan (3.2 mg/kg/day on day -5 to -3) and Fludarabine (50 mg/m<sup>2</sup>/day on day -5 to -3); Treo-Flu: Treosulfan (14 g/m<sup>2</sup>/day on day -6 to -4) and Fludarabine (30 mg/m<sup>2</sup>/day on day -6 to -2).



**Supplementary Table 2. Univariate analysis of the effect of predicted NK alloreactivity on major clinical endpoints.**

Endpoint	All Patients		Acute Myeloid Leukemia		AML in Complete Remission	
	Pts with predicted NK Alloreactivity (n=41)	Pts without predicted NK Alloreactivity (n=58)	Pts with predicted NK Alloreactivity (n=27)	Pts without predicted NK Alloreactivity (n=32)	Pts with predicted NK Alloreactivity (n=8)	Pts without predicted NK Alloreactivity (n=10)
<b>100-d CI of grade 2-4 aGVHD</b>	37% (CI: 22-51) p=0.53	33% (CI: 21-45)	26% (CI: 11-44) p=0.52	34% (CI: 19-51)	25% (CI: 3-58)	30% (CI: 6-59) p=0.69
<b>100-d CI of grade 3-4 aGVHD</b>	27% (CI: 14-41) p=0.4	21% (CI: 11-32)	19% (CI: 7-35) p=0.85	22% (CI: 10-38)	13% (CI: 1-45)	10% (CI: 1-37) p=0.83
<b>2-y CI of cGVHD</b>	30% (CI: 13-49) p=0.6	38% (CI: 23-52)	21% (CI: 4-46) p=0.61	37% (CI: 16-58)	38% (CI: 1-88)	60% (CI: 1-95) p=0.74
<b>2-y CI of extensive cGVHD</b>	5% (CI: 1-15) p=0.27	17% (CI: 8-30)	4% (CI: 1-16) p=0.34	19% (CI: 5-40)	0%	30% (CI: 1-80) p=0.53
<b>2-y CI of Relapse</b>	35% (CI: 21-50) p=0.9	34% (CI: 22-47)	39% (CI: 20-57) p=0.76	38% (CI: 21-54)	13% (CI: 1-45)	30% (CI: 6-60) p=0.46
<b>2-y CI of TRM</b>	18% (CI: 8-31) p=0.11	30% (CI: 19-43)	20% (CI: 7-37) p=0.66	19% (CI: 7-34)	13% (CI: 1-45)	10% (CI: 1-37) p=0.84
<b>2-y OS</b>	40% (CI: 23-57) p=0.38	43% (CI: 29-55)	45% (CI: 15-56) p=0.71	46% (CI: 28-62)	75% (CI: 23-92)	60% (CI: 25-83) p=0.6
<b>2-y PFS</b>	47% (CI: 31-62) p=0.15	36% (CI: 23-49)	42% (CI: 23-60) p=0.42	44% (CI: 27-60)	75% (CI: 32-93)	60% (23-82) p=0.64
<b>2-y GRFS<sup>^</sup></b>	31% (CI: 16-47) p=0.17	13% (CI: 5-24)	30% (CI: 11-52) p=0.55	21% (CI: 7-40)	38% (CI: 1-80)	30% (CI: 1-70) p=0.96

Abbreviations: CI=Cumulative Incidence; TRM=Transplant-Related Mortality; OS=Overall Survival; PFS=Progression-Free Survival;  
GRFS=GvHD-Free Relapse-Free Survival

<sup>^</sup>GRFS defined according to Holtan et al. Blood, 2015<sup>14</sup>

**Supplementary Table 3. Univariate analysis of the impact of NK cell maturity features at day 30 on disease-related clinical endpoints.**

Immune Parameter at day 30	2-y CI of Relapse		2-y PFS	
	< median (n=29)	≥ median (n=30)	< median (n=29)	≥ median (n=30)
<b>PB T cell counts (CD3<sup>+</sup> cells/μl) median: 221 cells/μl</b>	35% (CI: 18-52)	20% (CI: 8-36)	42% (CI: 26-30)	60% (CI: 40-75)
	p=0.20		p=0.29	
<b>PB NK cell counts (CD3<sup>+</sup>CD56<sup>+</sup> cells/μl) median: 9.3 cells/μl</b>	38% (CI: 20-55)	17% (CI: 6-32)	43% (CI: 24-60)	60% (CI: 41-75)
	p=0.08		p=0.36	
<b>PB memory-like NK cell counts (CD57<sup>+</sup>CD16<sup>+</sup>KIR<sup>+</sup>NKG2C<sup>+</sup> NK cells/μl) median: 0.07 cells/μl</b>	38% (CI: 20-55)	17% (CI: 6-32)	45% (CI: 27-62)	59% (CI: 38-74)
	p=0.07		p=0.20	
<b>%CD16/NK cells median: 40%</b>	31% (CI: 15-48)	23% (CI: 10-40)	51% (CI: 32-68)	52% (CI: 33-69)
	p=0.52		p=0.97	
<b>%CD57/NK cells median: 5%</b>	35% (CI: 18-52)	20% (CI: 8-36)	48% (CI: 30-65)	55% (CI: 35-71)
	p=0.26		p=0.57	
<b>%CD62L/NK cells median: 42%</b>	<b>14% (CI: 4-29)</b>	<b>40% (CI: 22-57)</b>	58% (CI: 37-73)	47% (CI: 28-63)
	<b>p=0.03</b>		p=0.33	
<b>%KIR/NK cells median: 22%</b>	<b>48% (CI: 29-65)</b>	<b>7% (CI: 1-19)</b>	<b>38% (CI: 21-55)</b>	<b>65% (CI: 45-80)</b>
	<b>p=0.0003</b>		<b>p=0.02</b>	
<b>%NKG2A/NK cells median: 88%</b>	31% (CI: 15-48)	23% (CI: 10-40)	54% (CI: 34-70)	50% (CI: 31-66)
	p=0.59		p=0.61	
<b>%NKG2C/NK cells median: 11%</b>	28% (CI: 13-45)	27% (CI: 12-43)	53% (CI: 33-70)	50% (CI: 31-66)
	p=0.96		p=0.55	
<b>%NK memory-like/NK cells median: 0.7%</b>	31% (CI: 15-48)	23% (CI: 10-40)	48% (CI: 30-65)	55% (CI: 36-71)
	p=0.52		p=0.45	

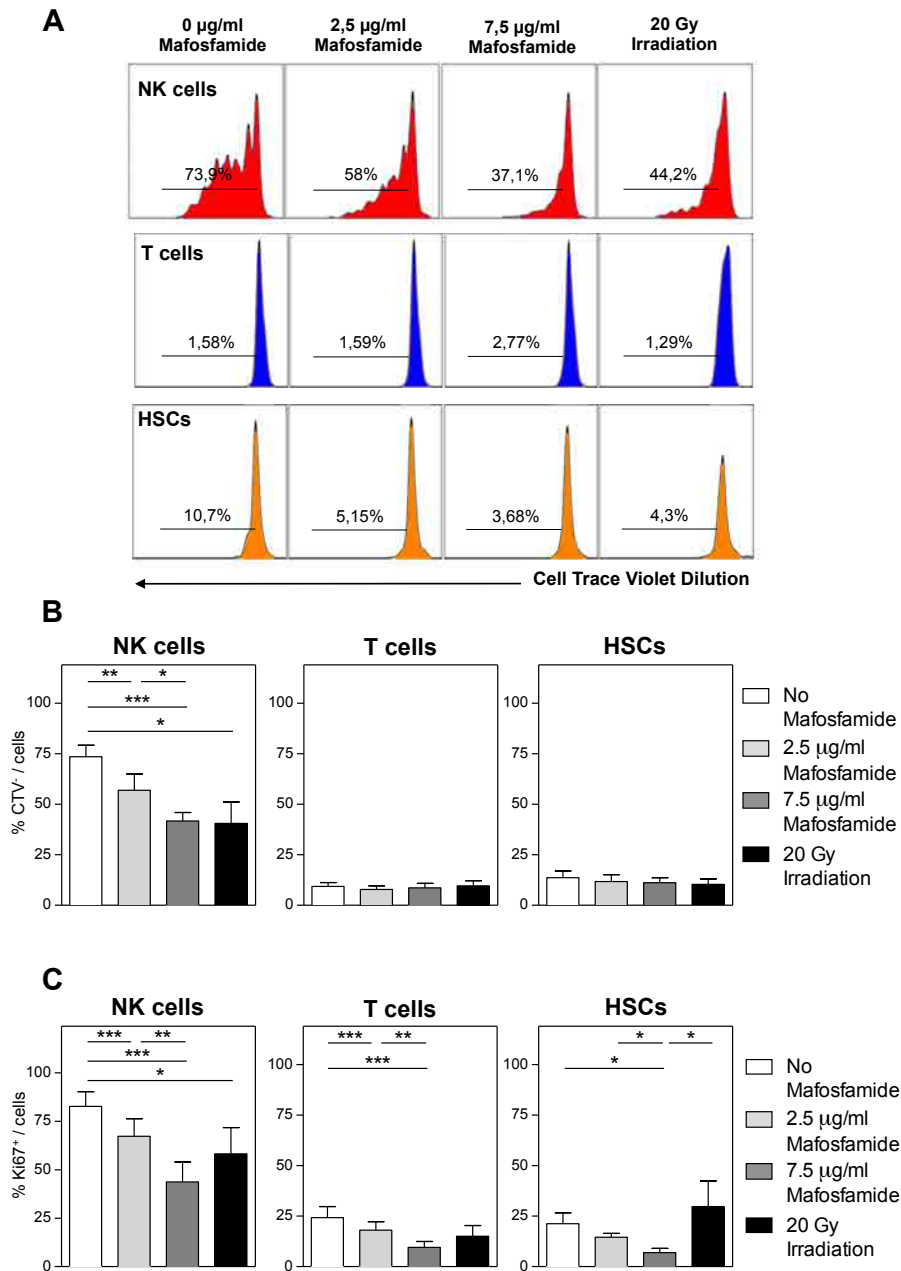
Abbreviations: CI=Cumulative Incidence; PFS=Progression-Free Survival; PB=Peripheral Blood

**Supplementary Table 4. Multivariate analysis of the impact of NK cell maturity features at day 30 on disease-related clinical endpoints.**

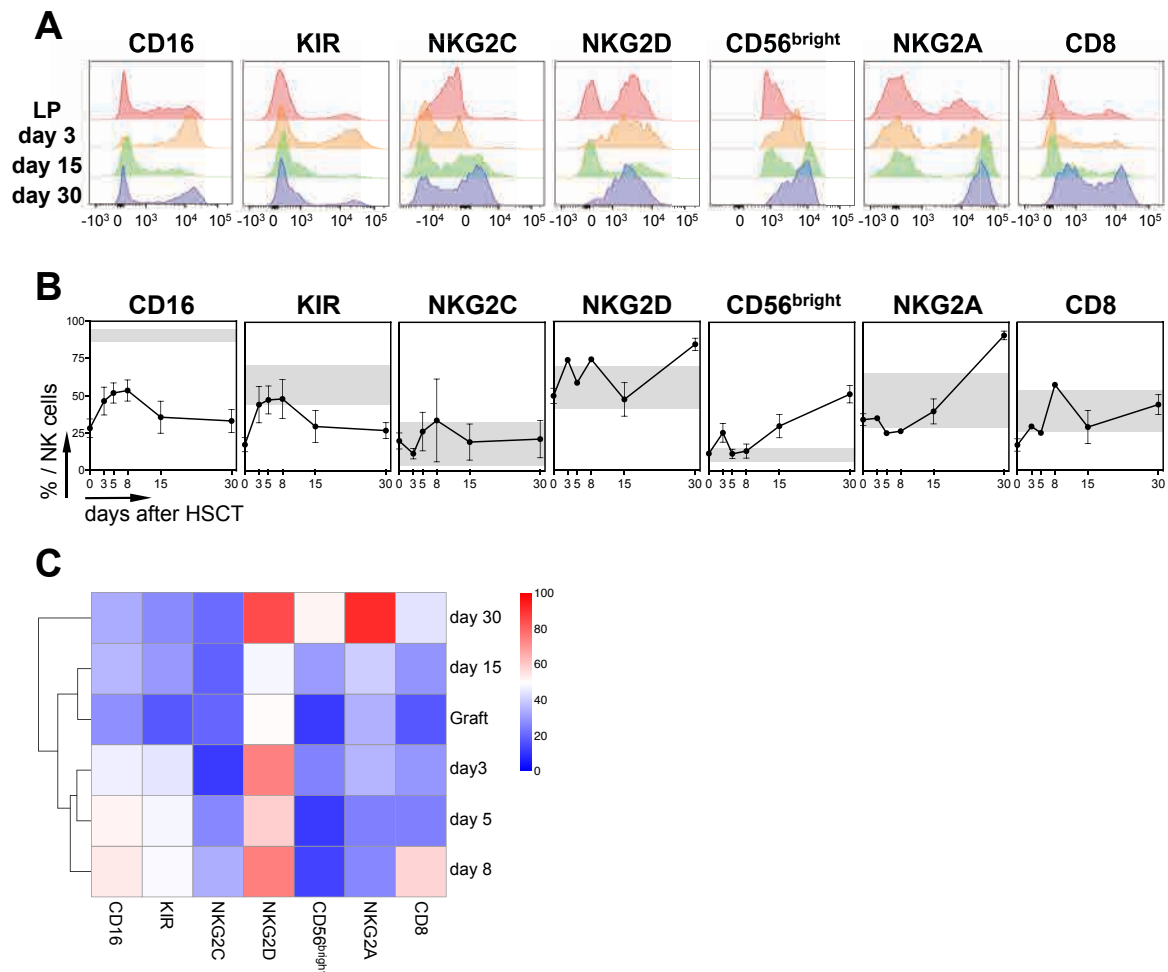
Variable	2-y CI of Relapse		2-y PFS	
	P value	HR (CI)	P value	HR (CI)
<b>Patient age (≥ 48y vs &lt; 48y)</b>	0.13	0.379 (0.108 – 1.332)	0.235	0.585 (0.242 – 1.418)
<b>Disease category (other diagnoses vs AML)</b>	0.888	0.911 (0.25 – 3.325)	0.31	1.612 (0.642 – 4.052)
<b>Disease status (advanced vs CR)</b>	<b>0.023</b>	<b>5.095 (1.247 – 20.821)</b>	<b>0.001</b>	<b>4.998 (1.863 – 13.411)</b>
<b>HCT-CI score<sup>^</sup> (≥ 3 vs &lt; 3)</b>	0.542	1.55 (0.379 – 6.347)	0.509	1.38 (0.531 – 3.591)
<b>PB T cells counts (≥ 221/μl vs &lt; 221/μl)</b>	0.784	0.829 (0.217 – 3.167)	1	1 (0.37 – 2.702)
<b>PB NK cell counts (≥ 9.3/μl vs &lt; 9.3/μl)</b>	0.318	2.264 (0.456 – 11.238)	0.285	1.839 (0.602 – 5.619)
<b>PB memory-like NK cells (≥ 0.07/μl vs &lt; 0.07/μl)</b>	0.532	0.628 (0.146 – 2.703)	0.198	0.479 (0.156 – 1.468)
<b>%CD62L/NK cells (≥ 42% vs &lt; 42%)</b>	0.229	2.302 (0.592 – 8.945)	0.765	1.145 (0.473 – 2.774)
<b>%KIR/NK cells (≥ 22% vs &lt; 22%)</b>	<b>0.012</b>	<b>0.1 (0.017 – 0.599)</b>	0.083	0.433 (0.168 – 1.116)

Abbreviations: CI=Cumulative Incidence; PFS=Progression-Free Survival; PB=Peripheral Blood; HCT-CI=Hematopoietic Cell Transplantation-Comorbidity Index

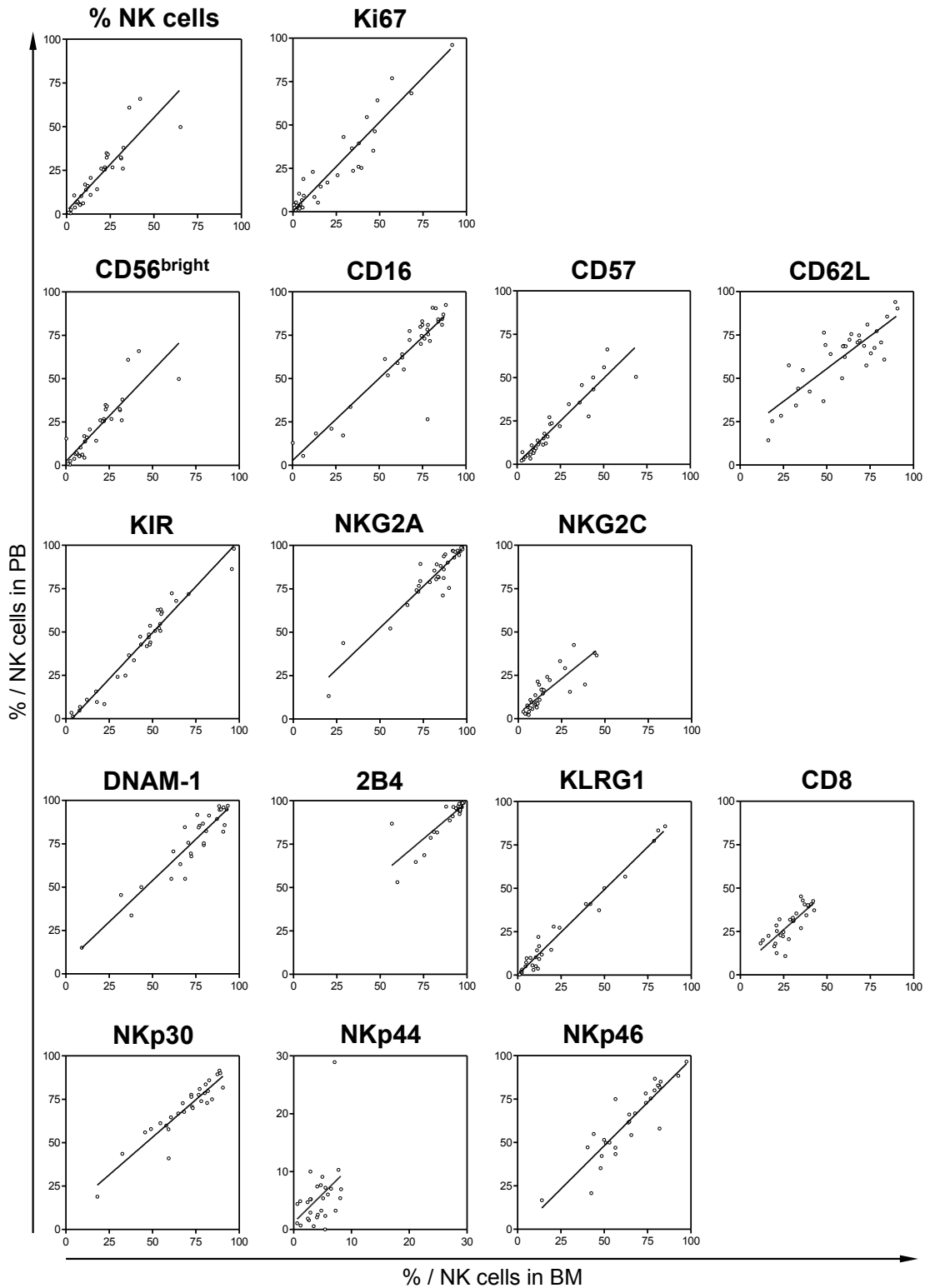
<sup>^</sup> HCT-CI calculated according to Sorror et al. *J Clin Oncol*, 2007<sup>12</sup>



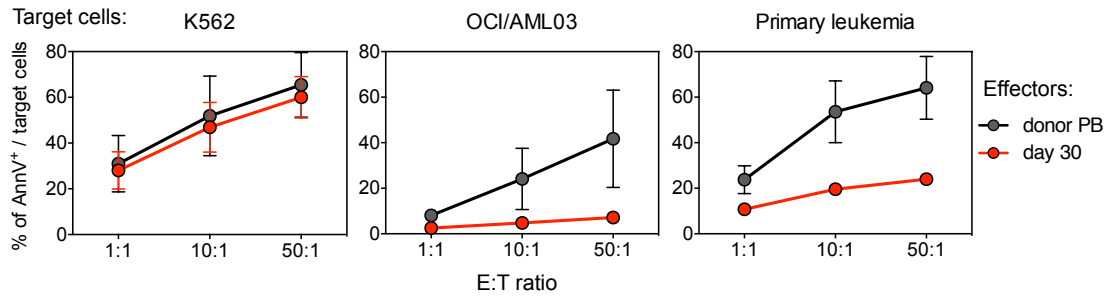
**Supplementary Figure 1. In vitro assessment of NK cell sensitivity to mafosfamide.** The leukapheresis product of 6 patients was stimulated with IL-15 at day 0 and exposed to different doses of mafosfamide or irradiation at day 3. Proliferation was measured at day 5 by flow cytometry. (A) Flow cytometry plots from a representative patient (OSR#2), depicting the in vitro dilution of cell trace violet (CTV) gated on CD56<sup>+</sup> CD3<sup>-</sup> NK cells (upper row, red curves), CD3<sup>+</sup> T cells (middle row, blue curves) or CD34<sup>+</sup> HSCs (bottom row, orange curves). (B-C) Graphs showing the frequency of proliferating cells as assessed by CTV dilution (B) or by Ki-67 expression (C) and measured on NK, T and HSCs, after no treatment (white bars), administration of different doses of mafosfamide (light grey bars: 2.5 µg/mL; dark grey bars: 7.5 µg/mL), and after irradiation (day 5, black bars). Unless otherwise specified, shown in all panels are average values with SEM.



**Supplementary Figure 2. Phenotypic analysis of NK cells circulating in JHU patients.** (A) Flow cytometry plots depicting expression of indicated maturation markers amongst CD56<sup>+</sup> CD3<sup>-</sup> NK cells from a representative patient (JHU#7) at the indicated time-points (LP, leukapheresis: red; day 3: orange; day 15: green; day 30: blue). (B) Graphs showing the expression of the indicated maturation markers measured by flow cytometry in NK cells from the graft (day 0) and from samples collected longitudinally after HSCT with PT-Cy from JHU patients (n=7). For each marker, normal reference values (mean  $\pm$  SD) measured in NK cells harvested from 5 healthy subjects are reported in grey. (C) Heat map and unsupervised hierarchical clustering of the average expression of maturation markers measured in NK cells from 7 JHU patients analyzed by multiparametric flow cytometry at the indicated time-points. The color scale is shown on the right.

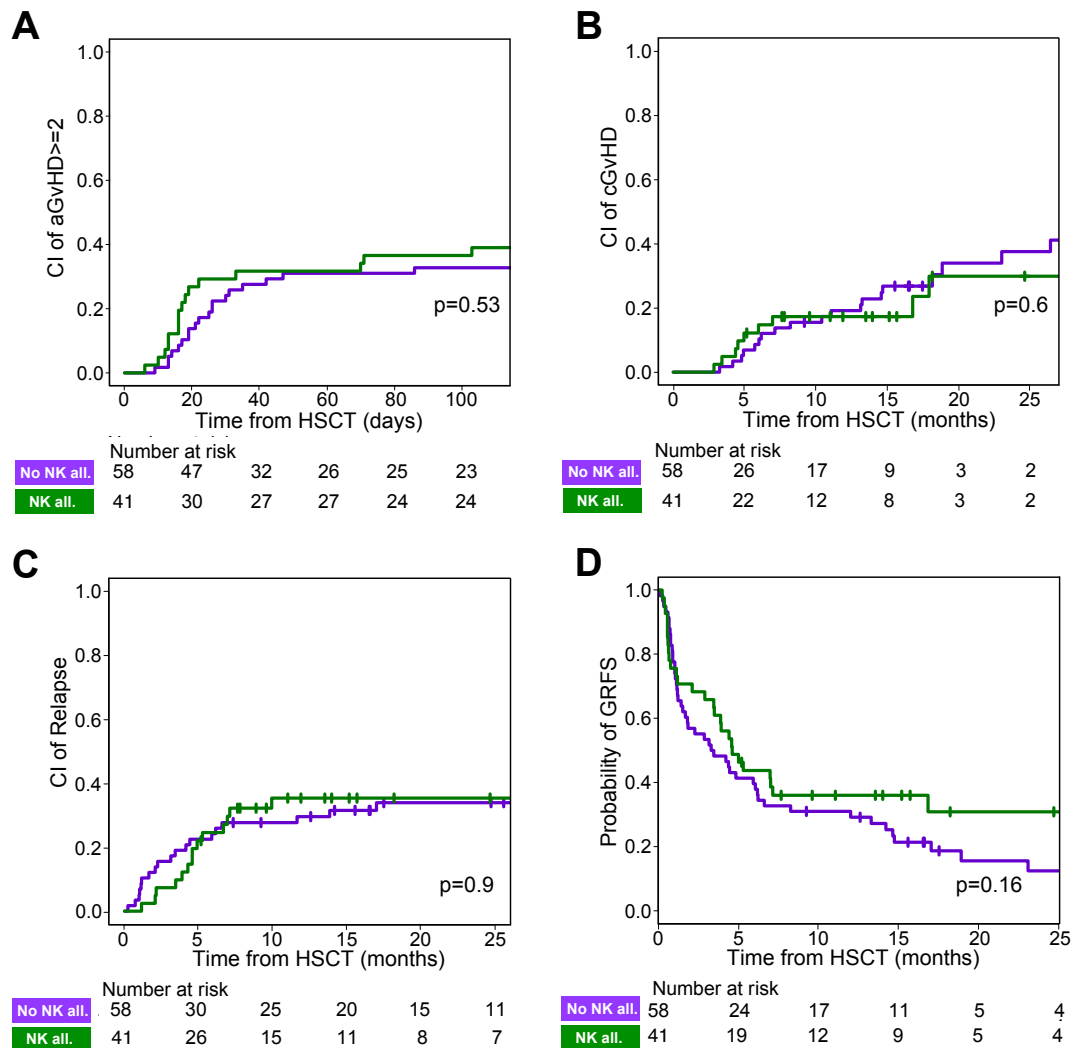


**Supplementary Figure 3. Comparison of NK cell immunophenotype in BM and PB.** The panels depict the correlation between the expression of each marker on NK cells harvested from BM (x axis) and PB (y axis) for all the samples. The black lines denote the best-fit line of the linear regression analysis, which is significant for all the plotted data ( $p < 0.05$ ).

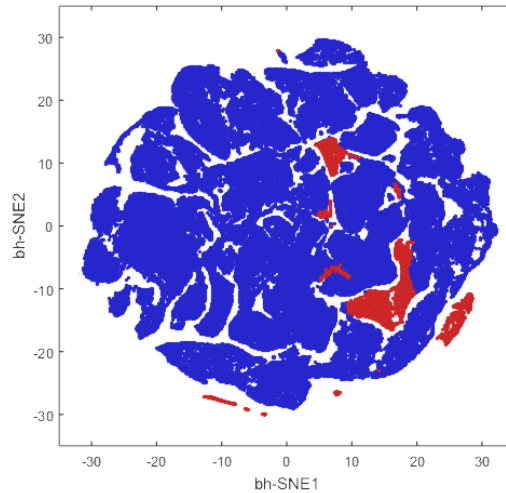


**Supplementary Figure 4. Impaired cytotoxicity of early-reconstituting patient NK cells against leukemic cells.** Target cell death, expressed as Annexin V positivity, measured on K562 cells, OCI/AML3 cells or primary leukemic cells after incubation at different effector:target ratios with NK cells purified from patient PB at day 30 after HSCT with PT-Cy (n=3, red dots) or from their respective donors PB (n=3, black dots). Shown are average values with SEM.





**Supplementary Figure 5. Impact of NK alloreactivity on other clinical endpoints.** Cumulative incidence of grade 2-4 acute GvHD (A), cumulative incidence of chronic GvHD (B), cumulative incidence of relapse (C) and GvHD- and Relapse-Free Survival (D) in patients who received PT-Cy-based haploidentical HSCT from donor with (green line, n=41) or without (purple line, n=58) predicted NK cell alloreactivity. Ticks represent censoring for live patients.



**Supplementary Figure 6. bhSNE analysis and unsupervised k-means clustering to identify memory-like NK cells.** Phenotypic data obtained through the analysis of our "NK cell maturation" panel in samples collected from patients at day 30 after haploidentical HSCT with PT-Cy (n=59) and from healthy individuals (n=9) were mapped on a bidimensional map using the bhSNE algorithm for multidimensional analysis. Subsequently, the k-means bioinformatic tool for unsupervised data clustering was used to identify in an unsupervised manner the position on the bhSNE map of  $CD57^+CD16^+KIR^+NKG2C^+$  memory-like NK cells (red clusters), and this knowledge was employed to quantify the proportion of such cells in each of the original samples.

## **Chapter 4.**

### **Bone marrow central memory and memory stem T-cell exhaustion in AML patients relapsing after HSCT**

Noviello M, Manfredi F, Ruggiero E, Perini T, Oliveira G, Cortesi F, De Simone P, Toffalori C, Gambacorta V, Greco R, Peccatori J, Casucci M, Casorati G, Dellabona P, Onozawa M, Teshima T, Griffioen M, Halkes CJM, Falkenburg JHF, Stölzel F, Altmann H, Bornhäuser M, Waterhouse M, Zeiser R, Finke J, Cieri N, Bondanza A, Vago L\*, Ciceri F\*, Bonini C\*

*Published in Nature Communications (2019)*

ARTICLE

<https://doi.org/10.1038/s41467-019-08871-1>

OPEN

# Bone marrow central memory and memory stem T-cell exhaustion in AML patients relapsing after HSCT

Maddalena Noviello<sup>1</sup>, Francesco Manfredi<sup>1</sup>, Eliana Ruggiero<sup>1</sup>, Tommaso Perini<sup>2</sup>, Giacomo Oliveira<sup>1</sup>, Filippo Cortesi<sup>3</sup>, Pantaleo De Simone<sup>1</sup>, Cristina Toffalori<sup>4</sup>, Valentina Gambacorta<sup>4</sup>, Raffaella Greco<sup>2</sup>, Jacopo Peccatori<sup>2</sup>, Monica Casucci<sup>5</sup>, Giulia Casorati<sup>3</sup>, Paolo Dellabona<sup>3</sup>, Masahiro Onozawa<sup>6</sup>, Takanori Teshima<sup>6</sup>, Marieke Griffioen<sup>7</sup>, Constantijn J.M. Halkes<sup>7</sup>, J.H.F. Falkenburg<sup>7</sup>, Friedrich Stölzel<sup>8</sup>, Heidi Altmann<sup>8</sup>, Martin Bornhäuser<sup>8</sup>, Miguel Waterhouse<sup>9</sup>, Robert Zeiser<sup>9</sup>, Jürgen Finke<sup>9</sup>, Nicoletta Cieri<sup>1,11</sup>, Attilio Bondanza<sup>5</sup>, Luca Vago<sup>4</sup>, Fabio Ciceri<sup>2,10</sup> & Chiara Bonini<sup>1,10</sup>

The major cause of death after allogeneic Hematopoietic Stem Cell Transplantation (HSCT) for acute myeloid leukemia (AML) is disease relapse. We investigated the expression of Inhibitory Receptors (IR; PD-1/CTLA-4/TIM-3/LAG-3/2B4/KLRG1/GITR) on T cells infiltrating the bone marrow (BM) of 32 AML patients relapsing (median 251 days) or maintaining complete remission (CR; median 1 year) after HSCT. A higher proportion of early-differentiated Memory Stem (T<sub>SCM</sub>) and Central Memory BM-T cells express multiple IR in relapsing patients than in CR patients. Exhausted BM-T cells at relapse display a restricted TCR repertoire, impaired effector functions and leukemia-reactive specificities. In 57 patients, early detection of severely exhausted (PD-1<sup>+</sup>Eomes<sup>+</sup>T-bet<sup>-</sup>) BM-T<sub>SCM</sub> predicts relapse. Accordingly, leukemia-specific T cells in patients prone to relapse display exhaustion markers, absent in patients maintaining long-term CR. These results highlight a wide, though reversible, immunological dysfunction in the BM of AML patients relapsing after HSCT and suggest new therapeutic opportunities for the disease.

<sup>1</sup>IRCCS San Raffaele Scientific Institute, Division of Immunology, Transplantation, and Infectious Diseases, Experimental Hematology Unit, via Olgettina 60, Milan 20132, Italy. <sup>2</sup>IRCCS San Raffaele Scientific Institute, Hematology and Hematopoietic Stem Cell Transplantation Unit, via Olgettina 60, Milan 20132, Italy. <sup>3</sup>IRCCS San Raffaele Scientific Institute, Division of Immunology, Transplantation and Infectious Diseases, Experimental Immunology Unit, via Olgettina 60, Milan 20132, Italy. <sup>4</sup>IRCCS San Raffaele Scientific Institute, Division of Immunology, Transplantation and Infectious Disease, Unit of Immunogenetics, Leukemia Genomics and Immunobiology, via Olgettina 60, Milan 20132, Italy. <sup>5</sup>IRCCS San Raffaele Scientific Institute, Division of Immunology, Transplantation and Infectious Diseases, Innovative Immunotherapies Unit, via Olgettina 60, Milan 20132, Italy. <sup>6</sup>Hokkaido University Faculty of Medicine, Graduate School of Medicine, Department of Hematology, 5 Chome Kita 8 Jonishi, Kita, Sapporo 060-0808, Japan. <sup>7</sup>Leiden University Medical Center (LUMC), Department of Hematology, Albinusdreef 2, Leiden 2333, The Netherlands. <sup>8</sup>Department of Internal Medicine I, University Hospital Carl Gustav Carus Dresden, Technical University Dresden, Fetsherstrasse 74, Dresden 01307, Germany. <sup>9</sup>University of Freiburg Medical Center, Department of Hematology, Oncology and Stem Cell Transplantation, Hugstetterstr 55, Freiburg 79106, Germany. <sup>10</sup>Università Vita-Salute San Raffaele, via Olgettina 60, Milan 20132, Italy. <sup>11</sup>Present address: University of Milan, via Festa del Perdono 7, Milan 20122, Italy. These authors contributed equally: Maddalena Noviello, Francesco Manfredi. These authors jointly supervised this work: Luca Vago, Fabio Ciceri, Chiara Bonini. Correspondence and requests for materials should be addressed to C.B. (email: [bonini.chiara@hsr.it](mailto:bonini.chiara@hsr.it))

In patients affected by high-risk hematological malignancies, such as acute myeloid leukemia (AML), allogeneic hematopoietic stem cells transplantation (HSCT) represents the most effective treatment option. Still, disease relapse and progression remain the major causes of treatment failure<sup>1</sup>. HSCT efficacy largely relies on the ability of donor T cells to eliminate residual tumor cells, through a phenomenon described as Graft-versus-Leukemia (GvL) effect<sup>2</sup>. Durable immunosurveillance after HSCT likely requires long-term persistence of such leukemia-reactive T cells, possibly maintained by a stem-cell-like memory T-cell pool<sup>3,4</sup>. Indeed, according to the hierarchical model of T-cell differentiation<sup>5</sup>, after antigen encounter, naive T cells differentiate into several functional subsets, including central memory (T<sub>CM</sub>), effector memory (T<sub>EM</sub>), and terminal effectors (T<sub>EM</sub>RA). Memory stem T cells (T<sub>SCM</sub>)<sup>6</sup> are a newly described subset that differentiate directly from naive T cells upon TCR engagement and retain the capacity of self-renewal and to hierarchically differentiate into all other memory T-cell subsets<sup>7,8</sup>. Clonal tracking of genetically modified T cells infused into patients affected by malignant and non-malignant diseases revealed the ability of T<sub>SCM</sub> to persist for decades in the host and to recapitulate the ontogeny of circulating memory T cells<sup>9,10</sup>.

Even when immune reconstitution is preserved and maintained long-term after transplant, leukemic blasts can escape the immune response by several mechanisms<sup>11</sup>. At the tumor cell level, a combination of genomic instability and a Darwinian process of immunoselection may ultimately lead to a loss of tumor immunogenicity. For instance, by monitoring patients relapsing after mismatched HSCT, we described the loss of the host's mismatched HLA haplotype by leukemic cells as a relevant biological mechanism leading to tumor escape and clinical disease recurrence<sup>12,13</sup>, particularly frequent in late relapses<sup>14</sup>. Alternatively, the presence of tolerogenic T<sub>regs</sub> or cells expressing inhibitory ligands such as PD-L1<sup>15</sup> may result in the loss of donor-mediated antitumor activity.

In the last years, the expression of multiple inhibitory receptors on the cell surface of antigen-experienced T cells has been associated to T-cell "exhaustion", a functional status characterized by concomitant loss of cytokines production, proliferative capacity, and lytic activity<sup>16</sup>. First described in chronic infections, T-cell exhaustion is considered a common and relevant phenomenon in cancer progression, as well demonstrated by the efficacy of immune checkpoint-blocking therapy, a paradigm-shifting treatment for several tumors<sup>17</sup>. In the setting of leukemia, a pioneering study reported the efficacy of anti-CTLA-4 blocking antibody as a treatment of post-transplantation relapse<sup>18</sup>. However, data on the role of immune checkpoints in the control of hematological malignancies are still limited.

In the current study, we investigated whether T-cell exhaustion is involved in the development of post-transplant leukemic relapse. To this end, we evaluated the expression of several inhibitory receptors on different bone marrow (BM) infiltrating memory CD4<sup>+</sup> and CD8<sup>+</sup> T-cell subsets in AML patients who received HSCT. We identified a PD-1<sup>+</sup> TIM-3<sup>+</sup> KLRG1<sup>+</sup> 2B4<sup>+</sup> exhaustion signature that characterizes early-differentiated CD8<sup>+</sup> BM-T<sub>SCM</sub> and T<sub>CM</sub> subsets, during disease relapse.

## Results

**Increased frequency of BM-T<sub>regs</sub> associates to AML relapse.** We analyzed BM and peripheral blood (PB) from 32 patients affected by AML who received HSCT from either HLA-matched (20 pts) or HLA-haploidentical (12 pts) donors. Clinical characteristics of patients are summarized in Table 1. Samples were collected at relapse (REL; median 251 days after HSCT; 16 pts) or, for patients who achieved and maintained complete remission (CR; 16 pts), at 1

year after HSCT. Samples from 11 healthy donors (HD) were used as controls. The gating strategy of the flow-cytometry analysis is reported in Supplementary Fig. 1. After transplant, T cells infiltrating the BM (BM-T cells) of patients in CR displayed an inverted CD4/CD8 ratio compared with HD ( $p < 0.0001$ ), consistent with a more rapid CD8<sup>+</sup> T-cell reconstitution, whereas relapsing patients displayed a wider variability in CD4/CD8 ratio both in BM (Supplementary Fig. 2a) and PB (Supplementary Fig. 2b). As already reported<sup>19</sup>, T regulatory cells (T<sub>regs</sub>), defined by the coexpression of CD4, CD25, and FoxP3, represented a small cellular population in the bone marrow. The frequency of BM-infiltrating T<sub>regs</sub> was significantly higher in REL patients compared with CR patients ( $p < 0.01$ ) and HD ( $p < 0.01$ ) (Supplementary Fig. 2c). This difference held also when separately evaluating naive (defined as CD45RA<sup>+</sup>FoxP3<sup>low</sup>) and activated (CD45RA<sup>-</sup>FoxP3<sup>high</sup>) cells (Supplementary Fig. 2d), the two major T<sub>reg</sub> subsets<sup>20</sup>. Interestingly, this observation was confined to tumor site, since no significant differences in T<sub>reg</sub> frequencies were observed among patient cohorts in PB (Supplementary Fig. 2e, f).

Next, we evaluated CD4<sup>+</sup> and CD8<sup>+</sup> T-cell differentiation by assessing CD62L, CD45RA, and CD95 expression<sup>4,21</sup> (Supplementary Fig. 2g). In transplanted patients, we observed a lower proportion of CD4<sup>+</sup> and CD8<sup>+</sup> BM-T naive (T<sub>naive</sub>) ( $p < 0.001$ ) and a concomitant increase of T<sub>EM</sub> ( $p < 0.0001$ ) lymphocytes than in HDs, with no significant differences between CR and REL patients (Fig. 1a). A similar T-cell distribution was observed in PB (Supplementary Fig. 2h, i). The analysis of the TCR repertoire indicated a skewed BM-T-cell clonal composition in transplanted patients, independent of clinical outcome. Analyses of TCR- $\alpha$  chain showed that the 10 most frequent clonotypes represent up to 33 and 39% of all detected clonotypes in CR and REL patients, respectively, and only 22% in HD; a similar T-cell skewing was observed upon TCR- $\beta$ -chain sequencing (Fig. 1b). These results show that the transplant procedure is the major factor promoting the expansion of CD8<sup>+</sup> T cells, their differentiation into effectors and the skewing of the TCR repertoire toward few dominant clones, whereas leukemia relapse is associated to a high frequency of T<sub>regs</sub>, specifically at the disease site.

**Exhausted phenotype of CD8<sup>+</sup> BM-T cells at AML relapse.** To assess the functional and exhaustion profile of BM-T cells, we analyzed the expression of costimulatory molecules and inhibitory receptors (IRs) on CD4<sup>+</sup> and CD8<sup>+</sup> lymphocytes and observed a different pattern of expression according to the level of HLA disparity between donor and host. The gating strategy of the flow-cytometry analysis is reported in Supplementary Fig. 1. Patients receiving HLA-haploidentical HSCT had lower percentages of CD27<sup>+</sup>CD4<sup>+</sup> T cells and CD28<sup>+</sup>CD8<sup>+</sup> T cells, compared with healthy donors, in line with the high proportion of effector T lymphocytes observed after HSCT. In this group of patients, with the exception of a slightly but significant lower proportion of T cells expressing LAG-3 in REL than in CR patients ( $p < 0.05$ ), the profile of IR expression in BM-T cells did not correlate with clinical outcome (Fig. 1c).

After HLA-identical HSCT, the expression profile of CD4<sup>+</sup> T cells appeared again dominated by the transplant procedure, and distinct from that of HD, with a higher percentage of CD4<sup>+</sup> T-cells expressing ICOS and inhibitory receptors in transplanted patients than in HD (Fig. 1d). In contrast, the exhaustion profile of CD8<sup>+</sup> BM-T cells varied significantly, according to the clinical outcome. In fact, we observed a higher proportion of CD8<sup>+</sup> BM-T cells expressing CTLA-4 (median 29.2%), PD-1 (44.1%), and TIM-3 (10.6%) inhibitory molecules in REL patients than in CR patients (CTLA-4 19.4%, PD-1 24.0%, TIM-3 2.8%;  $p < 0.05$ ) (Fig. 1d). Interestingly, some, but not all phenotypic

**Table 1 Patients' characteristics at long-term follow-up**

	HLA-matched HSCT long-term complete remission (CR)	HLA-matched HSCT relapse (REL)	Haploidentical HSCT long-term complete remission (CR)	Haploidentical HSCT relapse (REL)
Number of patients, <i>n</i>	10	10	6	6
Diagnosis <i>n</i> (%)				
AML	8 (80%)	9 (90%)	6 (100%)	5 (83%)
MDS	2 (20%)	1 (10%)	0 (0%)	1 (17%)
Donor type, <i>n</i> (%)				
HLA-matched sibling	5 (50%)	5 (50%)	0 (0%)	0 (0%)
HLA-matched MUD (9–10/10)	5 (50%)	5 (50%)	0 (0%)	0 (0%)
HLA-haploidentical	0 (0%)	0 (0%)	6 (100%)	6 (100%)
CMV serostatus donor/recipient, <i>n</i> (%)				
pos/pos	5 (50%)	7 (70%)	4 (67%)	4 (67%)
pos/neg	0 (0%)	0 (0%)	0 (0%)	0 (0%)
neg/pos	5 (50%)	2 (20%)	2 (33%)	2 (33%)
neg/neg	0 (0%)	1 (10%)	0 (0%)	0 (0%)
Disease status at transplant, <i>n</i> (%)				
Complete remission	8 (80%)	8 (80%)	3 (50%)	1 (17%)
Presence of disease	2 (20%)	2 (20%)	3 (50%)	5 (83%)
Conditioning regimen, <i>n</i> (%)				
Reduced-intensity	2 (20%)	3 (30%)	0 (0%)	0 (0%)
Myeloablative, treosulfan-based	6 (60%)	4 (40%)	6 (100%)	6 (100%)
Myeloablative, other	2 (20%)	3 (30%)	0 (0%)	0 (0%)
In vivo T-cell depletion, <i>n</i> (%)				
None	6 (60%)	5 (50%)	0 (0%)	0 (0%)
ATG	5 (50%)	1 (10%)	3 (50%)	0 (0%)
PT-Cy	0 (0%)	0 (0%)	3 (50%)	6 (100%)
ATG/PT-Cy	1 (10%)	4 (40%)	0 (0%)	0 (0%)
GvHD prophylaxis, <i>n</i> (%)				
CSA-based	8 (80%)	5 (50%)	0 (0%)	0 (0%)
Sirolimus-based	1 (10%)	2 (20%)	6 (100%)	6 (100%)
Other	1 (10%)	3 (30%)	0 (0%)	0 (0%)
Clinically relevant post-HSCT CMV reactivation*, <i>n</i> (%)				
Yes	4 (40%)	4 (40%)	1 (17%)	1 (17%)
No	6 (60%)	6 (60%)	5 (83%)	5 (83%)
Acute GvHD incidence, <i>n</i> (%)				
Grade 0-I	8 (80%)	9 (90%)	6 (100%)	6 (100%)
Grade II-IV	2 (20%)	1 (10%)	0 (0%)	0 (0%)
Chronic GvHD incidence, <i>n</i> (%)				
None	9 (90%)	8 (80%)	3 (50%)	6 (100%)
Mild	1 (10%)	1 (10%)	0 (0%)	0 (0%)
Moderate	0 (0%)	0 (0%)	0 (0%)	0 (0%)
Severe	0 (0%)	1 (10%)	3 (50%)	0 (0%)
Under treatment for GvHD at the time of sampling, <i>n</i> (%)				
None	10 (100%)	10 (100%)	6 (100%)	6 (100%)
Yes	0 (0%)	0 (0%)	0 (0%)	0 (0%)
Time point sampling (days after HSCT), median (range)	425 (270–1438)	589 (229–1299)	239 (137–364)	204 (149–237)

AML acute myeloid leukemia, MDS myelodysplasia, ATG anti-thymocyte antibodies, PT-Cy post-transplant cyclophosphamide, GvHD graft-versus-host disease, HSCT haematopoietic stem cell transplant, CMV cytomegalovirus

\*Clinically relevant CMV reactivation is defined as a CMV reactivation requiring systemic preemptive antiviral treatment in accordance to institutional guidelines (DNAemia > 1000 cp/ml, measured on plasma)

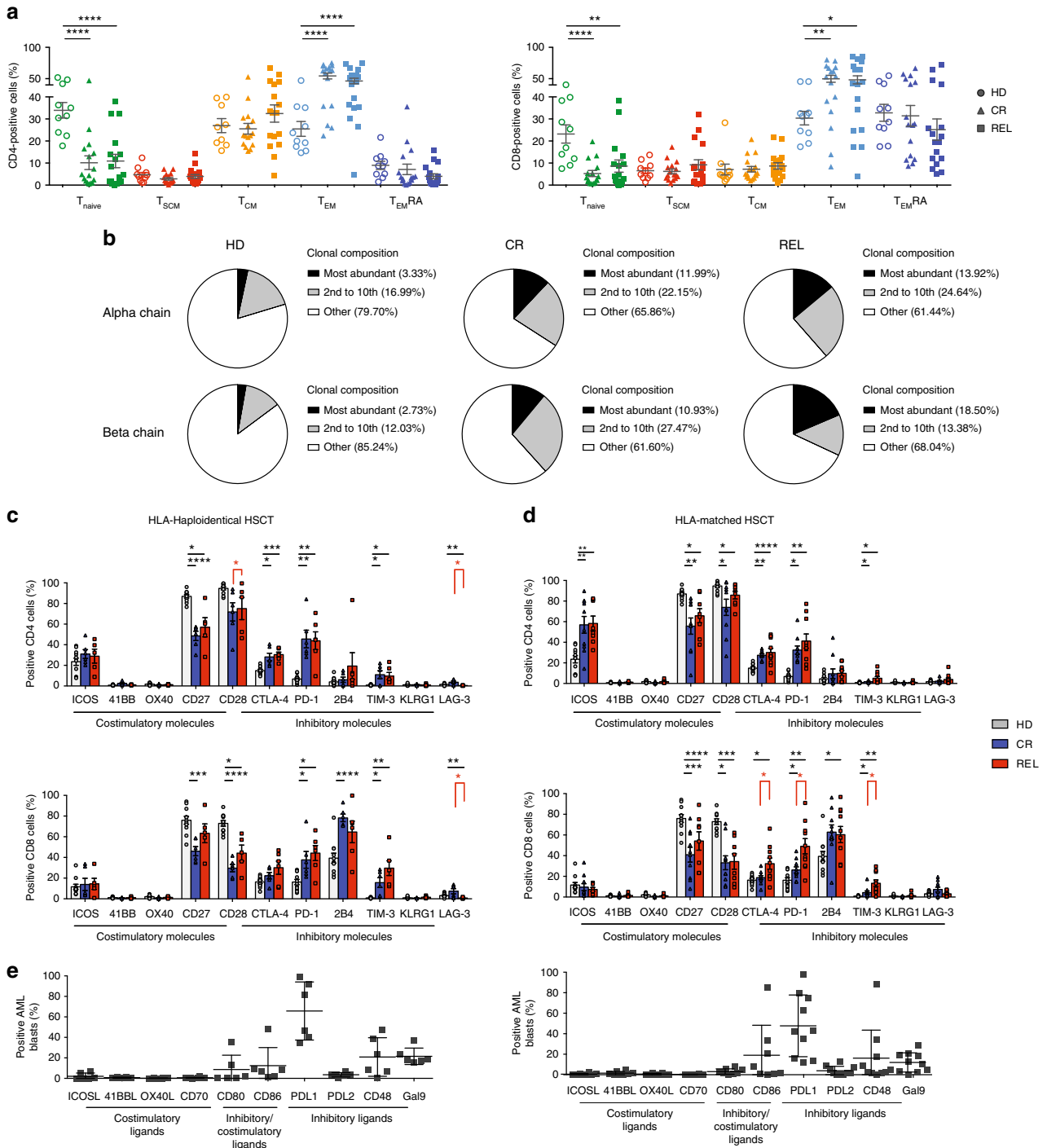
perturbations detected in BM-T cells were also observed in the peripheral blood (Supplementary Fig. 3a, b).

Of notice, at relapse, leukemic blasts expressed CD80 and CD86, ligands for both CD28 and CTLA-4, PD-L1 (ligand of PD-1), CD48 (ligand of 2B4), and Galectin-9 (ligand of TIM-3, Fig. 1e), suggesting that the inhibitory receptors expressed by BM-T cells could be triggered directly by the relapsing blasts. Interestingly, a positive correlation was observed between the proportion of TIM-3<sup>+</sup> CD8<sup>+</sup> T cells and the frequencies of Galectin-9<sup>+</sup> AML blasts in HLA-matched transplanted patients (Supplementary Fig. 3c).

Overall, our results reveal a dominant effect of the transplant procedure on the BM-T-cell functional profile, lasting 1 year after

transplant. In addition, in patients relapsing after HLA-matched HSCT, we observed that PD-1<sup>+</sup>CTLA-4<sup>+</sup>TIM-3<sup>+</sup> exhausted CD8<sup>+</sup> T cells accumulate in the bone marrow. The pattern of inhibitory ligand expression on AML blasts at relapse implies an active immunosuppressive process, underscoring the possible relevance of these IRs in AML progression. According to these observations, we further investigated the functional profile of BM-T cells in patients receiving HLA-matched HSCT.

**BH-SNE algorithm segregates IR<sup>+</sup> relapse-specific clusters.** To validate our findings by an unsupervised approach and identify putative cellular populations associated to clinical outcome, we



**Fig. 1** T-cell subset phenotype in the bone marrow of HSCT patients differs according to the clinical outcome and transplant type. **a** Proportion of naive ( $CD45RA^+CD62L^+CD95^-$ ,  $T_{naive}$ ), memory stem ( $CD45RA^+CD62L^+CD95^+$ ,  $T_{SCM}$ ), central memory ( $CD45RA^-CD62L^+$ ,  $T_{CM}$ ), effector memory ( $CD45RA^-CD62L^-$ ,  $T_{EM}$ ) T cells and terminal effectors ( $CD45RA^+CD62L^-$ ,  $T_{EMRA}$ ) over the total  $CD4^+$  and  $CD8^+$  BM-T-cell subsets in healthy donors (HD,  $N = 11$ ), in patients who achieved long-term complete remission (CR,  $N = 16$ ) and in patients who experienced relapse (REL,  $N = 16$ ) after HSCT. **b** Pie charts depicting the relative abundance of T-cell clones in each study group (HD,  $N = 3$ ; CR,  $N = 3$ ; REL,  $N = 3$ ) obtained after CDR3 sequencing of both TCR- $\alpha$  and TCR- $\beta$  chains. **c, d** Percentages of BM-infiltrating  $CD4^+$  and  $CD8^+$  T cells positive for costimulatory or inhibitory receptors in HLA-haploidentical ( $N = 12$ , **c**) or HLA-matched ( $N = 20$ , **d**) transplant settings; bone marrow samples from healthy donors were used as controls (HD,  $N = 11$ ). **e** Percentages of leukemic blasts at relapse expressing costimulatory or inhibitory ligands in patients receiving HLA-haploidentical (left) or HLA-matched (right) transplants. All the inhibitory receptors have been visualized by means of cell surface staining apart for CTLA-4, visualized after cell fixation and permeabilization. Individual patient data points, mean, and SEM are shown. Statistically significant differences between CR and REL groups are highlighted in red, the differences between patients' groups and HD in black. \* $p < 0.05$ ; \*\* $p < 0.01$ ; \*\*\* $p < 0.001$ ; \*\*\*\* $p < 0.0001$ ; nonparametric unpaired two-sided T test



analyzed our data with BH-SNE (Barnes-Hut Stochastic Neighbor Embedding<sup>22</sup>), a dimensionality reduction algorithm that attributes two new variables (BH-SNE1 and BH-SNE2) to each event (i.e., the single cell in flow cytometry), considering as discriminants all the fluorochromes at a time.

HLA-matched patients ( $N = 20$ ) and healthy donors ( $N = 10$ ) bone marrow samples were analyzed by BH-SNE after unsupervised and stochastic data downscaling, in which ~7500 events among CD3<sup>+</sup> lymphocytes were chosen from each file (Fig. 2a). The two newly calculated variables BH-SNE1 and BH-SNE2 allowed data to be visualized in a single two-dimensional plot. If divided according to three experimental groups, HD, CR, and REL, the events clustered in different areas. When considering a region of high density for each experimental group (black rectangles in Fig. 2a), higher mean fluorescence intensities (MFI) for inhibitory receptors in case of REL were observed.

To better identify discrete spatial regions of the BH-SNE plot specifically associated to each experimental group, we deployed the clustering algorithm K-means (Fig. 2b). First, we calculated K-means on BH-SNE1 and BH-SNE2 variables, dividing the plot in 200 meta-clusters; then, we attributed meta-clusters to either HD, CR or REL when more than 55% of the events were specific for one experimental group. Two series of BH-SNE analysis for each sample were performed, since the markers of interest were divided into two distinct flow-cytometry panels (panel 1 and panel 2, Fig. 2c). In total, 32 and 34 meta-clusters were attributed to HD in panel 1 and in panel 2, respectively; 9 and 16 meta-clusters were attributed to CR while 15 and 17 to REL. We calculated the relative fluorescence intensity (RFI) for each marker of each meta-cluster in panels 1 and 2 and observed a higher RFI in case of relapse for PD-1, KLRG1 and TIM-3 when compared with HD and CR (Fig. 2d). The analysis with BH-SNE algorithm also revealed that most (81.3%) HD meta-clusters did not express IRs, while only a fraction (17.7%) of them expressed only one IR. In the CR group, the majority (64.0%) of meta-clusters was negative for IRs, while in REL patients only one-third was IR negative and 67.8% expressed one or more IRs (Fig. 2e). In conclusion, this unsupervised approach revealed the presence, in relapsing patients, of distinct T-cell populations characterized by high expression of multiple inhibitory receptors.

### Early-differentiated CD8<sup>+</sup> BM-T cells at relapse are exhausted.

Since most differences in IR profiles observed in REL versus CR patients clustered in CD8<sup>+</sup> BM-T cells, we focused on this T-cell subset and investigated how the exhaustion profile was modulated at different stages of memory CD8<sup>+</sup> T-cell differentiation in the BM of patients after HLA-matched HSCT. The gating strategy of the flow-cytometry analysis is reported in Supplementary Fig. 1. In HD (Fig. 3a, b), the expression of inhibitory receptors 2B4 and PD-1 was confined to T<sub>EM</sub> (mean 2B4: 69.2%; PD-1: 25.7%) and terminal effectors T<sub>EM</sub>RA (2B4 69.8% and PD-1 11.0%), while CTLA-4 expression was more equally distributed in all differentiation stages, and TIM-3, KLRG1 and LAG-3 were barely detectable. In CR patients, CD8<sup>+</sup> BM-T cells recapitulated almost completely the pattern observed in HD. At relapse, T<sub>EM</sub> and T<sub>EM</sub>RA showed an inhibitory receptor profile similar to that of CR patients, with the exception of PD-1, more homogeneously expressed (46.4% and 29.6%, respectively in T<sub>EM</sub> and T<sub>EM</sub>RA). Strikingly, however, in REL patients, a high proportion of early-differentiated CD8<sup>+</sup> T cells displayed an exhausted phenotype. A higher frequency of T<sub>CM</sub> expressed 2B4 (mean 54.5%), PD-1 (33.8%), and TIM-3 (14.6%) in REL patients compared with HDs (2B4 12.0%,  $p < 0.0001$ ; PD-1 9.8%,  $p < 0.01$ ; TIM-3 1.9%,  $p < 0.01$ ). Furthermore, the proportion of TIM-3<sup>+</sup> T<sub>CM</sub> cells was higher in REL than in CR patients (3.6%,  $p < 0.01$ ). These

differences were even more pronounced in BM-T<sub>SCM</sub> cells, a higher percentage of which expressed PD-1 (30.6%), TIM-3 (15.1%), and KLRG1 (14.7%) in REL patients than in HDs (PD-1 3.8%, TIM-3 1.1%, KLRG1 1.6%;  $p < 0.001$ ) or CR patients (PD-1 7.6%,  $p < 0.01$ ; TIM-3 3.7%,  $p < 0.001$ ; KLRG1 1.4%,  $p < 0.001$ ). Finally, a higher proportion of BM-T<sub>SCM</sub> cells from REL patients expressed 2B4 (mean 51.0%) compared with HDs (2B4 23.0%,  $p < 0.05$ ).

Unsupervised clustering analysis summarized in the heatmap of Fig. 3c shows (left to right) an enrichment of BM-T cells expressing IRs correlating with progressive T-cell differentiation and unfavorable clinical outcome. Interestingly, the right part of the heatmap contains late differentiated T cells of all patient cohorts and early-differentiated T cells only belonging to relapsing patients, indicating that this T-cell subset is assimilated to more differentiated (and exhausted) effectors when relapse occurs. Altogether, these results show that early-differentiated CD8<sup>+</sup> BM-T cells in patients who relapse after HLA-matched HSCT display an exhausted phenotype.

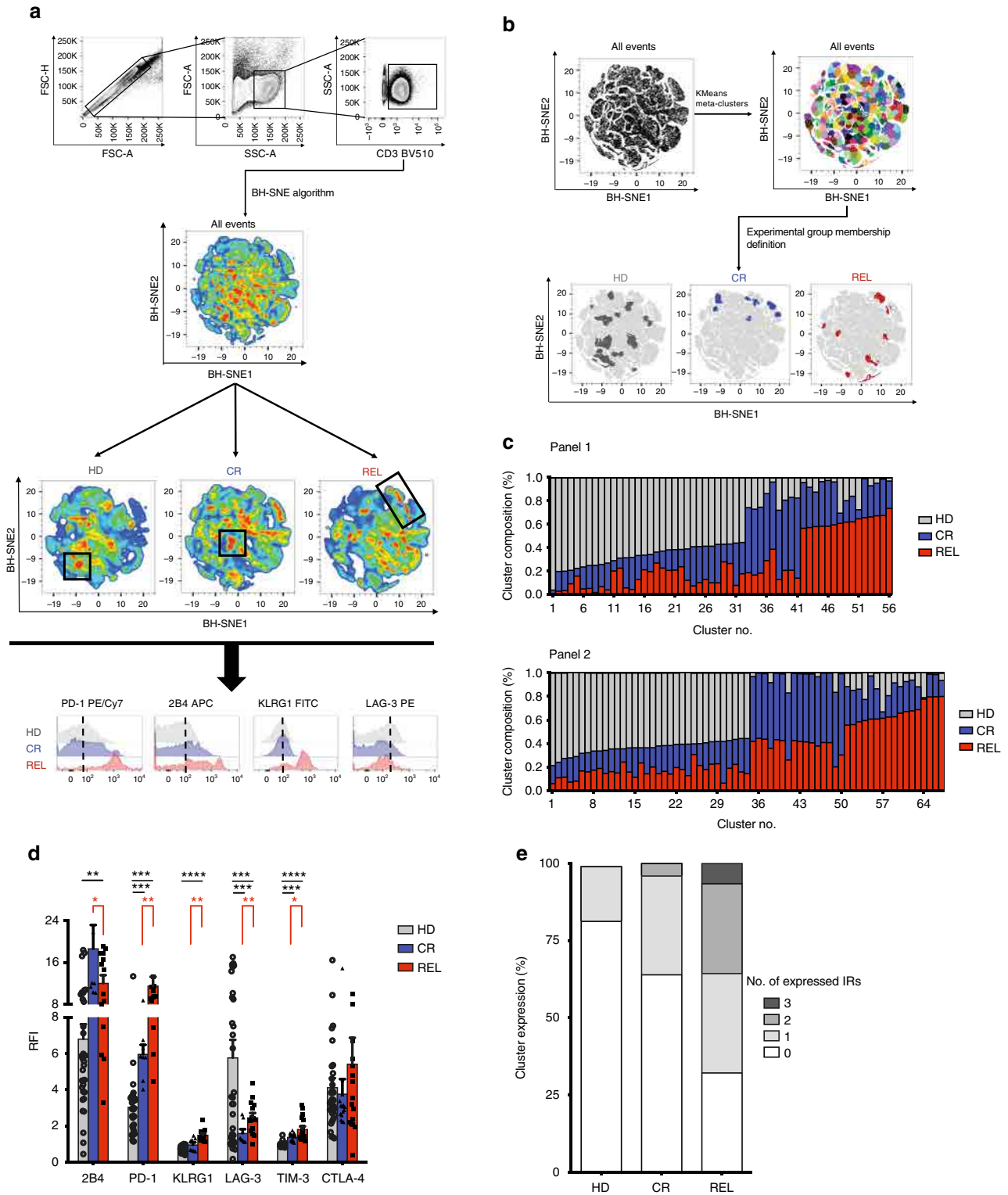
### BM-T cells at AML relapse are functionally impaired.

Polyfunctionality is a relevant measure of T-cell fitness<sup>23</sup>. We thus evaluated the function of BM-T cells by analyzing the production of IL-2, IFN- $\gamma$ , and TNF- $\alpha$  cytokines and the expression of CD107a upon activation with a polyclonal stimulus. The proportions of both early CD62L<sup>+</sup> (Fig. 4a) and late CD62L<sup>-</sup> (Fig. 4b) differentiated BM-T cells simultaneously displaying four effector functions were lower in REL patients compared with HD and CR. In relapsing patients, T-cell hyporesponsiveness appeared largely due to reduced degranulation, since both early- and late-differentiated T cells showed defects in CD107a expression, both when measured alone or in combination with cytokine production (Fig. 4a, b). Altogether these data indicate that at the primary disease site both early- and late-differentiated T cells manifest a partial functional impairment, in accordance with the inhibitory receptor profile in relapsing patients.

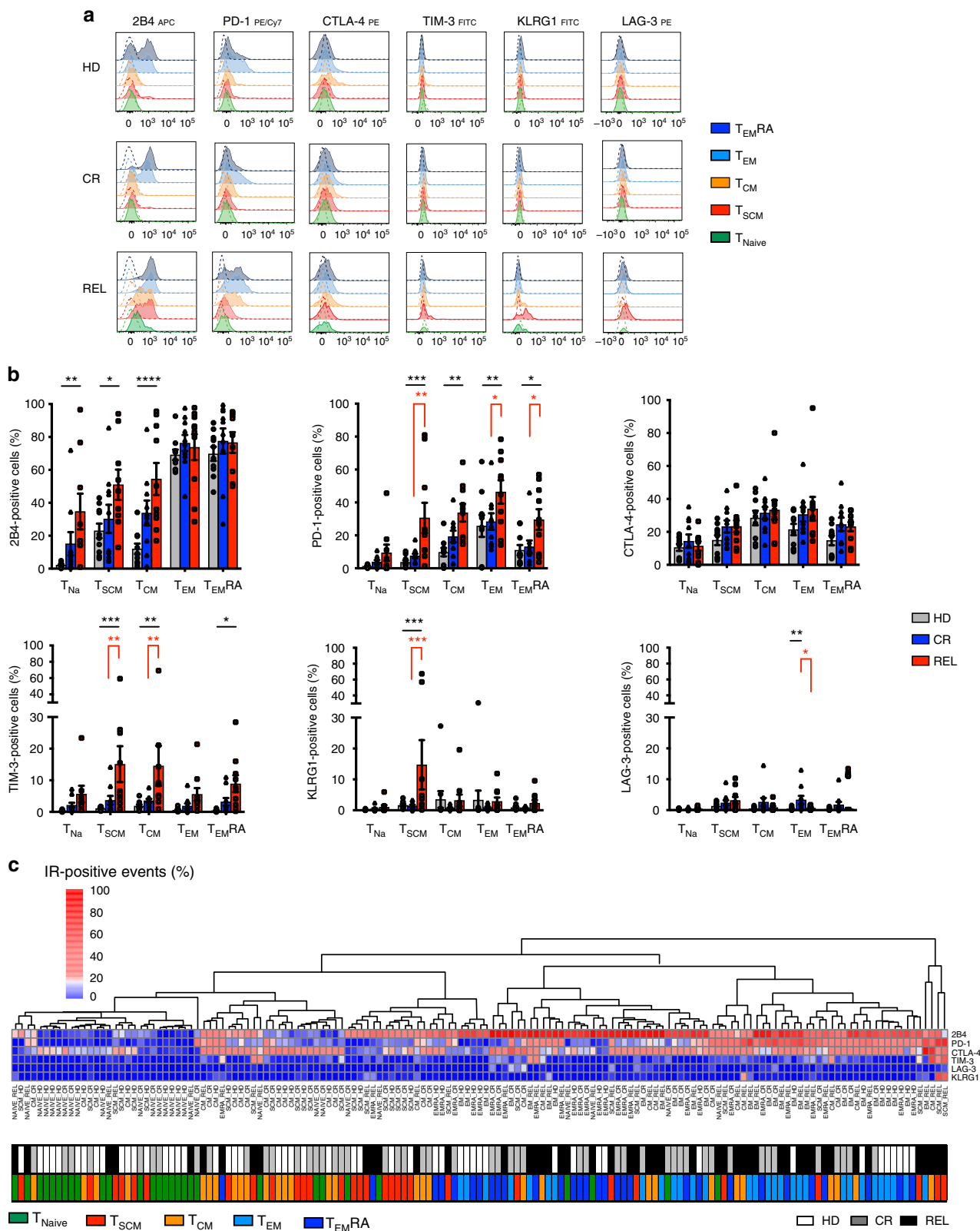
### IR<sup>+</sup> BM-T cells at relapse display leukemia specificities.

Exhaustion of tumor-infiltrating lymphocytes is currently ascribed to several mechanisms, including inhibitory signals and chronic antigen exposure promoted by cancer cells and tumor microenvironment<sup>24</sup>. It can thus be assumed that exhausted lymphocytes at the tumor site are enriched in tumor-specific T cells. To verify this hypothesis, BM-T cells from six REL patients were sorted in IR<sup>+</sup> cells, based on the expression of at least one inhibitory receptor, and IR<sup>-</sup> cells (Fig. 5a). The comparative analyses of the TCR repertoire showed a higher abundance of the 10 strongest clonotypes in IR<sup>+</sup> than in IR<sup>-</sup> lymphocytes, confirmed with both TCR- $\alpha$  and  $\beta$ -chain sequences (Fig. 5b), suggesting a more restricted T-cell repertoire in IR<sup>+</sup> cells. Sorted IR<sup>+</sup> and IR<sup>-</sup> BM-T cells expanded in vitro with a similar kinetic and magnitude upon rapid expansion protocol and high doses of IL-2<sup>25</sup> (Fig. 5c), indicating that the exhausted phenotype can be reverted in culture, as already reported<sup>26</sup>. Upon in vitro culture, IR<sup>+</sup> cells recovered the ability to degranulate and produce IFN- $\gamma$  and TNF- $\alpha$  (Fig. 5d, e); however, expanded cells differentiate in late effector T cells and, accordingly, did not fully recover IL-2 production capacity. Most interestingly, despite no enrichment for leukemia-specific T cells was performed in vitro, a higher proportion of IR<sup>+</sup> lymphocytes recognized autologous leukemic blasts compared with IR<sup>-</sup> cells in vitro, as demonstrated by granzyme A and B production (IR<sup>+</sup> and IR<sup>-</sup>: 762.6 pg/mL, vs. 0 pg/mL;  $p < 0.001$ ; Fig. 5f) and cytotoxicity (elimination index: 62.2% for IR<sup>+</sup> vs. 43.5% for IR<sup>-</sup> at 100:1 E:T ratio;  $p < 0.05$ ; Fig. 5g). Taken together, these results indicate that exhausted





**Fig. 2** BH-SNE and K-means tandem application evaluates IR coexpression. **a** A median of 7500 CD3<sup>+</sup> lymphocytes from bone marrow samples were studied with BH-SNE algorithm (top) and plotted according to the calculated variables BH-SNE1 and BH-SNE2 (mid); the events were then split into three density plots according to the study group they belong to (healthy donors,  $N = 10$  HD; patients achieving long-term remission after transplant, CR  $N = 10$ ; and patients experiencing post-transplant relapse, REL  $N = 10$ ); representative histograms of PD-1, 2B4, KLRG1, and LAG-3 from selected areas are reported (bottom). **b** K-means algorithm was applied to BH-SNE1 and BH-SNE2 variables, and a fraction of the identified meta-clusters were attributed to each experimental group (HD, CR, and REL). **c** Composition of meta-clusters ascribed to a specific experimental group (variables analyzed in panel 1 and panel 2 are detailed in the Methods section). **d, e** HD-, CR-, or REL-specific meta-clusters were described in terms of both relative fluorescence intensity (RFI, **d**) and multiple expression (**e**) of inhibitory receptors. Individual patients datapoint, means, and SEM are shown. Statistically significant differences between CR and REL groups are highlighted in red and the differences between patients' groups and HD in black. \* $p < 0.05$ ; \*\* $p < 0.01$ ; \*\*\* $p < 0.001$ ; \*\*\*\* $p < 0.0001$ ; nonparametric unpaired two-sided  $T$  test



T cells at the tumor site preferentially harbor specificities directed against leukemic blasts.

**Tumor-specific CD8<sup>+</sup> BM-T cells are exhausted early after HSCT.** Having observed that BM-infiltrating T cells of HLA-matched patients are exhausted at the time of disease recurrence,

we hypothesized that this dysfunctional profile could be detected also before relapse.

We retrospectively analyzed T cells harvested from the BM of 57 patients at early time points (median 68 days) after HLA-matched HSCT. Patients characteristics are detailed in Table 2, and gating strategies for flow-cytometry data are summarized in

**Fig. 3** Exhausted CD8<sup>+</sup> T<sub>SCM</sub> and T<sub>CM</sub> infiltrate the bone marrow of relapsing patients. **a** Representative histograms showing the inhibitory receptor expression profile in CD8<sup>+</sup> naive (CD45RA<sup>+</sup>CD62L<sup>+</sup>CD95<sup>-</sup>, T<sub>naive</sub>), memory stem (CD45RA<sup>+</sup>CD62L<sup>+</sup>CD95<sup>+</sup>, T<sub>SCM</sub>), central memory (CD45RA<sup>-</sup>CD62L<sup>+</sup>, T<sub>CM</sub>), effector memory (CD45RA<sup>-</sup>CD62L<sup>-</sup>, T<sub>EM</sub>) T cells, and terminal effectors (CD45RA<sup>+</sup>CD62L<sup>-</sup>, T<sub>EM</sub>RA) in healthy donors (HD, N = 10), in HLA-matched patients maintaining complete remission (CR, N = 10) or relapsing after transplant (REL, N = 10). Fluorescence-minus one (FMO) negative controls (dashed lines) are shown for each subpopulation. **b** Relative proportion of IR-expressing CD8<sup>+</sup> T cells in each memory subpopulation from the different experimental groups (HD, CR, and REL). **c** Heatmap representing percentage of positive cells for all samples classified according to the memory differentiation status (N = 5 inputs per samples, N = 150 total inputs); every input was associated with two colored tags, one referring to the memory status (T<sub>Na</sub> green, T<sub>CM</sub> orange, T<sub>SCM</sub> red, T<sub>EM</sub> light blue, T<sub>EM</sub>RA dark blue) and one to the experimental group (HD white, CR gray, REL black). All the inhibitory receptors have been visualized by means of cell surface staining apart for CTLA-4, visualized after cell fixation and permeabilization. Individual patient data points, means, and SEM are shown. Statistically significant differences between CR and REL groups are highlighted in red and the differences between patients' groups and HD in black. \**p* < 0.05; \*\**p* < 0.01; \*\*\**p* < 0.001; \*\*\*\**p* < 0.0001; two-way ANOVA with no matching coupled with Sidak multiple correction test

Supplementary Fig. 4. We detected a low CD4/CD8 T-cell ratio (Supplementary Fig. 5a) with a percentage of naive CD4<sup>+</sup> and CD8<sup>+</sup> BM-T cells lower in transplanted patients than in HD, independently of the clinical outcome, while effectors appeared enriched (Supplementary Fig. 5b, c). The expression of IRs was high and neither did not differ according to the clinical outcome, when studied on total CD8<sup>+</sup> BM-T cells, nor on T-cell memory subpopulations (Supplementary Fig. 5d, e) indicating that the transplant procedure dominates and shapes the CD8<sup>+</sup> T-cell profile early after transplant. We hypothesize that in this early phase, in which alloreactivity is dominant, the expression of inhibitory receptors might reflect the largely activated status of BM-T cells. According to this hypothesis, a large proportion of CD8<sup>+</sup> BM-T cells, at early time points expressed the HLA-DR activation marker (Supplementary Fig. 5d). In such a highly activated immunological setting, we attempted to identify putative terminally exhausted T cells among total CD8<sup>+</sup> BM-T cells, defined based on the expression of PD1, Eomes and T-bet<sup>27</sup>. As shown in Fig. 6a, we found a significant enrichment in PD-1<sup>+</sup> Eomes<sup>+</sup> T-bet<sup>-</sup> T<sub>SCM</sub> cells in the BM of REL patients compared with the CR ones, suggesting that a small fraction of severely exhausted memory T<sub>SCM</sub> preferentially accumulates early after transplant in patients prone to relapse. To verify our results with an unsupervised approach, sensitive to small cellular populations, we applied the BH-SNE algorithm, and observed that 6 (54%) out of 11 and 11 (84%) of the 13 clusters specific for CR and REL, respectively, were negative for the expression of HLA-DR. The analysis of these HLA-DR negative clusters revealed higher expression of TIM3, 2B4, LAG3, GITR, and KLRG1 in REL than in CR (Fig. 6b). Overall, this analysis indicates the presence of a small population of not activated (HLA-DR<sup>-</sup>) BM-T cells that differentially express IRs in patients prone to relapse versus patients destined to long-term CR. To verify whether dysfunctional T cells are enriched in tumor-specificities at this early time point, we took advantage of MHC dextramers to identify tumor-specific (WT1, PRAME, or EZH2) and control viral-specific (cytomegalovirus-CMV) CD8<sup>+</sup> T cells from patients. We observed that viral-specific T cells were IR<sup>-</sup> independently of the ultimate clinical outcome. Furthermore, also most tumor-specific T cells retrieved from CR patients did not express IRs. By contrast, a large number of tumor-specific T cells present in the REL group expressed IRs (Fig. 6c). In particular, >50% of tumor-specific T cells in the REL group expressed at least one IR, while 29% of these cells expressed four IRs, consistent with a profound functional exhaustion (Fig. 6d). Collectively, these data strongly suggest that antitumor T-cell reactivity is already impaired early after transplant in the patients who subsequently relapse.

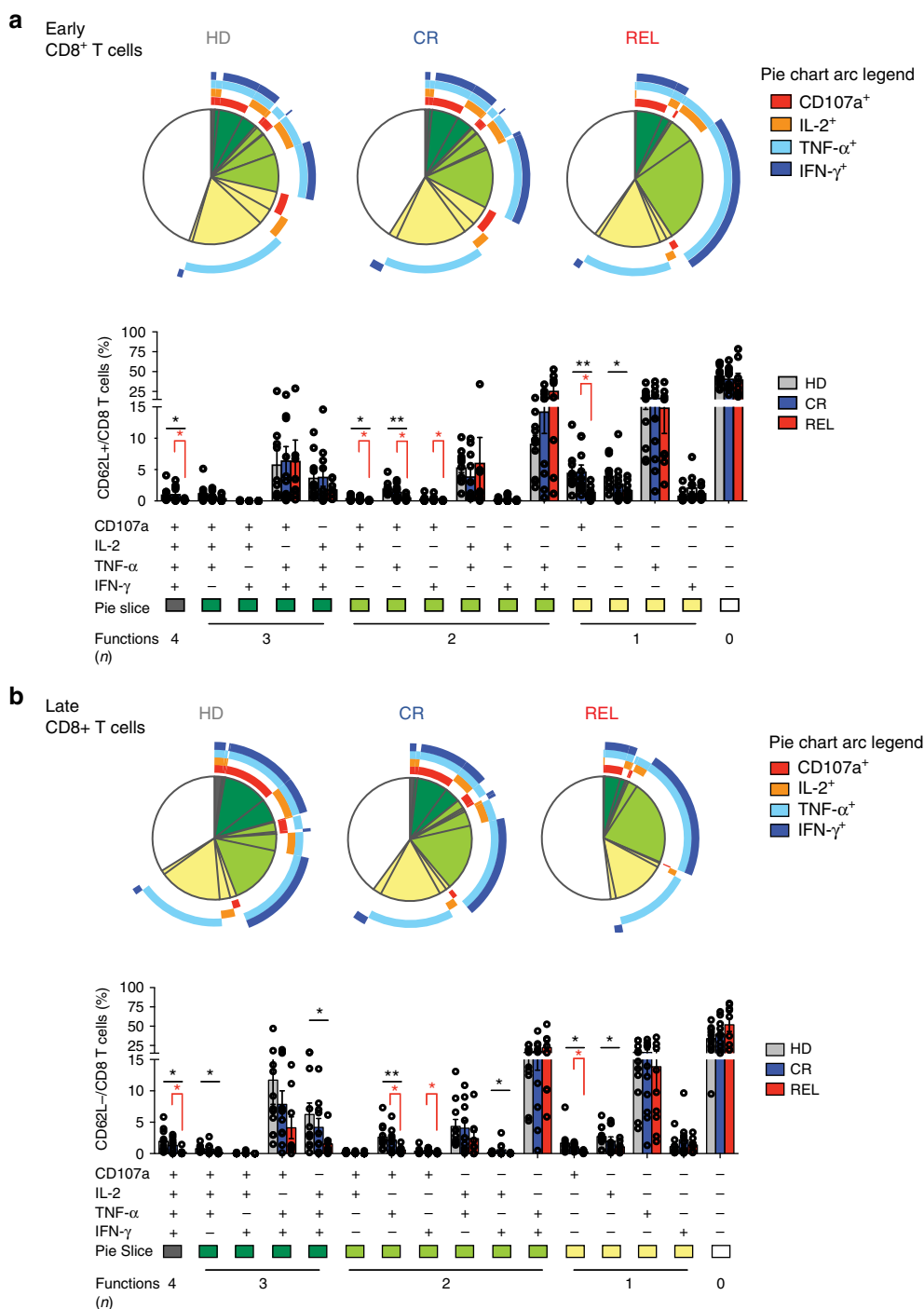
## Discussion

IRs modulate T-cell responsiveness and act as negative feedback mechanisms limiting T-cell activation during antigen exposure.

Recent findings show that tumors often hijack IRs to acquire protection from immune attack<sup>24</sup>. In the present work, we show that CD8<sup>+</sup> BM-T cells exhibit a unique exhaustion signature in patients relapsing after HLA-matched transplants and that such signature defines antitumor T cells in the setting of disease relapse. While in previous studies IR expression was assessed on circulating T cells and after transplant<sup>28–30</sup>, we concentrated our efforts mainly on T cells infiltrating the bone marrow, the primary site of the disease, based on the concept that cancer cells and their microenvironment play a critical role in modulating T-cell exhaustion<sup>31</sup>.

In this study, we focused on patients who relapsed after a phase of clinical remission lasting a median of 1 year. This choice had several reasons. First, in the early time points after HSCT, the pro-inflammatory milieu may alter the T-cell profile independently of disease recurrence, for example resulting in high expression of PD-1 on T lymphocytes in patients with aGvHD or CMV reactivation<sup>32</sup>. Second, leukemia-resistance mechanisms acquired against the immunological pressure imposed by HSCT might require time to fully unfold. Indeed, we reported that after HLA-haploidentical HSCT, HLA-loss occurs later than other forms of relapse<sup>14</sup>. To discriminate between the effects of the transplant procedure and those linked to the disease, the results obtained from relapsing patients were compared with those obtained both in healthy donors and in patients who maintained a long-term status of complete remission. We balanced the experimental groups with respect to relevant clinical variables, such as donor source, conditioning regimen, CMV serostatus, and GvHD incidence and evaluated patients in the absence of active inflammation, e.g., infections or GvHD.

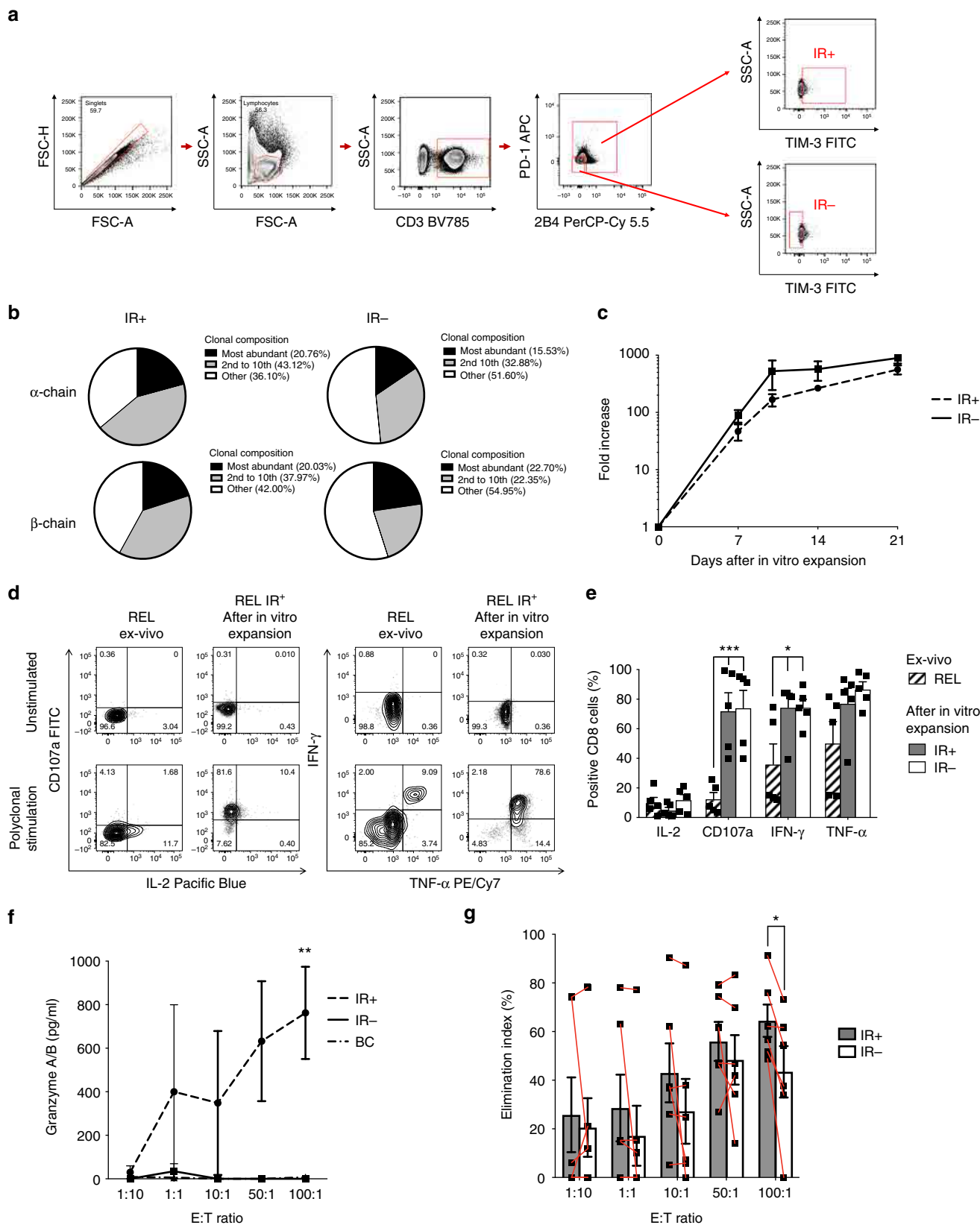
We initially investigated the distribution of T-cell subsets both in PB and BM of transplanted patients at early and late time points. In the context of T repleted haploidentical HSCT, we and others recently showed an early wave of T<sub>SCM</sub> cell accumulation in the peripheral blood within the first 30 days after HSCT<sup>7,8</sup>. Here, we focused on the time of relapse (1 year, for non-relapsing patients) showing that the proportion of T<sub>SCM</sub> cells, similarly to all other memory T-cell subsets, is not affected by clinical outcome. Our data suggest that, also at late time points the transplant procedure dominates in instructing T-cell differentiation by eroding the naive T-cell compartment and promoting T<sub>EM</sub> accumulation in the BM, in all transplant settings, an effect likely due to the continuous exposure to viral and/or allo-antigens after HSCT. Interestingly, we observed an increased frequency of T<sub>regs</sub> in the BM of REL patients compared with CR. The T<sub>reg</sub> accumulation has been linked to T-cell exhaustion in recent studies on chronic viral infections<sup>33</sup> and on relapsed/refractory lymphoma patients<sup>34</sup>. However, the phenotypic portrait of exhausted T cells appears more complex and driven by several IRs<sup>16,35</sup>. We screened T cells in the BM of HSCT patients for the expression of six different IRs, i.e., PD-1, CTLA-4, TIM-3, LAG-3, 2B4, and



**Fig. 4** CD8<sup>+</sup> BM-T cells from relapsing patients display defective polyfunctionality. Cytokine production (IL-2, TNF-α, IFN-γ) and degranulation capacity (CD107a expression) of CD8<sup>+</sup> T cells upon PMA/Ionomycin stimulation were evaluated in bone marrow samples. **a, b** Pie charts with arcs (upper part) and bar chart (lower part) showing the relative proportion of CD8<sup>+</sup> T cells performing four, three, or two multiple effector functions or one or no effector functions in early-differentiated (CD62L<sup>+</sup>, **a**) and late differentiated (CD62L<sup>-</sup>, **b**) subsets. Healthy donors (HD, N = 10), HLA-matched patients maintaining complete remission (CR, N = 10) or relapsing after transplant (REL, N = 10) were evaluated. Arcs represent which function was exerted, alone or in combination with the others (CD107a, IL-2, TNF-α, and IFN-γ). Individual patient data points, means, and SEM are shown. Statistically significant differences between CR and REL groups are highlighted in red and the differences between patients' groups and HD in black. \**p* < 0.05; \*\**p* < 0.01; \*\*\**p* < 0.001; \*\*\*\**p* < 0.0001, nonparametric unpaired two-sided *T* test

KLRG1. When subjects were segregated by transplant type, we found that in the HLA-matched HSCT context, the proportion of CD8<sup>+</sup> T cells infiltrating the BM of REL patients expressing PD-1, CTLA-4, and/or TIM-3 was higher than in patients in CR. This

was not the case in the haploidentical setting, and this effect, imputable to donor type, could be explained by the higher degree of HLA-mismatch between donor and host that could exacerbate the pro-inflammatory milieu in HLA-haploidentical patients,



independently of the occurrence of relapse. We cannot rule-out, however, a time-dependent effect, since post-transplant samples were harvested earlier in haplo-recipients than in HLA-identical HSCT.

Given the high number of markers screened, and with the aim of analyzing them simultaneously, we implemented the BH-SNE algorithm to allow low-dimensional embedding of complex flow-cytometry data<sup>36</sup>. In HLA-matched patients, the unsupervised



**Fig. 5** The functional exhaustion of IR<sup>+</sup> BM-T cells at relapse is reverted in vitro. BM-infiltrating CD8<sup>+</sup> T cells from  $N = 6$  patients experiencing relapse were isolated according to the expression of IRs and expanded in vitro. **a** Gating strategy for the definition of IR<sup>+</sup> (expression of at least one IR among TIM-3, PD-1, and 2B4) and IR<sup>-</sup> (TIM-3<sup>-</sup> PD-1<sup>-</sup> 2B4<sup>-</sup>) T cells. **b** Pie charts depicting the relative abundance of T-cell clones in IR<sup>+</sup> ( $N = 3$ ) and IR<sup>-</sup> ( $N = 2$ ) cells obtained after CDR3 sequencing of both TCR- $\alpha$  and TCR- $\beta$  chains. **c** Expansion rate of IR<sup>+</sup> and IR<sup>-</sup> T cells after in vitro polyclonal stimulation with OKT3 in presence of high doses of IL-2. **d, e** Representative plots (**d**) and bar graph (**e**) showing T-cell effector functions measured on ex vivo samples (dashed bars) or on in vitro expanded IR<sup>+</sup> (black bars) and IR<sup>-</sup> (white bars) T cells after short-term polyclonal stimulation (PMA/Ionomycin); two-way ANOVA with no matching coupled with Sidak multiple corrections test was used for statistical analyses. **f, g** IR<sup>+</sup> and IR<sup>-</sup> T cells, expanded in vitro upon polyclonal stimulation and in the absence of any procedure to enrich for leukemia-specific T cells, were co-cultured with matched AML blasts at different effector-to-target (E:T) ratios; at day 1, Granzyme A and B production was quantified (**f**), and at day 3 the elimination index (**g**) was calculated; two-way ANOVA with no matching coupled with Sidak multiple corrections test and nonparametric paired two-sided  $T$  test were used for statistical analyses, respectively. Means and SEM are shown. \* $p < 0.05$ ; \*\* $p < 0.01$ ; \*\*\* $p < 0.001$

BH-SNE analysis identified clusters of BM-T lymphocytes associated to relapse characterized by high levels of IRs and coexpression of multiple IRs, supporting the hypothesis that, at relapse, a large proportion of T cells are exhausted.

None of the IRs identified at the time of relapse was unequivocally associated to the clinical outcome when looking at the BM at early time points, before relapse. We hypothesized that this early phase after HSCT may be dominated by alloreactivity and that the expression of inhibitory receptors might reflect the largely activated status of BM-T cells, which masks the detection of exhausted cells. To better discriminate exhaustion from T-cell activation, a status that indeed includes IR expression on T cells, we took advantage of the BH-SNE algorithm and we observed that coexpression of multiple IRs on T cells lacking the HLA-DR activation marker, defines an exhausted T-cell population significantly enriched in patients prone to relapse.

The expression profile of IRs is often associated with the progressive T-cell differentiation status<sup>37,38</sup>. A quite remarkable finding of the present study is the observation that early-differentiated T<sub>SCM</sub> and T<sub>CM</sub> at relapse display an exhaustion signature suggesting a pervasive status of T-cell dysfunction associated with the failure to control the disease. A key question is what is the biological role of inhibited T<sub>SCM</sub>/T<sub>CM</sub>, whether they contribute to the development of leukemia relapse and whether they are responsible to the maintenance of the pool of exhausted effectors. Interestingly, a small population of PD-1<sup>+</sup> Eomes<sup>+</sup> T-bet<sup>-</sup> severely exhausted T cells, displaying a T<sub>SCM</sub> phenotype, were found enriched in the bone marrow of REL patients well before relapse occurred, and the coexpression of multiple IRs on BM T cells, early after HSCT, was highly associated with the risk of relapse. These results suggest that early-differentiated dysfunctional T cells may contribute to the establishment of an immunosuppressive tumor microenvironment, ultimately facilitating relapse, in accordance to the observations reported in the setting of chronic viral infections<sup>27</sup>. The generation of such exhausted T cells at an early time point might be the result of a continuous aberrant antigen presentation mediated by residual leukemic cells not detected by routine screening techniques. It is tempting to speculate that exhaustion of early-differentiated T cells might curtail the long-term reservoir of leukemia-reactive donor T cells, thus facilitating disease relapse. In accordance with this hypothesis, we observed that most tumor-specific T cells retrieved in patients prone to relapse, displayed an exhausted phenotype, whereas the same tumor specificities identified in CR patients were functionally fit and did not express IRs.

The T-cell exhaustion phenotype was challenged in functional assays. In relapsing patients, CD8<sup>+</sup> BM-T cells display a reduced IL-2 production and degranulation capacity, while retaining the ability to produce TNF- $\alpha$  and IFN- $\gamma$ , a functional profile compatible with initial signs of exhaustion<sup>39</sup>. Notably, in vitro activation with high doses of IL-2 reverted the functional defect, as already reported in melanoma patients<sup>26</sup>.

A recently published work reported the increased coexpression of inhibitory molecules on circulating T cells recognizing minor histocompatibility antigens after allo-HSCT<sup>40</sup>. Of notice, in our experimental setting, IR<sup>+</sup> T cells infiltrating the BM of AML patients at relapse display a skewed TCR repertoire and, after in vitro expansion, in the absence of any procedure aimed at enriching for leukemia-specific T cells, displayed a greater ability to recognize matched leukemic blasts, compared with the IR<sup>-</sup> counterparts, indicating that IR expression marks lymphocytes enriched for tumor specificity.

The success of antibodies blocking immune checkpoints in oncology led to their approval for the cure of advanced solid tumors and of relapsed Hodgkin lymphoma as the first hematological indication<sup>41</sup>. Our study provides a rationale for the treatment and prevention of AML post-transplant relapses with multiple immune checkpoints-blocking agents to restore the function of leukemia-reacting T cells. Due to the broad expression of multiple IRs on T cells after transplantation, and the risk of exacerbating GvHD by blocking all relevant immunomodulatory axes in the entire T-lymphocytes population, innovative cell manipulation procedures should be explored to design specific leukemia-reactive cellular products, able to counteract the immunosuppressive leukemic microenvironment.

## Methods

**Study design and human biological samples.** In this retrospective study, we considered 32 leukemic patients who underwent allogeneic hematopoietic stem cell transplantation. Inclusion criteria were a diagnosis of acute myeloid leukemia or myelodysplastic syndrome, a relapse-free survival of at least 4 months after HSCT, absence of moderate-to-severe active GvHD, CMV infections, or other complications at the time of sampling. Relapsing patients fulfilling these criteria were initially identified. Since those patients received HSCT under a variety of treatment schedule<sup>42–44</sup>, we selected control patients showing similar clinical characteristic who maintained a status of long-term complete remission (follow-up > 3 years) to avoid late events of disease recurrence and misinterpretation of the results. Samples from relapsing patients were collected at relapse. Patients who maintained CR were evaluated at matched time points. Bone marrow samples from 18 healthy donors were analyzed in parallel as control. For the analyses at early time point, we recruited 57 patients (20 prone to relapse, 37 destined to long-term CR), at a median of 68 (range 28–180) days after HLA-identical HSCT.

PBMC and bone marrow samples were retrieved from the BioBank facility at San Raffaele, at the University Hospital Carl Gustav Carus Dresden, at the Leiden University Medical Centre (LUMC), at the University of Freiburg Medical Center, and at the Hokkaido University Faculty of Medicine where they were collected under written informed consent in agreement with the Declaration of Helsinki. Sample availability is limited and their use is under control and approval from the Ethical Committee of each of the participating institutes.

**Multiparametric flow cytometry.** PBMC and bone marrow samples were thawed and kept overnight at 37 °C at a concentration of  $1 \times 10^6$  cells/ml in complete X-vivo: X-vivo (Lonza) supplemented with glutamine 1%, penicillin/streptomycin 1%, human serum 2%, DNase (Roche) 1 IU/ml, and IL-2 20 IU/ml (Novartis). Samples were then stained with mouse fluorochrome-associated monoclonal antibodies specific for human CD3-BV510 (BioLegend, clone OKT3), CD4-PE/Dazzle (BioLegend, clone RPA-T4), CD8-BV785 (BioLegend, clone RPA-T8), CD25-APC/Cy7 (BioLegend, clone BC96), CD45RA-AF700 (BioLegend, clone HI100), CD45RA-PerCP/Cy5.5 (BioLegend, clone HI100), CD62L-AF700 (BioLegend, clone DREG-

**Table 2 Patients' characteristics at early time point follow-up**

	Long-term complete remission (CR)	Relapse (REL)
Number of patients, n	37	20
Diagnosis, n (%)		
AML	33 (89%)	18 (90%)
MDS	4 (11%)	2 (10%)
Donor type, n (%)		
HLA-matched sibling	29 (78%)	19 (95%)
HLA-matched MUD (9-10/10)	8 (22%)	1 (5%)
CMV serostatus donor/recipient, n (%)		
N.A.	3 (8%)	1 (5%)
pos/pos	30 (81%)	18 (90%)
pos/neg	2 (5%)	1 (5%)
neg/pos	1 (3%)	0 (0%)
neg/neg	1 (3%)	0 (0%)
Disease status at transplant, n (%)		
N.A.	3 (8%)	1 (5%)
Complete remission	29 (78%)	15 (75%)
Presence of disease	5 (14%)	4 (20%)
Conditioning regimen, n (%)		
N.A.	3 (8%)	1 (5%)
Reduced-intensity	2 (5%)	6 (30%)
Myeloablative, treosulfan-based	8 (22%)	3 (15%)
Myeloablative, other	24 (65%)	10 (50%)
In vivo T-cell depletion, n (%)		
N.A.	3 (8%)	3 (15%)
None	15 (41%)	3 (15%)
ATG	3 (8%)	2 (10%)
PT-Cy	14 (38%)	12 (60%)
ATG/PT-Cy	0 (0%)	0 (0%)
Other	2 (5%)	0 (0%)
GvHD prophylaxis, n (%)		
N.A.	1 (3%)	1 (5%)
CSA-based	16 (43%)	8 (40%)
Sirolimus-based	10 (27%)	6 (30%)
Other	10 (27%)	5 (25%)
Acute GvHD incidence, n (%)		
N.A.	4 (11%)	1 (5%)
Grade 0-I	30 (81%)	18 (90%)
Grade II-IV	3 (8%)	1 (5%)
Chronic GvHD incidence, n (%)		
None	34 (92%)	19 (95%)
Mild	2 (5%)	1 (5%)
Moderate	1 (3%)	0 (0%)
Severe	0 (0%)	0 (0%)
Under treatment for GvHD at the time of sampling, n (%)		
None	34 (92%)	16 (80%)
Yes		
0-1 mg/kg steroid	3 (8%)	4 (20%)
Yes, other	0 (0%)	0 (0%)
Time point sampling (days after HSCT), mean ± SD (range)	71 ± 35 (28-180)	66 ± 39 (28-174)

AML acute myeloid leukemia, MDS myelodysplasia, ATG anti-thymocyte antibodies, PT-Cy post-transplant cyclophosphamide, GvHD graft-versus-host disease, HSCT haematopoietic stem cell transplant, CMV cytomegalovirus

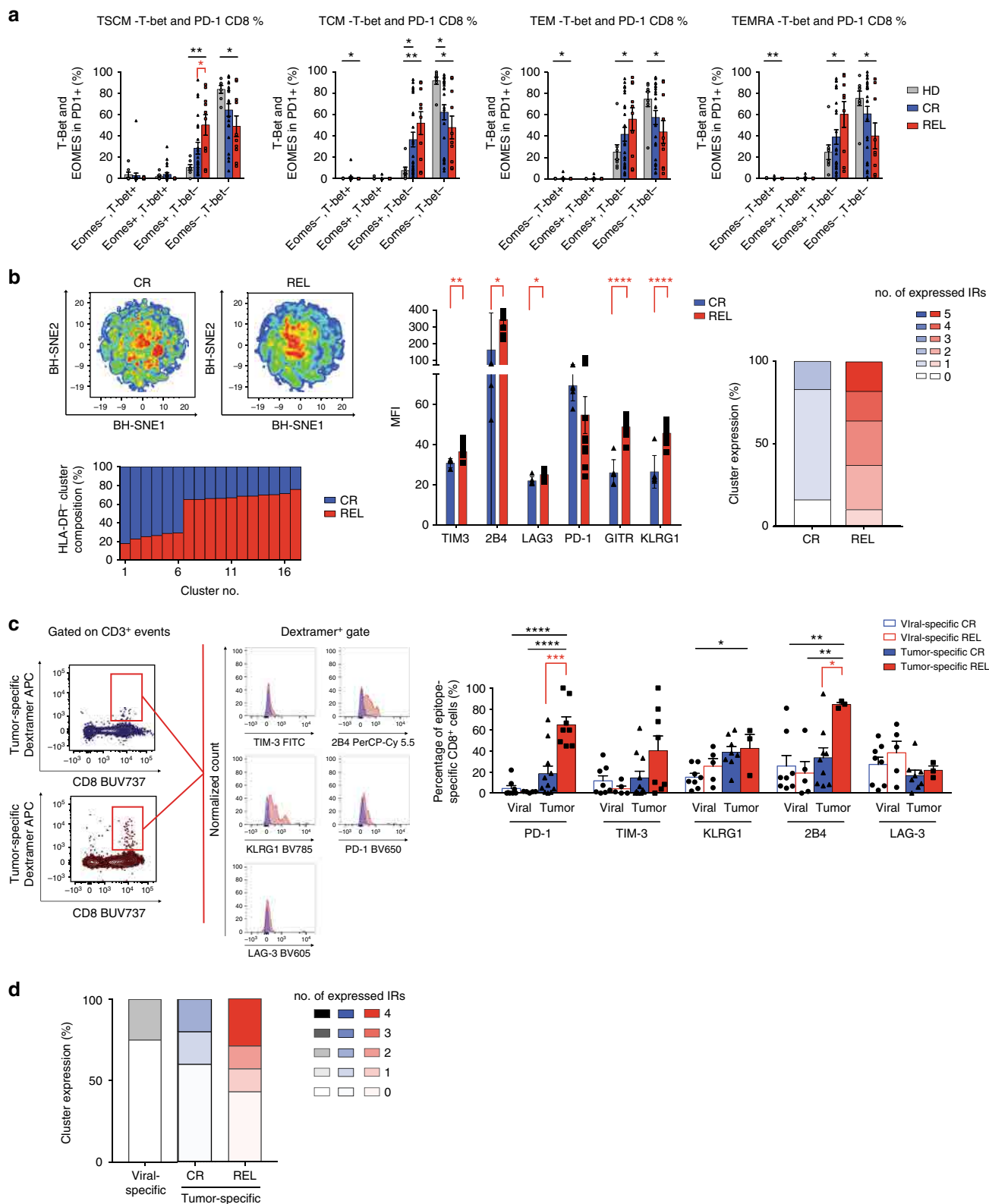
56), CD62L-APC/Cy7 (BioLegend, clone DREG-56), CD95-PB (BioLegend, clone DX2), CD95-PE/Cy7 (BioLegend, clone DX2), FOXP3-AF647 (BioLegend, clone 259D), ICOS-PB (BioLegend, clone C398.4A), KLRG1-FITC (BioLegend, clone 2Fi/KLRG1), OX40-APC (BioLegend, clone ACT35), PD-1-PE/Cy7 (BioLegend, clone EH12.2H7), 2B4-APC (BioLegend, clone CI.7), GITR-BV711 (BioLegend, clone 108-17), T-bet-BV605 (BioLegend, clone 4B10), Eomes-APC/Cy7

(BioLegend, clone WD1928), 41BB-AF700 (BioLegend, clone 4B4-1), CD27-FITC (BD Pharmingen, clone M-T271), CD28-PE (BD Pharmingen, clone L293), and CTLA-4-PE (BD Pharmingen, clone BNI-3) and for rat fluorochrome-associated monoclonal antibodies specific for TIM-3-AF488 (R&D, clone 295D) and goat fluorochrome-associated monoclonal antibodies specific for LAG-3-PE (R&D, clone Leu23-Leu450). In addition, for the study of leukemic blasts, samples at relapse were stained with the following fluorochrome-associated monoclonal antibodies: CD11b-BV785 (BioLegend, clone ICRF44), CD34-PB (BioLegend, clone 581), CD45-PE/Dazzle (BioLegend, clone HI30), CD48-FITC (BioLegend, clone BJ40), CD70-PerCp/Cy5.5 (BioLegend, clone 113-16), CD80-PE/Cy7 (BioLegend, clone 2D10), CD117-BV510 (BioLegend, clone 104D2), Galectin-9-APC (BioLegend, clone 9M1-3), OX40L-Biotin (BioLegend, clone ACT35), PD-L1-PE/Cy7 (BioLegend, clone 29E.2A3), PD-L2-PE (BioLegend, clone 24 F.10C12), 41BBL-PE (BioLegend, clone 5F4), CD86-FITC (BD Pharmingen, clone FUN-1), streptavidin-APC/Cy7 (BD Pharmingen), ICOSL-APC (R&D, clone 136726), and CD33-AF700 (eBiosciences, clone WM-53). Samples were incubated with antibodies for 15 min at 4 °C and washed with phosphate-buffered saline (PBS) containing 1% FBS. Fixation and permeabilization were required before CTLA-4<sup>45</sup>, FoxP3, T-bet, and Eomes staining and was performed using FoxP3 Fix/Perm buffer, FoxP3 Perm buffer, and Perm Wash Buffer (BioLegend) according to the manufacturer instructions. Flow-cytometry data were acquired using BD LSRFortessa cell analyzer and visualized with FlowJo software (TreeStar).

For the analysis of the antigen-specific CD8<sup>+</sup> T cells, staining with dextramers was preceded by 15 min staining with a Zombie Aqua Fixable Viability kit (BioLegend) and a round of washing (5 mins 1,500 rpm). The cell pellet was then resuspended in 50 µL of PBS containing 10% FBS and the specific dextramer added, namely dextramer Immudex anti-EZH2 HLA\*0201 (WB3257-PE), anti-WT1 HLA\*0201 (WB3787-PE), anti-WT1 HLA\*0201 (WB3469-APC), and anti-PRAME HLA\*0201 (WB3312-APC). After 30 min at 4 °C, the samples were washed and then stained 20 min at 4 °C with CD3-V500 (BioLegend, clone SK7), CD4-BUV395 (BioLegend, clone SK3), CD8-BUV737 (BD Biosciences, clone SK1), PD-1-BV650 (BioLegend, clone EH12.2H7), TIM3-AF488, LAG3-BV605 (BioLegend, clone 11C3C65), KLRG1-BV785 (BioLegend, clone 2F1-KLRG1), 2B4-PerCP-Cy5.5 (BioLegend, clone CI.7), Zombie Violet Viability Dye (BioLegend), CD62L-A700, CD45RA-PerCy7 (BioLegend, clone HI100), CD95-PB. Catalogue numbers and dilutions of each fluorochrome-conjugated monoclonal antibody are reported in Supplementary Table 1.

**CD107a degranulation and cytokines production assays.** After thawing and overnight incubation at 37 °C in complete X-vivo, cells were plated at the concentration of  $1 \times 10^6$  cells/ml in RPMI 1640 (Lonza) supplemented with glutamine 1%, penicillin/streptomycin 1%, fetal bovine serum 10%, IL-2 20 IU/ml, and in the presence of an inhibitor of metalloprotease activity (TAPI-2 200 microM<sup>46</sup>). After 1-h incubation at 37 °C, GolgiStop (0.66 µmol/ml, BD biosciences) and the fluorochrome-conjugated antibody CD107a-FITC (BD Biosciences) were added; in the stimulated wells only, PMA (50 ng/ml; Sigma) and Ionomycin (1 µg/ml; Sigma) were added. After 6 h at 37 °C, cells were first stained with fluorochrome-associated monoclonal antibodies specific for surface molecules, CD3-BV510, CD4-PE/Dazzle, CD8-BV785, CD45RA-PerCP/Cy5.5, CD62L-AF700 (BioLegend); next, cells underwent fixation and permeabilization for intracellular staining with monoclonal antibodies specific for the following cytokines: TFN-α-PE/Cy7, IFN-γ-APC/Cy7, and IL-2-PB (BioLegend). Catalogue numbers and dilutions of each fluorochrome-conjugated monoclonal antibody are reported in Supplementary Table 1. Flow-cytometry data were acquired using BD LSRFortessa cell analyzer and visualized with FlowJo software (TreeStar). Statistical analyses were performed with Prism5 software or later versions (GraphPad). Pie charts with arcs were created using SPICE software<sup>47</sup>.

**BH-SNE analysis.** BH-SNE is a dimensionality reduction algorithm that allows low-dimensional embedding of experimental data where each high-dimensional object (i.e., an event associated with many variables, such as a cell stained with many different fluorochromes) is collapsed in 2D space as a low-dimensional point associated to only two variables, BH-SNE1 and BH-SNE2. Such low-dimensional points are positioned in maps in a way that nearby points share similar high-dimensional profiles whereas distant points are dissimilar. BH-SNE runs on a Matlab plug-in called “\_Cyt”, a visualization platform developed by Dana Pe'er's lab of Computational Systems Biology<sup>36</sup>. BH-SNE algorithm analysis settings were perplexity = 30.00 and theta = 0.5, as suggested by the developers. For the analysis in Fig. 2, the algorithm was applied to downsampled (7500 events/sample) bone marrow CD3<sup>+</sup> events for both panels designed for flow-cytometry analysis, one including PD-1, LAG-3, KLRG1, and 2B4 (panel 1) and the other PD-1, TIM-3, and CTLA-4 (panel 2); for the analysis reported in Fig. 6, the algorithm was applied to downsampled (10,000 events/sample) bone marrow CD8<sup>+</sup> CD3<sup>+</sup> events from a single panel containing fluorophores specific for GITR, HLA-DR, TIM3, LAG3, 2B4, KLRG1, and PD-1. K-means algorithm was directly applied on BH-SNE1 and BH-SNE2 variables and it converged in 140-190 interactions, dividing the biaxial plot into 200 discrete areas (meta-clusters) for each BH-SNE analysis. Meta-clusters were studied by means of percentage, and then RFI was calculated and compared with the threshold for positivity defined from FlowJo analysis.



**Isolation and expansion of IR-expressing T cells.** For the isolation IR<sup>+</sup> and IR<sup>-</sup> cells and blasts, thawed bone marrow-derived mononuclear cells were stained with fluorochrome-conjugated antibodies, CD3-BV510, CD34-PB or CD33-AF700, PD-1-PE/Cy7, 2B4-APC, TIM-3-AF488. IR<sup>+</sup> cells were defined as CD3<sup>+</sup> cells expressing one or more IR according to the gating strategy shown in Fig. 5a. IR<sup>+</sup> and IR<sup>-</sup> (CD3<sup>+</sup>PD-1<sup>-</sup>2B4<sup>-</sup>TIM-3<sup>-</sup> cells) were sorted accordingly on a MoFlo XDP cell sorter (Beckman Coulter). From the same samples, leukemic blasts, defined as

CD34<sup>+</sup>CD3<sup>-</sup> or CD33<sup>+</sup>CD3<sup>-</sup>, according to the leukemia phenotype, were also retrieved. For all subsets, average purity was greater than 95%. Immediately after sorting, blasts were frozen whereas IR<sup>+</sup> and IR<sup>-</sup> lymphocytes underwent a round of in vitro activation and expansion, as previously described<sup>25</sup>. Briefly, 0.1–0.5 × 10<sup>6</sup> IR<sup>+</sup> and IR<sup>-</sup> T cells were activated with anti-CD3 OKT3 antibody (30 ng/ml, Miltenyi) in RPMI (Lonza) with FBS 10%, glutamine 1%, penicillin/streptomycin 1%, supplemented with recombinant human IL-2 (600 UI/ml, Novartis), and in the



**Fig. 6** A phenotype of exhaustion characterizes tumor-specific T cells early after transplant. **a** Proportion of PD-1<sup>+</sup> CD8<sup>+</sup> BM-T cells expressing T-bet and EOMES transcription factors in different T-cell subsets of healthy donors (HD,  $N = 8$ ), patients who will maintain long-term complete remission (CR,  $N = 37$ ) or will experience disease relapse (REL,  $N = 20$ ). **b** BH-SNE analysis of CR and REL CD8<sup>+</sup> BM-T cells at this early time point. The BH-SNE1/BH-SNE2 biaxial plot for CR and REL and the composition of HLA-DR<sup>-</sup> clusters are reported (left), together with the MFIs of inhibitory receptors (center) and the percentages (right) of CD8<sup>+</sup> BM-T cells expressing inhibitory receptors in the CR- and REL-specific HLA-DR<sup>-</sup> clusters. **c** Representative plot of inhibitory receptors expression by CR or REL tumor-specific CD8<sup>+</sup> T cells and their quantification by histograms, compared with viral-specific CD8<sup>+</sup> T cells. **d** Percentages of expression of multiple inhibitory receptors by viral and tumor-specific T cells. Individual patient data points, means, and SEM are shown. Statistically significant differences between CR and REL groups are highlighted in red and the differences between patients' groups and HD in black. \* $p < 0.05$ , \*\* $p < 0.01$ , \*\*\* $p < 0.001$ , \*\*\*\* $p < 0.0001$ , nonparametric unpaired two-sided  $T$  test

presence of irradiated (30 Gy) allogeneic PBMCs ( $1 \times 10^6$  cell/ml) obtained from a pool of three different healthy donors, and irradiated (100 Gy) lymphoblastoid cell lines ( $0.2 \times 10^6$  cell/ml). The medium and IL-2 were changed every 3–4 days, cells counted by Trypan Blue exclusion and resuspended at a concentration of  $0.5\text{--}1 \times 10^6$  cells/ml. When expansion reached plateau, IR<sup>+</sup> and IR<sup>-</sup> cells were functionally analyzed in a CD107a degranulation assay, in a cytokine release assay and a co-culture assay. Catalogue numbers and dilutions of each fluorochrome-conjugated monoclonal antibody are reported in Supplementary Table 1.

**Co-culture assay.** IR<sup>+</sup> and IR<sup>-</sup> cells were separately cultured for 3 days in U-bottom 96 wells in complete X-Vivo plus IL-2 60 IU/ml, IL-3 20 ng/ml, and G-CSF 20 ng/ml, in the presence of matched leukemic blasts, at increasing effector-to-target (E:T) ratios (1:10, 1:1, 10:1, 50:1, 100:1). As an internal control, leukemic blasts were cultured in the presence of unrelated PBMCs. After 24 h, supernatants were collected and, after a cycle of freezing and thawing, processed using LEGENDplex Human CD8/NK panel (Biolegend) and read at BD FACSCanto II HTS; this panel allows to measure molecules released upon activation, including Granzyme A and Granzyme B, in the co-culture supernatant. After 3 days of coculture, the total number of target cells was quantified upon staining with Zombie Aqua Viability kit (Biolegend), with fluorochrome-conjugated antibodies specific for CD3, CD4, CD8, CD33, or CD34 (according to the leukemia phenotype), CD45, CD117, HLA-DR-FITC (Biolegend). Data were acquired at BD LSRFortessa cell analyzer. Viable target cells were counted by using counting beads (Flow-count fluorospheres, Beckman Coulter), according to the manufacturer instructions. Elimination index was calculated according to the formula:  $[1 - (\text{total number of residual target cells cultured in presence of IR}^+ \text{ or IR}^- \text{ T cells}) / (\text{total number of residual target cells cultured in presence of unrelated PBMCs})] \times 100$ . Catalogue numbers and dilutions of each fluorochrome-conjugated monoclonal antibody are reported in Supplementary Table 1.

**Analysis of TCR- $\alpha$  and TCR- $\beta$  chains repertoire.** Sequencing of the TCR- $\alpha$  and - $\beta$  chains was performed on RNA by using a modified RACE PCR protocol, independently of multiplex PCRs<sup>48,49</sup>. Samples were sequenced using the MiSeq platform (Illumina) and raw reads were sorted according to the individual barcode combination used for each specimen. Analysis of the TCR clonotypes was carried out using the MiXCR software<sup>50</sup>.

**Statistical analysis.** Nonparametric unpaired two-sided  $T$  tests were performed for the analysis of the set of data throughout the study, with the exception of Figs 3b, 5d, where the comparison of the variables from three different experimental groups was carried out by two-way ANOVA with no matching coupled with Sidak multiple correction test, and Fig. 5g, where the comparison between the two experimental T-cell subsets IR<sup>+</sup> and IR<sup>-</sup> isolated from the same patients at the same time point was compared by means of paired two-tail  $T$  test.

Statistical analyses were performed with Prism5 software or later versions (GraphPad). The heatmap of Fig. 2 was created by using Rstudio software, packages "pheatmap", "ggplot2", and "RColorBrewer".

## Data availability

The TCR sequences data that support the findings of this study are available in SRA database with the identifier PRJNA510967. Further data are available from the corresponding author on reasonable request.

Received: 3 November 2018 Accepted: 20 January 2019

Published online: 25 March 2019

## References

- Horowitz, M. et al. Epidemiology and biology of relapse after stem cell transplantation. *Bone Marrow Transplant.* 1–11. <https://doi.org/10.1038/s41467-018-0171-z> (2018).
- Horowitz, M. M. et al. Graft-versus-leukemia reactions after bone marrow transplantation. *Blood* **75**, 555–562 (1990).
- Fearon, D. T., Manders, P. & Wagner, S. D. Arrested differentiation, the self-renewing memory lymphocyte, and vaccination. *Science* **293**, 248–250 (2001).
- Gattinoni, L. et al. A human memory T cell subset with stem cell-like properties. *Nat. Med.* **17**, 1290–1297 (2011).
- Lanzavecchia, A. & Sallusto, F. Progressive differentiation and selection of the fittest in the immune response. *Nat. Rev. Immunol.* **2**, 982–987 (2002).
- Zhang, Y., Joe, G., Hexner, E., Zhu, J. & Emerson, S. G. Host-reactive CD8<sup>+</sup> memory stem cells in graft-versus-host disease. *Nat. Med.* **11**, 1299–1305 (2005).
- Cieri, N. et al. Generation of human memory stem T cells after haploidentical T-replete hematopoietic stem cell transplantation. *Blood* **125**, 2865–2874 (2015).
- Roberto, A. et al. Role of naive-derived T memory stem cells in T cell reconstitution following allogeneic transplantation. *Blood* **125**, 2855–2865 (2015).
- Oliveira, G. et al. Tracking genetically engineered lymphocytes long-term reveals the dynamics of T cell immunological memory. *Sci. Transl. Med.* **7**, 317ra198 (2015).
- Biasco, L. et al. In vivo tracking of T cells in humans unveils decade-long survival and activity of genetically modified T memory stem cells. *Sci. Transl. Med.* **7**, 273ra13 (2015).
- Schreiber, R. D., Old, L. J. & Smyth, M. J. Cancer immunoeediting: integrating immunity's roles in cancer suppression and promotion. *Sci. (80-)* **331**, 1565–1570 (2011).
- Vago, L. et al. Loss of mismatched HLA in leukemia after stem-cell transplantation. *N. Engl. J. Med.* **361**, 478–488 (2009).
- Toffalori, C. et al. Genomic loss of patient-specific HLA in acute myeloid leukemia relapse after well-matched unrelated donor HSCT. *Blood* **119**, 4813–4815 (2012).
- Crucitti, L. et al. Incidence, risk factors and clinical outcome of leukemia relapses with loss of the mismatched HLA after partially incompatible hematopoietic stem cell transplantation. *Leukemia* **29**, 1143–1152 (2015).
- Zhou, Q. et al. Program death-1 (PD-1) signaling and regulatory T cells (Tregs) collaborate to resist the function of adoptively transferred cytotoxic T lymphocytes (CTLs) in advanced acute myeloid leukemia (AML). *Blood* **116**, 2484–2493 (2010).
- Wherry, E. J. & Kurachi, M. Molecular and cellular insights into T cell exhaustion. *Nat. Rev. Immunol.* **15**, 486–499 (2015).
- Callahan, M. K., Postow, M. A. & Wolchok, J. D. Targeting T cell co-receptors for cancer therapy. *Immunity* **44**, 1069–1078 (2016).
- Davidson, M. S. et al. Ipilimumab for patients with relapse after allogeneic transplantation. *N. Engl. J. Med.* **375**, 143–153 (2016).
- Tian, T. et al. The profile of T helper subsets in bone marrow microenvironment is distinct for different stages of acute myeloid leukemia patients and chemotherapy partly ameliorates these variations. *PLoS One* **10**, e0131761 (2015).
- Miyara, M. et al. Functional delineation and differentiation dynamics of human CD4<sup>+</sup> T cells expressing the FoxP3 transcription factor. *Immunity* **30**, 899–911 (2009).
- Cieri, N. et al. IL-7 and IL-15 instruct the generation of human memory stem T cells from naive precursors. *Blood* **121**, 573–584 (2013).
- Yang, Z., Peltonen, J. & Kaski, S. Scalable optimization of neighbor embedding for visualization. *Icml* **28**, 786–794 (2013).
- Wherry, E. J. T cell exhaustion. *Nat. Immunol.* **13**, 492–499 (2011).
- Anderson, K. G., Stromnes, I. M. & Greenberg, P. D. Obstacles posed by the tumor microenvironment to T cell activity: a case for synergistic therapies. *Cancer Cell* **31**, 311–325 (2017).
- Riddell, S. R. & Greenberg, P. D. The use of anti-CD3 and anti-CD28 monoclonal antibodies to clone and expand human antigen-specific T cells. *J. Immunol. Methods* **128**, 189–201 (1990).
- Gros, A. et al. PD-1 identifies the patient-specific CD8<sup>+</sup> tumor-reactive repertoire infiltrating human tumors. *J. Clin. Invest.* **124**, (2014).

27. Paley, M. A. et al. Progenitor and terminal subsets of CD8+ T cells cooperate to contain chronic viral infection. *Sci. (80-.)* **338**, 1220–1225 (2012).
28. Schade, H. et al. Programmed death 1 expression on CD4+ T cells predicts mortality after allogeneic stem cell transplantation. *Biol. Blood. Marrow Transplant.* **22**, 2172–2179 (2016).
29. Kong, Y. et al. PD-1hiTIM-3+ T cells associate with and predict leukemia relapse in AML patients post allogeneic stem cell transplantation. *Blood Cancer J.* **5**, e330–e330 (2015).
30. Merindol, N., Champagne, Ma, Duval, M. & Soudeyns, H. CD8+ T-cell reconstitution in recipients of umbilical cord blood transplantation and characteristics associated with leukemic relapse. *Blood* **118**, 4480–4488 (2011).
31. Ahmadzadeh, M. et al. Tumor antigen – specific CD8 T cells infiltrating the tumor express high levels of PD-1 and are functionally impaired tumor antigen – specific CD8 T cells infiltrating the tumor express high levels of PD-1 and are functionally impaired. *Blood* **114**, 1537–1544 (2009).
32. Gallez-Hawkins, G. M. et al. Increased programmed death-1 molecule expression in cytomegalovirus disease and acute graft-versus-host disease after allogeneic hematopoietic cell transplantation. *Biol. Blood. Marrow Transplant.* **15**, 872–880 (2009).
33. Penalzoza-MacMaster, P. CD8 T-cell regulation by T regulatory cells and the programmed cell death protein 1 pathway. *Immunology* **151**, 146–153 (2017).
34. Merryman, R. W. et al. Safety and efficacy of allogeneic hematopoietic stem cell transplant after PD-1 blockade in relapsed/refractory lymphoma. *Blood* **129**, 1380–1388 (2017).
35. Blackburn, S. D. et al. Coregulation of CD8+ T cell exhaustion by multiple inhibitory receptors during chronic viral infection. *Nat. Immunol.* **10**, 29–37 (2009).
36. Amir, E. D. et al. viSNE enables visualization of high dimensional single-cell data and reveals phenotypic heterogeneity of leukemia. *Nat. Biotechnol.* **31**, 545–552 (2013).
37. Legat, A., Speiser, D. E., Pircher, H., Zehn, D. & Fuentes Marraco, S. A. Inhibitory receptor expression depends more dominantly on differentiation and activation than “exhaustion” of human CD8 T cells. *Front. Immunol.* **4**, 1–15 (2013).
38. Schnorfeil, F. M. et al. T cells are functionally not impaired in AML: increased PD-1 expression is only seen at time of relapse and correlates with a shift towards the memory T cell compartment. *J. Hematol. Oncol.* **8**, 93 (2015).
39. Wherry, E. J., Blattman, J. N., Murali-krishna, K., Most, R. VanDer & Ahmed, R. Viral persistence alters CD8 T-cell immunodominance and tissue distribution and results in distinct stages of functional impairment viral persistence alters CD8 T-cell immunodominance and tissue distribution and results in distinct stages of functional Im. *J. Virol.* **77**, 4911–3927 (2003).
40. Hutten, T. J. A. et al. Increased coexpression of PD-1, TIGIT, and KLRG-1 on tumor-reactive CD8 + T cells during relapse after allogeneic stem cell transplantation. *Biol. Blood Marrow Transplant.* **24**, 666–677 (2018).
41. Jelinek, T., Mihalyova, J., Kascak, M., Duras, J. & Hajek, R. PD-1/PD-L1 inhibitors in haematological malignancies: update 2017. *Immunology* **152**, 357–371 (2017).
42. Peccatori, J. et al. Sirolimus-based graft-versus-host disease prophylaxis promotes the in vivo expansion of regulatory T cells and permits peripheral blood stem cell transplantation from haploidentical donors. *Leukemia* **29**, 396–405 (2015).
43. Cieri, N. et al. Post-transplantation cyclophosphamide and sirolimus after haploidentical hematopoietic stem cell transplantation using a treosulfan-based myeloablative conditioning and peripheral blood stem cells. *Biol. Blood. Marrow Transplant.* **21**, 1506–1514 (2015).
44. Greco, R. et al. Posttransplantation cyclophosphamide and sirolimus for prevention of GVHD after HLA-matched PBSC transplantation. *Blood* **128**, 1528–1531 (2016).
45. Walker, L. S. K. & Sansom, D. M. Confusing signals: recent progress in CTLA-4 biology. *Trends Immunol.* **36**, 63–70 (2015).
46. Jabbari, A. & Hartly, J. T. Simultaneous assessment of antigen-stimulated cytokine production and memory subset composition of memory CD8 T cells. *J. Immunol. Methods* **313**, 161–168 (2006).
47. Roederer, M., Nozzi, J. L. & Nason, M. C. SPICE: exploration and analysis of post-cytometric complex multivariate datasets. *Cytom. Part A* **79A**, 167–174 (2011).
48. Bolotin, D. A. et al. Next generation sequencing for TCR repertoire profiling: platform-specific features and correction algorithms. *Eur. J. Immunol.* **42**, 3073–3083 (2012).
49. Ruggiero, E. et al. High-resolution analysis of the human T-cell receptor repertoire. *Nat. Commun.* **6**, 8081 (2015).
50. Bolotin, D. A. et al. MiXCR: software for comprehensive adaptive immunity profiling. *Nat. Methods* **12**, 380–381 (2015).

## Acknowledgements

This work was supported by EU-FP7 (SUPERSIST) to C.B., by the Italian Association for Cancer Research (AIRC-IG-18458 to C.B., Start-Up Grant #14162 to L.V.), by the Italian Ministry of University and Research (MIUR-2015NZWSEC\_001) to C.B., the Italian Ministry of Health (RF-FSR-2008-1202648 to Fabio Ciceri, RF-2011-02351998 to Fabio Ciceri and L.V., RF-2011-02348034 to L.V. and TRANSCAN HLALOSS to L.V.), by the ASCO Conquer Cancer Foundation (2014 Young Investigator Award to L.V.), and by the DKMS Mechtild Harf Foundation (DKMS Mechtild Harf Research Grant 2015 to L.V.). E.R. was supported by a fellowship from the European Union's Horizon 2020 research and innovation program under the Marie Skłodowska-Curie grant agreement THAT IS HUNT 752717. This work was partially supported by the Italian Ministry of Health (GR-2016-02364847) to E.R.

## Author contributions

M.N. designed the study, conducted laboratory experiments, analyzed and interpreted data, and wrote the paper; F.M. conducted laboratory experiments and BH-SNE analysis, analyzed and interpreted data, and wrote the paper; E.R. performed and analyzed experiments of TCR sequencing; T.P., R.G., and J.P. provided clinical data and participated in the data interpretation; G.O. and N.C. participated to the design of the study and data discussion; Filippo Cortesi participated to the BH-SNE analysis; P.D.S. participated to laboratory experiments; C.T. and V.G. participated in the data interpretation; M.C. participated to co-culture experiments and data discussion; G.C. and P.D.B. participated to the interpretation of results and reviewed the paper; M.O., T.T., G.M., H.C.J.M., F.J.H. F., S.F., H.H., B.M., M.W., R.Z., and J.F. provided clinical data and bone marrow samples, and participated in data interpretation; A.B. participated to data discussion and interpretation of the results; L.V., Fabio Ciceri, and C.B. designed and supervised the study and wrote the paper.

## Additional information


**Supplementary Information** accompanies this paper at <https://doi.org/10.1038/s41467-019-08871-1>.

**Competing interests:** C.B. received research support from Molmed s.p.a and Intellia Therapeutics. A.B. received research support from TxCell. L.V. received research support from GenDx and Moderna Therapeutics. The remaining authors declare no competing interests.

**Reprints and permission** information is available online at <http://npg.nature.com/reprintsandpermissions/>

**Journal peer review information:** *Nature Communications* thanks the anonymous reviewers for their contributions to the peer review of this work. Peer reviewers reports are available.

**Publisher's note:** Springer Nature remains neutral with regard to jurisdictional claims in published maps and institutional affiliations.

 **Open Access** This article is licensed under a Creative Commons Attribution 4.0 International License, which permits use, sharing, adaptation, distribution and reproduction in any medium or format, as long as you give appropriate credit to the original author(s) and the source, provide a link to the Creative Commons license, and indicate if changes were made. The images or other third party material in this article are included in the article's Creative Commons license, unless indicated otherwise in a credit line to the material. If material is not included in the article's Creative Commons license and your intended use is not permitted by statutory regulation or exceeds the permitted use, you will need to obtain permission directly from the copyright holder. To view a copy of this license, visit <http://creativecommons.org/licenses/by/4.0/>.

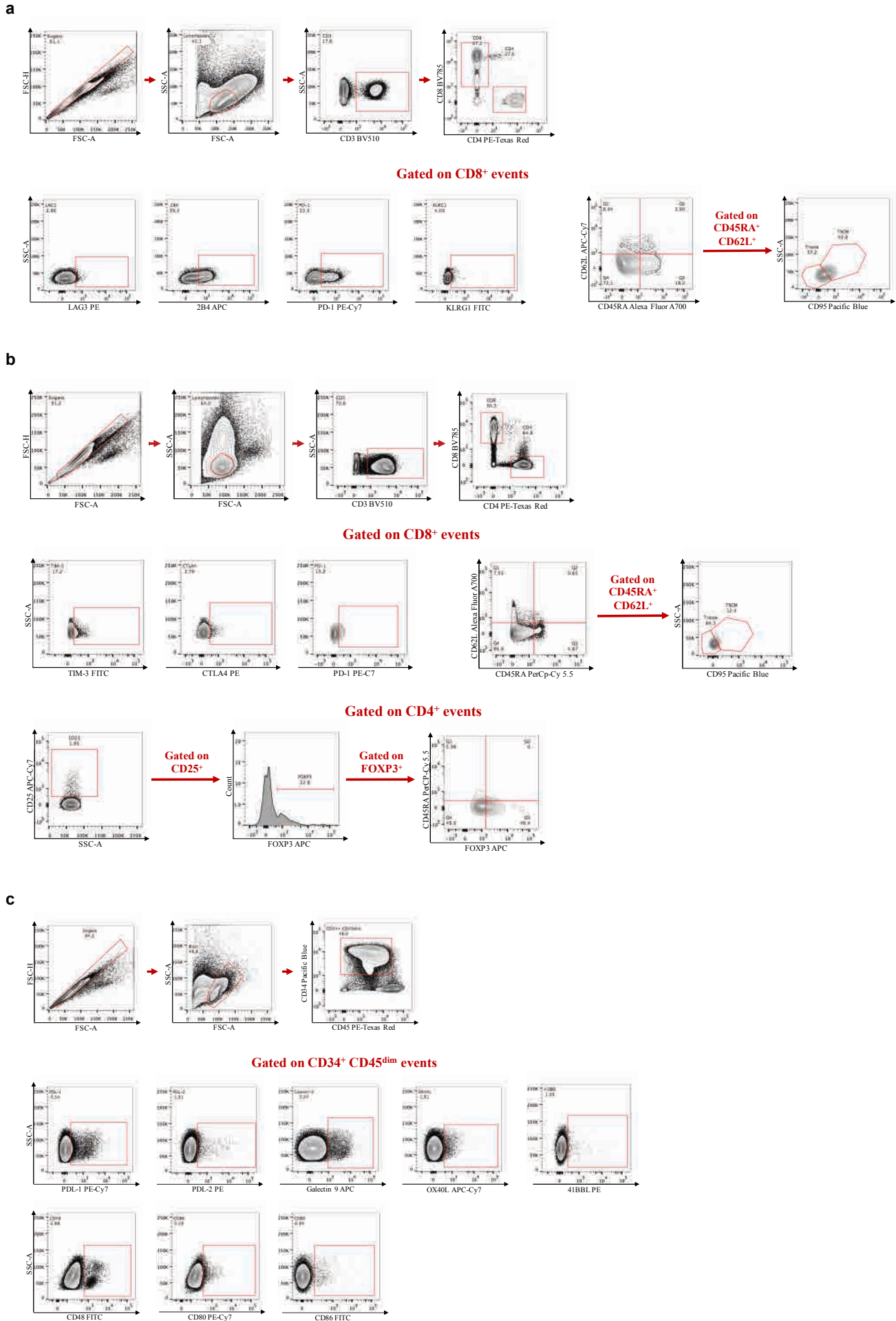
© The Author(s) 2019

# Bone marrow central memory and memory stem T-cell exhaustion in AML patients relapsing after HSCT

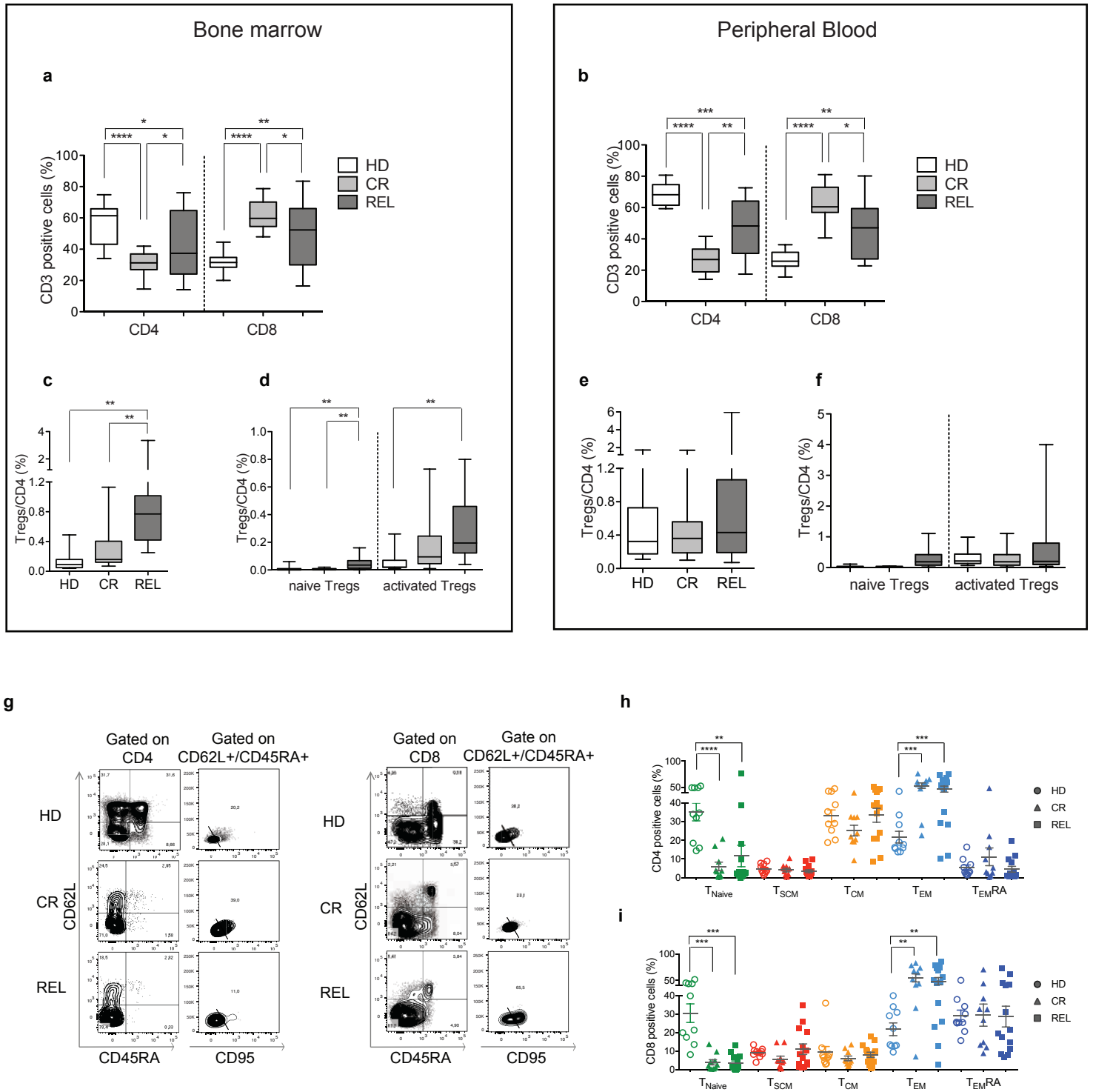
Noviello, Manfredi et al.

## **Supplementary Information**

# Supplementary figures

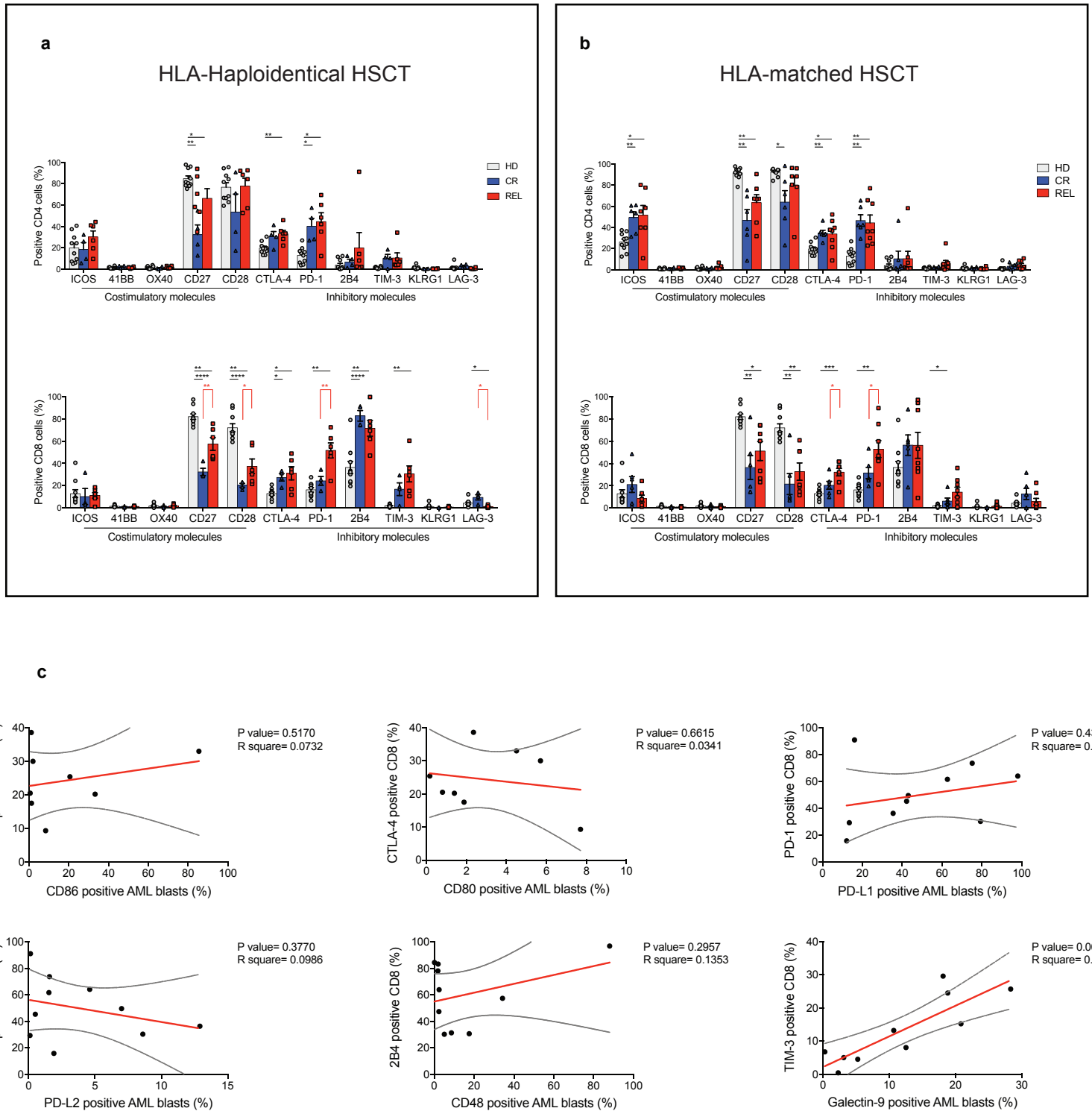


**Supplementary Figure 1.** Gating strategy used for multiparametric flow cytometry analysis. Sequential gating for the analysis reported in Fig.1, Fig3 and Supplementary Fig2, for all the different flow cytometry panels used. (a) Inhibitory receptors and memory differentiation markers on the cell surface. (b) Inhibitory receptors and Treg differentiation markers on the cell surface and after cell fixation and permeabilization. (c) Gating strategy for the analysis of blasts at relapse.



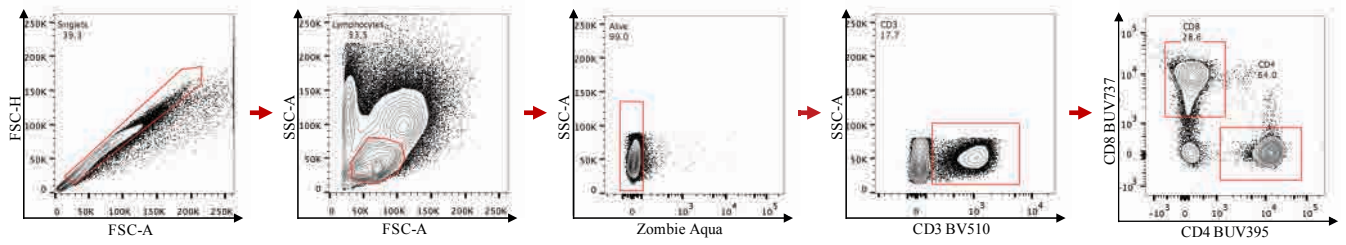
**Supplementary Figure 2.** T-cell subset distribution in the bone marrow and in peripheral blood of HSCT patients according to transplant outcome. The T-cell subset distribution of healthy donors (HD), patients who achieved long-term complete remission (CR) and patients who experienced relapse (REL) after HSCT was evaluated in the Bone Marrow (HD=10, CR=16, REL=16) and in Peripheral Blood (HD=10, CR=14, REL=10). (a-b) Proportion of CD4<sup>+</sup> and CD8<sup>+</sup> subsets on total CD3<sup>+</sup> T cells in HD, CR and REL patients for BM-infiltrating (a) and circulating (b) T cells. (c-f) Relative proportion of Tregs and proportion of naïve and activated Tregs over total CD4<sup>+</sup> T cells in either BM-infiltrating (c-d) and circulating (e-f) T cells. (g) Representative plots of the gating strategy for the visualization of T-cell memory subsets in one HD, one CR and one REL patient. (h-i) Relative proportion of naïve (CD45RA<sup>+</sup>CD62L<sup>+</sup>CD95<sup>-</sup>, T<sub>Naive</sub>), memory stem (CD45RA<sup>+</sup>CD62L<sup>+</sup>CD95<sup>+</sup>, T<sub>SCM</sub>), central memory (CD45RA<sup>-</sup>CD62L<sup>+</sup>, T<sub>CM</sub>), effector memory (CD45RA<sup>-</sup>CD62L<sup>-</sup>, T<sub>EM</sub>) T cells and terminal effectors (CD45RA<sup>+</sup>CD62L<sup>-</sup>, T<sub>EMRA</sub>) over the total CD4<sup>+</sup> (h) or CD8<sup>+</sup> (i) T-cell subsets in peripheral blood samples harvested from HD, CR or REL. Individual data points, means, and SEM are shown. Median, min and max values are reported for box-and-whiskers plots. \*, p<0.05; \*\*, p<0.01; \*\*\*, p<0.001; \*\*\*\*, p<0.0001, nonparametric unpaired two-sided T-test.



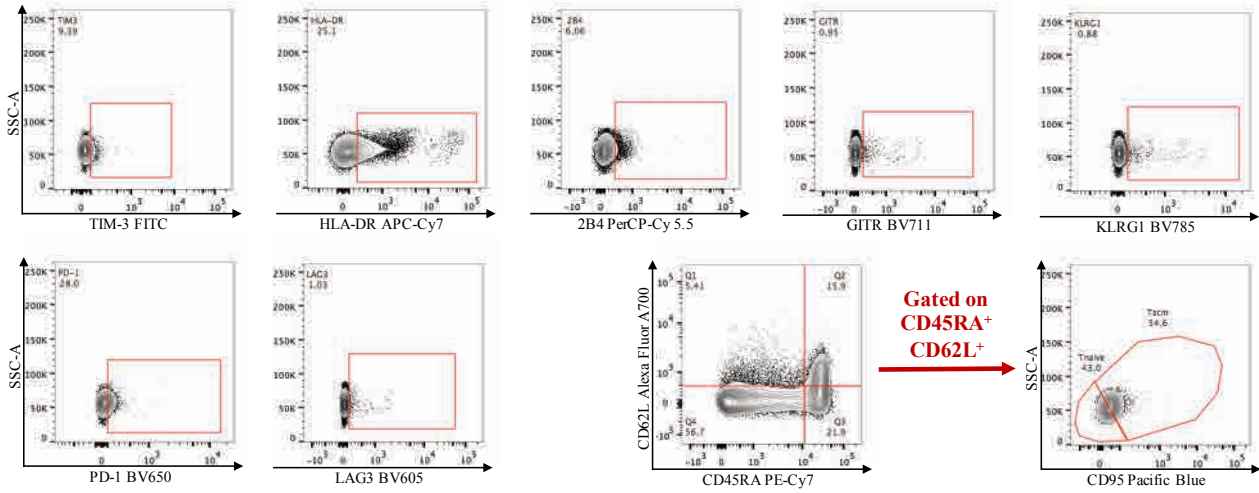


**Supplementary Figure 3.** Expression of inhibitory receptors and costimulatory molecules on circulating T cells of HSCT patients according to clinical outcome and transplant type. (a-b) HLA-matched (N=14) and HLA-haploidentical (N=10) patient samples were analyzed for the expression of inhibitory and costimulatory molecules on circulating T cells; peripheral blood samples from healthy donors were used as controls (HD, N=10). The percentage of CD4<sup>+</sup> and CD8<sup>+</sup> BM-T cells positive for costimulatory or inhibitory receptors in the HLA-haploidentical (a) and HLA-matched (b) transplant settings is reported (HD CR REL). Individual data points, means, and SEM are shown. Statistically significant differences between CR and REL groups are highlighted in red, the differences between patients' groups and HD in black. \*, p<0.05; \*\*, p<0.01; \*\*\*, p<0.001; \*\*\*\*, p<0.0001, nonparametric unpaired two-sided T-test. (c) Linear regression analysis between the relative proportion of PD-1, 2B4, CTLA-4 and TIM-3-expressing CD8<sup>+</sup> BM-T cells of patients undergoing HLA-identical HSCT and the relative proportion of their respective ligands on leukemic blasts. Linear regression, confidence intervals, P-value and R square are shown. All the inhibitory receptors have been visualized by means of cell surface staining apart for CTLA-4, visualized after cell fixation and permeabilization.

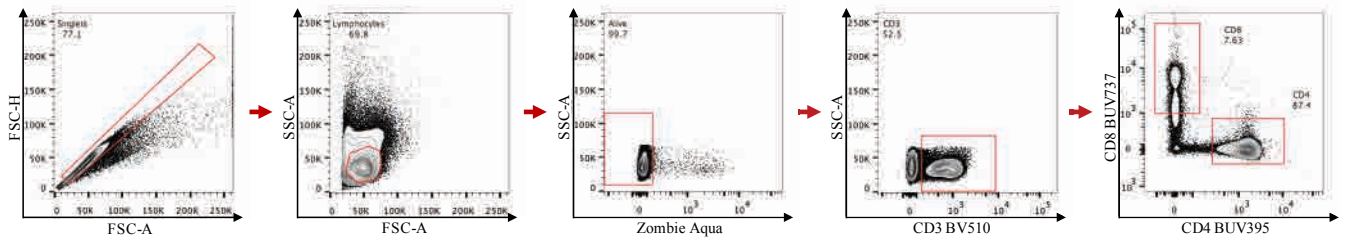
**a**



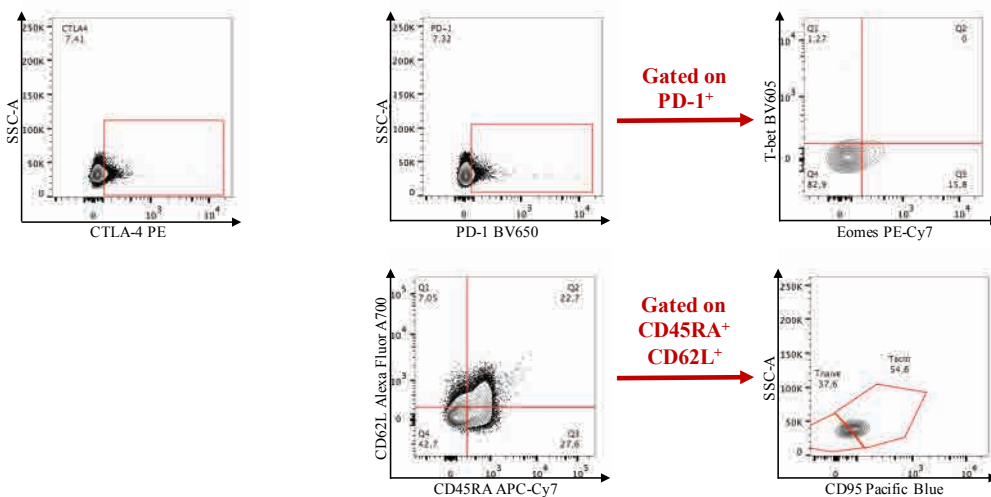
**Gated on CD8<sup>+</sup> events**



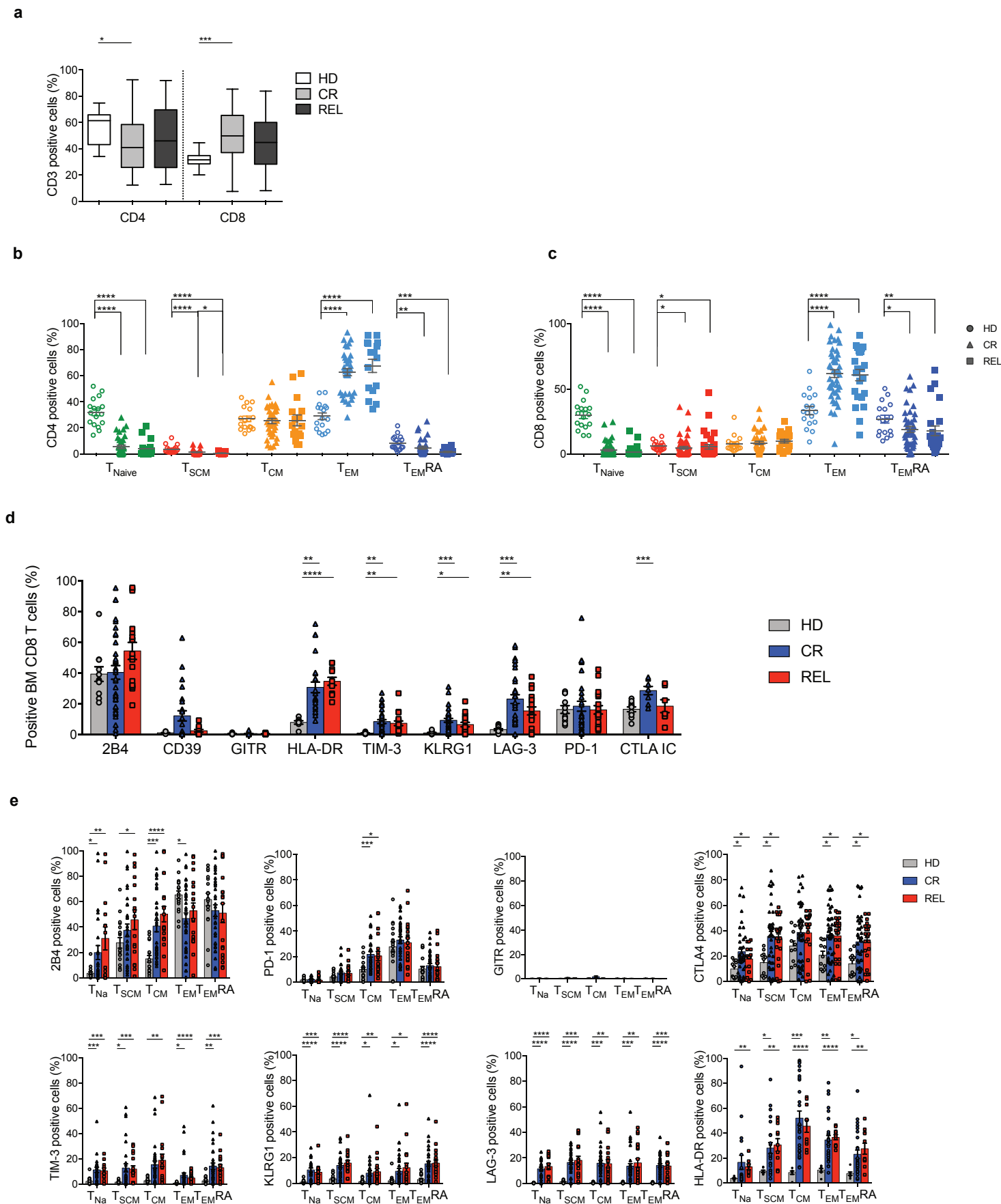
**b**



**Gated on CD8<sup>+</sup> events**



**Supplementary Figure 4.** Gating strategy used for multiparametric flow cytometry analysis. Sequential gating for the analysis reported in Fig.6 and Supplementary Fig.5, for all the different flow cytometry panels used. (a) Inhibitory receptors and memory differentiation markers on the cell surface. (b) Inhibitory receptors and transcription factors visualization on the cell surface and after cell fixation and permeabilization.



**Supplementary Figure 5. Circulating and BM-T cell subsets and exhaustion profile of CD8<sup>+</sup> BM-T cells at early time points.** The T-cell subset distribution was evaluated in the Bone Marrow of HLA-matched transplanted patients who will maintain long-term complete remission (CR, N=37) or will experience disease relapse (REL, N=20) at the median time of 68 days after HSCT, when all patients were in CR. BM-T cells from healthy donors were used as controls (HD, N=18). **(a)** Proportion of CD4<sup>+</sup> and CD8<sup>+</sup> subsets on total CD3<sup>+</sup> BM-T cells in HD, CR and REL patients. **(b-c)** Relative proportion of memory T-cell subsets over the total CD4<sup>+</sup> **(b)** and CD8<sup>+</sup> **(c)** T cells, in each study group. **(d-e)** Percentages of BM-T cells expressing inhibitory receptors in both total CD8<sup>+</sup> T cells **(d)** and in each CD8<sup>+</sup> T-cell memory subset in each study group **(e)**. All the inhibitory receptors have been visualized by means of cell surface staining apart for CTLA-4, visualized after cell fixation and permeabilization. Statistically significant differences between CR and REL groups are highlighted in red, the differences between patients' groups and HD in black. Individual data points, means, and SEM are shown. \*, p<0.05; \*\*, p<0.01; \*\*\*, p<0.001; \*\*\*\*, p<0.0001, nonparametric unpaired T-test.



**Supplementary Table**

Fluorochrome-conjugated monoclonal antibody	Clone	Vendor	Catalogue number	Dilution
2B4-APC	CI.7	BioLegend	329512	1:400
2B4-PerCP-Cy5.5	C1.7	Biolegend	329516	1:100
41BB-AF700	4B4-1	BioLegend	304120	1:70
41BBL-PE	5F4	BioLegend	311504	1:100
CD107a-FITC	H4A3	BD Biosciences	555800	1:50
CD117-BV510	104D2	BioLegend	313220	1:100
CD11b-BV785	ICRF44	BioLegend	301345	1:200
CD25-APC/Cy7	BC96	BioLegend	302614	1:100
CD27-FITC	M-T271	BD Pharmingen	555440	1:100
CD28-PE	L293	BD Pharmingen	555729	1:100
CD3-BV510	OKT3	BioLegend	317333	1:200
CD3-BV510	SK7	BioLegend	344828	1:200
CD33-AF700	WM-53	eBiosciences	56-0338	1:200
CD34-PB	581	BioLegend	343512	1:100
CD4-BUV395	SK3	BD Biosciences	563550	1:200
CD4-PE/Dazzle	RPA-T4	BioLegend	300548	1:200
CD45-PE/Dazzle	HI30	BioLegend	304052	1:200
CD45RA-AF700	HI100	BioLegend	304120	1:400
CD45RA-PeCy7	HI100	Biolegend	304126	1:100
CD45RA-PerCP/Cy5.5	HI100	BioLegend	304122	1:100
CD48-FITC	BJ40	BioLegend	336706	1:400
CD62L-AF700	DREG-56	BioLegend	304820	1:70
CD62L-APC/Cy7	DREG-56	BioLegend	304814	1:100
CD70-PerCp/Cy5.5	113-16	BioLegend	355108	1:200
CD8-BUV737	SK1	BD Biosciences	564629	1:200
CD8-BV785	RPA-T8	BioLegend	301046	1:200
CD80-Pe/Cy7	2D10	BioLegend	305218	1:200
CD86-FITC	FUN-1	BD Pharmingen	555657	1:100
CD95-PB	DX2	BioLegend	305619	1:70
CD95-PE/Cy7	DX2	BioLegend	305622	1:200
CTLA-4-PE	BNI-3	BD Pharmingen	560939	1:100
Eomes APC/Cy7	WD1928	Invitrogen	25-4877-42	1:70
FOXP-3-AF647	259D	BioLegend	320214	1:100
Galectin-9-APC	9M1-3	BioLegend	348908	1:70
GITR-BV711	108-17	Biolegend	371212	1:70
HLA-DR-AF700	L243	Biolegend	307626	1:100
ICOS-PB	C398.4A	BioLegend	313522	1:100
ICOSL-APC	136726	R&D	FAB165A	1:70
IFN- $\gamma$ -APC/Cy7	4S.B3	BioLegend	502530	1:100
IL-2-PB	MQ1-17H12	BioLegend	500324	1:100
KLRG1-BV785	2F1-KLRG1	Biolegend	138429	1:70
KLRG1-FITC	2Fi/KLRG1	BioLegend	138410	1:100
LAG-3-PE	Leu23-Leu450	R&D	FAB2319P	1:70
LAG3-BV605	11C3C65	Biolegend	369324	1:70
OX40-APC	ACT35	BioLegend	350008	1:100
OX40L-Biotin	ACT35	BioLegend	326306	1:100
PD-1-BV650	EH12.2H7	Biolegend	329950	1:200
PD-1-PE/Cy7	EH12.2H7	BioLegend	329918	1:70
PD-L1-PE/Cy7	29E.2A3	BioLegend	329718	1:70
PD-L2-PE	24F.10C12	BioLegend	329606	1:200
T-bet-BV605	4B10	Biolegend	644817	1:70
TFN- $\alpha$ -PE/Cy7	Mab11	BioLegend	502930	1:100
TIM-3-AF488	295D	R&D	FAB2365G	1:70

**Supplementary Table 1.** *List of the used fluorochrome-conjugated Monoclonal Antibodies.*



## Chapter 5.

### **Immune signature drives leukemia escape and relapse after hematopoietic cell transplantation**

Toffalori C, Zito L\*, Gambacorta V\*, Riba M\*, Oliveira G, Bucci G, Barcella M, Spinelli O, Greco R, Crucitti L, Cieri N, Noviello M, Manfredi F, Montaldo E, Ostuni R, Naldini MM, Gentner B, Waterhouse M, Zeiser R, Finke J, Hanoun M, Beelen D, Gojo I, Luznik L, Onozawa M, Teshima T, Devillier R, Blaise D, Halkes CJM, Griffioen M, Carrabba MG, Bernardi M, Peccatori J, Barlassina C, Stupka E, Lazarevic D., Tonon G, Rambaldi A, Cittaro D, Bonini C, Fleischhauer K, Ciceri F\*, Vago L\*

*Published in Nature Medicine (2019)*

# Immune signature drives leukemia escape and relapse after hematopoietic cell transplantation

Cristina Toffalori<sup>1</sup>, Laura Zito<sup>1,21</sup>, Valentina Gambacorta<sup>1,2,21</sup>, Michela Riba<sup>3,21</sup>, Giacomo Oliveira<sup>1,4,19</sup>, Gabriele Bucci<sup>1,3</sup>, Matteo Barcella<sup>5</sup>, Orietta Spinelli<sup>6</sup>, Raffaella Greco<sup>7</sup>, Lara Crucitti<sup>7,20</sup>, Nicoletta Cieri<sup>4,7,20</sup>, Maddalena Noviello<sup>4</sup>, Francesco Manfredi<sup>4</sup>, Elisa Montaldo<sup>8</sup>, Renato Ostuni<sup>8</sup>, Matteo M. Naldini<sup>9</sup>, Bernhard Gentner<sup>7,9</sup>, Miguel Waterhouse<sup>10</sup>, Robert Zeiser<sup>10</sup>, Jurgen Finke<sup>10</sup>, Maher Hanoun<sup>11</sup>, Dietrich W. Beelen<sup>11</sup>, Ivana Gojo<sup>12</sup>, Leo Luznik<sup>12</sup>, Masahiro Onozawa<sup>13</sup>, Takanori Teshima<sup>13</sup>, Raynier Devillier<sup>14</sup>, Didier Blaise<sup>14</sup>, Constantijn J. M. Halkes<sup>15</sup>, Marieke Griffioen<sup>15</sup>, Matteo G. Carrabba<sup>7</sup>, Massimo Bernardi<sup>7</sup>, Jacopo Peccatori<sup>7</sup>, Cristina Barlassina<sup>5</sup>, Elia Stupka<sup>3,19</sup>, Dejan Lazarevic<sup>3</sup>, Giovanni Tonon<sup>3</sup>, Alessandro Rambaldi<sup>6,16</sup>, Davide Cittaro<sup>3</sup>, Chiara Bonini<sup>4,17</sup>, Katharina Fleischhauer<sup>1,18</sup>, Fabio Ciceri<sup>7,17,22</sup> and Luca Vago<sup>1,7,22\*</sup>

**Transplantation of hematopoietic cells from a healthy individual (allogeneic hematopoietic cell transplantation (allo-HCT)) demonstrates that adoptive immunotherapy can cure blood cancers: still, post-transplantation relapses remain frequent. To explain their drivers, we analyzed the genomic and gene expression profiles of acute myeloid leukemia (AML) blasts purified from patients at serial time-points during their disease history. We identified a transcriptional signature specific for post-transplantation relapses and highly enriched in immune-related processes, including T cell costimulation and antigen presentation. In two independent patient cohorts we confirmed the deregulation of multiple costimulatory ligands on AML blasts at post-transplantation relapse (PD-L1, B7-H3, CD80, PVRL2), mirrored by concomitant changes in circulating donor T cells. Likewise, we documented the frequent loss of surface expression of HLA-DR, -DQ and -DP on leukemia cells, due to downregulation of the HLA class II regulator CIITA. We show that loss of HLA class II expression and upregulation of inhibitory checkpoint molecules represent alternative modalities to abolish AML recognition from donor-derived T cells, and can be counteracted by interferon- $\gamma$  or checkpoint blockade, respectively. Our results demonstrate that the deregulation of pathways involved in**

**T cell-mediated allorecognition is a distinctive feature and driver of AML relapses after allo-HCT, which can be rapidly translated into personalized therapies.**

The efficacy of allo-HCT in curing hematological malignancies strongly relies on transferring from the donor to the patient an immune system that is capable of eliminating residual tumor cells<sup>1,2</sup>. Still, relapses are frequent and, due to the lack of effective salvage therapies, represent the first cause of death in transplanted patients<sup>3</sup>.

Previous studies have documented that in partially incompatible allo-HCTs, genomic loss of the mismatched HLAs represents a frequent mechanism by which leukemia evades recognition from donor T cells and outgrows into clinically evident relapse<sup>4-7</sup>.

Here, we comprehensively assessed the genomic and transcriptional changes occurring at post-transplantation relapse in two independent cohorts of patients without genomic loss of HLA, documenting that immune-related changes are also prevalent in these patients and describing more patterns of immune evasion leading to recurrence.

We started by analyzing a discovery cohort of 40 adult patients transplanted for AML and for whom samples had been collected at the time of diagnosis, relapse after sole chemotherapy (available in three of the patients) and relapse after allo-HCT (Supplementary Tables 1 and 2). On purification of leukemia cells, genomic changes

<sup>1</sup>Unit of Immunogenetics, Leukemia Genomics and Immunobiology, Division of Immunology, Transplantation and Infectious Disease, IRCCS San Raffaele Scientific Institute, Milano, Italy. <sup>2</sup>Unit of Senescence in Stem Cell Aging, Differentiation and Cancer, San Raffaele Telethon Institute for Gene Therapy, IRCCS San Raffaele Scientific Institute, Milano, Italy. <sup>3</sup>Center for Translational Genomics and Bioinformatics, IRCCS San Raffaele Scientific Institute, Milano, Italy. <sup>4</sup>Experimental Hematology Unit, Division of Immunology, Transplantation and Infectious Disease, IRCCS San Raffaele Scientific Institute, Milano, Italy. <sup>5</sup>Genomic and Bioinformatics Unit, Department of Health Sciences, University of Milano, Milano, Italy. <sup>6</sup>Hematology and Bone Marrow Transplant Unit, ASST Papa Giovanni XXIII, Bergamo, Italy. <sup>7</sup>Unit of Hematology and Bone Marrow Transplantation, IRCCS San Raffaele Scientific Institute, Milano, Italy. <sup>8</sup>Genomics of the Innate Immune System Unit, San Raffaele Telethon Institute for Gene Therapy, IRCCS San Raffaele Scientific Institute, Milano, Italy. <sup>9</sup>Translational Stem Cell and Leukemia Unit, San Raffaele Telethon Institute for Gene Therapy, IRCCS San Raffaele Scientific Institute, Milano, Italy. <sup>10</sup>Department of Hematology, Oncology and Stem Cell Transplantation, Universitätsklinikum Freiburg, Freiburg, Germany. <sup>11</sup>Department of Bone Marrow Transplantation, Universitätsklinikum Essen, Essen, Germany. <sup>12</sup>Sidney Kimmel Comprehensive Cancer Center, Johns Hopkins University School of Medicine, Baltimore, MD, USA. <sup>13</sup>Department of Hematology, Hokkaido University Faculty of Medicine, Graduate School of Medicine, Sapporo, Japan. <sup>14</sup>Department of Haematology, Institut Paoli Calmettes, Marseille, France. <sup>15</sup>Department of Hematology, Leiden University Medical Center, Leiden, The Netherlands. <sup>16</sup>Department of Oncology and Hemato-Oncology, University of Milano, Milano, Italy. <sup>17</sup>San Raffaele Vita-Salute University, Milano, Italy. <sup>18</sup>Institute for Experimental Cellular Therapy, Universitätsklinikum Essen, Essen, Germany. <sup>19</sup>Present address: Dana-Farber Cancer Institute, Boston, MA, USA. <sup>20</sup>Present address: University of Milano, Milano, Italy. <sup>21</sup>These authors contributed equally: Laura Zito, Valentina Gambacorta and Michela Riba. <sup>22</sup>These authors jointly directed this work: Fabio Ciceri and Luca Vago. \*e-mail: [vago.luca@hsr.it](mailto:vago.luca@hsr.it)

were assessed by single nucleotide polymorphism (SNP) arrays, and transcriptional changes by genome-wide microarrays (Fig. 1a).

SNP profiling evidenced the appearance of new chromosomal insertions or deletions in 7 out of 12 post-transplantation relapses (Extended Data Fig. 1 and Supplementary Table 3) and of new copy-neutral loss-of-heterozygosity (CN-LOH) events in 2 of 12, always involving chromosome 13 and resulting in doubled allele burden of FLT3-internal tandem duplications (-ITD). FLT3-ITD allele burden also increased at post-transplantation relapse in three more patients by relative expansion of the mutated subclones (Supplementary Table 3).

Our observation of frequent de novo genomic alterations at post-transplantation relapse, in line with previous reports<sup>5</sup>, indicates that AML clonal evolution also continues after allo-HCT. However, the macro-alterations we identified here are clustered in well-known hotspots for AML both at diagnosis<sup>8</sup> and at relapse after chemotherapy<sup>9</sup>, indicating that they are unlikely to be linked to the immunological effects of allo-HCT, but rather to the clonal dynamics characteristic of tumors, canalized by the selective bottleneck imposed by the transplant conditioning regimen.

We next pairwise compared the gene expression profiles of AML blasts purified at diagnosis and at post-transplantation relapse, identifying a signature of 110 differentially expressed genes (DEGs) (Supplementary Table 4). Gene ontology analysis revealed that this signature was significantly enriched in immune-related genes (Fig. 1b). In-depth analysis of the three cases for which samples after sole chemotherapy were available evidenced that the immune-related changes were specific for post-transplantation relapses (Fig. 1c–e), possibly imprinted by the graft-versus-leukemia (GvL) effect.

To overcome the redundancy of gene ontology categorization, we assessed the semantic distance between the significantly deregulated biological processes using the GOSemSim Bioconductor R package<sup>10</sup> and identified two deregulated ‘macro-clusters’ encompassing genes linked to T cell costimulation and to antigen processing and presentation via HLA class II molecules (Fig. 1f). This result was confirmed by an independent bioinformatic analysis with the ClueGO package from Cytoscape<sup>11</sup> (Extended Data Fig. 2).

Given the deregulation of the T cell costimulation process highlighted in the previous analyses, we retrieved from the original dataset the expression levels of 32 genes known to be relevant in conveying activating or inhibitory signals to T cells and used them to create a heatmap representing the fold change in the expression of these genes between leukemia at diagnosis and its counterparts at relapse after chemotherapy or allo-HCT (Fig. 2a). This allowed us to appreciate the downregulation in post-transplantation relapses of multiple activatory ligands and adhesion molecules, including CD11A/LFA-1, and largely unchanged expression of

inhibitory ligands, except for a modest increase in the expression of B7-H3.

However, since most of these genes are poorly covered by expression arrays, we further analyzed by immunophenotypic analysis AML blasts and T cells collected before and after allo-HCT from 33 discovery cohort patients (Supplementary Table 2).

After gating on leukemia blasts (Supplementary Fig. 1), we assessed the positivity (Fig. 2b) and RFI (Fig. 2c) of 13 T cell ligands. We confirmed the changes in B7-H3 and CD11A levels detected by gene expression analysis, and documented in addition upregulation in relapsed leukemia of PD-L1 (significant in terms of percentage but not of RFI), PVRL2 and CD80.

Notably, the changes we observed in the expression profile of leukemia cells at post-transplantation relapse were mirrored by corresponding alterations in T cells (Fig. 2d). In particular, we observed that the percentage of T cells expressing PD-1 was significantly higher in AML patients before allo-HCT than in healthy controls, was similarly high in transplanted patients in remission and rose further at post-transplantation relapse. The percentage of T cells expressing PD-1 at post-transplantation relapse correlated significantly with the changes observed in the expression of PD-L1 between pre- and post-transplant analysis (Fig. 2e), hinting that upregulation of the ligand in leukemia blasts might have induced an exhausted phenotype in the corresponding T cells. For all the other receptors analyzed, except CTLA4, we documented significant differences between healthy individuals and patients at diagnosis, but either no change between the T cells at diagnosis and at relapse (for TIGIT, ICOS, OX40 and ICAM-1) or changes that were similarly observed in the lymphocytes of patients in remission after transplant (for DNAM-1 and CD28), indicating a principal role of the post-transplantation immune environment in driving their altered expression.

Taken together, these data demonstrate that the costimulatory interface between T cells and leukemia changes significantly after allo-HCT, with loss of costimulatory interactions (CD28/CD80, ICAM-1/CD11A) and enforcement of inhibitory ones (PD-1/PD-L1).

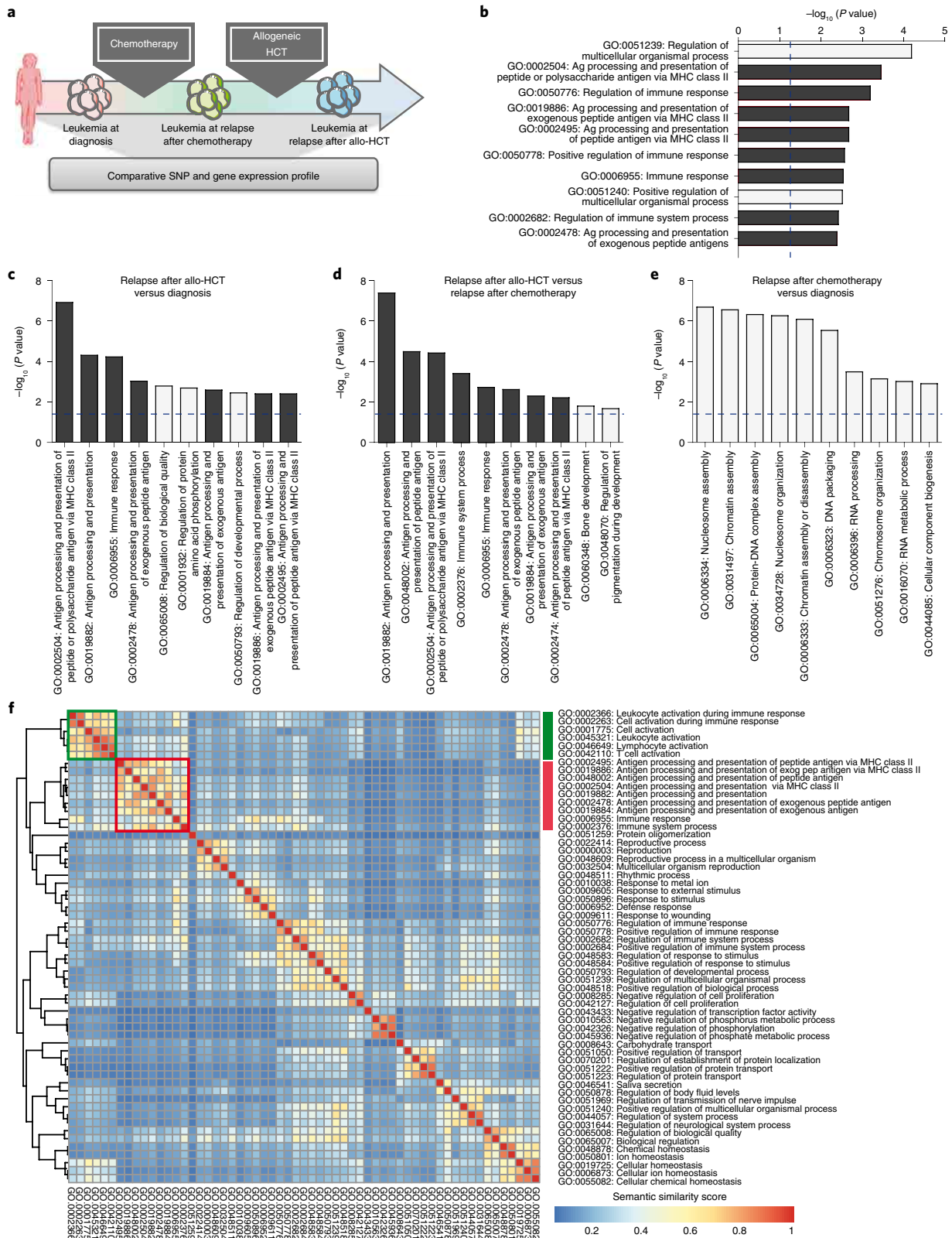
To address the functional and translational relevance of these findings, we studied more in detail the case of a patient who relapsed 200 days after HCT with PD-L1<sup>+</sup> leukemia (UPN 24). We observed that during the post-transplantation follow-up the increase in the expression of PD-1 on donor-derived T cells paralleled the rise of minimal residual disease markers and anticipated clinical relapse (Fig. 2f). In ex vivo coculture experiments, addition of an anti-PD-L1 blocking antibody increased both the proliferation (Fig. 2g) and the release of IFN- $\gamma$  (Fig. 2h) of donor-derived T cells against the patient leukemia blasts. Although this single patient observation should be considered cautiously, it suggests

**Fig. 1 | Immune-related changes in leukemia relapsing after allo-HCT.** **a**, Outline of the experimental work-flow: peripheral blood and bone marrow samples were longitudinally collected from AML patients at the time of disease diagnosis, relapse after sole chemotherapy and relapse after allo-HCT. Leukemia blasts were purified from each sample by FACS-sorting and then subjected to genomic and transcriptional profile analysis. **b**, Histogram outlining the ten most significantly deregulated biological processes (classified by gene ontology terms) identified from the pairwise comparison of AML blasts collected and purified from discovery cohort patients at disease diagnosis and at relapse after allo-HCT ( $n=9$ ). The length of each bar is proportional to the significance of enrichment, calculated by a two-sided Fisher's exact test, with  $P$  values  $<0.05$  to the right of the dashed blue line. Dark bars denote immune-related biological processes. **c–e**, Histograms outlining biological processes identified as significantly deregulated from all pairwise comparisons performed for cases in which leukemia samples were available at disease diagnosis, at relapse after sole chemotherapy and at relapse after allo-HCT: a summary of the results obtained from the comparison between relapse after allo-HCT and disease at diagnosis (**c**), a summary of the results obtained from the comparison between relapse after allo-HCT and relapse after chemotherapy (**d**) and a summary of the results obtained from the comparison between relapse after chemotherapy and disease at diagnosis (**e**). The height of each bar is proportional to the significance of enrichment, calculated by a two-sided Fisher's exact test, with  $P < 0.05$  above the dashed blue line. **f**, Heatmap representing the semantic similarity between all gene ontology terms identified as significantly deregulated ( $P < 0.05$ ) from the pairwise comparison of AML blasts collected at disease diagnosis and at relapse after allo-HCT from discovery cohort patients ( $n=9$ ). Red indicates high similarity in gene content between two gene ontologies, blue indicates low similarity. Gene ontology terms are clustered according to their semantic distance, thus allowing the identification of significantly deregulated ‘macro-processes’ (yellow/red squares in the heatmap), including one encompassing gene ontology terms linked to T cell costimulation (in green) and one encompassing gene ontology terms linked to antigen processing and presentation via HLA class II (in red).

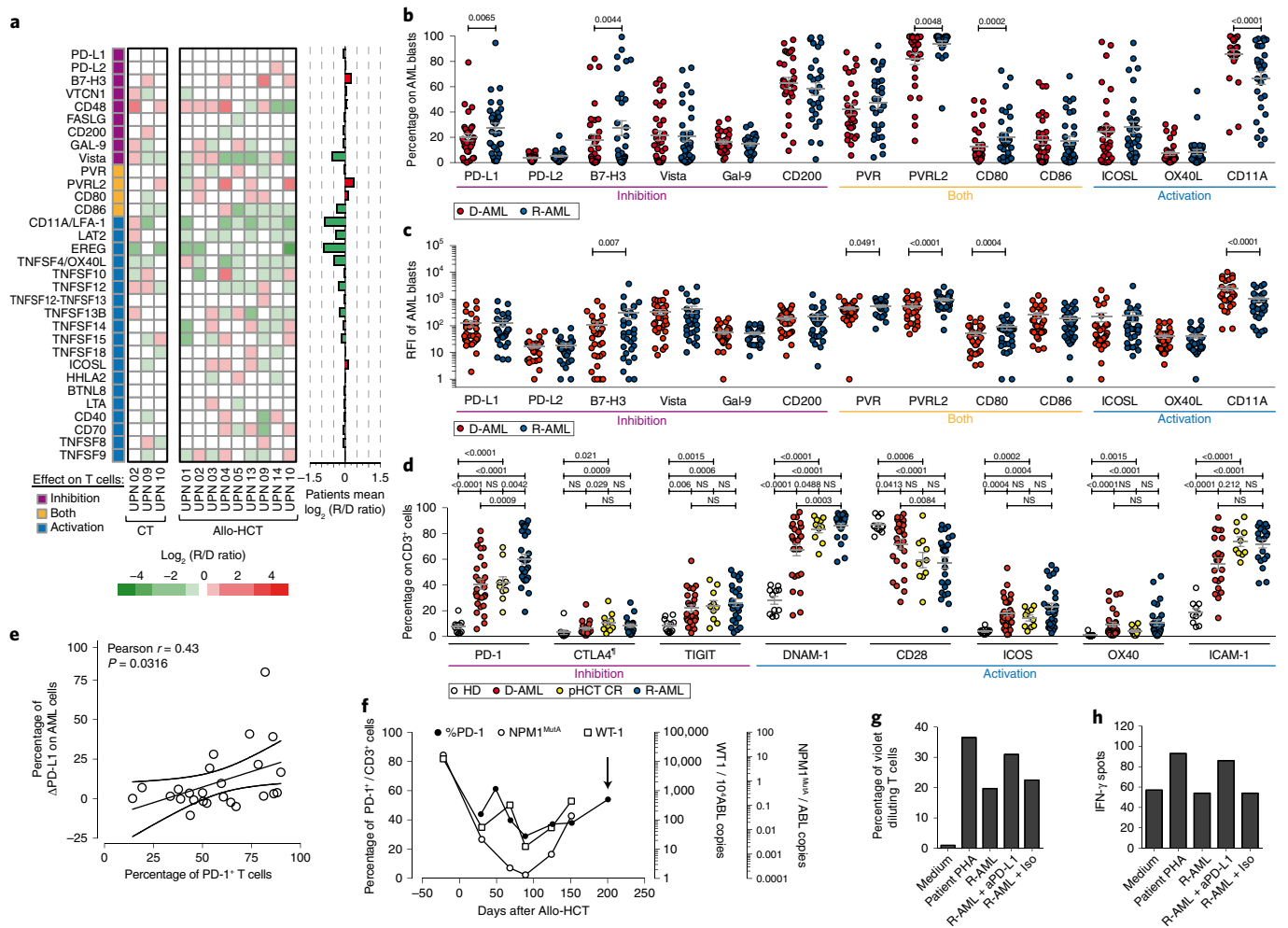
that at least in some patients with deregulation of the PD-1/PD-L1 axis, checkpoint blockade might restore a proficient GvL effect against the relapsed disease.

We next extracted from our dataset the expression of transcripts involved in peptide proteolysis and HLA presentation, selected from the Reactome database<sup>12</sup>. This analysis revealed the frequent and significant downregulation at post-transplantation relapse of

almost all HLA class II transcripts and of their known regulator CIITA (Fig. 3a), which was confirmed by locus-specific quantitative PCR (Fig. 3b) and not explained by genomic alterations detectable by SNP arrays (Extended Data Fig. 1 and Supplementary Table 3). Comparative immunophenotypic analysis of leukemia blasts collected before and after allo-HCT confirmed loss of HLA-DR and -DP cell surface expression in 7/33 relapses (Fig. 3c,d). In all cases,







**Fig. 2 | Impaired T cell costimulation by leukemia blasts at post-transplantation relapse.** **a**, Heatmap representing fold expression changes in transcripts for molecules known to exert an inhibitory effect on T cells (purple markers), activating them (blue markers) or able to mediate both effects, depending on the cognate receptor expressed by T cells (yellow markers). Transcript levels were assessed by microarrays, comparing leukemia at diagnosis with relapses after chemotherapy (CT,  $n = 3$ ) or allo-HCT (allo-HCT CT,  $n = 9$ ). Red and green indicate transcript upregulation and downregulation at relapse, respectively. Bars on the right side of the heatmap summarize average fold changes at post-transplantation relapse. **b, c**, Percentage of cell surface expression (**b**) and relative fluorescence intensity (RFI) (**c**) of inhibitory (in purple), activatory (in blue) or dual-functional (in yellow) ligands, assessed by immunophenotypic analysis of leukemia cells pairwise collected from discovery cohort patients before allo-HCT (red dots) and at post-transplantation relapse (blue dots) ( $n = 33$ ). Shown are mean  $\pm$  s.e.m.;  $P$  values were calculated by a two-sided Wilcoxon matched-pairs signed rank test at a 95% confidence interval (CI). **d**, Expression on the T cell surface of inhibitory (in purple) or activatory (in blue) receptors, assessed by immunophenotypic analysis of peripheral blood samples collected from healthy volunteers (in white,  $n = 10$ ), from discovery cohort patients before allo-HCT (red dots) and at post-transplantation relapse (blue dots) ( $n = 33$ ), and from patients in complete remission 2 months after allo-HCT (yellow dots,  $n = 10$ ). Expression of CTLA4 is tested by intracellular staining and shown on CD4<sup>+</sup> T cells. Shown are mean  $\pm$  s.e.m.;  $P$  values were calculated by a two-sided unpaired or paired  $t$  test at 95% CI, as appropriate. **e**, Correlation between the expression of PD-1 on T cells at post-transplantation relapse ( $x$  axis) and the change in expression of PD-1 on AML blasts between diagnosis and relapse ( $y$  axis) in 25 evaluable sample pairs. Shown are results of two-sided Pearson correlation analysis, with linear regression line and 95% CI. **f**, Time course of the expression of PD-1 on unique patient number (UPN) 24 T cells over time after allo-HCT (black circles) in relation to the levels of the NPM1<sup>mutA</sup> and WT1 transcripts in the patient bone marrow (white circles and squares, respectively). The black arrow indicates the time of the hematological relapse. Each patient-derived sample has been analyzed once, with three technical replicates for the molecular analyses. **g, h**, T cells collected from UPN 24, 150 days after allo-HCT and 50 days before relapse (38% positive for PD-1 at the time of sampling) were tested for their ability to proliferate (**g**, showing the percentage of vital dye diluting cells in each condition tested) and release IFN- $\gamma$  (**h**, showing for each condition the number of IFN- $\gamma$  spots detected from one out of three technical replicates) in response to patient PHA-stimulated lymphocytes (patient PHA), leukemia blasts collected from the same patient at post-transplantation relapse (41% positive for PD-1, R-AML), the same blasts preincubated with an anti-CD11A blocking antibody (R-AML + aPD-1) or the same blasts preincubated with a control isotype antibody (R-AML + Iso). Proliferation was assessed by dilution of the CellTrace Violet membrane dye, cytokine release by IFN- $\gamma$  ELISpot assay. Shown are results from a single experiment.

analyzed expression of HLA class I remained high at post-transplantation relapse (Extended Data Fig. 3).

We showed in cytotoxicity assay (Fig. 3e), IFN- $\gamma$  ELISpot (Fig. 3f) and antigen-specific activation assay (Fig. 3g) that T cells collected from a patient who experienced relapse with loss of HLA class II

expression (UPN 10) responded to the leukemia at diagnosis, and not to its relapsed counterpart.

Taken together, these data indicate that not only genomic loss of a mismatched HLA haplotype, but also the transcriptional silencing of HLA class II molecules occur frequently in leuke-

mia relapses after allo-HCT, abrogating leukemia recognition by donor-derived T cells.

On the basis of the observation that in a patient-derived xenograft model HLA class II expression could be recovered on cross-recognition of minor histocompatibility antigens presented by leukemia blasts via HLA class I molecules and/or by xeno-reactivity against murine tissues (Extended Data Fig. 4), primary blasts from UPN 17 at post-transplantation relapse were cultured *in vitro* in the presence or absence of the same cytokines that were analyzed in the mouse sera, documenting that only IFN- $\gamma$  was able to re-induce the surface expression of HLA-DR (Fig. 3h). Also, in the other cases of relapse with loss of HLA class II expression, exposure of leukemia cells to IFN- $\gamma$  increased the expression of HLA class II (Fig. 3i,k) and rescued effective recognition of relapsed leukemia cells by donor-derived T cells (Fig. 3l).

By analyzing the expression of immune markers of interest in leukemia relapses after sole chemotherapy (Extended Data Fig. 5) and in non-malignant counterparts of AML (Supplementary Fig. 2 and Extended Data Fig. 6) we could demonstrate that the changes in T cell costimulation and antigen presentation that we documented occur only after allo-HCT, and only in leukemia cells.

To confirm the robustness of our findings, we analyzed by RNA-seq and immunophenotypic profiling a validation set of 36 pre- and post-transplantation AML samples collected from seven different transplantation centers (Supplementary Tables 1 and 5). Despite the many differences between the two cohorts in terms of type of transplant, disease status and graft-versus-host disease (GvHD) prophylaxis, the 110-gene signature derived from our discovery series was also highly consistent in this validation set (Fig. 4a), as were the patterns and relative frequency of the transcriptional changes documented in genes involved in T cell costimulation and HLA class II presentation (Fig. 4b and Extended Data Fig. 7).

To analyze the reciprocal interactions of the two newly identified modalities of relapse, the immunophenotypic datasets originated from the two cohorts were clustered on the basis of profile similarity (Fig. 4c,d). This allowed to clearly distinguish in both cohorts a subset of patients with downregulation of HLA class II molecules (top clusters, 45% of cases in the discovery set and 39% in the validation set), and a second macro-cluster characterized by minor changes (middle sub-clusters) or upregulation (lower sub-clusters) of HLA class II molecules, accompanied by more evident upregulation of inhibitory markers, including PD-L1. Concordantly, high-dimensional analysis identified relapse-specific clusters with lower HLA-DR expression and increased PD-L1 expression as compared to their diagnosis-specific counterparts (Extended Data Fig. 8). Correlation analysis evidenced that inhibitory ligands were mostly upregulated in cases with conserved or increased expression of HLA-DR and -DP (Fig. 4e,f).

We finally integrated our results regarding immune-related changes with known clinical and immunogenetic variables. The distribution of patients among relapse modalities did not correlate with most of the features analyzed, including cytogenetics, leukemia driver mutations and donor-recipient HLA matching. The only variables that showed a significant correlation with HLA class II downregulation at relapse were the use of a peripheral blood stem cell graft and the dose of infused T cells, consistent in each patient cohort and reaching statistical significance only when the two were merged (Extended Data Fig. 9).

The results from the present study complement and reinforce previous work on genomic HLA loss<sup>4,6,7</sup> in supporting the hypothesis that post-transplantation relapses might frequently represent the end-result of mechanisms enacted by leukemia cells to evade immune control, and that immune pressure might substantially deviate the trajectory of leukemia clonal evolution<sup>13,14</sup>.

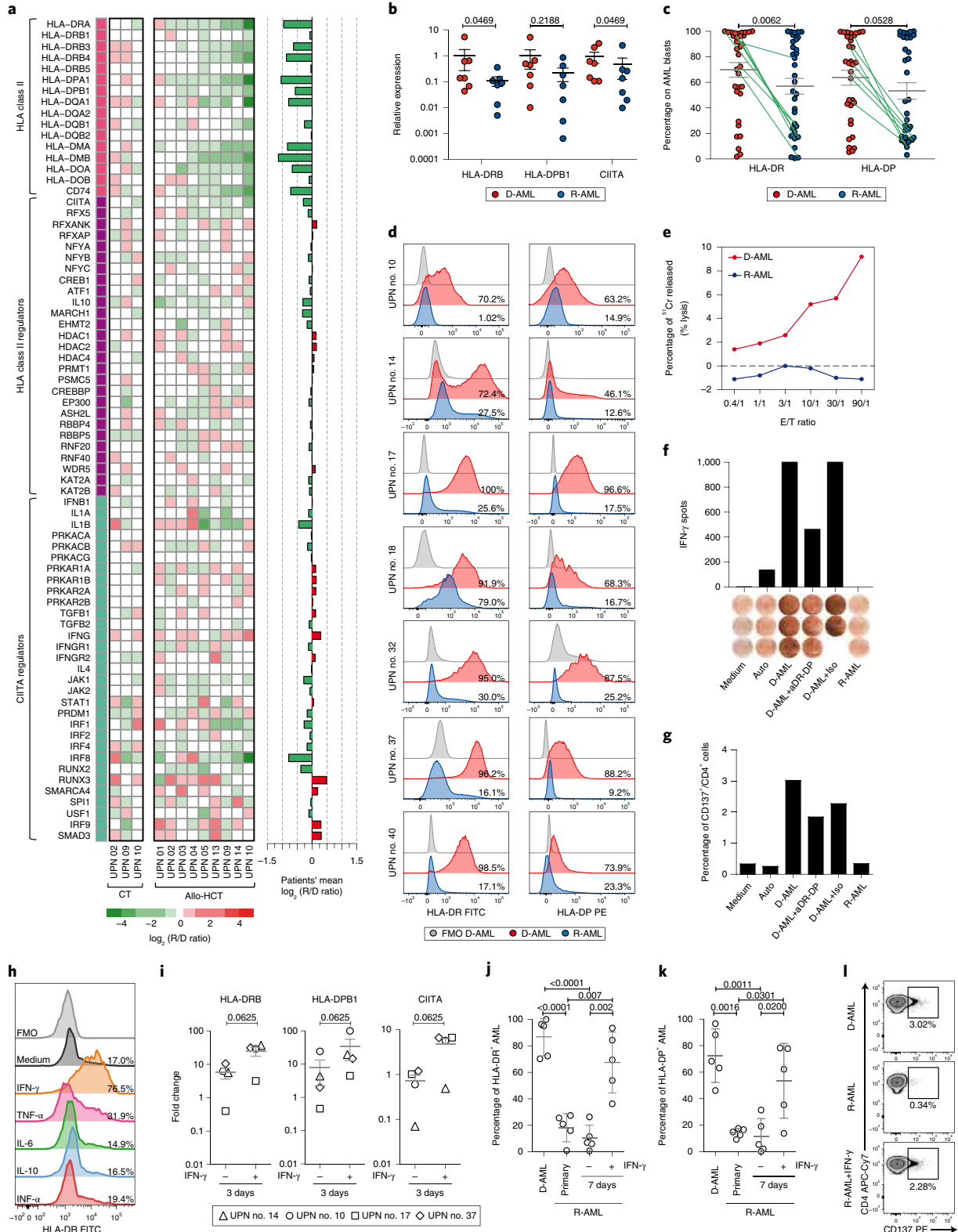
**Fig. 3 | Loss of HLA class II expression in leukemia cells at post-transplantation relapse.** **a**, Heatmap representing fold expression changes in HLA class II transcripts (fuchsia markers), their regulators (purple markers) and regulators of CIITA (teal markers), assessed by microarrays, comparing leukemia at diagnosis with relapses after chemotherapy (CT,  $n=3$ ) or after allo-HCT (allo-HCT,  $n=9$ ). Red and green indicate transcript upregulation and downregulation at relapse, respectively. Bars on the right side of the heatmap summarize average fold changes at post-transplantation relapse. **b**, mRNA expression levels of HLA-DRB, HLA-DPB1 and CIITA measured by locus-specific quantitative PCR in leukemia blasts purified from discovery cohort patients at diagnosis (red dots) and at post-transplantation relapse (blue dots) ( $n=7$ ). Shown are mean  $\pm$  s.e.m.;  $P$  values were calculated by a two-sided Wilcoxon matched-pairs signed rank test at 95% CI. **c,d**, Expression on the cell surface of leukemia blasts of HLA-DR and HLA-DP molecules, assessed by immunophenotypic analysis in samples pair-wise collected from discovery cohort patients before allo-HCT (red dots) and at post-transplantation relapse (blue dots) ( $n=33$ ) (**c**). Shown are mean  $\pm$  s.e.m.;  $P$  values calculated by a two-sided Wilcoxon matched-pairs signed rank test at 95% CI. Green lines link pre- and post-transplantation assessments in the seven patients for whom histogram plots are shown in **d**. Gray histograms in **d** represent fluorescence-minus-one (FMO) controls of AML blasts at diagnosis. For each histogram, the percentage displayed refers to the comparison with the relevant FMO control. All of these samples have been analyzed at least twice with similar results. **e-g**, T cells collected from UPN 10, 310 days after allo-HCT and 30 days before relapse were stimulated with leukemia blasts collected from the same patient at diagnosis, and tested by standard 4-h chromium release cytotoxicity assay (**e**, showing one out of three technical triplicates from one out of two independent experiments), by IFN- $\gamma$  ELISpot assay (**f**, showing for each condition the number of IFN- $\gamma$  spots detected from one out of two or three technical replicates from one out of two independent experiments) and by CD137/4-1BB upregulation assay (**g**, showing the percentages of CD137<sup>+</sup> CD4<sup>+</sup> T cells in each condition tested, calculated using as reference for gating the spontaneous expression in CD4<sup>+</sup> T cells cultured in medium alone; shown are results from one out of two independent experiments). Targets for the cytotoxicity assay were patient leukemia cells collected at diagnosis (red line) and at post-transplantation relapse (blue line). Targets for IFN- $\gamma$  ELISpot and CD137/4-1BB assays were donor autologous PHA-stimulated lymphocytes (auto), the patient leukemia cells at diagnosis incubated with medium alone (D-AML), with anti-HLA-DR and anti-HLA-DP blocking antibodies (D-AML+aDR-DP) or with an isotype control antibody (D-AML+Iso), and the patient leukemia cells at post-transplantation relapse (R-AML). **h**, Leukemia blasts collected from UPN 17 at post-transplantation relapse were tested for recovery of HLA-DR expression after 72 h of culture in the presence of medium alone or supplemented with human cytokines. The gray histogram represents the FMO control of the sample cultured in medium alone. Shown are results from a single experiment. **i**, Fold change in HLA class II transcripts on IFN- $\gamma$  treatment of AML post-transplantation relapses from UPN 14 (triangle), 10 (circle), 17 (square) and 37 (diamond). Leukemia cells were incubated for 3 days with IFN- $\gamma$  or medium alone. Numbers above graphs indicate  $P$  obtained from two-sided Wilcoxon matched-pairs signed rank test at 95% CI. **j,k**, Dot plots represent the percentage of leukemia blasts expressing HLA-DR (**j**) and HLA-DP (**k**), assessed by immunophenotypic analysis of samples collected from five patients at diagnosis (D-AML) and at relapse after allo-HCT (R-AML). Relapse samples were also tested after 7 days of culture in the presence or absence of human IFN- $\gamma$ . Shown are mean  $\pm$  s.d.;  $P$  values were calculated by one-way analysis of variance (ANOVA) with Bonferroni correction post-test. **l**, T cells collected from UPN 10, 310 days after allo-HCT and 30 days before relapse were stimulated with patient leukemia blasts collected from the same patient at time of diagnosis, and tested for expression of the activation marker CD137/4-1BB on the cell surface of CD4<sup>+</sup> cells on rechallenge with patient leukemia cells at diagnosis (D-AML), patient leukemia cells at relapse (R-AML) or the same relapsed leukemia cultured for 7 days in the presence of human IFN- $\gamma$  (R-AML+IFN- $\gamma$ ). Shown are the percentages of CD137<sup>+</sup> CD4<sup>+</sup> T cells in each condition tested, calculated using as reference for gating the spontaneous expression of CD137 in CD4<sup>+</sup> T cells cultured in medium alone. Shown are results from one out of two independent experiments.

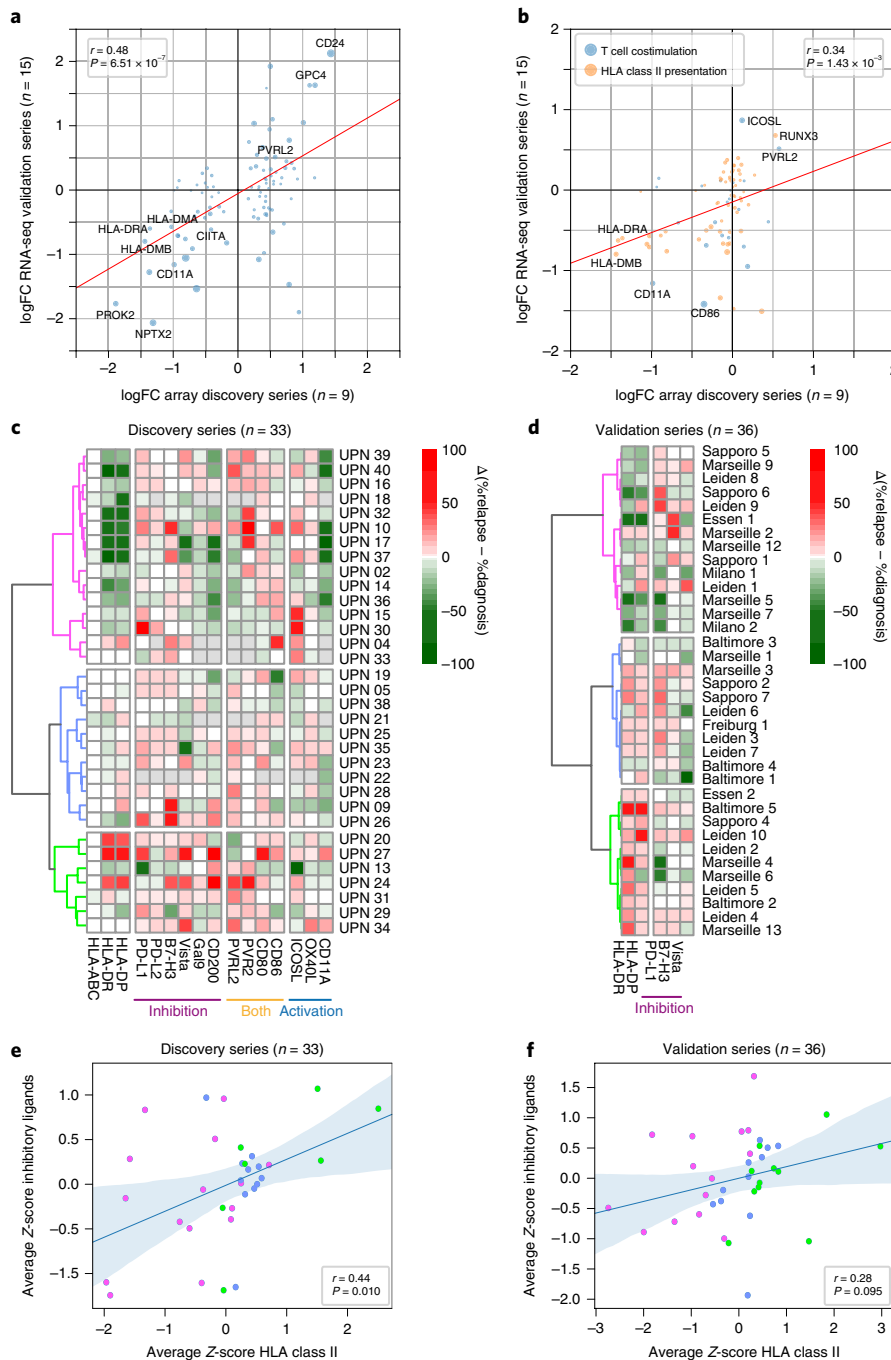


Whereas the previously described mechanism of HLA loss relied on large-scale genomic alterations<sup>4</sup>, here we observed transcriptional changes that were not explained by genomics, indicating they might have a primarily epigenetic origin. This intriguing hypothesis is supported by recent studies highlighting the extents of AML epigenetic clonal evolution<sup>15</sup>, by the preclinical evidence of immune-related effects of epigenetic drugs<sup>16,17</sup> and by the promising

results achieved by these same therapies against post-transplantation relapse<sup>18,19</sup>.

Several previous reports have shown that AML blasts can express multiple inhibitory ligands to dampen T cell recognition<sup>20-23</sup>. Here we show that this feature becomes even more prevalent at relapse after allo-HCT. Despite some very promising preliminary results<sup>24,25</sup>, the implementation of checkpoint blockade





**Fig. 4 | Validation, frequency and reciprocal interplay of the two newly identified modalities of post-transplantation leukemia relapse.** **a**, Scatter plot displaying the fold changes in the levels of transcripts belonging to the 110-gene signature of post-transplantation relapse detected by microarray analysis of paired diagnosis-relapse samples from the discovery cohort (x axis,  $n = 9$ ) and by RNA-seq analysis of paired diagnosis-relapse samples from the validation cohort (y axis,  $n = 15$ ). Size of the dots is proportional to the significance of the deregulation in the validation dataset. Shown are the results of two-sided Pearson correlation analysis. **b**, Scatter plot displaying the fold changes in the levels of transcripts from genes known to be involved in T cell costimulation (in cyan) or HLA class II presentation (in light orange) detected by microarray analysis of paired diagnosis-relapse samples from the discovery cohort (x axis,  $n = 9$ ) and by RNA-seq analysis of paired diagnosis-relapse samples from the validation cohort (y axis,  $n = 15$ ). Size of the dots is proportional to the significance of the deregulation in the validation dataset. Shown are the results of two-sided Pearson correlation analysis. **c,d**, The datasets generated from the immunophenotypic analysis of the full panel of antigen presentation and T cell costimulation molecules in the discovery cohort ( $n = 33$ , **c**) and in the validation cohort ( $n = 36$ , **d**) were employed to generate two heatmaps of fold changes in the expression of each marker. Unsupervised clustering was then performed to group together patients with similar patterns of phenotypical changes. By ANOVA analysis, HLA-DR and -DP resulted as the most significant contributors in determining the clustering. Red indicates surface marker upregulation at relapse, green indicates surface marker downregulation at relapse. Light gray squares indicate markers not tested in the relevant patient. **e,f**, Scatter plots displaying the correlation between changes in the surface expression of HLA class II molecules from diagnosis to relapse (on the x axis, expressed as average Z score) and changes in the overall expression of inhibitory ligands in the same leukemia sample pair (on the y axis, expressed as average Z score) in the discovery cohort ( $n = 33$ , **e**) and in the validation cohort ( $n = 36$ , **f**). Colors of the dots relate to the three patient clusters indicated in **c** and **d**. Shown are results of two-sided Pearson correlation analysis. The blue line represents the best fit regression line and the light blue area indicates the 95% CI.

in the context of allo-HCT has been restrained by concerns regarding the risk of inducing severe GvHD<sup>26,27</sup>. Our results indicate that in selected patients checkpoint blockade may be highly effective in restoring the GvL effect, although the multiplicity of different patterns of co-expression of inhibitory ligands and the observation that most changes are subtle quantitative deregulations indicated that combinatorial therapy will probably be required to achieve clinically meaningful results.

The second relapse modality identified in this study depends on the downregulation of HLA class II molecules from the surface of leukemia blasts. Analogously to genomic HLA loss<sup>6</sup>, this mechanism also appeared to be directly correlated with the dose of T cells infused with the graft. However, different from its genomic counterpart, loss of HLA class II expression did not correlate with the number of donor-recipient HLA incompatibilities and also occurred after HLA-matched HCTs, where it may favor immune evasion by dramatically narrowing the antigenic repertoire presented to donor T cells. In the single case in which functional ex vivo validation was possible, loss of HLA class II molecules abrogated recognition of leukemia by donor T cells, supporting previous studies on the role of incompatible HLA class II molecules as preferential targets of GvL<sup>28,29</sup>, and pointing to a central role of CD4<sup>+</sup> T cells in post-transplantation leukemia immunosurveillance.

Of note, the mechanisms we described sit on two opposite poles of interferon-mediated responses: while in fact IFN- $\gamma$  can rescue the surface expression of HLA class II molecules on relapsed leukemia, it is also known to promote the expression of PD-L1 and other inhibitory ligands<sup>30–32</sup>. This dichotomy has a translational impact, since promoting IFN- $\gamma$  systemic release, such as by inducing non-severe chronic GvHD, might be beneficial to patients in which relapse depends on the loss of HLA expression and detrimental to those in which relapse is driven by the enhancement of inhibitory axes.

Including cases with genomic loss of HLA, we can now recognize a defined immune pattern in more than two-thirds of relapses, each targetable by a precise salvage therapy: re-transplantation from a different donor for patients with genomic HLA loss<sup>6,33,34</sup>, checkpoint blockade for those with upregulation of inhibitory ligands and establishment of mild chronic GvHD for those with loss of HLA class II expression. Recent data have shown that, even in cases in which relapse depends on the FLT3-ITD oncogene amplification, it is possible to exploit the transplanted immune system in a tailored approach<sup>35</sup>. Whereas each of these strategies may yield mixed results when employed without a clear patient selection criterion, their efficacy can be substantially improved when it is based on a specific biological rationale, fulfilling the logic of personalized medicine.

### Online content

Any methods, further references, Nature Research reporting summaries, source data, statements of data availability and associated accession codes are available at <https://doi.org/10.1038/s41591-019-0400-z>.

Received: 15 March 2018; Accepted: 15 February 2019;

Published online: 25 March 2019

### References

- Copelan, E. A. Hematopoietic stem-cell transplantation. *N. Engl. J. Med.* **354**, 1813–1826 (2006).
- Kolb, H.-J. Graft-versus-leukemia effects of transplantation and donor lymphocytes. *Blood* **112**, 4371–4383 (2008).
- Horowitz M et al. Epidemiology and biology of relapse after stem cell transplantation. *Bone Marrow Trans.* **53**, 1379–1389 (2018).
- Vago, L. et al. Loss of mismatched HLA in leukemia after stem-cell transplantation. *N. Engl. J. Med.* **361**, 478–488 (2009).
- Waterhouse, M. et al. Genome-wide profiling in AML patients relapsing after allogeneic hematopoietic cell transplantation. *Biol. Blood Marrow Trans.* **17**, 1450–1459.e1 (2011).
- Crucitti, L. et al. Incidence, risk factors and clinical outcome of leukemia relapses with loss of the mismatched HLA after partially incompatible hematopoietic stem cell transplantation. *Leukemia* **29**, 1143–1152 (2015).
- Vago, L., Toffalori, C., Ciceri, F. & Fleischhauer, K. Genomic loss of mismatched human leukocyte antigen and leukemia immune escape from haploidentical graft-versus-leukemia. *Semin. Oncol.* **39**, 707–715 (2012).
- Gupta, M. et al. Novel regions of acquired uniparental disomy discovered in acute myeloid leukemia. *Genes Chromosom. Cancer* **47**, 729–739 (2008).
- Raghavan, M. et al. Segmental uniparental disomy is a commonly acquired genetic event in relapsed acute myeloid leukemia. *Blood* **112**, 814–821 (2008).
- Yu, G. et al. GOSemSim: an R package for measuring semantic similarity among GO terms and gene products. *Bioinformatics* **26**, 976–978 (2010).
- Bindea, G. et al. ClueGO: a Cytoscape plug-in to decipher functionally grouped gene ontology and pathway annotation networks. *Bioinformatics* **25**, 1091–1093 (2009).
- Fabregat, A. et al. The Reactome Pathway Knowledgebase. *Nucleic Acids Res.* **46**, D649–D655 (2018).
- Ding, L. et al. Clonal evolution in relapsed acute myeloid leukaemia revealed by whole-genome sequencing. *Nature* **481**, 506–510 (2012).
- Shlush, L. I. et al. Tracing the origins of relapse in acute myeloid leukaemia to stem cells. *Nature* **547**, 104–108 (2017).
- Li, S. et al. Distinct evolution and dynamics of epigenetic and genetic heterogeneity in acute myeloid leukemia. *Nat. Med.* **22**, 792–799 (2016).
- Goodyear, O. et al. Induction of a CD8<sup>+</sup> T-cell response to the MAGE cancer testis antigen by combined treatment with azacitidine and sodium valproate in patients with acute myeloid leukemia and myelodysplasia. *Blood* **116**, 1908–1918 (2010).
- Goodyear, O. C. et al. Azacitidine augments expansion of regulatory T cells after allogeneic stem cell transplantation in patients with acute myeloid leukemia (AML). *Blood* **119**, 3361–3369 (2012).
- de Lima, M. et al. Maintenance therapy with low-dose azacitidine after allogeneic hematopoietic stem cell transplantation for recurrent acute myelogenous leukemia or myelodysplastic syndrome: a dose and schedule finding study. *Cancer* **116**, 5420–5431 (2010).
- Platzbecker, U. et al. Azacitidine for treatment of imminent relapse in MDS or AML patients after allogeneic HSCT: results of the RELAZA trial. *Leukemia* **26**, 381–389 (2012).
- Zhou, Q. et al. Program death-1 signaling and regulatory T cells collaborate to resist the function of adoptively transferred cytotoxic T lymphocytes in advanced acute myeloid leukemia. *Blood* **116**, 2484–2493 (2010).
- Norde, W. J. et al. PD-1/PD-L1 interactions contribute to functional T-cell impairment in patients who relapse with cancer after allogeneic stem cell transplantation. *Cancer Res.* **71**, 5111–5122 (2011).
- Hobo, W., Hutten, T. J. A., Schaap, N. P. M. & Dolstra, H. Immune checkpoint molecules in acute myeloid leukaemia: managing the double-edged sword. *Br. J. Haematol.* **181**, 38–53 (2018).
- Knaus, H. A., Kanakry, C. G., Luznik, L. & Gojo, I. Immunomodulatory drugs: immune checkpoint agents in acute leukemia. *Curr. Drug Targets* **18**, 315–331 (2017).
- Bashey, A. et al. CTLA4 blockade with ipilimumab to treat relapse of malignancy after allogeneic hematopoietic cell transplantation. *Blood* **113**, 1581–1588 (2009).
- Davids, M. S. et al. Ipilimumab for patients with relapse after allogeneic transplantation. *N. Engl. J. Med.* **375**, 143–153 (2016).
- Blazar, B. R. et al. Blockade of programmed death-1 engagement accelerates graft-versus-host disease lethality by an IFN-gamma-dependent mechanism. *J. Immunol.* **171**, 1272–1277 (2003).
- Haverkos, B. M. et al. PD-1 blockade for relapsed lymphoma post-allogeneic hematopoietic cell transplant: high response rate but frequent GVHD. *Blood* **130**, 221–228 (2017).
- Stevanović, S., van Schie, M. L. J., Griffioen, M. & Falkenburg, J. H. HLA-class II disparity is necessary for effective T cell mediated graft-versus-leukemia effects in NOD/scid mice engrafted with human acute lymphoblastic leukemia. *Leukemia* **27**, 985–987 (2013).
- Fleischhauer, K. & Shaw, B. E. HLA-DP in unrelated hematopoietic cell transplantation revisited: challenges and opportunities. *Blood* **130**, 1089–1096 (2017).
- Abiko, K. et al. IFN- $\gamma$  from lymphocytes induces PD-L1 expression and promotes progression of ovarian cancer. *Br. J. Cancer* **112**, 1501–1509 (2015).
- García-Díaz, A. et al. Interferon receptor signaling pathways regulating PD-L1 and PD-L2 expression. *Cell Rep.* **19**, 1189–1201 (2017).
- Berthon, C. et al. In acute myeloid leukemia, B7-H1 (PD-L1) protection of blasts from cytotoxic T cells is induced by TLR ligands and interferon-gamma and can be reversed using MEK inhibitors. *Cancer Immunol. Immunother.* **59**, 1839–1849 (2010).
- Imus P H et al. Major histocompatibility mismatch and donor choice for second allogeneic bone marrow transplantation. *Biol. Blood Marrow Trans.* **23**, 1887–1894 (2017).

34. Vago, L. & Ciceri, F. Choosing the alternative. *Biol. Blood Marrow Trans.* **23**, 1813–1814 (2017).
35. Mathew, N. R. et al. Sorafenib promotes graft-versus-leukemia activity in mice and humans through IL-15 production in FLT3-ITD-mutant leukemia cells. *Nat. Med.* **24**, 282–291 (2018).

### Acknowledgements

This work was supported by the Italian Ministry of Health (no. RF-FSR-2008-1202648 to K.F., F.C. and C.Barlassina, no. RF-2011-02351998 to F.C. and L.V., no. RF-2011-02348034 to L.V. and TRANSCAN HLALOSS to L.V. and K.F.), by the Italian Ministry of University and Research (no. MIUR-2015NZWSEC-001 to C.Bonini), by the CARIPLO Foundation (no. 2009-2665 to K.F., A.R. and C.Barlassina), by the Associazione Italiana per la Ricerca sul Cancro (IG no. 18458 to C.Bonini, IG no. 12042 to K.F. and F.C. and Start-Up Grant no. 14162 to L.V.), by the ASCO Conquer Cancer Foundation (2014 Young Investigator Award to L.V.), EU-FP7 (SUPERSIST to C.Bonini), the Deutsche José Carreras Leukämie Stiftung (grant nos. DJCLS R 15-02 and DJCLS 01 R/2017 to K.F.) and by the DKMS Mechtild Harf Foundation (DKMS Mechtild Harf Research Grant 2015 to L.V.). C.T. was supported by an Associazione Italiana per la Ricerca sul Cancro post-doctoral fellowship. G.O. was supported by a Fondazione Matarelli fellowship from the Associazione Italiana Leucemie and by a Fondazione Umberto Veronesi fellowship.

### Author contributions

C.T., C.Bonini, K.F., F.C. and L.V. designed the study, analyzed the data and wrote the paper. C.T., L.Z. and V.G. performed the ex vivo and in vitro experiments. C.T. and G.O. performed the in vivo experiments. M.R., G.B., M.Barcella and D.C. performed

the bioinformatic analyses. N.C., O.S., R.G., L.C., M.W., R.Z., J.F., M.H., D.W.B., I.G., L.L., M.O., T.T., R.D., D.B., C.J.M.H., M.G., M.G.C., M.Bernardi, J.P., A.R. and F.C. collected and analyzed patient samples and clinical data. C.Barlassina, E.S., D.L., G.T. and D.C. supervised the high-throughput studies. N.C., M.N., F.M. and C.Bonini provided reagents and scientific advice on the analysis of T cell dynamics. E.M., R.O., M.M.N. and B.G. provided reagents and scientific advice on the analysis of the immature and mature myeloid compartments.

### Competing interests

C.Bonini received research support from Molmed s.p.a and Intellia Therapeutics. K.F. received research support from GenDx. L.V. received research support from GenDx and Moderna Therapeutics. None of the other authors has any relevant conflicts of interest to disclose.

### Additional information

**Extended data** is available for this paper at <https://doi.org/10.1038/s41591-019-0400-z>.

**Supplementary information** is available for this paper at <https://doi.org/10.1038/s41591-019-0400-z>.

**Reprints and permissions information** is available at [www.nature.com/reprints](http://www.nature.com/reprints).

**Correspondence and requests for materials** should be addressed to L.V.

**Publisher's note:** Springer Nature remains neutral with regard to jurisdictional claims in published maps and institutional affiliations.

© The Author(s), under exclusive licence to Springer Nature America, Inc. 2019



## Methods

**Study design: patient and transplant characteristics.** In this retrospective study, on the basis of material availability, we selected a discovery cohort ( $n=40$ ) and a validation cohort ( $n=36$ ) of patients with a diagnosis of de novo or secondary AML who experienced non-HLA loss disease relapse after allo-HCT, and for whom paired pre- and post-transplant viable leukemic samples had been collected on specific written informed consent, in agreement with the Declaration of Helsinki. Discovery cohort samples came from the San Raffaele Leukemia Biobank (Protocol 'ALLO-RELAPSE' approved by the San Raffaele Ethics Committee on 3 November 2017 and Protocol 'Banca Neoplasie Ematologiche' approved by the San Raffaele Ethics Committee on 5 October 2010, latest amendment on 14 June 2012) and the Northern Italy Leukemia Group (NILG) BioBank (protocol NILG AML 02/06, NCT00495287). Validation cohort samples came from the San Raffaele Leukemia Biobank, the Universitätsklinikum Essen Biobank, the Universitätsklinikum Freiburg Biobank, the Hokkaido University Biobank, the Leiden University Medical Center Biobank, the Johns Hopkins University Biobank and the Institut Paoli-Calmettes Biobank. Supplementary Table 1 summarizes patient and transplant characteristics for both cohorts, and Supplementary Tables 2 and 5 provide a summary of the analyses conducted for each sample.

**Processing of biological samples.** Samples containing leukemia cells were thawed and kept overnight at 37 °C in X-Vivo-15 medium (Lonza) supplemented with 5% human serum (HS, Euroclone) at a concentration of  $1-2 \times 10^6$  cells per ml. Leukemia blasts were labeled in 100  $\mu$ l of complete medium for 20 min at 4 °C using fluorescent antibodies according to their leukemia associated immunophenotype (LAIP), using in all cases at least CD45, CD3 and two markers among CD34, CD33, CD117 (all from BD Biosciences) and CD14 (BioLegend). Leukemia samples were washed with 10 ml of complete medium, filtered with a cell strainer and then FACS-purified using a MoFloTM XDP (Beckman Coulter) or a FACS Diva (BD Biosciences) cell sorter. AML blast purity after sorting, assessed by flow cytometry, was  $93.56 \pm 1.16\%$  for samples employed for microarray analysis and  $91.99 \pm 1.20\%$  for samples employed for RNA-seq, with a respective T cell contaminant of  $1.29 \pm 0.57\%$  and  $0.26 \pm 0.18\%$ , superimposable between diagnosis and relapse samples.

Genomic DNA and total RNA were extracted using the Qiagen Mini Blood Kit (Qiagen) and the Trizol reagent (Invitrogen, used for samples analyzed by microarrays) or RNeasy Plus Mini or Micro Kits (Qiagen, used for samples analyzed by RNA-seq), respectively, following the manufacturer's indications. Nucleic acid quantification was performed using a Nanodrop-2000c spectrophotometer (Thermo Fisher Scientific), and quality control was performed taking advantage of the Agilent Bioanalyzer technology or the RNA Screen Tape System (both from Agilent).

**SNP array and data analysis.** Genomic profiling was performed using the Illumina Human 660W-Quad BeadChip array (Illumina), capable of assessing over 550,000 tag SNPs plus 100,000 further markers (targeting regions of common copy number variations). A total of 200 ng per sample of high-quality DNA were amplified, tagged and hybridized according to the manufacturer's protocol. The array slides were scanned on an iScan Reader (Illumina). The estimations of  $\log_2$  Ratio ( $\log_2R$ ) and B-allele frequency (BAF) were generated using default settings of the GT module of GenomeStudio v.9.4 (Illumina), taking into consideration the HapMap control set provided by the manufacturer. On the basis of the  $\log_2R$  and BAF values, Nexus Copy Number 5.0 (BioDiscovery) with default settings was used for calling copy number variation and/or LOH events, with the UCSC built Hg18—Human Mar. 2006 (NCBI36/hg18) assembly as reference. Raw data tables from GenomeStudio were then imported and processed by the DNACopy R package for segmentation analysis estimation<sup>36</sup>. The  $\log_2R$ , BAF and the segmentation data were converted into a BED graph and segment files, and alterations previously identified were confirmed by visual inspection on IGV v.2.4.8 (ref. <sup>37</sup>). Supplementary Table 3 lists all duplications, deletions and CN-LOHs larger than 0.1 Mb detected by our analysis, together with estimates of clonality of the alterations, through a method adapted from Paulsson et al.<sup>38</sup>.

**Gene expression profile array and data analysis.** Gene expression profiling for samples belonging to the discovery set was performed using the Illumina HumanHT-12 v.3.0 or v.4.0 Expression BeadChips array (Illumina), covering up to 35,000 annotated genes with more than 48,000 probes derived from the National Center for Biotechnology Information Reference Sequence (NCBI) RefSeq (Build v.36.2, Release 22) and the UniGene (Build 1999) databases. A first step of RNA amplification generating biotinylated, amplified RNA for hybridization was performed with the Illumina TotalPrep RNA Amplification Kit (Life Technologies), according to previously published protocols and to the manufacturer's recommendations<sup>39</sup>. Briefly, up to 200 ng of total RNA was reverse transcribed into complementary DNA with T7 Oligo(dT) primers, and the double stranded cDNA was then in vitro transcribed to synthesize cRNA using a biotin-NTP mix. The resulting cRNA was quantified on a Nanodrop-2000c spectrophotometer (Thermo Fisher Scientific), and the quality was assessed on a Agilent Bioanalyzer chip (Agilent). A total of 250 ng of cRNA were then hybridized to the BeadChip at 58 °C overnight and the fluorescent signal was developed with streptavidin-Cy3, followed

by quantitative detection of fluorescence emission by the array Illumina iScan scanner and computation by the Illumina GenomeStudio software (both from Illumina). Gene expression data were normalized using the quantile algorithm implemented in the Illumina GenomeStudio software.

Among the 30,000 genes assessed in the microarray, a matrix of expressed genes was generated by selecting all transcripts with intensity values that differed significantly from background (detection  $P < 0.01$ ) in at least one sample of the entire series. The LIMMA Bioconductor package was used to extract the DEGs considering a factorial design model and pairwise comparisons<sup>40</sup>. A post-test was used to select putative DEGs in each contrast, under the Benjamini–Hochberg multiple comparison correction. Genes with an adjusted  $P < 0.1$  were considered differentially expressed.

A gene ontology enrichment analysis for biological processes was performed with the DAVID v.6.7 online interface<sup>41,42</sup>, using default parameters and considering as background all the genes expressed in our dataset and as genes of interest those differentially expressed in each specific contrast. For each comparison,  $P < 0.05$  was used to define a significantly enriched biological process. The GOSemSim package release 2.12 (ref. <sup>43</sup>) and the ClueGO package from Cytoscape<sup>44</sup> were used to cluster together related gene ontology biological processes.

**RNA-seq and data analysis.** Gene expression profiling for samples belonging to the validation set was performed using RNA-seq, starting from 300 ng of total RNA and using the TruSeq Stranded mRNA library preparation kit (Illumina) in accordance with low-throughput protocol. After PCR enrichment (15 cycles) and purification of adapter-ligated fragments, the concentration and length of DNA fragments were measured using D1000 Screen Tape System (Agilent), obtaining a median insert size of 311 nucleotides. Then, RNA-seq libraries were sequenced using the Illumina Next-Seq 500 high platform to obtain a minimum of  $30 \times 10^6$  paired-end reads per sample.

To quantify gene expression levels, read tags were pseudoaligned to genome v.28 transcripts<sup>45</sup> using kallisto v.0.44.0<sup>44</sup> (parameters: -t 8—single—rf-stranded -l 200 -s 20). Abundancies were summarized to genes using txImport package<sup>45</sup> and analyzed using edgeR<sup>46</sup> with a design matrix including sample identity, disease condition and coordinates of the first two components of multidimensional scaling of the count matrix (~sample\_id + condition + X + Y). Fold change was then calculated on the 'condition' covariate.

**Quantitative PCR quantification of gene transcripts.** qPCR assays for the quantification of HLA-A, HLA-C, HLA-DRB, HLA-DPB1 and CIITA transcripts were developed in house or adapted from previous studies<sup>47–49</sup>. For all reactions, 250–500 ng of total RNA were retro-transcribed with the High Capacity cDNA Reverse Transcription Kit (Applied Biosystems), using random hexamers and RNase Inhibitor. Gene expression levels were measured by real-time quantitative PCR (RT-qPCR) on an ABI 7500 Real-Time PCR System (Applied Biosystems) using the Sybr Green chemistry (Applied Biosystems), using the following thermal cycler conditions for all reactions: 1 cycle 95 °C for 10 min, followed by 40 cycles at 95 °C for 10 s, and at 60 or 63 °C for 35 s, ending with 15 °C incubation. The nucleotide sequences of primers used for RT-qPCR are provided in Supplementary Table 6. The  $\Delta\Delta C_T$  method was used to define gene expression levels using RNaseP as the reference gene and the  $\Delta C_T$  mean of each transcript at diagnosis as a reference sample value. For all the assays, efficiency was confirmed to be superior to 80% by serial dilutions of the template in water, and specificity was validated by in silico analysis and Sanger sequencing of the amplification products.

**Multiparametric flow cytometry.** To assess their phenotype, mononuclear cells derived from the peripheral blood or bone marrow of patients and healthy individuals were stained with human fluorochrome-conjugated monoclonal antibodies (mAb). The complete list of mAbs used in the study is provided as part of the Life Sciences Reporting Summary.

For immunophenotypic analysis samples were thawed in complete medium. A total of  $(0.2-1) \times 10^6$  cells were washed in 1  $\times$  PBS, 2% FBS and then labeled with the appropriate antibodies mix in 50  $\mu$ l 1  $\times$  PBS, 2% FBS in a FACS tube. Staining was performed at 4 °C for 15–20 min, followed by washing with 1 ml of 1  $\times$  PBS, 2% FBS before the analysis. For staining of intracellular antigens (CTLA4), after surface staining, cells were fixed and permeabilized using the BD Cytofix/Cytoperm fixation and permeabilization solution kit (BD Biosciences).

For data analysis, a first logical gate was based on side scatter and CD45 intensity, followed by a second gate on the patient-specific LAIP to identify leukemia cells and on CD3 for T cells. At least 200,000 events in the live cells gate were acquired per sample. Analysis of human samples was performed using a Canto II flow cytometer equipped with 405, 488 and 633 nm lasers, or using a LSR Fortessa flow cytometer equipped with 355 nm, 405, 488, 561 and 640 nm lasers (both from BD Biosciences). Analysis of mouse samples was performed using a Gallios flow cytometer equipped with 488, 638 and 405 nm lasers (Beckman Coulter). Each acquisition was calibrated using Rainbow Calibration Particles (Spherotech) to correct for day-to-day laser intensity variations. Data were processed using FCS 4 Express (De Novo Software), FlowJo v.9.8.5 (Tree Star) or Kaluza (Beckman Coulter). Representative plots with gating strategy and controls are shown in Supplementary Figs. 1 and 2.

Differences in percentages were used to calculate sample clustering, using correlation coefficient as distance measure and Ward's method for agglomerative clustering. An ANOVA *F*-value was used to rank the relative influence of each marker in determining clusters. Heatmaps were elaborated using the heatmap package<sup>50</sup>.

High-dimensional analysis of flow cytometry data from the entire validation sample cohort (72 samples, 36 from diagnoses and 36 from relapses) was performed using the Barnes–Hut-stochastic neighbor embedding (BH–SNE) dimensionality reduction algorithm downscaling each sample to 5,000 CD3<sup>+</sup> events. BH–SNE was visualized on MATLAB (MathWorks, Inc.) by the plug-in 'cyt', developed by D. Pe'er's laboratory<sup>51</sup>. BH–SNE algorithm analysis settings were perplexity = 30.00 and theta = 0.5, as suggested by the developers. The *K*-means algorithm was directly applied on BH–SNE1 and BH–SNE2 variables, converging in approximately 190 interactions and dividing the bi-axial plot into 200 discrete areas (meta-clusters) on the basis of the mean fluorescence intensity of the HLA-DR, HLA-DP, PD-L1, B7-H3 and Vista markers. Each cluster was then studied for their composition, and appointed to either the 'relapse' or the 'diagnosis' subgroup if more than 75% of those events fell specifically in one of the two groups.

**Mixed lymphocyte cultures (MLCs).** Peripheral blood mononuclear cells (PBMCs) collected from patients with full donor chimerism after allo-HCT and before clinical relapse were stimulated with the respective patient irradiated leukemic blasts at a responder/stimulator ratio of 1/1. Cells were cultured in Iscove's Modified Dulbecco's Media supplemented with 1% glutamine (G), 1% penicillin/streptomycin (P/S), 10% HS and IL-2 at a final concentration of 150 U ml<sup>-1</sup>. IL-2 was replaced every 3–4 days and responders were re-stimulated every 7 days. PBMCs from an HLA-disparate healthy individual were tested in parallel as a positive control of the ability of leukemic cells to induce an all-response. After each round of stimulation, donor-derived T cells from the MLCs were characterized by flow cytometry for their phenotype, and tested against targets of choice for antigen-specific activation, cytokine release, proliferation and cytotoxicity.

**Functional assays for T cell recognition of target cells.** Briefly, T cell activation in response to the relevant target cells was tested on 24-h co-incubation with the targets of interest using the 4–1BB (CD137) upregulation assay<sup>52</sup>. CD4 and CD8 T cell populations were identified by excluding target cells, marked by the CellTrace Violet Cell Proliferation dye (Invitrogen) and staining the samples with CD45 (Clone HI30), CD3 (Clone SK7), CD4 (Clone OKT4 or SK3)—all from BioLegend, CD8 (Clone SK1) and CD137 (Clone 4B4-1), both from BD Biosciences. Each condition was assessed in duplicates and pooled before flow cytometry analysis to acquire at least 20,000 effector cells per condition.

Cytokine release was tested by means of IFN- $\gamma$  ELISpot assay. Briefly, 5  $\times$  10<sup>4</sup> responder T cells from the MLCs were re-challenged overnight at 37 °C in 5% CO<sub>2</sub> with 5  $\times$  10<sup>4</sup>  $\gamma$ -irradiated targets in 200  $\mu$ l of complete medium. Primary leukemic blasts were irradiated at 30 Gy. Spots were counted by a KS ELISpot Reader (Zeiss). All conditions were assessed, at least in duplicates.

Cytotoxicity was measured by standard 4-h <sup>51</sup>Cr release assay, testing different effector/target (E/T) ratios. After 4 h co-incubation of responder T cells with the <sup>51</sup>Cr labeled targets of interest, the supernatants were collected and analyzed using a  $\gamma$ -counter. Specific lysis was expressed according to the formula: 100  $\times$  (average experimental cpm – average spontaneous cpm)/(average maximum cpm – average spontaneous cpm).

For mAb blocking experiments, target cells were pre-incubated for 1 h at room temperature before addition to the functional assays described above. The following neutralizing mAb were used: anti-HLA-DR (clone L243, BioLegend) used at the final concentration of 30  $\mu$ g ml<sup>-1</sup>, anti-HLA-DP (clone B7/21, Cancer Research Technology) at a final concentration of 30  $\mu$ g ml<sup>-1</sup> or anti-PDL1 (clone MIH1, Thermo Fisher Scientific) at a final concentration of 10  $\mu$ g ml<sup>-1</sup>.

**In vivo experiments.** All in vivo experiments were performed on approval by the San Raffaele Institutional Animal Care and Use Committee (IACUC, protocol number 651), by the San Raffaele Ethic Committee (protocol AML-PDX, approved on 3 November 2017) and by the Italian Ministry of Health (Authorization number 97/2015-PR on 18 February 2015).

For in vivo experiments, the T cells were depleted from the leukemia samples by column selection (Miltenyi Biotec) taking advantage of the human CD3 microbeads (Miltenyi Biotec). At least 1  $\times$  10<sup>6</sup> CD3-depleted primary human leukemia cells collected at diagnosis or relapse after allo-HCT were engrafted into 4-week-old non-irradiated immunodeficient NOD scid gamma (NSG) mice. Human chimerism in the peripheral blood of the mice was assessed twice a week by flow cytometry, evaluating the counts per  $\mu$ l by addition of count beads into each sample (Beckman Coulter). A first gate was set to discriminate between cells positive for mouse or human CD45 and, among human CD45-positive cells, the absolute counts of leukemia blasts and T cells were quantified on gating on the patient-specific LAIP or on CD3<sup>+</sup> T cells, respectively.

Donor T cells were expanded from PBMCs on in vitro stimulation with anti-CD3/CD28-conjugated magnetic beads (Dynabeads ClinExVivo CD3/CD28; or human CD3/CD28 (Invitrogen) in a bead/T cell ratio of 3/1 with the addition

of IL-7 and IL-15 at 5 ng ml<sup>-1</sup> each (PeproTech)<sup>53</sup>. Cytokines and medium were replaced every 3–4 days. After 2 weeks of stimulation, T cell cultures were stored in nitrogen until infusion into mice. On the appearance of human AML blasts in the peripheral blood (threshold set at 25 leukemic cells per  $\mu$ l), the relevant groups of mice were treated with a single infusion of human T cells from the respective allogeneic HCT donor.

Each experiment included at least three mice per group.

For immunophenotypic analysis a total of 50  $\mu$ l mice peripheral blood, previously treated with heparin, were stained with the relevant mixture of antibodies with the addition of 100  $\mu$ l of 1  $\times$  PBS, 2% FBS, for 20 min at 4 °C. The erythrocytes were eliminated from the samples by incubating with 3–5 ml ammonium chloride potassium lysis buffer for 4 min at room temperature. Cells were pelleted by centrifugation (300g for 10 min) and washed with 3 ml of 1  $\times$  PBS and then re-suspended in 50  $\mu$ l of 1  $\times$  PBS and 25  $\mu$ l of count beads. Mice sera were collected before and after the infusion of donor T cells (once a week) and stored at –20 °C before evaluation of human cytokines (see Extended Data Fig. 4a for the experimental outline).

**Quantification of human cytokines in mouse sera.** Human Th1 cytokines (IL-2, IL-6, IL-10, IFN- $\gamma$  and TNF- $\alpha$ ) were quantified in murine sera using Human LegendPlex 5-plex (BioLegend) according to the manufacturer's instructions. For each time-point and each experimental condition the sera of three biological replicates were analyzed. For each studied cytokine, a high-sensitivity standard curve was generated by serial dilutions of recombinant proteins. Data were analyzed using LEGENDplex v.7.0 (BioLegend).

**Leukemia blasts in vitro culture.** Leukemia blasts were cultured in X-Vivo 15, 5% HS, 1% P/S, 1% G for 1 week in the presence or absence of human recombinant cytokines: IFN- $\gamma$  (10 ng  $\mu$ l<sup>-1</sup>), TNF- $\alpha$  (5 ng  $\mu$ l<sup>-1</sup>), IFN- $\alpha$  (5 ng  $\mu$ l<sup>-1</sup>), IL-10 (10 ng  $\mu$ l<sup>-1</sup>) and IL-6 (10 ng  $\mu$ l<sup>-1</sup>). At 3 and 7 days after stimulation, cell surface expression of HLA class I, HLA-DR and -DP was analyzed on the leukemia blast population identified as described above. Dead cells were excluded from the analysis by Annexin-V (BioLegend) staining. After IFN- $\gamma$  stimulation and in the absence of any cytokine, as control, the blasts were also recovered for total RNA extraction.

**Analysis of leukemia driver mutations.** FLT3-ITD status and allele burden was determined by PCR followed by capillary electrophoresis using 100 ng of genomic DNA extracted from purified leukemic blasts, as described by Jilani and collaborators<sup>54</sup>. Analysis of mutations in NPM1 and quantification of transcripts of NPM1 mutation A and WT1 were performed using the methods described by Brambati and collaborators<sup>55</sup>.

**Statistical analyses.** For all relevant comparisons, after testing for normal distribution through the Kolmogorov–Smirnov test, comparative analyses between two groups were performed, as appropriate, by two-sided paired or unpaired Student's *t*-tests at 95% CI. In case of not-normally distributed data, the Wilcoxon matched-pair signed rank test at 95% CI was used. A *P* < 0.05 was set as threshold for significance. If more than two groups were tested, a one-way ANOVA test with the Bonferroni correction was used. All statistical analyses were carried out using the GraphPad Prism v.7.0a software.

Animal numbers were chosen according to the variability observed in pilot experiments and on the basis of leukemia cell availability. In all in vivo experiments, at least three biological replicates per group were tested.

Regression analysis between relapse modalities and known clinical variables was performed through a univariate model, calculating for each variable of interest the odds ratio with the associated 95% CI.

**Reporting Summary.** Further information on research design is available in the Nature Research Reporting Summary linked to this article.

## Data availability

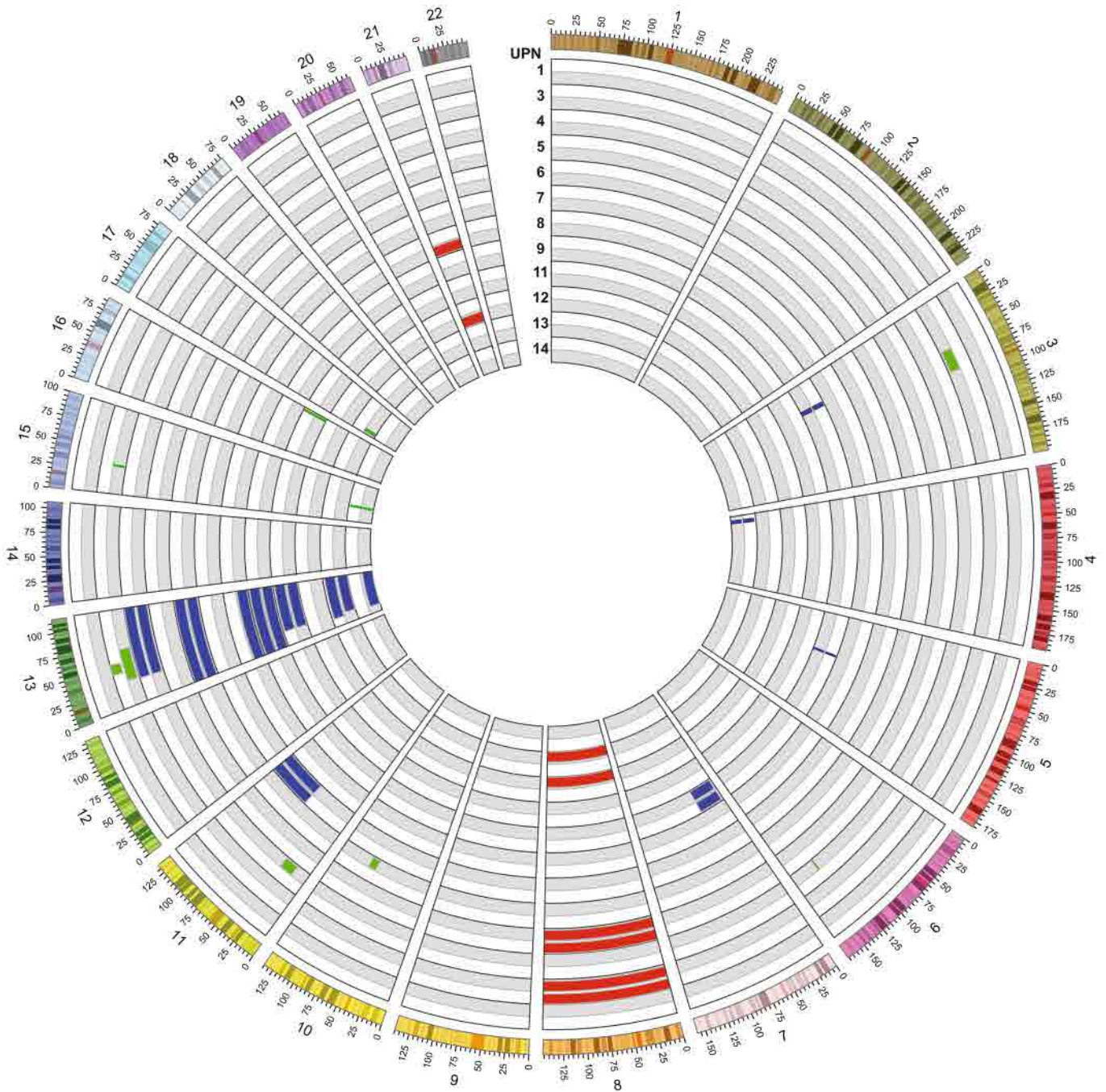
SNP array, microarray and RNA-seq data generated and analysed during the current study are available through ArrayExpress (<https://www.ebi.ac.uk/arrayexpress/>) with accession numbers E-MTAB-7631, E-MTAB-7628, E-MTAB-7630 and E-MTAB-7456.

## References

- Olshen, A. B., Venkatraman, E. S., Lucito, R. & Wigler, M. Circular binary segmentation for the analysis of array-based DNA copy number data. *Biostatistics* **5**, 557–572 (2004).
- Robinson, J. T. et al. Integrative genomics viewer. *Nat Biotechnol* **29**, 24–26 (2011).
- Paulsson, K., Lindgren, D. & Johansson, B. SNP array analysis of leukemic relapse samples after allogeneic hematopoietic stem cell transplantation with a sibling donor identifies meiotic recombination spots and reveals possible correlation with the breakpoints of acquired genetic aberrations. *Leukemia* **25**, 1358–1361 (2011).

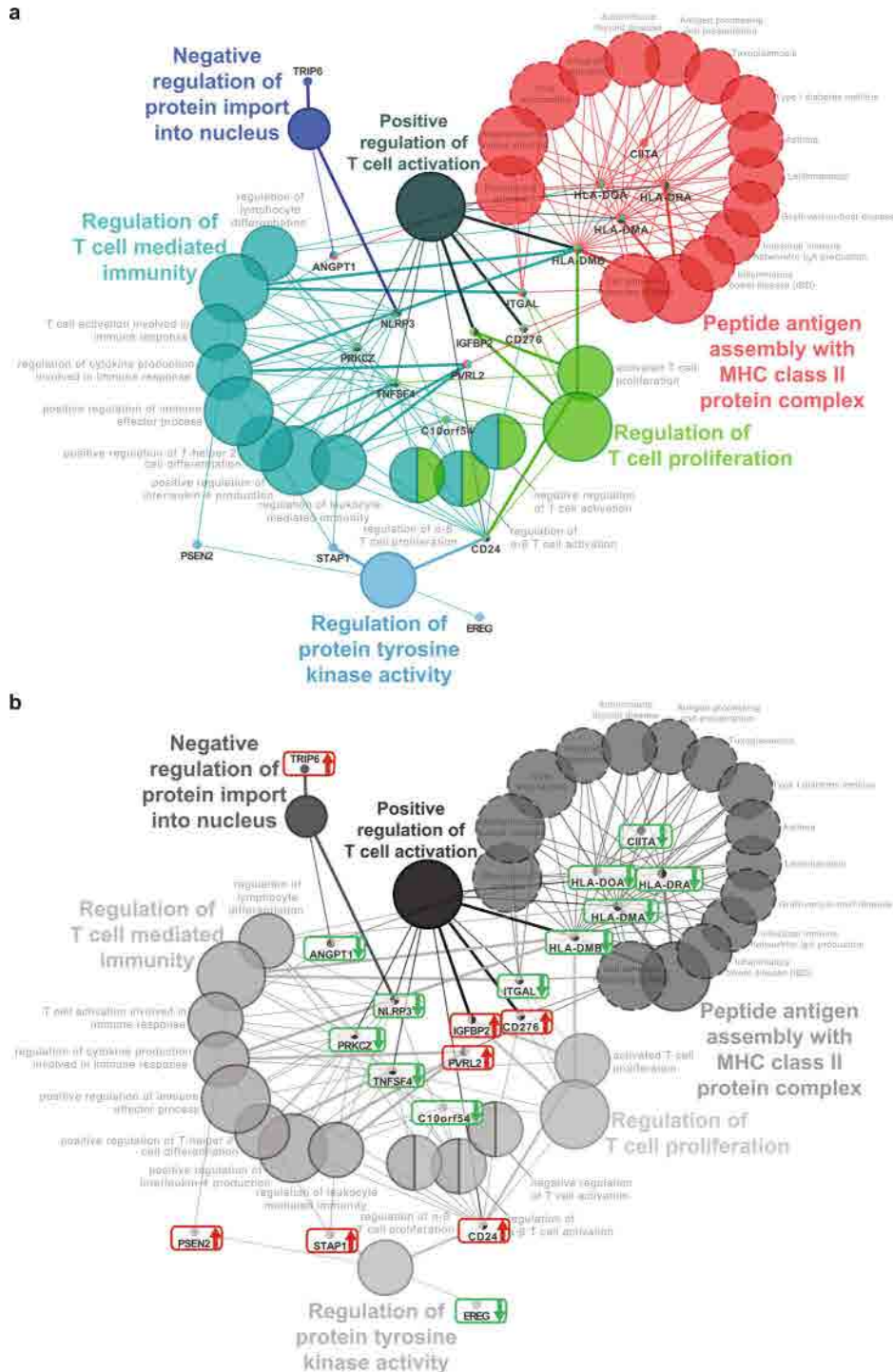
39. Van Gelder, R. N. et al. Amplified RNA synthesized from limited quantities of heterogeneous cDNA. *Proc. Natl Acad. Sci. USA* **87**, 1663–1667 (1990).
40. Smyth, G. K., Michaud, J. & Scott, H. S. Use of within-array replicate spots for assessing differential expression in microarray experiments. *Bioinformatics* **21**, 2067–2075 (2005).
41. Huang, D. W., Sherman, B. T. & Lempicki, R. A. Systematic and integrative analysis of large gene lists using DAVID bioinformatics resources. *Nat. Protoc.* **4**, 44–57 (2009).
42. Huang, D. W., Sherman, B. T. & Lempicki, R. A. Bioinformatics enrichment tools: paths toward the comprehensive functional analysis of large gene lists. *Nucleic Acids Res.* **37**, 1–13 (2009).
43. Harrow, J. et al. GENCODE: the reference human genome annotation for The ENCODE Project. *Genome Res.* **22**, 1760–1774 (2012).
44. Bray, N. L., Pimentel, H., Melsted, P. & Pachter, L. Near-optimal probabilistic RNA-seq quantification. *Nat. Biotechnol.* **34**, 525–527 (2016).
45. Sonesson, C., Love, M. I. & Robinson, M. D. Differential analyses for RNA-seq: transcript-level estimates improve gene-level inferences. *F1000Res* **4**, 1521 (2015).
46. Robinson, M. D., McCarthy, D. J. & Smyth, G. K. edgeR: a Bioconductor package for differential expression analysis of digital gene expression data. *Bioinformatics* **26**, 139–140 (2010).
47. García-Ruano, A. B. et al. Analysis of HLA-ABC locus-specific transcription in normal tissues. *Immunogenetics* **62**, 711–719 (2010).
48. Ulbricht, T. et al. PML promotes MHC class II gene expression by stabilizing the class II transactivator. *J. Cell Biol.* **199**, 49–63 (2012).
49. Wang, J., Roderiquez, G., Jones, T., McPhie, P. & Norcross, M. A. Control of in vitro immune responses by regulatory oligodeoxynucleotides through inhibition of pIII promoter directed expression of MHC class II transactivator in human primary monocytes. *J. Immunol.* **179**, 45–52 (2007).
50. Kolde, R. Pheatmap: Pretty heatmaps. R package version 0.6.1. <https://cran.r-project.org/web/packages/pheatmap/index.html> (2012).
51. Amir, E. D. et al. viSNE enables visualization of high dimensional single-cell data and reveals phenotypic heterogeneity of leukemia. *Nat. Biotechnol.* **31**, 545–552 (2013).
52. Wolff, M. et al. Activation-induced expression of CD137 permits detection, isolation, and expansion of the full repertoire of CD8+T cells responding to antigen without requiring knowledge of epitope specificities. *Blood* **110**, 201–210 (2007).
53. Cieri, N. et al. IL-7 and IL-15 instruct the generation of human memory stem T cells from naive precursors. *Blood* **121**, 573–584 (2013).
54. Jilani, I. et al. Better detection of FLT3 internal tandem duplication using peripheral blood plasma DNA. *Leukemia* **17**, 114–119 (2003).
55. Brambati, C. et al. Droplet digital polymerase chain reaction for DNMT3A and IDH1/2 mutations to improve early detection of acute myeloid leukemia relapse after allogeneic hematopoietic stem cell transplantation. *Haematologica* **101**, e157–e161 (2016).



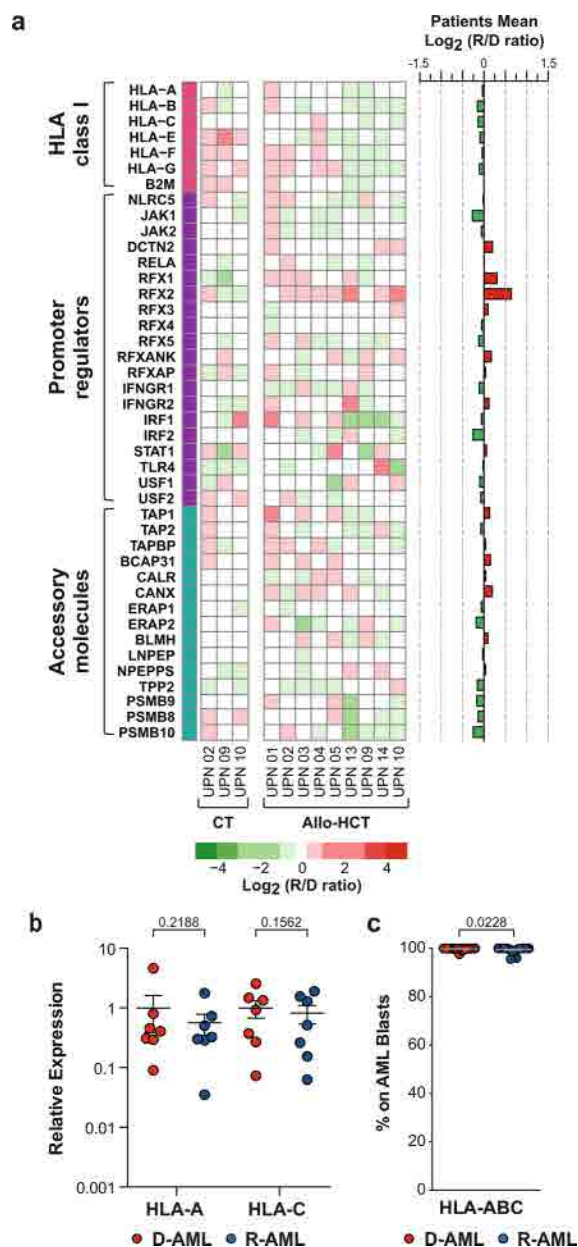


**Extended Data Fig. 1 | Genomic alterations detected in sorted AML blasts of paired samples at diagnosis and relapse after allo-HCT.** SNP array analyses were performed on high-quality DNA extracted from AML blasts sorted according to the patient-specific LAIP, collected at diagnosis or relapse after allo-HCT from patients from the discovery cohort ( $n=12$ ). The Circos plot summarizes the duplications (red bars), deletions (green bars) and CN-LOH (blue bars) detected in leukemic blasts at diagnosis (white corona) or relapse after allo-HCT (gray corona) for each patient (UPN) in each chromosome.

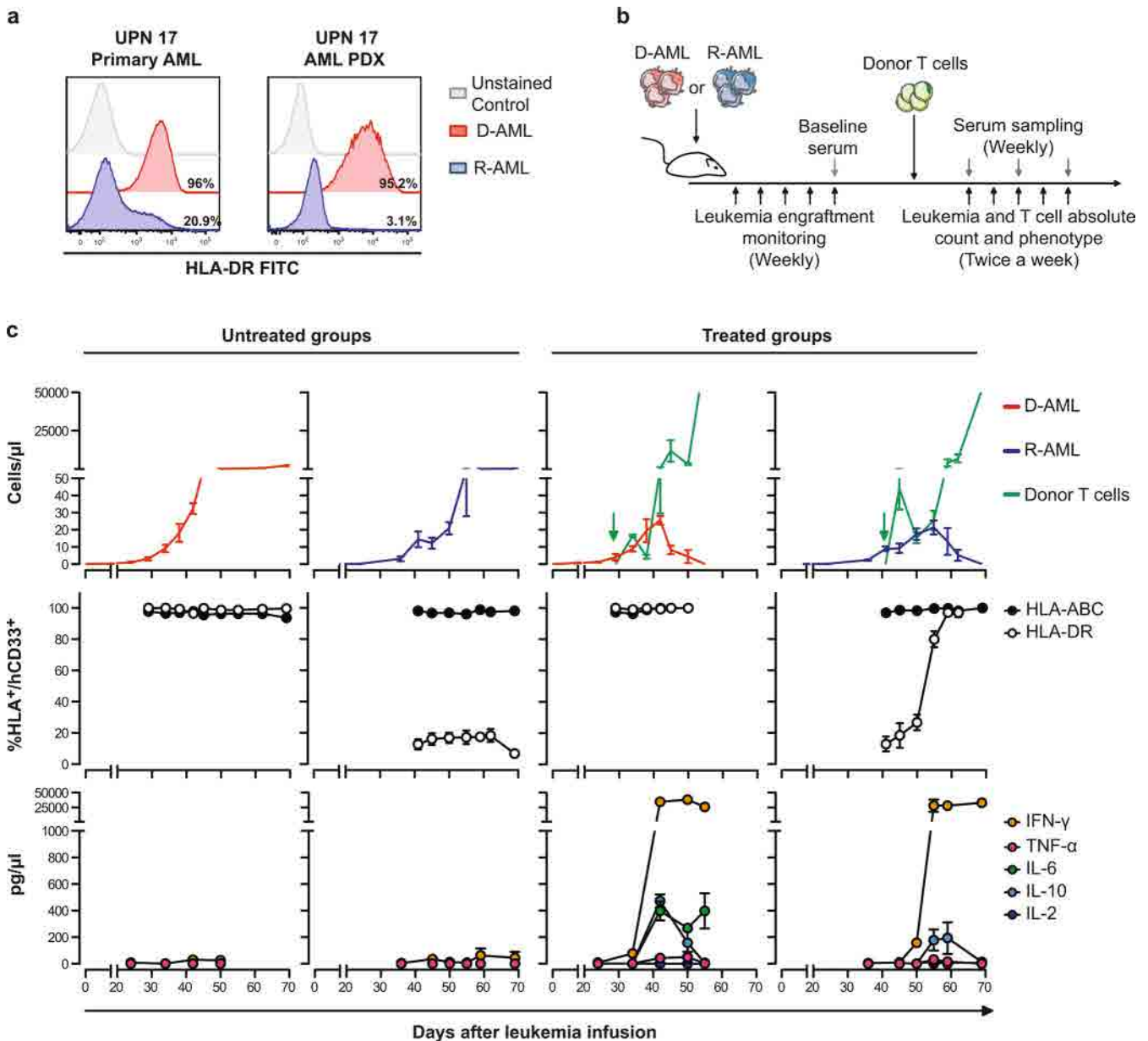




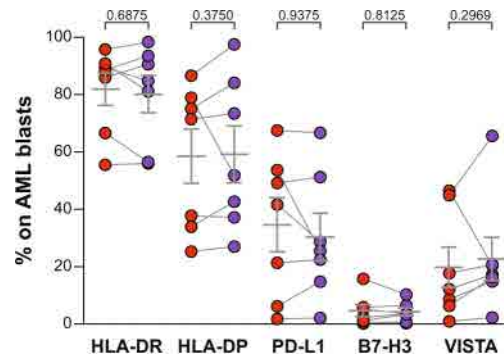
**Extended Data Fig. 2 | ClueGO networks of biologic processes deregulated at post-transplantation relapse. a**, Network representing the mutual relationship between gene ontology, KEGG and BioCarta terms related to the 110-gene signature identified from the pairwise comparison of AML blasts collected at disease diagnosis and at relapse after allo-HCT from discovery cohort patients ( $n = 9$ ), as evidenced by the ClueGO package of Cytoscape. Dots and colored circles represent genes and biological terms, respectively. The amplitude of the circles represents the adjusted  $P$  value (calculated by a two-sided Fisher's exact test, Bonferroni step-down correction) of each term enrichment. The thickness of each line correlating genes with biological terms represents the strength of interaction as defined by the kappa score. The enriched terms are clustered by function according to their gene content similarity: 'positive regulation of T cell activation' (in dark green), 'peptide antigen assembly with MHC class II protein complex' (in red), 'negative regulation of protein import in the nucleus' (in blue) and 'regulation of protein tyrosine kinase activity' (in light blue). **b**, The gray-scale image represents the same network of panel **a**, with the direction of deregulation of genes: red represents upregulation at relapse, green represents downregulation.



**Extended Data Fig. 3 | Expression of HLA class I molecules at post-transplantation relapse. a**, Heatmap representing fold expression changes in HLA class I gene transcripts (fuchsia markers), their regulators (purple markers) and accessory molecules involved in HLA class I presentation (teal markers). Transcript levels were assessed by microarrays, comparing leukemia at diagnosis with relapses after chemotherapy (CT,  $n=3$ ) or allo-HCT (allo-HCT,  $n=9$ ). Red and green indicate transcript upregulation and downregulation at relapse, respectively. Bars on the right side of the heatmap summarize mean fold changes at post-transplantation relapse. **b**, mRNA expression levels of HLA-A and -C measured by locus-specific qPCR in leukemia blasts pairwise collected and purified from patients at diagnosis (red dots) and at post-transplantation relapse (blue dots) ( $n=7$ ). Dots indicate values from single patients, lines indicate mean  $\pm$  s.e.m.  $P$  values were calculated by a two-sided Wilcoxon matched-pairs signed rank test at 95% CI. **c**, HLA class I cell surface expression by leukemia blasts, assessed by immunophenotypic analysis in samples pairwise collected from discovery series patients before allo-HCT (red dots) and at post-transplantation relapse (blue dots) ( $n=33$ ). Dots indicate values from single patients, lines indicate mean  $\pm$  s.e.m.  $P$  values were calculated by a two-sided Wilcoxon matched-pairs signed rank test at 95% CI.

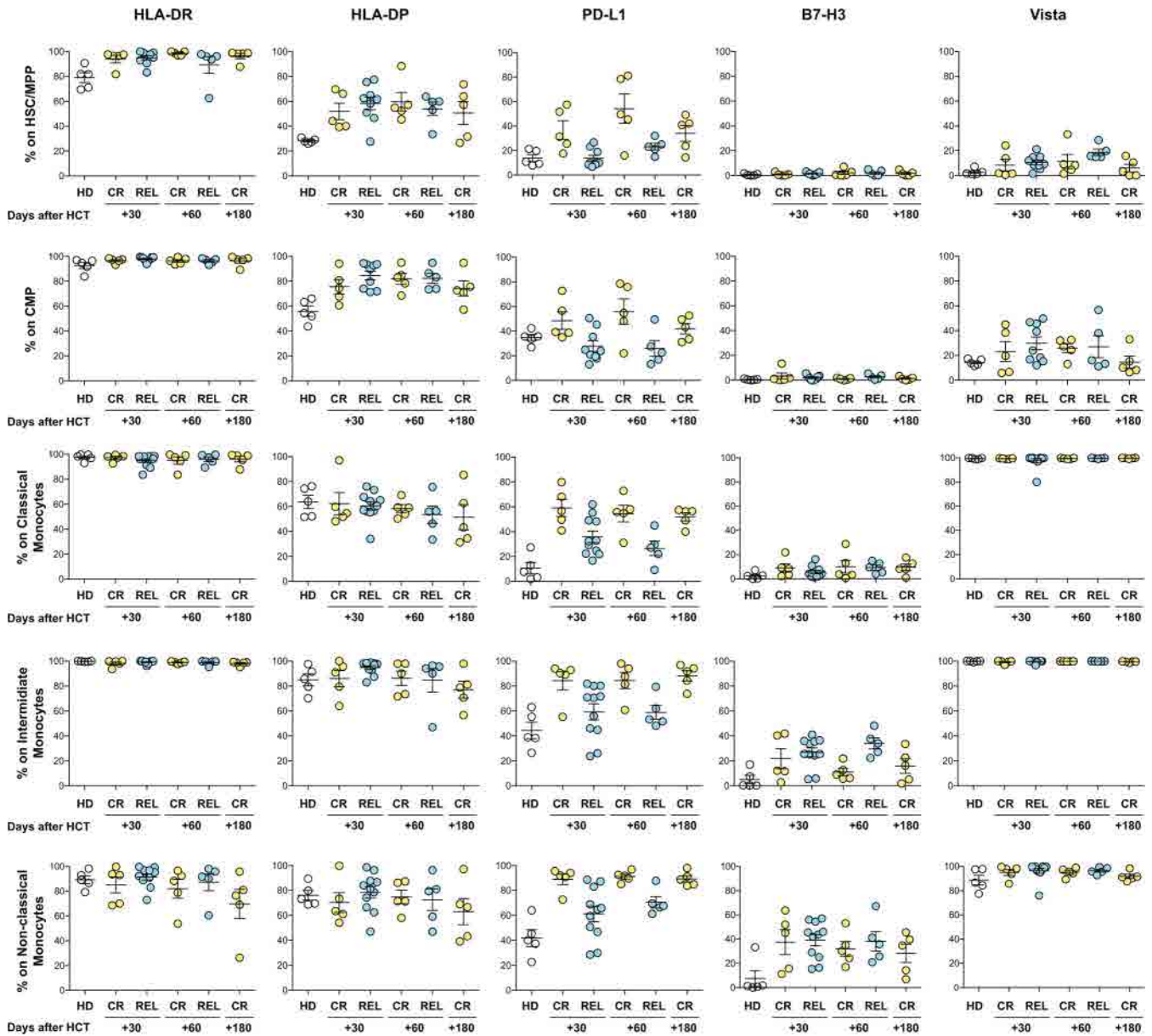


**Extended Data Fig. 4 | In vivo rescue of HLA class II expression on exposure of relapsed leukemia to IFN- $\gamma$ .** **a**, HLA-DR expression on primary leukemia cells collected from UPN 17 at diagnosis (in red) and at relapse after allo-HCT (in blue), re-assessed before infusion in NSG mice (left side panel) and on the respective patient-derived xenografts (PDXs). The gray histograms represent the FMO control of AML blasts at diagnosis. For each histogram, the percentage displayed refers to the comparison with the relevant FMO control. Shown are results representative for two independent experiments with primary leukemias and with PDXs originated from UPN 17 leukemia at diagnosis ( $n=3$  per experiment) and at post-transplantation relapse ( $n=4$  per experiment). **b**, Layout of the in vivo experiment: AML blasts purified from UPN 17 at diagnosis (D-AML) or at relapse after allo-HCT (R-AML) were infused by tail vein injection into 4-week-old NSG mice. Mice were monitored weekly for leukemia engraftment and, on appearance in their peripheral blood of human leukemic cells, received the infusion of T cells collected and ex vivo expanded from UPN 17 donor. **c**, From left to right are shown results obtained in mice receiving only leukemia cells gathered from UPN 17 at diagnosis ( $n=3$ ), mice receiving only leukemia cells gathered from UPN 17 at relapse after allo-HCT ( $n=4$ ), mice receiving leukemia cells gathered from UPN 17 at diagnosis followed by donor T cell infusion (green arrow,  $n=4$ ) and mice receiving leukemia cells gathered from UPN 17 at relapse after allo-HCT followed by donor T cell infusion (green arrow,  $n=4$ ). The top panel row displays the absolute counts of circulating human T cells (in green) and leukemia cells in diagnosis (in red) or relapse (in blue) PDXs. The middle panel row displays the expression on the surface of PDXs of HLA class I (black dots) and HLA-DR (white dots) molecules. The lower panel row displays the concentration of human IFN- $\gamma$  (in orange), TNF- $\alpha$  (in fuchsia), IL-6 (in green), IL-10 (in light blue) and IL-2 (in violet) measured in the peripheral blood of the mice during the experiment. All the data are displayed as mean  $\pm$  s.e.m. Shown are results representative for two independent experiments.

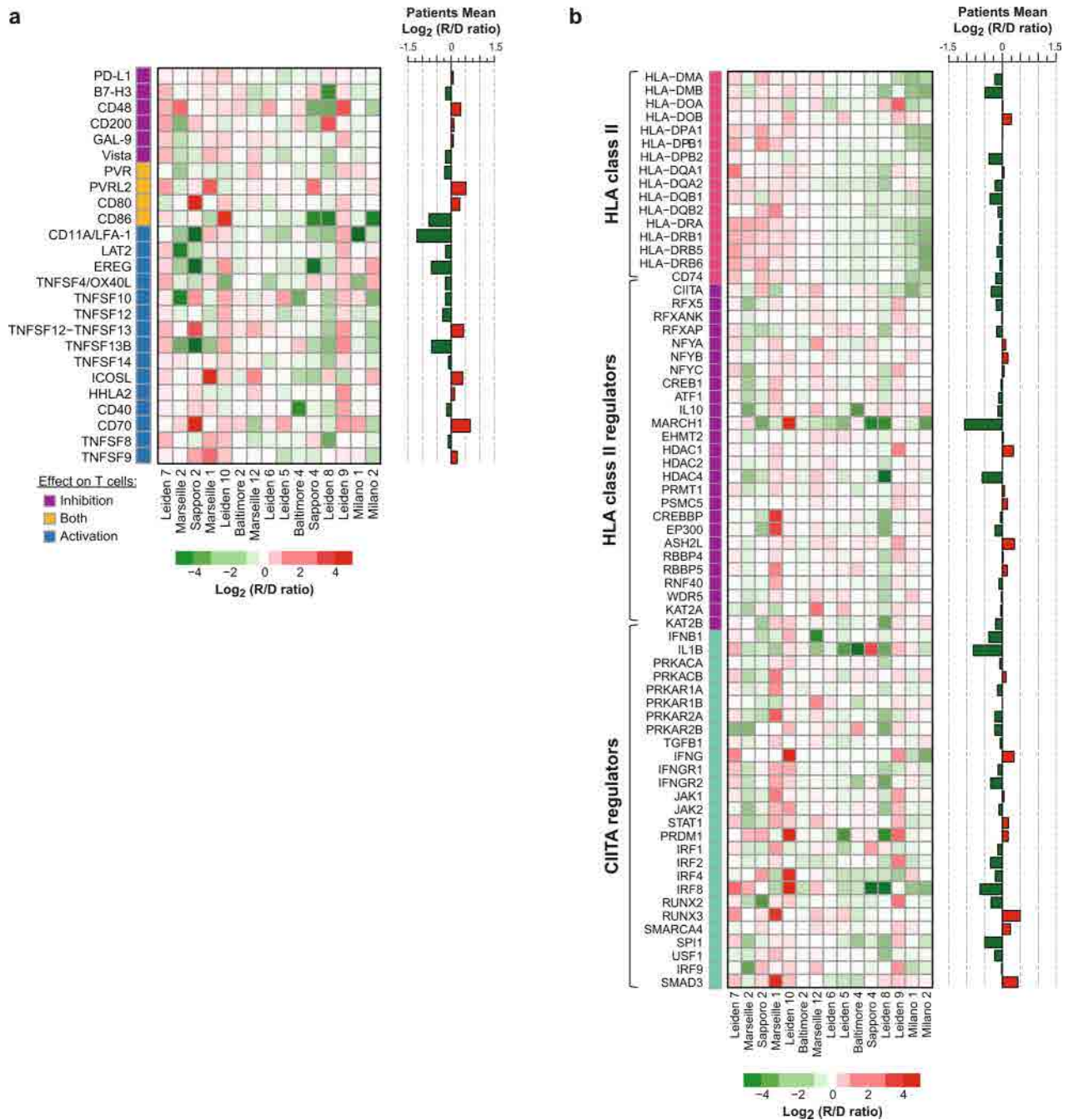


**Extended Data Fig. 5 | Expression of HLA class II molecules and inhibitory ligands on leukemia blasts at relapse after sole chemotherapy.** Surface expression of HLA-DR, HLA-DP, PD-L1, B7-H3 and Vista was assessed by immunophenotypic analysis in samples pairwise collected from patients at diagnosis (red dots) and at relapse after sole chemotherapy (purple dots) ( $n=7$ ). Dots indicate values from single patients, lines indicate mean  $\pm$  s.e.m. by a two-sided Wilcoxon matched-pairs signed rank test at 95% CI.

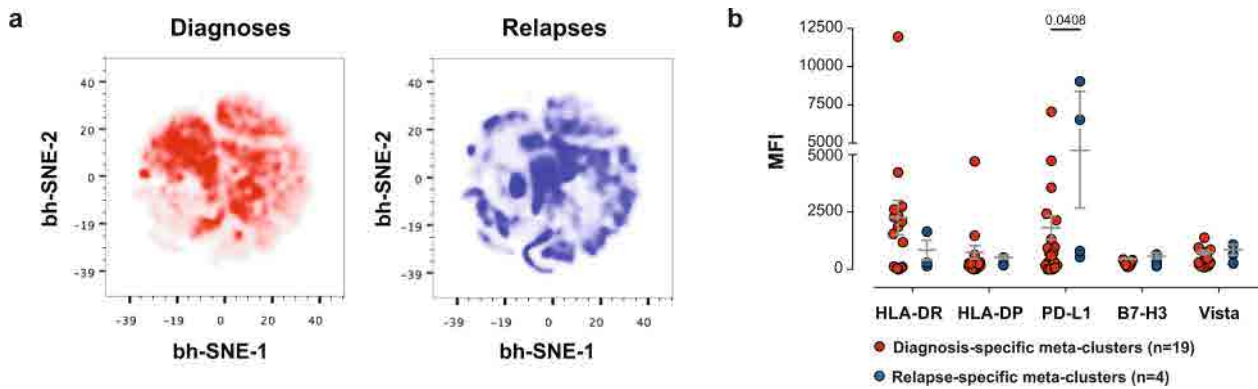




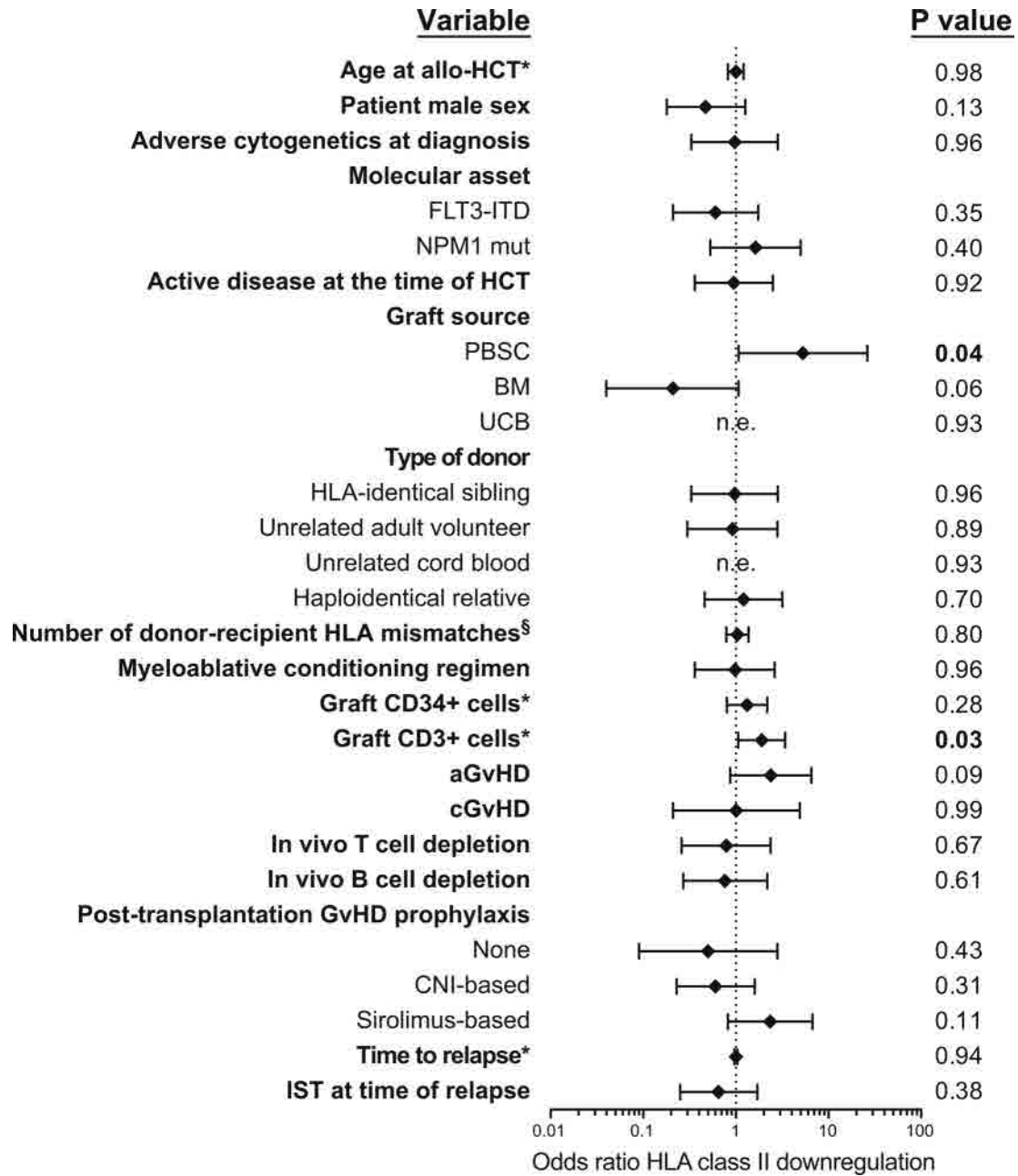
**Extended Data Fig. 6 | Expression of HLA class II molecules and inhibitory ligands on hematopoietic progenitors and monocytes from healthy individuals and transplanted patients.** Using multiparametric flow cytometry and the gating strategy summarized in Supplementary Fig. 2, we analyzed the surface expression profile of bone marrow myeloid progenitors and peripheral blood monocytes in samples from healthy individuals ( $n=5$ , in white, HD), patients from the discovery cohort who subsequently relapsed with one of the two newly described relapse modalities ( $n=10$ , in cyan, REL) and transplanted patients who achieved long-term disease remission ( $n=10$ , in yellow, CR). Dots indicate values from single patients, lines indicate mean  $\pm$  s.e.m.



**Extended Data Fig. 7 | Changes in the transcript levels of genes related to HLA class II antigen presentation and T cell costimulation in the validation cohort. a,b**, Heatmaps mirroring those shown in Figs. 2a and 3a for the discovery cohort, representing fold expression changes in transcripts for molecules involved in HLA class II presentation (a) and T cell costimulation (b) assessed by RNA-seq of leukemia sample pairwise collected and purified from validation cohort patients ( $n=15$ ). Red and green indicate transcript upregulation and downregulation at relapse, respectively. Bars on the right side of the heatmap summarize mean fold changes at post-transplantation relapse.



**Extended Data Fig. 8 | High-dimensional analysis of immunophenotypic data obtained from the validation cohort. a,** Color maps obtained using the BH-SNE bioinformatic algorithm for single-cell analysis, allowing the visualization in a two-dimensional map of complex datasets of high-dimensional objects (in this case, single cells stained with 16 different fluorochromes), plotted in the map on the basis of their reciprocal similarity. Shown are maps obtained from the full dataset of immunophenotypic analyses performed in our validation cohort, encompassing all the events registered in the analysis of paired diagnosis-relapse samples from the validation cohort ( $n=36$ ). The BH-SNE map relative to expression of HLA-DR, HLA-DP, PD-L1, B7-H3 and Vista was colored to evidence the differential positioning (and consequently phenotypic dissimilarity) of events originating from diagnosis samples (in red, left panel) or relapse samples (in blue, right panel). **b,** On the basis of *K*-means analysis of the BH-SNE map, meta-clusters of events unique for diagnoses ( $n=19$ ) and relapses ( $n=4$ ) were identified, and the mean fluorescence intensity of the markers characterizing them are plotted in red and blue, respectively. *P* values were calculated by a two-sided unpaired *t*-test at 95% CI.



**Extended Data Fig. 9 | Clinical and immunogenetic correlates of HLA class II downregulation at post-transplantation relapse.** Forest plot represents the odds ratio (diamonds) and 95% CI (error bars) of belonging to the 'HLA class II downregulation' clusters identified in Fig. 4c, d, calculated in the entire study population ( $n = 69$ ) using an univariate logistic regression model for demographic, disease-related, immunogenetic and transplant-related variables. \*These variables were considered as continuous in the model. <sup>§</sup>Considering allelic mismatches in the graft-versus-host direction in HLA-A, -B, -C and -DRB1.



## Reporting Summary

Nature Research wishes to improve the reproducibility of the work that we publish. This form provides structure for consistency and transparency in reporting. For further information on Nature Research policies, see [Authors & Referees](#) and the [Editorial Policy Checklist](#).

### Statistical parameters

When statistical analyses are reported, confirm that the following items are present in the relevant location (e.g. figure legend, table legend, main text, or Methods section).

n/a Confirmed

- The exact sample size ( $n$ ) for each experimental group/condition, given as a discrete number and unit of measurement
- An indication of whether measurements were taken from distinct samples or whether the same sample was measured repeatedly
- The statistical test(s) used AND whether they are one- or two-sided  
*Only common tests should be described solely by name; describe more complex techniques in the Methods section.*
- A description of all covariates tested
- A description of any assumptions or corrections, such as tests of normality and adjustment for multiple comparisons
- A full description of the statistics including central tendency (e.g. means) or other basic estimates (e.g. regression coefficient) AND variation (e.g. standard deviation) or associated estimates of uncertainty (e.g. confidence intervals)
- For null hypothesis testing, the test statistic (e.g.  $F$ ,  $t$ ,  $r$ ) with confidence intervals, effect sizes, degrees of freedom and  $P$  value noted  
*Give  $P$  values as exact values whenever suitable.*
- For Bayesian analysis, information on the choice of priors and Markov chain Monte Carlo settings
- For hierarchical and complex designs, identification of the appropriate level for tests and full reporting of outcomes
- Estimates of effect sizes (e.g. Cohen's  $d$ , Pearson's  $r$ ), indicating how they were calculated
- Clearly defined error bars  
*State explicitly what error bars represent (e.g.  $SD$ ,  $SE$ ,  $CI$ )*

*Our web collection on [statistics for biologists](#) may be useful.*

### Software and code

Policy information about [availability of computer code](#)

#### Data collection

SNP array and gene expression data were generated by the Illumina iScan Reader (Illumina, San Diego, CA, USA). The RNA-seq libraries were sequenced using the Illumina Next-Seq 500 high platform (Illumina, San Diego, CA, USA). Leukemia samples were FACS-purified using a MoFloTM XDP (Beckman Coulter, Brea, CA, USA) or a FACS Diva (BD Biosciences, Franklin Lakes, NJ, USA) cell sorter. Total RNA and DNA fragments were measured and checked for quality on a Agilent Bioanalyser chip or an D1000 Screen Tape System (both from Agilent, Santa Clara, CA, USA). Spots of the ELISpot assays were acquired by the KS Elispot Reader (Zeiss, Oberkochen, Germany). Quantitative PCR data were generated and analyzed by the ABI7500 Real-Time PCR System (Applied Biosystems, Foster City, CA, USA). Analysis of human samples was performed using a Canto II flow cytometer equipped with 405nm, 488nm, and 633nm lasers, or using a LSR Fortessa flow cytometer equipped with 355nm, 405nm, 488nm, 561nm and 640nm lasers (both from BD Biosciences, Franklin Lakes, NJ, USA), both using the DB FacsDIVA Software version 7 (BD Biosciences, Franklin Lakes, NJ, USA). Analysis of mouse samples was performed using a Gallios flow cytometer equipped with 488nm, 638nm and 405nm lasers (Beckman Coulter, Brea, CA, USA) using the Summit software (Beckman Coulter, Brea, CA, USA). Cytofluorimetric data were next processed using FCS 4 Express (De Novo Software, Los Angeles, CA), FlowJo version 9.8.5 (Tree Star, Ashland, OR, USA), or Kaluza (Beckman Coulter, Brea, CA, USA).

#### Data analysis

For SNP array analysis GenomeStudio version 1.9.4 (Illumina, San Diego, CA, USA), Nexus Copy Number 5.0 (BioDiscovery, El Segundo, CA, USA) and DNACopy (Olshen, A.B et al., Biostatistics, 2004) were used. - Gene expression array data were analyzed using the Illumina GenomeStudio software (Illumina, San Diego, CA, USA), the R software taking advantage of different Bioconductor packages (<https://www.bioconductor.org/>): in particular LIMMA (Smyth, G.K., at al., Bioinformatics, 2005) and GoSEMSim v2.12 (Yu, G., Bioinformatics,

2010), the online interface DAVID version 6.7 (Huang D., Nat Protoc., 2009) and the Cluego Cytoscape package (Bindea, G., Bioinformatics, 2009). - The RNA-seq libraries were pseudoaligned to gencode v28 transcripts (Harrow, J., Genome Res., 2012) using kallisto v 0.44.0 (Bray, N., Nat. Biotechnol., 2016). The abundancies were summarized to genes using txlmpack package (Soneson, C., F1000Res, 2015) and analyzed using edgeR (Robinson, M.D., Bioinformatics, 2010). - Cytokine quantification was performed using LEGENDplex v7.0 (BioLegend, San Diego, CA, USA). All the statistical analysis were performed using GraphPad Prism Version 5.0 or 7.0a (La Jolla, CA, USA). - High-dimensional analysis of flow cytometry was performed using the BH-SNE dimensionality reduction algorithm, running on the MatLab plug-in "cyt" developed by Dana Pe'er's lab (Amir, E.D., Nat. Biotechnol., 2013)

For manuscripts utilizing custom algorithms or software that are central to the research but not yet described in published literature, software must be made available to editors/reviewers upon request. We strongly encourage code deposition in a community repository (e.g. GitHub). See the Nature Research [guidelines for submitting code & software](#) for further information.

## Data

Policy information about [availability of data](#)

All manuscripts must include a [data availability statement](#). This statement should provide the following information, where applicable:

- Accession codes, unique identifiers, or web links for publicly available datasets
- A list of figures that have associated raw data
- A description of any restrictions on data availability

SNP array, microarray and RNA-Seq data generated and analysed during the current study are available through ArrayExpress (<https://www.ebi.ac.uk/arrayexpress/>) with accession numbers E-MTAB-7631, E-MTAB-7628, E-MTAB-7630 and E-MTAB-7456.

All the other relevant data generated and/or analysed in the current study are included in the manuscript or in supplementary information.

## Field-specific reporting

Please select the best fit for your research. If you are not sure, read the appropriate sections before making your selection.

Life sciences  Behavioural & social sciences

For a reference copy of the document with all sections, see [nature.com/authors/policies/ReportingSummary-flat.pdf](https://www.nature.com/authors/policies/ReportingSummary-flat.pdf)

## Life sciences

### Study design

All studies must disclose on these points even when the disclosure is negative.

Sample size	All patient samples coming from the Biobank of the different centres had been collected upon specific written consent in agreement with the Declaration of Helsinki. Selection of samples of interest was operated on the basis of availability of viable samples containing at least 5% leukemic blasts pairwise collected before and after allogeneic HSCT and no evidence of genomic HLA loss at relapse. For the high-throughput analyses also the expected yield of an adequate amount of purified leukemic blasts upon sorting was considered a criterion for sample choice. All samples meeting these requirements were tested, and sample size was determined by their availability and considered adequate upon analysis of the interindividual variability in the variables of interest. The study was approved by the scientific and ethic committee of the San Raffaele Hospital Scientific Institute (Milan, IT). For in vivo experiments, number of animals was selected based on variability observed in pilot experiments and on primary leukemia cells availability. All in vivo experiments performed were approved by the San Raffaele Animal Care and Use Committee (IACUC), by the San Raffaele Ethic Committee and by the Italian Ministry of Health.
Data exclusions	No data were excluded.
Replication	For gene expression profiling, leukemic cell purification and microarray profiling was for each sample performed in triplicate whenever possible. For all other experiments performed using patient-derived samples, each sample was tested in a single experiment, with an appropriate number of experimental replicates within the experiments. All attempts at replication of presented data were successful.
Randomization	Not applicable to our study design (retrospective observational).
Blinding	Analysis of biological features was blinded to the clinical data, which were linked for correlation analysis only in a later stage.

## Materials & experimental systems

Policy information about [availability of materials](#)

n/a	Involved in the study
<input type="checkbox"/>	<input checked="" type="checkbox"/> Unique materials
<input type="checkbox"/>	<input checked="" type="checkbox"/> Antibodies
<input checked="" type="checkbox"/>	<input type="checkbox"/> Eukaryotic cell lines
<input type="checkbox"/>	<input checked="" type="checkbox"/> Research animals
<input type="checkbox"/>	<input checked="" type="checkbox"/> Human research participants

### Unique materials

#### Obtaining unique materials

For primary leukemia and PDX samples used in this study material restrictions depends on sample availability and are ruled by the San Raffaele Scientific Institute. All the samples used had been collected upon specific written consent under a specific protocol approved by the scientific and ethic committee of the San Raffaele Hospital Scientific Institute (Milan, IT)

### Antibodies

#### Antibodies used

Here below the list of anti-human fluorochrome-conjugated antibodies:

CD34 PerCP-Cy5.5 (BD Biosciences, Clone 8G12, Catalog. N° 347222, Lot N°4092951, 1:30)  
 CD34 PE (BD Biosciences, Clone 8G12, Catalog. N° 345802, Lot N°77166, 1:50)  
 CD34 APC (BD Biosciences, Clone 8G12, Catalog. N° 345804, Lot N°6229872, 1:50)  
 CD34 FITC (BD Biosciences, Clone 8G12, Catalog. N° 345801, Lot N°42362, 1:50)  
 CD33 PerCP-Cy5.5 (BD Biosciences, Clone P67.6, Catalog. N° 333146, Lot N°37722)  
 CD117 PerCP-Cy5.5 (BD Biosciences, Clone YB5.B8, Catalog. N° 562094, Lot N°4002885, 1:30)  
 CD86 FITC (BD Biosciences, Clone 2331, Catalog. N° 555657, Lot N°3338536, 1:50)  
 HLA-DR FITC (BD Biosciences, Clone L243, Catalog. N° 347400, Lot N°6180996, 1:100)  
 HLA-DR PE-CF594 (BD Biosciences, Clone G46-6, Catalog. N°562304, Lot N°7191553, 1:100)  
 DNAM-1 FITC (BD Biosciences, Clone DX11, Catalog. N° 559788, Lot N°4287752, 1:50)  
 CD137 PE (BD Biosciences, Clone 4B4-1, Catalog. N° 555956, Lot N°33587, 1:100)  
 CD45 BUV395 (BD Biosciences, Clone HI30, Catalog. N°563792, Lot N°7298798, 1:100)  
 CD38 BUV737 (BD Biosciences, Clone HB7, Catalog. N°564686, Lot N°7352565, 1:100)  
 CD14 BV510 (BD Biosciences, Clone M P9, Catalog. N°563079, Lot N°7341719, 1:30)  
 CD10 BV786 (BD Biosciences, Clone HI10a, Catalog. N°564960, Lot N°8045564, 1:50)  
 CD200 PE-Cy7 (BD Biosciences, Clone MRC OX-104, Catalog. N°562125, Lot N°5023724, 1:50)  
 CTLA-4 APC (BD Biosciences, Clone BNI3, Catalog. N°555855, Lot N°4066549, 1:50)  
 CD45 PC7 (BioLegend, Clone HI30, Catalog. N° 304016, Lot N°B229089, 1:100)  
 CD45 Pacific Blue (BioLegend, Clone HI30, Catalog. N° 304029, Lot N°B180440, 1:100)  
 CD3 FITC (BioLegend, Clone SK7, Catalog. N° 344804, Lot N°B231398, 1:100)  
 CD3 APC-H7 (BioLegend, Clone SK7, Catalog. N° 344818, Lot N°B206985, 1:100)  
 CD3 BV605 (BioLegend, Clone OKT3, Catalog. N°3173322, Lot B24061, 1:100)  
 CD11a APC (BioLegend, Clone HI111, Catalog. N° 301212, Lot N°B170015, 1:100)  
 HLA-ABC Pacific Blue (BioLegend, Clone W6/32, Catalog. N° 311418, Lot N°B191431, 1:200)  
 GAL-9 APC (BioLegend, Clone 9M1-3, Catalog. N° 348908, Lot N°B188210, 1:50)  
 PVR12 PE (BioLegend, Clone TX31, Catalog. N° 337410, Lot N°B177553, 1:50)  
 OX40 APC (BioLegend, Clone ACT35, Catalog. N° 350008, Lot N°B161270, 1:50)  
 PD-1 FITC (BioLegend, Clone EH12.2H7, Catalog. N° 329904, Lot N°B169871, 1:100)  
 CD28 Pacific Blue (BioLegend, Clone CD28.2, Catalog. N° 302928, Lot N°B147378, 1:100)  
 ICOS PB (BioLegend, Clone C398.4A, Catalog. N° 313522, Lot N°B170453, 1:50)  
 CD4 APC-Cy7 (BioLegend, Clone OKT4, Catalog. N° 317418, Lot N°B171483, 1:100)  
 CD4 Pacific Blue (BioLegend, Clone OKT4, Catalog. N° 317429, Lot N°B195687, 1:100)  
 CD4 FITC (BioLegend, Clone SK3, Catalog. N° 344604, Lot N°B205589, 1:100)  
 CD8 APC-Cy7 (BioLegend, Clone SK1, Catalog. N° 344714, Lot N°B233288, 1:100)  
 CD14 FITC (BioLegend, Clone M5E2, Catalog. N° 301804, Lot N°B163436, 1:100)  
 CD33 PerCP-Cy5.5 (BioLegend, Clone WM53, Catalog. N°303414, Lot B261779, 1:30)  
 PD-L1 PE-Cy7 (BioLegend, Clone 29E.2A3, Catalog. N°329718, Lot N°B227182, 1:50)  
 CD45RA Alexa700 (BioLegend, Clone HI100, Catalog. N°304120, Lot N°B227350, 1:50)  
 CD16 APC-Cy7 (BioLegend, Clone 3G8, Catalog. N°302018, Lot N°B260177, 1:50)  
 ICAM-1 PE (BioLegend, Clone HA58, Catalog. N°353106, Lot N°B169127, 1:50)  
 ICOSL PE (Thermo Fisher Scientific, Clone MIH12, Catalog. N° 12-5889-42, Lot N°E14114-103, 1:50)  
 PD-L1 PE (Thermo Fisher Scientific, Clone MIH1, Catalog. N°12-5983-42, Lot N°E13991-104, 1:50)  
 PD-L2 APC (Thermo Fisher Scientific, Clone MIH18, Catalog. N° 17-5888-42, Lot N°E17310-101, 1:50)  
 TIGIT PE-Cy7 (Thermo Fisher Scientific, Clone MBSA43, Catalog. N° 25-9500-42, Lot N°E25046-101, 1:50)  
 B7-H3 APC (R&D Systems, Clone 85504, Catalog. N° FAB1027A, Lot N°AAPJ0213061, 1:50)  
 OX40L PE (R&D Systems, Clone 159403, Catalog. N° FAB10541P, Lot N°ABJJ0313111, 1:50)  
 VISTA FITC (R&D Systems, Clone 730804, Catalog. N° FAB71261G, Lot N°ADJM0113091, 1:50)  
 HLA-DP PE (Leinco Technologies, Clone B7/21, Catalog. N° H130, Lot N°0313L280, 1:200)  
 PVR FITC (Lifespan Biosciences, Clone TX21, Catalog. N° LS-C179432, Lot N°66802, 1:50)  
 CD80 PE (Invitrogen, Clone MEM-233, Catalog. N° MHCD8004, Lot N°1369609B, 1:50)  
 CD34 Vioblue (Miltenyi Biotech, Clone AC136, Catalog. N°130-095-393, Lot N°5150415145, 1:50)

The only anti-mouse antibody used is the pan CD45 PerCp5.5 (Clone 30-F11, Catalog. N° 103132, Lot N° B199699, 1:200) from BioLegend, (San Diego, CA, USA), utilized only for the in vivo experiments.

#### Validation

All the antibodies used in the flow cytometry experiments were from commercial vendors and they were validated for specificity to original targets by the manufacturers. The Certificate of Analysis is available from the manufacturers. All these commercially-available antibodies were also tested on cell lines reported to be positive for the markers of interest and titrated for optimal on target/off target activity.

#### Research animals

Policy information about [studies involving animals](#); [ARRIVE guidelines](#) recommended for reporting animal research

##### Animals/animal-derived materials

For in vivo experiments four week-old male non-irradiated immunodeficient NOD-SCID interleukin (IL)-2Rgamma(null) (NSG) mice were used.

#### Human research participants

Policy information about [studies involving human research participants](#)

##### Population characteristics

In this retrospective study, we selected based on material availability a discovery cohort (n=40) and a validation cohort (n=36) of patients with diagnosis of de novo or secondary AML who experienced non-HLA loss disease relapse after allo-HCT, and for whom paired pre- and post-transplant viable leukemic samples had been collected upon specific written informed consent, in agreement with the Declaration of Helsinki. Discovery cohort samples came from the San Raffaele Leukemia Biobank (Protocol "ALLO-RELAPSE" approved by the San Raffaele Ethic Committee on 03/11/17 and Protocol "Banca Neoplasie Ematologiche" approved by the San Raffaele Ethic Committee on 10/05/10, latest amendment on 06/14/12) and the Northern Italy Leukemia Group (NILG) BioBank (protocol NILG AML 02/06, NCT00495287). Validation cohort samples came from the San Raffaele Leukemia Biobank, the Universitätsklinikum Essen Biobank, the Universitätsklinikum Freiburg Biobank, the Hokkaido University Biobank, the Leiden University Medical Center Biobank, the Johns Hopkins University Biobank and the Institut Paoli-Calmettes Biobank.

All the covariate-relevant population characteristics of the human cohorts here analyzed are listed in Supplementary Table 1. Supplementary Table 2 and 5 provide a summary of the analyses conducted for each sample.

## Method-specific reporting

n/a | Involved in the study

- ChIP-seq  
  Flow cytometry  
  Magnetic resonance imaging

## Flow Cytometry

### Plots

Confirm that:

- The axis labels state the marker and fluorochrome used (e.g. CD4-FITC).  
 The axis scales are clearly visible. Include numbers along axes only for bottom left plot of group (a 'group' is an analysis of identical markers).  
 All plots are contour plots with outliers or pseudocolor plots.  
 A numerical value for number of cells or percentage (with statistics) is provided.

### Methodology

#### Sample preparation

FACS-Sorting: Samples containing leukemia cells were thawed in and kept overnight at 37 °C in X-Vivo-15 medium supplemented with 5% human serum (complete medium) at a concentration of 1-2x10<sup>6</sup> cells/ml. Leukemia blasts were labeled using the appropriate mixture of antibodies in 100 µl of complete medium and kept for 20 min at 4 °C. Before sorting, cells were washed with 10 ml of complete medium and filtered with round bottom tube with cell a strainer cap.

Immunophenotypic analysis: Samples were thawed in complete medium. A total of 0.2-1 x 10<sup>6</sup> cells were washed in 1XPBS, 2% FBS and then labeled with the appropriate antibodies mix in 50 µl 1XPBS, 2% FBS in a FACS tube. Staining was performed at 4 °C for 15-20 min and washed with 1 ml of 1XPBS, 2% FBS.

Mice samples: In total 50 µl mice peripheral blood, previously treated with heparin, were stained with the relevant mixture of antibodies with the addition of 100 µl of 1X PBS, 2% FBS, for 20 min at 4 °C. The erythrocytes were eliminated from the samples by incubating with 3-5 ml ACK lysis buffer for 4 min at RT. Cells were pelleted by centrifugation (300g for 10 min) and washed with 3 ml of 1X PBS and then re-suspended in 50 µl of 1X PBS and 25 µl of count beads.

#### Instrument

Sorting of the relevant population was performed using MoFlo™ XDP (Beckman Coulter, Brea, CA, USA) or a FACS Diva (BD Biosciences, Franklin Lakes, NJ, USA) cell sorters.

Analysis of human samples was performed using a Canto II flow cytometer equipped with 405nm, 488nm, and 633nm lasers, or a LSR Fortessa flow cytometer equipped with 355nm, 405nm, 488nm, 561nm and 640nm lasers (both from BD Biosciences, Franklin Lakes, NJ, USA). Analysis of mouse samples was performed using a Gallios flow cytometer equipped with 488nm, 638nm and 405nm lasers (Beckman Coulter, Brea, CA, USA).

## Software

Data were processed using FCS 4 Express (De Novo Software, Los Angeles, CA), FlowJo version 9.8.5 (Tree Star, Ashland, OR, USA), or Caluza (Beckman Coulter, Brea, CA, USA).

## Cell population abundance

The relevant leukemic cell populations were sorted using MoFlo™ XDP (Beckman Coulter, Brea, CA, USA) or a FACS Diva (BD Biosciences, Franklin Lakes, NJ, USA) cell sorters. The cell purity was analyzed by flow cytometry by comparing the cell populations before and after sorting. All the post-sort fractions were at least 90% pure. For in vivo experiments the T cells were depleted from the leukemia samples by column selection (Miltenyi Biotec GmbH, Bergisch Gladbach, Germany) after staining the cells with human CD3 microbeads (Miltenyi Biotec GmbH, Bergisch Gladbach, Germany) according to manufacturer's instructions.

## Gating strategy

The gating strategy for analysis of markers of interest on leukemia and T cells is provided in Supplementary Fig. 1, and the gating strategy for analysis of markers of interest on bone marrow myeloid progenitors and peripheral blood monocytes is provided in Supplementary Fig. 2.

Tick this box to confirm that a figure exemplifying the gating strategy is provided in the Supplementary Information.

In the format provided by the authors and unedited.

# Immune signature drives leukemia escape and relapse after hematopoietic cell transplantation

Cristina Toffalori<sup>1</sup>, Laura Zito<sup>1,21</sup>, Valentina Gambacorta<sup>1,2,21</sup>, Michela Riba<sup>3,21</sup>, Giacomo Oliveira<sup>1,4,19</sup>, Gabriele Bucci<sup>1,3</sup>, Matteo Barcella<sup>5</sup>, Orietta Spinelli<sup>6</sup>, Raffaella Greco<sup>7</sup>, Lara Crucitti<sup>7,20</sup>, Nicoletta Cieri<sup>4,7,20</sup>, Maddalena Noviello<sup>4</sup>, Francesco Manfredi<sup>4</sup>, Elisa Montaldo<sup>8</sup>, Renato Ostuni<sup>8</sup>, Matteo M. Naldini<sup>9</sup>, Bernhard Gentner<sup>7,9</sup>, Miguel Waterhouse<sup>10</sup>, Robert Zeiser<sup>10</sup>, Jürgen Finke<sup>10</sup>, Maher Hanoun<sup>11</sup>, Dietrich W. Beelen<sup>11</sup>, Ivana Gojo<sup>12</sup>, Leo Luznik<sup>12</sup>, Masahiro Onozawa<sup>13</sup>, Takanori Teshima<sup>13</sup>, Raynier Devillier<sup>14</sup>, Didier Blaise<sup>14</sup>, Constantijn J. M. Halkes<sup>15</sup>, Marieke Griffioen<sup>15</sup>, Matteo G. Carrabba<sup>7</sup>, Massimo Bernardi<sup>7</sup>, Jacopo Peccatori<sup>7</sup>, Cristina Barlassina<sup>5</sup>, Elia Stupka<sup>3,19</sup>, Dejan Lazarevic<sup>3</sup>, Giovanni Tonon<sup>3</sup>, Alessandro Rambaldi<sup>6,16</sup>, Davide Cittaro<sup>3</sup>, Chiara Bonini<sup>4,17</sup>, Katharina Fleischhauer<sup>1,18</sup>, Fabio Ciceri<sup>7,17,22</sup> and Luca Vago<sup>1,7,22\*</sup>

<sup>1</sup>Unit of Immunogenetics, Leukemia Genomics and Immunobiology, Division of Immunology, Transplantation and Infectious Disease, IRCCS San Raffaele Scientific Institute, Milano, Italy. <sup>2</sup>Unit of Senescence in Stem Cell Aging, Differentiation and Cancer, San Raffaele Telethon Institute for Gene Therapy, IRCCS San Raffaele Scientific Institute, Milano, Italy. <sup>3</sup>Center for Translational Genomics and Bioinformatics, IRCCS San Raffaele Scientific Institute, Milano, Italy. <sup>4</sup>Experimental Hematology Unit, Division of Immunology, Transplantation and Infectious Disease, IRCCS San Raffaele Scientific Institute, Milano, Italy. <sup>5</sup>Genomic and Bioinformatics Unit, Department of Health Sciences, University of Milano, Milano, Italy. <sup>6</sup>Hematology and Bone Marrow Transplant Unit, ASST Papa Giovanni XXIII, Bergamo, Italy. <sup>7</sup>Unit of Hematology and Bone Marrow Transplantation, IRCCS San Raffaele Scientific Institute, Milano, Italy. <sup>8</sup>Genomics of the Innate Immune System Unit, San Raffaele Telethon Institute for Gene Therapy, IRCCS San Raffaele Scientific Institute, Milano, Italy. <sup>9</sup>Translational Stem Cell and Leukemia Unit, San Raffaele Telethon Institute for Gene Therapy, IRCCS San Raffaele Scientific Institute, Milano, Italy. <sup>10</sup>Department of Hematology, Oncology and Stem Cell Transplantation, Universitätsklinikum Freiburg, Freiburg, Germany. <sup>11</sup>Department of Bone Marrow Transplantation, Universitätsklinikum Essen, Essen, Germany. <sup>12</sup>Sidney Kimmel Comprehensive Cancer Center, Johns Hopkins University School of Medicine, Baltimore, MD, USA. <sup>13</sup>Department of Hematology, Hokkaido University Faculty of Medicine, Graduate School of Medicine, Sapporo, Japan. <sup>14</sup>Department of Haematology, Institut Paoli Calmettes, Marseille, France. <sup>15</sup>Department of Hematology, Leiden University Medical Center, Leiden, The Netherlands. <sup>16</sup>Department of Oncology and Hemato-Oncology, University of Milano, Milano, Italy. <sup>17</sup>San Raffaele Vita-Salute University, Milano, Italy. <sup>18</sup>Institute for Experimental Cellular Therapy, Universitätsklinikum Essen, Essen, Germany. <sup>19</sup>Present address: Dana-Farber Cancer Institute, Boston, MA, USA. <sup>20</sup>Present address: University of Milano, Milano, Italy. <sup>21</sup>These authors contributed equally: Laura Zito, Valentina Gambacorta and Michela Riba. <sup>22</sup>These authors jointly directed this work: Fabio Ciceri and Luca Vago. \*e-mail: [vago.luca@hsr.it](mailto:vago.luca@hsr.it)

## SUPPLEMENTARY INFORMATION

### **Immune signature drives leukemia escape and relapse after hematopoietic cell transplantation**

Toffalori C., Zito L., Gambacorta V., Riba M., Oliveira G., Bucci G., Barcella M., Spinelli O., Greco R., Crucitti L., Cieri N., Noviello M., Manfredi F., Montaldo E., Ostuni R., Naldini M.M., Gentner B., Waterhouse M., Zeiser R., Finke J., Hanoun M., Beelen D., Gojo I., Luznik L., Onozawa M., Teshima T., Devillier R., Blaise D., Halkes C.J.M., Griffioen M., Carrabba M.G., Bernardi M., Peccatori J., Barlassina C., Stupka E., Lazarevic D., Tonon G., Rambaldi A., Cittaro D., Bonini C., Fleischhauer K., Ciceri F., Vago L.

#### **Index**

Supplementary Tables.....	page 2
Supplementary Figures.....	page 8

## Supplementary Tables

Supplementary Table 1. Patient and transplant characteristics.

	Discovery Cohort (n=40)		Validation Cohort (n=36)	
	No.	%	No.	%
<b>Age at Transplant</b>				
Years, Median (Range)	47	(29 – 74)	55	(21 – 76)
<b>Sex ratio</b>				
Male/Female		0.6		1.4
<b>Disease Diagnosis</b>				
<i>De novo Acute Myeloid Leukemia</i>	35	87.5	28	77.8
Secondary Acute Myeloid Leukemia	5	12.5	8	22.2
<b>Cytogenetics</b>				
Favorable	2	5.0	2	5.6
Intermediate	31	77.5	20	55.6
Adverse	6	15.0	14	38.8
Not Available	1	2.5	0	0.0
<b>Molecular Alterations</b>				
FLT3-ITD	19	47.5	7	22.6
NPM1	16	40.0	4	13.8
<b>Status at Transplant</b>				
Complete Remission	13	32.5	22	61.2
Active Disease	27	67.5	14	38.8
<b>Graft Source</b>				
PBSCs	33	82.5	29	80.6
Bone Marrow	5	12.5	7	19.4
Umbilical Cord Blood	2	5.0	0	0.0
<b>Graft Composition</b>				
CD34+ *10e6/Kg, Median (Range)	6	(0.05–9.5)	5.4	(0.7–17.8)
CD3+ *10e6/Kg, Median (Range)	188	(1.46–439.0)	154.2	(43–457)
<b>Type of Donor</b>				
HLA-identical Sibling	7	17.5	14	38.8
Matched Unrelated	8	20.0	11	30.6
10/10	5	12.5	9	25.0
9/10	3	7.5	2	5.6
Cord Blood	2	5.0	0	0.0
Haploidentical	23	57.5	11	30.6
<b>Conditioning Regimens</b>				
Myeloablative	28	70.0	18	50.0
Non-myeloablative	12	30.0	18	50.0
<b>In vivo T cell Depletion</b>				
No	5	12.5	12	33.3
Anti Thymocyte Globulin	18	45.0	4	11.2
Post-Transplant Cyclophosphamide	15	37.5	11	30.6
Alemtuzumab	2	5.0	8	22.2
Anti Thymocyte Globulin + Alemtuzumab	0	0.0	1	2.7
<b>In vivo B cell Depletion</b>				
No	24	60.0	27	75.0
Rituximab	14	35.0	0	0.0
Alemtuzumab	2	5.0	9	25.0
<b>Post-transplantation GvHD Prophylaxis</b>				
None	0	0.0	7	19.4
CsA	0	0.0	9	25.0
Tacr/MMF	1	2.5	9	25.0
Sirolimus/MMF	22	55.0	0	0.0
CsA/MTX	12	30.0	2	5.6
CsA/MMF	5	12.5	5	13.8
Other	0	0.0	4	11.2
<b>aGvHD</b>				
No	23	57.5	26	72.2
Grade 1	8	20.0	3	8.3
Grade 2	5	12.5	3	8.3
Grade 3	4	10.0	2	5.6
Grade 4	0	0.0	2	5.6
<b>cGvHD</b>				
No	35	87.5	33	91.7
Limited	1	2.5	2	5.6
Extensive	4	10.0	1	2.7
<b>Relapse</b>				
Time to Relapse (Days), Median (Range)	65	(15-895)	153	(21-2165)
On IS at the Time of Relapse	24	60.0	15	41.7



**Supplementary Table 2.** Summary of the analyses carried out in the discovery cohort.

Patient Code	Type of allo-HCT	Donor-Recipient HLA mismatches	Days from allo-HCT to Relapse	SNP Array	Micro Array	Phenotypic analysis	qPCR	Functional Assays
UPN 1	HLA-identical	-	294	✓	✓			
UPN 2	HLA-identical	-	86		✓	✓	✓	
UPN 3	HLA-identical	-	233	✓	✓			
UPN 4	HLA-identical	-	29	✓	✓	✓	✓	
UPN 5	HLA-identical	-	15	✓	✓	✓	✓	
UPN 6	HLA-Matched Unrelated	B*	58	✓				
UPN 7	HLA-Matched Unrelated	C*	96	✓				
UPN 8	Cord Blood	DRB1 <sup>§</sup>	242	✓				
UPN 9	Cord Blood	A, (C), DQB1	54	✓	✓	✓	✓	
UPN 10	HLA-Haploidentical	(A), DRB1, DQB1, DPB1*	102		✓	✓	✓	✓
UPN 11	HLA-Haploidentical	(A), B, C, DRB1, DQB1, (DPB1)	53	✓				
UPN 12	HLA-Haploidentical	A, B, C, DRB1, DQB1, DPB1	190	✓				
UPN 13	HLA-Haploidentical	A, (B), (C), DQB1, DPB1	26	✓	✓	✓	✓	
UPN 14	HLA-Haploidentical	A, B, C, DRB1, DQB1, DPB1	41	✓	✓	✓	✓	✓
UPN 15	HLA-identical	-	27			✓		
UPN 16	HLA-identical	-	17			✓		
UPN 17	HLA-Matched Unrelated	(DPB1)	33			✓		✓
UPN 18	HLA-Matched Unrelated	DPB1	895			✓		
UPN 19	HLA-Matched Unrelated	DPB1	91			✓		
UPN 20	HLA-Matched Unrelated	DPB1	86			✓		
UPN 21	HLA-Matched Unrelated	-*	29			✓		
UPN 22	HLA-Matched Unrelated	C, DPB1	67			✓		
UPN 23	HLA-Haploidentical	(DRB1), (DQB1), DPB1	62			✓		
UPN 24	HLA-Haploidentical	A, (DRB1), (DQB1)	198			✓		✓
UPN 25	HLA-Haploidentical	A, B, DRB1, DQB1, DPB1	34			✓		
UPN 26	HLA-Haploidentical	A, B, C, DRB1, DPB1	49			✓		
UPN 27	HLA-Haploidentical	A, B, C, DRB1	29			✓		
UPN 28	HLA-Haploidentical	B, C, DRB1, DQB1, DPB1	132			✓		
UPN 29	HLA-Haploidentical	B, C, DRB1, DQB1	60			✓		
UPN 30	HLA-Haploidentical	A, B, C, DRB1, DQB1, (DPB1)	344			✓		
UPN 31	HLA-Haploidentical	B, C, DRB1, DQB1, DPB1	92			✓		
UPN 32	HLA-Haploidentical	A, B, C, DRB1, DQB1, DPB1	62			✓		✓
UPN 33	HLA-Haploidentical	A, (B), C, (DRB1), (DQB1), DPB1	38			✓		
UPN 34	HLA-Haploidentical	A, B, C, DRB1, DQB1, DPB1	551			✓		
UPN 35	HLA-Haploidentical	A, B, C, DRB1, DQB1, DPB1	146			✓		
UPN 36	HLA-Haploidentical	A, B, C, DRB1, DQB1, DPB1	104			✓		
UPN 37	HLA-Haploidentical	A, B, C, DRB1, DQB1, DPB1	90			✓		✓
UPN 38	HLA-Haploidentical	A, B, C, DRB1, DQB1, DPB1	59			✓		
UPN 39	HLA-Haploidentical	A, B, C, DRB1, DQB1, DPB1	856			✓		
UPN 40	HLA-Haploidentical	A, B, C, DRB1, DQB1	63			✓		

\* HLA-DPB1 typing not available, <sup>§</sup> HLA-DQB1 and -DPB1 typing not available

**Supplementary Table 3.** Summary of genomic alterations detected by SNP array analysis.

UPN#	Diagnosis			Relapse after allo-HCT		
	Alteration	Size	Clonality	Alteration	Size	Clonality
1	None			None		
	+8	Whole Chr.	Clonal	+8	Whole Chr.	Clonal
	-13(q13.3-14.3)	12.0 Kb	Subclonal (65-75%)	-13(q12.3-21.32)	36.9 Kb	Clonal
3				-3(p12.3-14.3)	28 Mb	Subclonal (25-30%)
				-15(q14)	0.11 Mb	Subclonal (25-30%)
4	CN-LOH 13q	85.7 Mb	Subclonal (80-90%)	CN-LOH 13q	85.7 Mb	Clonal
				-6(q23.3)	0.53 Mb	Clonal
				-11(p13-15.1)	17.1 Mb	Clonal
5	+8	Whole Chr.	Clonal	+8	Whole Chr.	Clonal
6	CN-LOH 13q	85.7 Mb	Subclonal (30-45%)	CN-LOH 13	Whole Chr.	Clonal
				-10(p22.3-23.2)	10.9 Mb	Subclonal (20-30%)
7	CN-LOH 11(q13.3-ter)	66.5 Mb	Clonal	CN-LOH 11(q13.3-ter)	66.5 Mb	Clonal
8	None			CN-LOH 13	Whole Chr.	Subclonal (40-50%)
				+21	Whole Chr.	Clonal
	CN-LOH 3(p21.3)	6.7 Mb	Clonal	CN-LOH 3(p21.3)	6.7 Mb	Clonal
9	CN-LOH 5(q13.2)	2.4 Mb	Clonal	CN-LOH 5(q13.2)	2.4 Mb	Clonal
	CN-LOH 7(p12.3-14.3)	40.6 Mb	Clonal	CN-LOH H 7(p12.3-14.3)	40.6 Mb	Clonal
	CN-LOH H 13	Whole Chr.	Subclonal (15-20%)	CN-LOH 13	Whole Chr.	Subclonal (85-95%)
11	CN-LOH 13q	86.8 Mb	Clonal	CN-LOH 13q	86.8 Mb	Clonal
	-16(q23.1)	1 Mb	Subclonal (65-75%)	-16(q23.1)	1 Mb	Clonal
12				+8	Whole Chr.	Clonal
				+21	Whole Chr.	Clonal
13	CN-LOH 13q	95 Mb	Clonal	CN-LOH 13q	87.6 Mb	Clonal
				+8	Whole Chr.	Clonal
				-17(p13.2-p13.1)	0.82 Mb	Clonal
14	CN-LOH 4(p15.32)	7.2 Mb	Clonal	CN-LOH 4(p15.32)	7.2 Mb	Clonal
	-15(q15.1)	1.2 Mb	Clonal	-15(q15.1)	1.2 Mb	Clonal
				CN-LOH 13q	94.1 Mb	Clonal

**Supplementary Table 4.** List of the 110 genes deregulated between AML collected at disease diagnosis and relapse after allo-HCT, with respective gene IDs and symbols (provided as a separate excel file).

**Supplementary Table 5.** Summary of the analyses carried out in the validation cohort.

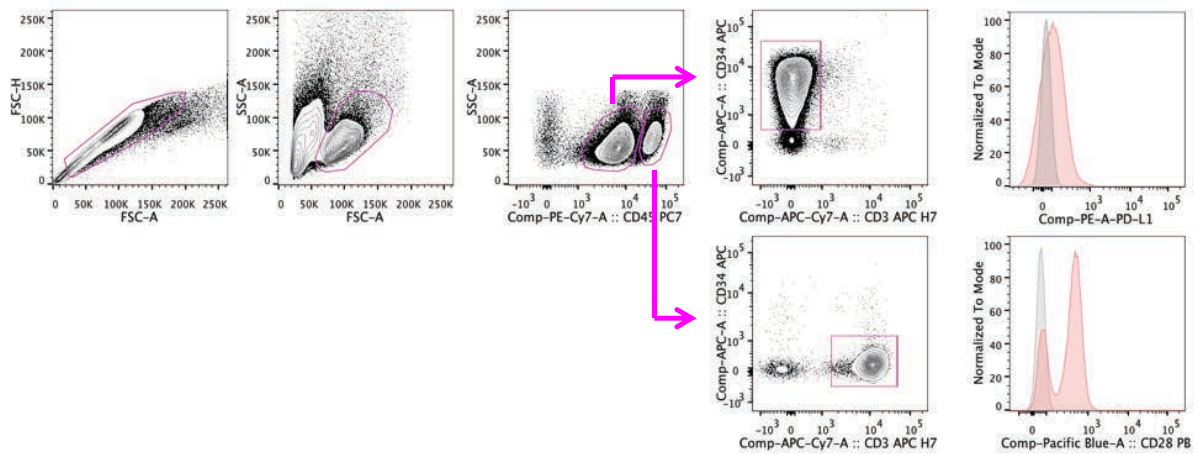
Patient Code	Type of allo-HCT	Donor-Recipient HLA mismatches	Days from allo-HCT to Relapse	RNA-Seq	Phenotypic analysis
Milano 1	HLA-identical	-	62	✓	✓
Milano 2	HLA-identical	-	702	✓	✓
Essen 1	HLA-Matched Unrelated	-*	304		✓
Essen 2	HLA-identical	-	2165		✓
Freiburg 1	HLA-Matched Unrelated	(DQB1)*	65		✓
Marseille 1	HLA-Haploidentical	(B), C*	838	✓	✓
Marseille 2	HLA-Haploidentical	A, B, C, DRB1, DQB1*	92	✓	✓
Marseille 3	HLA-Matched Unrelated	-*	94		✓
Marseille 4	HLA-Matched Unrelated	C*	890		✓
Marseille 5	HLA-Matched Unrelated	-*	139		✓
Marseille 6	HLA-Matched Unrelated	-*	597		✓
Marseille 7	HLA-Matched Unrelated	-*	404		✓
Marseille 9	HLA-Haploidentical	(A), B, C*	153		✓
Marseille 12	HLA-identical	-	558	✓	✓
Marseille 13	HLA-identical	-	128		✓
Baltimore 1	HLA-Haploidentical	(A), B, C, DRB1, DQB1*	166		✓
Baltimore 2	HLA-identical	-	163	✓	✓
Baltimore 3	HLA-Haploidentical	A, B, C, DRB1, (DQB1)*	99		✓
Baltimore 4	HLA-identical	-	59	✓	✓
Baltimore 5	HLA-Haploidentical	A, B, C, DRB1, (DQB1)*	114		✓
Leiden 1	HLA-Matched Unrelated	-*	537		✓
Leiden 2	HLA-identical	-	349		✓
Leiden 3	HLA-Matched Unrelated	(DPB1)	267		✓
Leiden 4	HLA-identical	-	108		✓
Leiden 5	HLA-Matched Unrelated	DPB1	307	✓	✓
Leiden 6	HLA-identical	-	141	✓	✓
Leiden 7	HLA-identical	-	184	✓	✓
Leiden 8	HLA-Matched Unrelated	(DPB1)	351	✓	✓
Leiden 9	HLA-identical	-	78	✓	✓
Leiden 10	HLA-identical	-	153	✓	✓
Sapporo 1	HLA-Haploidentical	A, B, C, DRB1 <sup>§</sup>	142		✓
Sapporo 2	HLA-Haploidentical	A, B, C, DRB1 <sup>§</sup>	30	✓	✓
Sapporo 4	HLA-identical	-	109	✓	✓
Sapporo 5	HLA-Haploidentical	B, C, DRB1 <sup>§</sup>	21		✓
Sapporo 6	HLA-Haploidentical	A, B, C, DRB1 <sup>§</sup>	88		✓
Sapporo 7	HLA-Haploidentical	A, B, (C), DRB1 <sup>§</sup>	55		✓

\* HLA-DPB1 typing not available, <sup>§</sup> HLA-DQB1 and -DPB1 typing not available

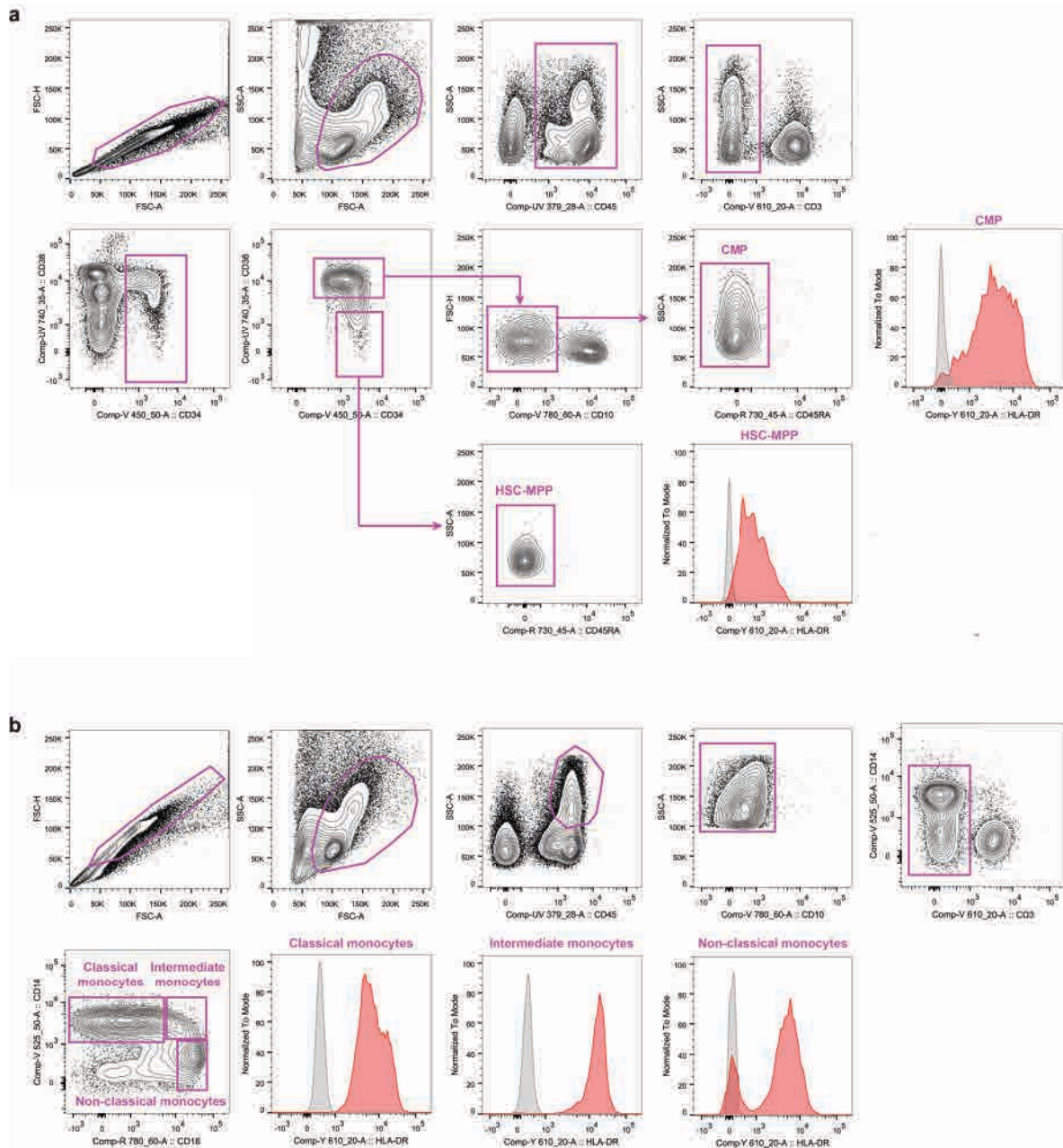
**Supplementary Table 6.** Primer sequences for qPCR assays.

	<b>Forward Sequence</b>	<b>Reverse Sequence</b>	<b>Reference</b>
<b>CIITA</b>	5'-AGCCTTTCAAAGCCAAGTCC-3'	5'-TTGTTCTCACTCAGCGCATC-3'	<i>Ulbricht T., et al., 2012<sup>48</sup></i>
<b>HLA-A</b>	5'-TCCTTGGAGCTGTGATCACT-3'	5'-AAGGGCAGGAACAACCTTG-3'	<i>García-Ruano A.B., et al., 2010<sup>47</sup></i>
<b>HLA-C</b>	5'-TCCTGGYTGCCTAGCTGTC-3'	5'-CAGGCTTTACAAGTGATGAG-3'	<i>García-Ruano A.B., et al., 2010<sup>47</sup></i>
<b>HLA-DRB</b>	5'-CGTGACAAGCCCTCTCACAG-3'	5'-TGTGCAGATTCAGACCGTGC-3'	<i>Wang J. et al., 2007<sup>49</sup></i>
<b>HLA-DPB1</b>	5'-GCAGGGCCACTCCAGAGAA-3'	5'-CCATTAACGCGTAGCATTCC-3'	Developed in house

## Supplementary Figures



**Supplementary Figure 1.** Gating strategy for the immunophenotypic analysis of the expression of HLA molecules, costimulatory ligands or receptors on AML blasts and T cells. Shown are representative flow cytometry plots with the sequential logical gates. According to physical parameters, live cells are gated upon the inclusion of singlets only. Based on the level of CD45 expression, immature myeloid cells ( $CD45^{dim}$ ) are discriminated from lymphocytes and monocytes ( $CD45^{high}$ ). The bulk  $CD45^{dim}$  leukemia population was defined as CD34 or CD33 or CD117-positive and CD3-negative. The  $CD45^{high}$  T cell population was identified as CD34 or CD33 or CD117-negative and CD3-positive subset. To determine the autofluorescence of the cell surface markers of interest in leukemia blasts and T cells, for each sample a negative control was generated using only lineage markers (CD45, CD33 or CD34 or CD117, and CD3).



**Supplementary Figure 2.** Gating strategies for the immunophenotypic analysis of the expression of HLA molecules and inhibitory ligands on bone marrow progenitors (panel **a**) and different subsets of peripheral blood monocytes (panel **b**). Shown are representative flow cytometry plots with the sequential logical gates. **a**, According to physical parameters, live cells are gated upon the inclusion of singlets only. Based on the expression of CD45, hematopoietic cells are selected, followed by exclusion of CD3<sup>+</sup> T cells and by gating on CD34<sup>+</sup> progenitors. Amongst these, hematopoietic stem cells/multipotent progenitors (HSCs/MPPs) are identified as CD38<sup>-</sup> and CD45RA<sup>-</sup> and common myeloid progenitors (CMPs) as CD38<sup>+</sup>CD10<sup>-</sup>. **b**, According to physical parameters, live cells are gated upon the inclusion of singlets only. CD45<sup>high</sup>SSC<sup>high</sup> cells are selected, followed by exclusion of CD10<sup>+</sup> neutrophils and CD3<sup>+</sup> lymphocytes. In the resulting subpopulation, classical monocytes are identified as CD14<sup>high</sup>CD16<sup>-</sup>, non-classical monocytes as CD14<sup>dim</sup>CD16<sup>+</sup>, and intermediate monocytes as CD14<sup>bright</sup>CD16<sup>dim</sup>. To determine the autofluorescence of the cell surface markers of interest (HLA-DR, -DP, PD-L1, B7-H3, VISTA) in the different cell subsets, for each sample a negative control was generated using only lineage markers (CD3, CD10, CD14, CD16, CD34, CD38, CD45, CD45RA).





**Chapter 6.**

**Mechanisms of Leukemia Immune Evasion and Their Role in  
Relapse after Haploidentical Hematopoietic Cell transplantation**

Rovatti PE\*, Gambacorta V\*, Lorentino F\*, Ciceri F and Vago L

*Under second revision in Frontiers in Immunology*

1 **Mechanisms of Leukemia Immune Evasion and Their Role in Relapse after Haploidentical**  
2 **Hematopoietic Cell Transplantation**

3  
4 Pier Edoardo Rovatti<sup>1,2,\*</sup>, Valentina Gambacorta<sup>1,3,\*</sup>, Francesca Lorentino<sup>2,\*</sup>, Fabio Ciceri<sup>2,4</sup>, Luca  
5 Vago<sup>1,2</sup>

6  
7 <sup>1</sup>Unit of Immunogenetics, Leukemia Genomics and Immunobiology, IRCCS San Raffaele Scientific Institute, Milano,  
8 Italy; <sup>2</sup>Hematology and Bone Marrow Transplantation Unit, IRCCS San Raffaele Scientific Institute, Milano, Italy;

9 <sup>3</sup>Unit of Senescence in Stem Cell Aging, Differentiation and Cancer; San Raffaele Telethon Institute for Gene Therapy,  
10 IRCCS San Raffaele Scientific Institute, Milano, Italy; <sup>4</sup>Vita-Salute San Raffaele University, Milano, Italy.

11 \* indicates equal contribution from these Authors  
12  
13  
14  
15  
16  
17  
18  
19  
20  
21  
22  
23  
24  
25  
26  
27  
28  
29  
30  
31  
32  
33  
34  
35  
36  
37

38 **RUNNING TITLE:** Immune Evasion and Relapse after Haploidentical HCT

39 **ABSTRACT/TEXT WORD COUNT:** 200/6820

40 **FIGURES/TABLES/REFERENCES:** 2/0/203  
41  
42  
43  
44  
45  
46  
47  
48  
49  
50

51 **CORRESPONDENCE:** Dr. Luca Vago, Unit of Immunogenetics, Leukemia Genomics and  
52 Immunobiology, IRCCS San Raffaele Scientific Institute, via Olgettina 60, Milano, Italy. Phone:  
53 +390226434341. Fax: +390226436198. E-mail: vago.luca@hsr.it

1 **ABSTRACT**

2 Over the last decade, the development of multiple strategies to allow the safe transfer from the  
3 donor to the patient of high numbers of partially HLA-incompatible T cells has dramatically  
4 reduced the toxicities of haploidentical hematopoietic cell transplantation (haplo-HCT), but this was  
5 not accompanied by a similar positive impact on the incidence of post-transplantation relapse.  
6 In the present review, we will elaborate on how the unique interplay between HLA-mismatched  
7 immune system and malignancy that characterizes haplo-HCT may impact on relapse biology,  
8 shaping the selection of disease variants that are resistant to the "graft-versus-leukemia" effect.  
9 In particular, we will present current knowledge on genomic loss of HLA, a relapse modality first  
10 described in haplo-HCT and accounting for a significant proportion of relapses in this setting, and  
11 discuss other more recently identified mechanisms of post-transplantation immune evasion and  
12 relapse, including the transcriptional downregulation of HLA class II molecules and the  
13 enforcement of inhibitory checkpoints between T cells and leukemia.  
14 Ultimately, we will review the available treatment options for patients who relapse after haplo-HCT  
15 and discuss on how a deeper insight into relapse immunobiology might inform the rational and  
16 personalized selection of therapies to improve the largely unsatisfactory clinical outcome of  
17 relapsing patients.

1 **MAIN TEXT**

2  
3 **Introduction**

4  
5 Allogeneic hematopoietic cell transplantation from haploidentical family members represents a  
6 promising solution to offer allogeneic HCT to virtually all patients with an indication to transplant  
7 but lacking a fully compatible and/or rapidly available donor. However, from the immunological  
8 standpoint, it also represents the most challenging allogeneic HCT setting, counterpoising two  
9 largely HLA-incompatible immune systems and thus posing a severe risk of graft-versus-host  
10 disease (GvHD) and immune rejection. To overcome this obstacle, over the last few decades many  
11 strategies have been developed to improve the feasibility and safety of haplo-HCT (1,2).  
12 Noticeably, some of these platforms have demonstrated remarkable success, leading to an  
13 exponential increase in the number of haplo-HCT performed worldwide (3,4).  
14 The development of innovative strategies to render haplo-HCT feasible was fueled by intensive  
15 research on the immunobiology of allo-HCT, leading to a number of observations that were  
16 subsequently extended to other transplantation settings or even served as the foundation to explain  
17 the physiological metrics of immune responses to pathogens and tumors.  
18 In the present review we will present one of the most paradigmatic examples of this process, by  
19 describing how investigation of mechanisms of relapse after haplo-HCT paved the way to  
20 understand the interplay between transplanted immune system and tumor also in other  
21 transplantation settings and, importantly, to the development of new rationales for relapse therapy.

22  
23 **Tumor-Intrinsic Mechanisms of Relapse**

24  
25 Seminal studies conducted by the Seattle group more than 25 years ago led to the identification of  
26 donor-derived T cells as one of the major drivers of the "graft-versus-leukemia" (GvL) effect (5). It  
27 is thus no surprise that all the best characterized tumor-intrinsic mechanisms of immune evasion  
28 and relapse after allo-HCT have as a final output the abrogation of interactions between T cells and  
29 the tumor. This can occur either because leukemia cells become "invisible" to patrolling T cells, for  
30 instance through genetic or epigenetic alterations in the antigen processing and presenting  
31 machinery, or because they enact mechanism to render the encounter ineffectual, as happens when  
32 inhibitory immune checkpoints are enforced (Figure 1).

33  
34 Genomic Loss of HLA

35  
36 Alterations in the expression and functionality of HLA class I and II molecules have long been  
37 characterized in solid tumors, underlining also in this setting the importance of T cell-mediated  
38 responses in shaping tumor immunogenicity.

39 Interestingly, in hematological tumors, and acute myeloid leukemia (AML) in particular, alterations  
40 in the HLA region are quite uncommon, especially at the time of diagnosis (6,7). This feature is  
41 critical, since the donor T cell-mediated GvL effect of allo-HCT mostly depends on the HLA  
42 molecule expression on the surface of leukemic cells. As part of the antigen presenting machinery,  
43 HLA molecules serve as restriction elements for minor histocompatibility antigens and tumor-  
44 associated antigens or, when incompatible, as direct targets of primary alloreactivity. Especially in  
45 haplo-HCT, where an entire HLA haplotype is mismatched between patient and donor, T cell-  
46 mediated alloreactivity converges against the incompatible molecules, that rapidly become the  
47 immunodominant GvL targets.

48 Given this fundamental role of HLAs in the biology of haplo-HCT, it is reasonable that a possible  
49 getaway for malignant cells to escape the bottleneck of immunological pressure might be to exploit  
50 alterations in the HLA locus, mirroring what happens in solid tumors.

1 The first characterization of such a strategy being used in AML after haplo-HCT was provided  
2 nearly ten years ago, when genomic loss of the mismatched HLA haplotype (from this point on  
3 referred as "HLA loss") was first reported (8). Behind this discovery there is a curious case of  
4 serendipity: while investigating intermediate-resolution genomic HLA typing of bone marrow  
5 aspirate samples as an alternative technique for the assessment of hematopoietic chimerism (9), our  
6 group encountered several cases of AML post-transplantation relapse that typed negative for the  
7 patient HLAs. Genomic HLA typing of leukemic blasts purified from these relapses confirmed the  
8 absence of all HLA class I and class II genes encoded on the mismatched patient-specific HLA  
9 haplotype. A deeper examination of this phenomenon was then carried out exploiting whole-  
10 genome single-nucleotide polymorphism (SNP) arrays, demonstrating loss of heterozygosity (LOH)  
11 of chromosome 6p in the absence of copy number variations (CNVs), thus suggesting an event of  
12 acquired somatic uniparental disomy (aUPD). UPD has been described as a common chromosomal  
13 aberration in different tumor types, both solid and hematological (10–12). This genomic alteration  
14 consists in the loss of a chromosome region which is subsequently replaced by the homologous  
15 copy, resulting in acquired homozygosity of that region without the actual loss of genomic material.  
16 The consequences of this event can be diverse: we can witness an increase in the expression of  
17 oncogenes, loss of heterozygosity of mutated tumor-suppressors or, in this specific context, the loss  
18 of the HLA molecules not shared between donor and recipient, which represented the most  
19 immunodominant targets for donor T cell alloreactivity. The observed rearrangements had variable  
20 boundaries and extension in the different patients, but in most cases encompassed the entire HLA  
21 region, and therefore included all HLA class I and class II loci.

22 *Ex vivo* coculture of donor T cells with leukemic cells demonstrated that when HLA loss occurs, the  
23 mutated blasts become completely invisible to donor T cells that were capable to recognize them  
24 before transplantation, thus taking the upper hand over other clones and rapidly becoming the  
25 predominant population (8,13). Documentation of HLA loss not only provides an explanation on  
26 how disease escaped a pre-existing control, but also contraindicates the infusion of additional donor  
27 T cells as a strategy to try to revert relapse, since also these cells would fail to find a target to attack.  
28 Conversely, HLA loss variants that become invisible to donor T cell allorecognition could in  
29 principle still represent viable targets for alloreactive donor natural killer (NK) cells. Indeed, while  
30 the mechanism of aUPD does not reduce the overall surface levels of HLA class I molecules on the  
31 leukemia cell surface, thus avoiding to trigger "missing self" recognition by NK cells (14), the HLA  
32 alleles that are lost by leukemia cells often also represent ligands for donor inhibitory KIRs (15).  
33 Nonetheless, HLA loss relapses still occur and the biology at the basis of NK cell failure in  
34 preventing or controlling the emergence of HLA loss relapses needs to be investigated further. This  
35 is highly relevant from the translational standpoint, since an improved understanding of NK cell  
36 responses in the context of HLA loss could also serve as a springboard to design adoptive  
37 immunotherapy trials based on NK cells to treat, or even prevent, these relapse variants.

38 One of the most relevant open issue regarding HLA loss is to understand when the genetic  
39 alteration occurs or, in other terms, if an infinitesimally small immune-resistant clone exists before  
40 allo-HCT or not. To date, the molecular drivers of aUPD are poorly known. It has been  
41 demonstrated that an increased susceptibility for chromosomal breaks and the effects of DNA  
42 damage inducers, including chemotherapeutic agents, might lead to higher aUPD risk in tight  
43 proximity of mitotic recombination sites (11), jeopardizing those heavily treated patients who  
44 undergo the transplantation procedure after multiple lines of chemotherapy. However, there is also  
45 evidence that aUPD can also be a common finding in AML samples at the time of diagnosis, with a  
46 large study on 454 samples reporting aUPD frequency of 15-20%. This alteration mainly affects  
47 specific chromosome arms, including 13q, 11p, and 11q (16). Of notice, in these reports the  
48 involvement of the HLA region located in chromosome 6p is exceptional, with an estimated 3-4%  
49 of myeloid malignancies characterized by HLA LOH at disease onset (17,18).

50 Some suggestions on the biological origin of HLA loss relapses come from retrospective clinical  
51 studies. In the largest analysis on this topic performed to date (19), HLA loss relapses were shown

1 to occur significantly later than their "classical" counterparts and to be strongly associated to allo-  
2 HCTs performed in an active disease stage. A possible explanation linking these two observations  
3 might be that patient transplanted with a sizable leukemia burden probably present also much  
4 higher intratumoral heterogeneity than those transplanted with minimal or even undetectable  
5 residual disease, and are thus also more likely to carry a clone with HLA loss or with high  
6 predisposition to aUPD, that may then slowly but steadily grow in the subsequent months  
7 following transplantation.

8 Soon after the initial description (8), a number of other studies reported cases of HLA loss relapses  
9 after haplo-HCT, with an incidence ranging between 20-40% of all relapses occurring in this setting  
10 (13,20,21). Of interest, analysis of two different cohorts transplanted at our Institution using the  
11 same haplo-HCT backbone and differing only for the use of anti-thymocyte globulin (22) or high-  
12 dose cyclophosphamide (23) as in vivo T cell-depleting agent, showed superimposable frequency of  
13 HLA loss relapses, suggesting that regardless of the strategy used a significant population of  
14 alloreactive T cells escapes the initial purging and is capable to mediate significant antileukemic  
15 immune pressure. Studies specifically focused on T cell-depleted haplo-HCTs are to date lacking,  
16 but available data from T cell replete platforms indicate that the frequency of HLA loss is directly  
17 associated to the number of T cells transferred as part of the graft or after that (19), thus suggesting  
18 that in "T cell naked" transplants HLA loss might be a rare event and relapses might have different  
19 underlying biology.

20 Interestingly, HLA loss relapse has also been reported in other transplantation settings, in particular  
21 after matched unrelated donor HCT (24–27). Although these reports originate from small cohorts of  
22 patients and therefore cannot provide an accurate estimate of the actual incidence of HLA loss in  
23 this setting. they appear to indicate a lower incidence of the phenomenon in this setting. We can  
24 speculate that this lower frequency might indicate that when donor-recipient incompatibilities are  
25 fewer T cell alloreactivity and GvL effect might be less pronouncedly focused against incompatible  
26 HLAs and possibly outperformed by immunodominant minor histocompatibility antigens, that in  
27 the unrelated setting are far more numerous than in allo-HCT from family donors.

28 It has already been stated how the occurrence of this genomic alteration greatly impairs T cell  
29 allorecognition, prompting the need for a more personalized clinical management of these relapses.  
30 As a consequence, the acute leukemia working party (ALWP) of the EBMT recently made  
31 recommendations for testing eventual HLA loss at the time of relapse before employing donor  
32 lymphocyte infusions (DLIs) (28). However, until recently, documentation of HLA loss at relapse  
33 required the presence of a considerable tumor burden to perform HLA typing of either unprocessed  
34 bone marrow samples or, when possible, sorted leukemic blasts (9). To overcome these limitations  
35 we recently developed "HLA-KMR", a rapid, reliable and economic assay based on quantitative  
36 PCR (qPCR) (29) that almost immediately became a commercially available diagnostic tool  
37 (GenDx, The Netherlands). The rationale of "HLA-KMR" is to combine the detection of non-HLA-  
38 polymorphisms together with ad hoc qPCR reactions targeting the most common HLA allele  
39 groups. Therefore, in "classical" relapses non-HLA and patient-specific HLA markers are  
40 concordantly positive, whereas the absence of HLA-specific signal indicates HLA loss relapse. This  
41 tool provides a sensitive method to detect HLA loss relapses event at early stages, allowing fast  
42 clinical decision-making and the use of a personalized therapeutic approach for every patient.

43 Finally, what should be the most appropriate therapeutic approach for HLA loss relapses occurring  
44 after haplo-HCT? Taking into consideration the mechanism and immunological consequences of  
45 this genomic alteration, a possible strategy could be a second haploidentical transplantation from an  
46 alternative donor, selected to target the remaining HLA haplotype. This originates a unique  
47 situation, where donor T cells still share one haplotype with non-hematopoietic tissues, while being  
48 fully mismatched with the leukemic blasts, possibly providing an even stronger GvL effect (30). As  
49 a proof of concept, this approach was the one associated with the longest survival after relapse for  
50 patients experiencing HLA loss at our center (19), and might explain the superior outcome  
51 described by Imus and collaborators upon choosing donors with a different HLA-haplotype for

1 second haplo-HCT (31). Unfortunately, a second allo-HCT is often not feasible in elderly or heavily  
2 pretreated patients, prompting further preclinical and clinical studies to treat HLA loss relapses  
3 using non HLA-restricted immunotherapy approaches, including bispecific antibodies and chimeric  
4 antigen receptor- (CAR-) modified T cells.

#### 5 6 Downregulation of HLA Class II molecules 7

8 Two very recent studies provided remarkable evidence that genomic haplotype loss is not the only  
9 strategy used by leukemic cells to alter their HLA asset and avoid detection by donor-derived T  
10 cells. In both studies, comparison of samples pairwise collected from patients before and after allo-  
11 HCT led to appreciate that in up to 40% of post-transplantation relapses the surface expression of  
12 HLA class II molecules (HLA-DR, -DQ and -DP) becomes virtually absent, and this translates in  
13 failure of donor T cells primed against the original disease to recognize the relapse variants (32,33).  
14 Supporting previous studies conducted in animal models (34), this evidence suggests that  
15 interactions between HLA class II molecules and CD4 T cells are necessary for a proficient GvL  
16 effect, and that this non redundant arm of the antitumor immunity represents a vulnerability that is  
17 easily exploited by leukemia to reemerge. It should be noted, however, that HLA Class II  
18 expression is also emerging as a relevant prognostic parameter in a number of other malignancies.  
19 HLA class II negativity has in fact been linked to unfavorable outcome in patients germinal center  
20 B-cell like diffuse large B cell lymphoma (35,36) and with microsatellite stable carcinomas (37). In  
21 a study performed on relapsed/refractory classical Hodgkin's lymphoma, in addition to the  
22 positivity for PD-L1, also high surface expression of HLA class II molecules correlated with a  
23 better response to the anti PD-1 monoclonal antibody nivolumab (38).

24 Coming back to leukemia post-transplantation relapses, similarly to the previously described  
25 genomic HLA loss mechanism, also in this case a higher dose of T cells infused with the graft is  
26 associated to a higher likelihood to experience also this modality of relapse (32). However,  
27 differently from haplotype loss, class II downregulation has to date been observed with similar  
28 frequencies in both HLA-compatible and incompatible transplants (32,33). This observation  
29 suggests that the driver of this event might not be alloreactivity toward incompatible HLA Class II  
30 molecules, but against their presented repertoire of tumor-specific antigens and minor  
31 histocompatibility antigens.

32 Of notice, in both studies that first described this immune escape modality, in-depth genetic  
33 profiling of the relapsed leukemia found no evidence of mutations in HLA genes or their regulators,  
34 arguing toward an epigenetic origin of the observed phenotype. Gene expression analysis,  
35 performed to assess the mechanism of HLA class II expression defects, revealed a significant  
36 downregulation of the major histocompatibility class II transactivator CIITA (*MHC2TA*) (32,33),  
37 which in some patients was linked to hypermethylation of its promoters (33). We further showed  
38 that this feature is stably maintained upon transplantation and serial passages in immune  
39 compromised mice, with levels of surface expression of HLA class II molecules in patient-derived  
40 xenografts (PDXs) perfectly mirroring those observed in the corresponding primary human samples  
41 (32).

42 Unexpectedly, however, when we infused donor-derived T cells to animals harboring the HLA class  
43 II-expressing diagnosis or the HLA class II-defective relapse, we observed that, although with a  
44 slower kinetics, also the latter was eventually recognized and eradicated. An in-depth study of this  
45 phenomenon showed that cross recognition of murine antigens by the infused T cells led to the  
46 release of high levels of interferon- $\gamma$  (IFN- $\gamma$ ) in the animal plasma, and that this was followed by the  
47 recovery of HLA class II expression on leukemic cells (32). These findings were also confirmed by  
48 *ex vivo* experiments in which post-transplantation leukemic blasts exposed to recombinant human  
49 IFN- $\gamma$  recovered HLA class II expression, and this in turn reconvened donor T cell-mediated  
50 recognition (32,33). From a translational perspective, these results imply that a proinflammatory

1 environment, driven by GvHD or recognition of antigens presented by HLA class I molecules,  
2 might actually revert this mechanism of relapse and re-establish a proficient antileukemic response.  
3 Whereas the description of deregulated HLA Class II expression as a mechanism of AML post-  
4 transplantation relapse is extremely recent, there are a number of other malignancies in which  
5 alterations in HLA Class II have been extensively investigated, and that might provide precious  
6 hints on the molecular driver of the phenomenon in AML. For instance, there have been several  
7 reports of HLA class II downregulation in lymphoma cells as a consequence of deletions and point  
8 mutations of HLA Class II genes and their regulators, including CIITA (35,36). Moreover, in  
9 lymphomas, CIITA has been reported to be a recurrent fusion partner of the programmed death-  
10 ligands *CD274/PD-L1* and *CD273/PD-L2*, leading to the downregulation of HLA class II genes and  
11 the upregulation of PD-L1 and PD-L2 (39,40). In addition, loss of HLA class II expression has also  
12 been linked to epigenetic silencing, as a consequence of mutations in epigenetic regulators (e.g.  
13 enhancer of zeste homolog 2, *EZH2*) or of hypermethylation or hypoacetylation of the promoters of  
14 HLA genes and/or CIITA (33,35,36,41). Finally, Tarafdar and colleagues also proposed a cytokine-  
15 mediated pathway of HLA class II silencing active in chronic myeloid leukemia: in this disease,  
16 tumor cells can produce anti-inflammatory cytokines including IL-4 (42) and TGF- $\beta$  (43) that  
17 downregulate the expression of CIITA, rendering themselves less immunogenic and susceptible to  
18 T cell recognition (42,44).

#### 20 Upregulation of T Cell Inhibitory Ligands

21  
22 While genomic and epigenetic alterations in HLA genes have all the final effect of turning tumor  
23 cells invisible to the donor-derived immune system, there is emerging evidence that leukemic cells  
24 can also hide in plain sight, using their encounter with T cells to transit inhibitory signals that stun  
25 and impair antigen-specific responses. A number of reports have in fact shown that over the course  
26 of treatments and in particular after allo-HCT, hematologic malignancies increase their expression  
27 of molecules that inhibit T cell responses or drive their exhaustion, including members of the  
28 programmed death-ligand family (32,45). In a recent study, retrospectively analyzing samples  
29 pairwise collected from AML patients at the time of diagnosis and at post-transplantation relapse,  
30 we showed increased expression of the inhibitory molecules PD-L1, CD276/B7-H3 and  
31 CD155/PVRL2 in up to 40% of cases of relapse. PD-L1 overexpression on AML blasts impaired  
32 donor T cell functions *ex vivo* and antileukemic responses could be partially restored upon  
33 treatment with anti-PD-L1 monoclonal antibody (32). It should be noted however that in most  
34 patients the landscape of expression of inhibitory ligands at time of relapse was quite composite,  
35 with high inter-patient variability, hinting to the fact that blocking a single interaction might yield  
36 limited clinical benefits, and efforts should rather be aimed at identifying and targeting a shared  
37 regulator of these molecules.

38 However, to date, little is known about the molecular drivers of this phenotype in the post-  
39 transplantation setting, and most of the currently available knowledge relates to PD-L1 and its  
40 regulation in other malignancies. Activation of aberrant janus kinase (JAK) signaling through  
41 9p24.1 amplification has been shown to be a potent driver of PD-L1 upregulation in Hodgkin's  
42 lymphoma (46). Also myeloproliferative neoplasms bearing the *JAK<sup>V617F</sup>* point mutation showed  
43 the same effect on PD-L1 expression (47). On the other hand, loss-of-function mutations in the  
44 JAK/STAT pathway observed in several other tumor types (e.g. melanoma), have been proved to be  
45 associated to resistance to PD-1/PD-L1 blockade (48–50). Also Myc-driven lymphomas display  
46 constitutive upregulation of inhibitory molecules: Myc oncogenic signaling has been shown in fact  
47 to increase the expression of PD-L1 and of the 'don't eat me' signal CD47 in tumor cells, impairing  
48 interactions with T lymphocytes and dendritic cells (51). Beside oncogenes driving PD-L1  
49 overexpression, also several epigenetic mechanisms have been reported. Expression of PD-L1 has  
50 been shown for instance to be inversely correlated with methylation of its promoter, and robustly  
51 induced upon treatment of tumor cells with hypomethylating agents (52). Also micro RNAs



1 (miRNAs), have been implicated in the regulation of PD-L1 expression by binding to the PD-L1  
2 mRNA and driving its degradation; in AML, for instance, the levels of miRNA-34a showed inverse  
3 correlation with PD-L1 expression (53). Another emerging layer of regulation of PD-L1 is  
4 represented by post-translational modifications, for instance through glycosylation of the mature  
5 protein (54).

6 In addition to all the tumor-intrinsic mechanisms of PD-L1 regulation mentioned in the previous  
7 paragraph, also pro-inflammatory molecules (e.g. IFN- $\gamma$ ) secreted in the tumor microenvironment  
8 can potently drive upregulation of PD-L1 on tumor cells (55). This might be extremely relevant in  
9 the setting of leukemia post-transplantation relapses, since, as discussed in the previous section,  
10 induction of a pro-inflammatory microenvironment conversely represents the key to revert  
11 epigenetic downregulation of HLA class II molecules. Indeed, when data regarding expression of  
12 HLA molecules and inhibitory ligands at relapse in our patient cohorts were plotted together, it  
13 appeared quite evidently that these two modalities of relapse are largely non-overlapping (32), and  
14 should prospectively be discriminated one from the other to enact the most appropriate salvage  
15 treatments.

16 Noticeably, the phenotypic features of T cells circulating in patients at the time of relapse mirror the  
17 changes observed in leukemic cells, with significant upregulation of inhibitory receptors in the  
18 patients whose leukemias express the respective ligands (32,56). Recent studies showed that  
19 expression of inhibitory receptors such as PD-1 on T lymphocytes can at least in part be prompted  
20 by the intense stimulation conveyed to the donor immune system upon transfer into an allogeneic  
21 environment (57), as suggested also by the observation of higher expression of inhibitory receptors  
22 on the T cells of patients who received haplo-HCTs (56). However, in-depth analysis of T cells  
23 from patients who did or did not experience relapse allowed the identification of specific exhaustion  
24 features in T cells from relapsing patients, with co-expression of multiple inhibitory receptors not  
25 only in terminally-differentiated effectors but also in early-differentiated memory stem and central  
26 memory T cells (56,58). The exhausted phenotype was particularly evident in the patients' bone  
27 marrow, where T cell-leukemia interactions are mainly expected to occur, and associated with a  
28 skewed T cell receptor (TCR) repertoire (56). Importantly, backtracking the clinical follow-up of  
29 patients who eventually relapsed, it was possible to identify the T cell exhaustion signature even  
30 months before relapse (32,56) and in patients who relapsed after sole chemotherapy (59),  
31 suggesting that upon further validation these features might be used as an indicator to guide pre-  
32-emptive therapeutic approaches.

### 33 34 **Tumor-Extrinsic Mechanisms of Relapse**

35  
36 Beside altering their features to increase aggressiveness and reduce immunogenicity, malignant  
37 cells can also accelerate disease progression by rewiring the microenvironment to their advantage,  
38 coopting the niche and the physiological mechanisms at the basis of immune tolerance. Mostly  
39 investigated in the context of solid tumors, interactions between cancer cells and the  
40 microenvironment are starting to gain more attention also in hematological diseases, and gain an  
41 additional layer of complexity upon allo-HCT, when the niche becomes an admixture of  
42 pathological and non-pathological elements of both host- and donor-origin.

43 One of the best characterized modalities employed by hematological tumors to alter the immune  
44 microenvironment that surrounds them is switching from the production of pro-inflammatory  
45 cytokines to the release of immunosuppressive molecules, including interleukin 10 and TGF-beta.  
46 For instance, it has been shown that during transformation, myeloid cells can reduce their  
47 production of granulocyte colony-stimulating factor (G-CSF), IL-15 and IFN- $\gamma$ . Defects in IFN- $\gamma$   
48 production have been correlated to a specific polymorphism, which has been also linked to clinical  
49 risk parameters (e.g. prednisone response) in patients affected by B-lineage acute lymphocytic  
50 leukemia (ALL) (60). Strongly produced by normal myeloid progenitors, the physiological function  
51 of IL-15 is to expand and activate effector T and NK cells (61) and to promote the generation of

1 memory stem T cell subset (62). Therefore, it is not difficult to understand why high levels of this  
2 cytokine in tumor microenvironment are unfavorable for leukemic cells. In post-transplantation  
3 setting, low plasma levels of IL-15 have been correlated to higher risk of relapse in patient affected  
4 by different hematological malignancies (63). One recently discovered mechanism at the basis of  
5 the reduced production of IL-15 by AML cells is the internal tandem duplication (ITD) of the FLT3  
6 tyrosine kinase (FLT3-ITD) (64).  
7 Even though in non-transplantation setting, the dysregulated effect of several metabolites has been  
8 shown to mediate immune suppression. The expression of indoleamine 2,3-dioxygenase-1 (IDO1)  
9 by leukemia cells was for instance correlated with unfavorable prognosis in childhood AML (65).  
10 IDO1 is the first actor of an enzymatic cascade resulting in the inhibition of T cell function and the  
11 T regulatory cell reprogramming (66). Moreover, AML exhibits the ability to block T cell function  
12 through the amino acid arginase which can also drive macrophages towards the suppressive M2-like  
13 phenotype (67). Other two enzymes that are gaining recent attention for their possible role in  
14 inducing leukemia immune escape are the ectonucleotidase CD73 (68) and the ectonucleoside  
15 triphosphate diphosphohydrolase-1 CD39 (69).  
16 Recently, moreover, studies conducted in solid tumors highlighted a major role of tumor-induced  
17 metabolic remodeling in altering T cell state and function. Specifically, Vodnala and colleagues  
18 revealed that the elevated presence of extracellular potassium in the tumor microenvironment can  
19 promote a state of functional starvation in tumor-specific T cells. The starvation response results in  
20 induction of autophagy and in epigenetic reprogramming, impairing T cell differentiation and  
21 function (70).

## 22 23 **Translating Relapse Biology Into Rationales for Treatment**

24  
25 The ideal strategies to treat relapse after allo-HCT should both exert a direct anti-tumor activity and  
26 enhance the alloreactive GvL effect of allogeneic T cells, sparing the risks of inducing significant  
27 cytopenias, immunosuppression or GvHD. Moreover, considering the numerous and complexly  
28 combined modalities of relapse that were summarized in previous section, it should be considered  
29 that ideally only using combinatorial therapies it might be possible to hit a target without exposing  
30 the flank to compensatory responses that ultimately select alternative mechanisms of escape.  
31 Here we summarize the most recent evidence about post-HCT relapse treatment modalities,  
32 categorizing strategies that rely on cellular therapies or that aim at boosting or redirecting the pre-  
33 existent donor-derived immune system.

### 34 35 Cellular therapies

36  
37 *Donor lymphocyte infusions.* One of the simplest and most intuitive ways to induce a GvL response  
38 after allogeneic HCT is to administer donor-lymphocyte infusions (DLIs). The main advantage of  
39 this strategy is the induction of a polyclonal T cell response able to target multiple antigens on  
40 malignant cells, reducing the risks of escaping T cell recognition just by loss of a single antigen.  
41 However, donor T cells may also recognize and attack non-hematopoietic tissues, with the risk of  
42 triggering GvHD.

43 As discussed in previous sections, when considering the therapeutic use of DLI for relapses after  
44 haplo-HCT, it is fundamental to rapidly determine if relapse is sustained by HLA loss immune-  
45 escape leukemia variants, that represent a clear counter indication to DLI administration. In fact, the  
46 genomic loss of the unshared HLA haplotype in leukemia cells not only renders them invisible to  
47 the major HLA alloreactivity exerted by infused T cells but also does not impact on their  
48 recognition of healthy tissues, leaving the risk of DLI-induced GvHD largely unaltered. For these  
49 reasons, upon documentation of HLA loss, other salvage options should be prioritized as treatment  
50 strategies (8,30).

1 Outside of this specific context, a considerable body of literature exists on the use of DLI as therapy  
2 of relapse after haplo-HCT. The first study after unmanipulated haplo-HCT performed under ATG-  
3 based GvHD prophylaxis utilized a median dose of donor T cells of  $0.6 \times 10^8$  CD3<sup>+</sup>/Kg, reporting  
4 significant risks of both severe acute GvHD (aGvHD, 30%) and chronic GvHD (cGvHD, 64%)  
5 (71). More recently, a study testing DLI after post-transplant cyclophosphamide (PTCy)-based  
6 GvHD prophylaxis, yielded a 30% complete remission (CR) rate, with a risk of developing grade  
7 III-IV aGvHD or cGvHD of 15% and 8%, respectively. In this trial, a dose of  $1 \times 10^6$  CD3<sup>+</sup>/Kg was  
8 considered a reasonable starting dose (72). Another study showed that escalating doses of DLI after  
9 PTCy-based haplo-HCT were accompanied by at least a 33% CR rate, a 14% risk of grade II-III  
10 aGvHD and no cases of grade III-IV aGvHD or cGvHD. In this study the initial administered DLI  
11 dose was  $1 \times 10^5$  CD3<sup>+</sup>/Kg in case of molecular relapse and higher (from  $1 \times 10^6$  rising to  $1 \times 10^7$   
12 CD3<sup>+</sup>/Kg) in case of hematological relapse (73).

13 Several studies also reported results from combinatorial administration of DLI and  
14 immunomodulating agents, with the aim of increasing the immunogenicity of tumor cells, rendering  
15 them more susceptible to DLI action. The diverse dose-schedules and time points of infusions  
16 preclude a clear guideline, but most trials employed a starting dose of  $1 \times 10^5$  CD3<sup>+</sup>/Kg, eventually  
17 escalating in the absence of GvHD development (72,74–82).

18  
19 *Second allogeneic transplantation.* Second allogeneic transplantation (allo-HCT2) to treat relapse  
20 after the first allo-HCT has recently gained more popularity thanks to the introduction of reduced-  
21 intensity conditioning and improvements of supportive therapies, that have significantly reduced  
22 toxicities after allo-HCT2, historically burdened by treatment-related mortality up to 40-50%  
23 (83,84). As in the case of DLI, when considering HCT2 for relapse after HLA-mismatched HCT, it  
24 is mandatory to discriminate whether relapse after the first transplant was classical or HLA loss.  
25 Especially in the second case, as mentioned above, selecting a second haploidentical donor with a  
26 different HLA haplotype provided some very promising preliminary results (31). Unfortunately, for  
27 all the studies on this subject, the inevitable selection bias of patients fit to receive a second  
28 conditioning and further transplantation must be taken into account, and clinical decisions must  
29 balance individual patient comorbidities and alternative therapeutic strategies.

30  
31 *Adoptive immunotherapy with genetically-redirected immune cells.* Over the last few years, a  
32 number of landmark studies have demonstrated the feasibility and efficacy of using gene therapy to  
33 redirect immune cells in a non HLA-restricted fashion against antigens of choice. The most striking  
34 example is provided by chimeric antigen receptor (CAR) T cells, that are capable of binding to the  
35 surface antigen of choice without the need for TCR-HLA interactions, thus representing a  
36 promising therapeutic option for patients relapsing with HLA loss or HLA downregulation.  
37 Moreover, CAR potent synthetic co-stimulatory domains may bypass the effect of the immune-  
38 suppressive signals expressed by tumor cells or microenvironment (85,86).

39 CAR T cells targeting CD19 are to date the best studied, and have demonstrated significant activity  
40 in chemotherapy refractory CLL, B-cell lymphomas and B-ALL in the autologous setting (87–92).  
41 There is also growing evidence of the efficacy of donor-origin CD19 CAR T cells in patients  
42 relapsing after allo-HCT (86,92–95) or even haplo-HCT (96,97). In this scenario, the infusion of  
43 allogeneic CAR T cells could carry the theoretical risk of GvHD: however, incidence of this  
44 fearsome complication in early trials was quite low, and an elegant study in mouse models showed  
45 that the CAR-driven and TCR-driven signal actually adds up, accelerating exhaustion and limiting  
46 alloactions (85). Still, a number of studies are focusing on the development of improved strategies  
47 to further enhance CAR T efficacy and persistence without risking to induce GvHD, such as by  
48 transducing recipient-derived donor T cells (97), by using genome editing approaches to knock out  
49 the endogenous TCR (85,98), or by modifying with the CAR different immune cells, less prone to  
50 induce GvHD (99–101).

51

1 Redirecting or Boosting the Donor-Derived Immune System

2  
3 *Bispecific antibodies.* Based on a principle similar to the one that guided the development of CAR T  
4 cells, also bispecific antibodies can enable redirection of immune cells towards malignant cells,  
5 forcing the formation of an immunological synapsis through the binding of an antigen expressed on  
6 effectors (such as CD3 on T cells or CD16 on NK cells) with one expressed by the tumor target  
7 (such as CD19 for lymphoid malignancies or CD33 for myeloid leukemias) (102,103). This results  
8 in the release of cytotoxic granules in close proximity to target cells, with the ultimate step of  
9 apoptosis induction and elimination, also fueled by inflammatory cytokines production and antigen  
10 spreading mechanisms (104). This strategy could be another useful way to circumvent HLA-  
11 restriction of TCR, with the potential added value of being readily available off-the-shelf and taking  
12 advantage of cells that are already circulating in the patient and tolerized against his healthy tissues.  
13 However, other immune-evasion mechanisms (related to the induction of inhibitory checkpoint  
14 molecules, the production of immunosuppressive cytokines or metabolites), have been shown to  
15 rapidly emerge upon treatment with bispecifics, suggesting that full exploitation of the anti-tumoral  
16 activity of these promising molecules could pass by enhancing costimulatory pathways or blocking  
17 immune checkpoints (105–110).

18  
19 *Epigenetic therapies.* The two commercially available hypomethylating agents (HMAs),  
20 azacytidine (Aza) and decitabine (DAC), are frequently used for post-HCT relapse treatment in  
21 AML or myelodysplastic syndromes (MDS). HMAs indirectly inhibit DNA methyltransferases  
22 significantly altering DNA methylation patterns with consequent induction of cell cycle arrest,  
23 DNA damage accumulation, apoptosis and differentiation (111–117). More recently, also immune-  
24 related effects of hypomethylating agents have been described. In particular, Aza stimulates  
25 antitumor immunity inducing the upregulation on leukemic cells of leukemia-associated and minor-  
26 histocompatibility antigens, including PRAME, MAGE-A, NY-ESO1 and HA-1 (114,115,118–  
27 121). Aza can also lead to increased HLA class-I and II expression and modulate tumor-  
28 immunogenicity through the upregulation on leukemic cell surface of costimulatory molecules,  
29 such as CD80, CD86, ULBP and MIC-A (122). Among the reported effects, HMAs can induce the  
30 expression of important players involved in anti-viral responses, including IFN- $\gamma$  and cytokines.  
31 Interestingly, Aza can also promote upregulation of endogenous retroviral elements on tumor cells,  
32 inducing a “viral mimicry” response that ultimately results in the induction of anti-tumor immunity  
33 (123–125). However, Aza can also act as a double-edged sword, since it can upregulate PD-1, PD-  
34 L1/L2 and CTLA-4 inhibitory pathways and induce the expansion of regulatory T cells (116),  
35 potentially hampering the intensity and duration of cytotoxic T cell responses and facilitating the  
36 tolerization and exhaustion of tumor-specific T cells (126,127).

37 Due to their reported immune-related effects, HMAs have been frequently employed in  
38 combination with DLI. To date, we have data on more than 600 patients undergoing salvage  
39 regimens including Aza and DLI, reporting very variable results in terms of clinical outcome (128–  
40 133). Because of the heterogeneous results obtained so far and lack of consent on treatment  
41 schedules, two retrospective surveys have analyzed the correlates of efficacy of Aza+DLI  
42 combinations in more homogeneous cohorts, one facilitated by the German Cooperative Transplant  
43 Study Group (130) and the other by the European Society for Blood and Marrow Transplantation  
44 (EBMT) (131). These studies reported that patients that benefitted the most from Aza+DLI  
45 combinatorial approach were those who presented low disease burden at the time of relapse  
46 (molecular relapse or less than 20% blasts in bone marrow) and those with a longer interval from  
47 allo-HCT to relapse. These variables can be adopted to predict treatment response through a score  
48 assignment (AZA relapse prognostic score – ARPS), even if an independent cohort validation is  
49 still lacking (131).

50 Histone acetylation is another epigenetic mechanism of immune regulation, balanced between the  
51 activity of histone acetyl-transferases (HATs) and histone deacetylases (HDACs) (134). HDAC

1 inhibitors, such as vorinostat and panobinostat, have been associated with the upregulation of  
2 major-histocompatibility and co-stimulatory molecules on AML cell surface through the induction  
3 of an open and readable structure of chromatin (135,136). To date, two prospective phase I/II trials  
4 of post-HCT therapy with panobinostat for AML/MDS patients, alone or in combination with DAC  
5 and DLI, have been reported (137,138).

6  
7 *Immune checkpoint blockade.* Immune checkpoint inhibition through the administration of  
8 monoclonal antibodies that target the PD-1/PD-L1 and CTLA-4/B7 axis is emerging as an attractive  
9 strategy to enhance alloreactive T cell function and rewire the immunosuppressive milieu in which  
10 disease relapse often occurs (139–141). Clinical trials exploring the efficacy of immune checkpoint  
11 inhibitors after allo-HCT have shown some promise using the anti-CTLA4 antibody ipilimumab  
12 (142,143) and more modest results using PD-1 inhibitors in diseases other than Hodgkin's  
13 lymphoma (144–147). Moreover, post-transplantation treatment with checkpoint inhibitors appears  
14 to be associated to a significant risk of severe and treatment-refractory GvHD and immune-related  
15 events (148).

16 However, as the balance of stimulatory and inhibitory signals determines the magnitude of immune  
17 responses against tumor cells, combining HMAs and immune-checkpoint blockade therapies may  
18 represent an interesting approach to release the “break” signal received by tumor-reactive immune  
19 cells (149–151). A phase II trial exploring the combination of the anti-PD1 monoclonal antibody  
20 Nivolumab and Aza in relapsed AML, reported an overall response rate of 33% (152), and several  
21 ongoing trials are assessing the efficacy of HMAs and immune checkpoint inhibitor combinations,  
22 some of them recruiting also post-transplantation relapsed patients (NCT02890329, NCT02845297,  
23 NCT02996474, NCT02397720).

24  
25 *Cytokine therapies.* The use of exogenous cytokines to boost or restore T and NK cell impaired  
26 effector functions have been object of intense investigation in cancer therapy, and especially in the  
27 field of hematological malignancies. Interleukin 2 (IL2), IFN- $\alpha$  and IL-15 are the best studied. IL-  
28 2 has been shown to stimulate the anti-tumor effect of lymphocytes, polarizing helper T cell  
29 responses towards type 1, and exerting both immune-enhancing and immune-suppressive activities  
30 (153–155). However, application of IL-2 monotherapy against AML has yielded very limited  
31 clinical benefit, both for the induction of regulatory T cells that impaired antileukemic activity and  
32 for the rapid drop in effector functions due to T cells terminal differentiation and exhaustion (156–  
33 159). IFN- $\alpha$ , on the other hand, exerts pleiotropic functions, since it has a direct antileukemic effect  
34 and also possesses immune-stimulatory properties, leading to dendritic cells stimulation,  
35 enhancement of NK-cell cytotoxicity and sensitization of T cells to other inflammatory cytokines,  
36 such as IL-2 (160–163). Despite these theoretical premises, IFN- $\alpha$  failed to demonstrate significant  
37 activity as single agent in post-transplantation relapse (164–167). As previously described, IL-15 is  
38 a potent immunostimulatory cytokine, that potentiates both T and NK cell immune responses,  
39 promoting the generation and maintenance of high-avidity and long-lived CD8<sup>+</sup> memory T cells.  
40 IL-15 also prevents activation-induced T cell death, and does not induce the expansion of  
41 immunosuppressive regulatory T cells (62,168–172). A phase I trial testing the IL-15 super-agonist  
42 complex ALT-803 in patients relapsing after allo-HCT showed a very promising response rate  
43 (19% of evaluable patients), correlated to the expansion of both NK and T cells (173). Recently,  
44 novel approaches to vehicle high concentration of cytokines to the tumor site and reduce their  
45 systemic effects are emerging, including gene therapy "trojan horse" strategies (174) and the use of  
46 lipid nanoparticles to convey to the tumor site mRNAs encoding cytokines (175).

47  
48 *Immune-related effects of targeted therapies.* The growing armamentarium of targeted therapies is  
49 providing new evidence that beside their direct effects, some of them can also promote antitumor  
50 immunity. A recent work testing the effect of the tyrosine-kinase inhibitor sorafenib in a mouse  
51 model of leukemia showed that the treatment increased the production of IL-15 by leukemic cells

1 bearing FLT3-ITD. This resulted in enhanced CD8<sup>+</sup> T cell effector function (via their increased  
2 metabolic capacity) and leukemia eradication. Mechanistically, sorafenib induced transcription of  
3 IL-15 acting by inhibition of the transcription factor ATF435 that in turn suppresses the IL-15  
4 activator interferon regulatory factor 7 (IRF7) (64).  
5 Another example of tyrosine-kinase inhibitor exerting “off-target” immune mechanisms is  
6 represented by imatinib, which is indicated in Philadelphia-positive (Ph<sup>+</sup>) leukemias, namely  
7 chronic myeloid leukemia (CML) and Ph<sup>+</sup> acute lymphoblastic leukemia (ALL). Allogeneic HCT  
8 remains the only curative option for Ph<sup>+</sup> ALL and advanced-phase CML, and there is general  
9 consensus about imatinib administration following HCT (176,177). In addition to targeting  
10 Bcr/Abl1 and KIT oncogene products, imatinib modulates the proliferation, polarization and  
11 functionality of different subsets of myeloid and lymphoid cells (178–181). This modulation can  
12 exert both inhibitory or stimulating immune effects. Among the inhibitory effects are the inhibition  
13 of dendritic cells expansion, resulting in less efficient priming of cytotoxic T cells (182–185), the  
14 polarization towards a M2-like anti-inflammatory phenotype of tumor-associated macrophages  
15 (186,187), the reduction of effector-cytokine production by CD4<sup>+</sup> T cells in response to TCR-  
16 signaling (188,189) and the reduction of IgM-producing memory B-cell frequency (190–192). On  
17 the other hand, imatinib has also stimulating effect such as: decreased expression of 2,3-IDO and  
18 consequent apoptosis in regulatory T cells (193,194), reduction of myeloid-derived suppressor cells,  
19 thus restoring a T cell cytotoxic response (195–197), reduced secretion of VEGF with subsequent  
20 antiangiogenic effect (198,199), polarization towards a higher Th1/Th2 ratio (200–202); and  
21 preferential expression of activating NK receptors (203).

22

### 23 **Conclusions and Perspectives**

24

25 The landscape of allo-HCT, and haplo-HCT in particular, is rapidly changing, with multiple  
26 platforms able to achieve remarkable long-term outcome results. The reduced risk of treatment-  
27 related toxicities and mortality has also opened the possibility to implement innovative  
28 pharmacological or cellular therapies in the post-transplantation follow-up, transforming the  
29 perception of allo-HCT from that of a final consolidation therapy to a "platform" to build on. In this  
30 new scenario, it will be of utmost relevance to associate to the analysis of clinical endpoints also a  
31 detailed study on how changing the recipe of allo-HCT influences its immunobiology. It is now  
32 evident that the success or failure of transplantation is linked to our ability to take full advantage of  
33 the many features endowed in the immune system and to combine them with targeted therapies to  
34 hit as many tumor targets as possible, reducing the chances of selection of escape variants.  
35 Generation of new quantitative systems to map tumor immune targets, characterization of the tumor  
36 immune microenvironment by multi-omics single-cell technologies and generation of more refined  
37 humanized mouse model to mirror allo-HCT all appear promising avenues to advance knowledge  
38 on allo-HCT immunobiology, and, ultimately, to generate new rationales to further improve clinical  
39 outcome.

40

1 **AUTHOR CONTRIBUTIONS**

2 P.E.R., V.G. and F.L. reviewed available literature and drafted the paper. F.C. and L.V. provided  
3 critical discussion and revised the manuscript draft.

4

5 **CONFLICT OF INTEREST**

6 LV received research funding from GenDx (Utrecht, The Netherlands) and Moderna Therapeutics  
7 (Cambridge, MA, USA). All other authors declare no competing financial interests.

8

9 **ACKNOWLEDGMENTS**

10 The Authors would like to thank all members of the Unit of Immunogenetics, Leukemia Genomics  
11 and Immunobiology, IRCCS San Raffaele Scientific Institute, Milano for critical reading and  
12 discussion on the text. L.V. would like to acknowledge support from the Italian Ministry of Health  
13 (RF-2011-02351998, RF-2011-02348034 and TRANSCAN HLALOSS), the Associazione Italiana  
14 per la Ricerca sul Cancro (Start-Up Grant #14162 and IG #22197) and the DKMS Mechtild Harf  
15 Foundation (DKMS Mechtild Harf Research Grant 2015).

1 **REFERENCES**

- 2 1. Kanakry CG, Fuchs EJ, Luznik L. Modern approaches to HLA-haploidentical blood or  
3 marrow transplantation. *Nat Rev Clin Oncol* (2016) **13**:10–24.  
4 doi:10.1038/nrclinonc.2015.128
- 5 2. Patriarca F, Luznik L, Medeot M, Zecca M, Bacigalupo A, Di Bartolomeo P, Arcese W,  
6 Corradini P, Ciceri F, Vago L, et al. Experts' considerations on HLA-haploidentical stem  
7 cell transplantation. *Eur J Haematol* (2014) **93**:187–197. doi:10.1111/ejh.12322
- 8 3. Passweg JR, Baldomero H, Basak GW, Chabannon C, Corbacioglu S, Duarte R, Kuball J,  
9 Lankester A, Montoto S, de Latour RP, et al. The EBMT activity survey report 2017: a  
10 focus on allogeneic HCT for nonmalignant indications and on the use of non-HCT cell  
11 therapies. *Bone Marrow Transplant* (2019) doi:10.1038/s41409-019-0465-9
- 12 4. D'Souza A, Fretham C. D'Souza A, Fretham C. Current Uses and Outcomes of Hematopoietic  
13 Cell Transplantation (HCT): CIBMTR Summary Slides, 2018. Available at  
14 <https://www.cibmtr.org>.
- 15 5. Horowitz MM, Gale RP, Sondel PM, Goldman JM, Kersey J, Kolb HJ, Rimm AA, Ringdén O,  
16 Rozman C, Speck B. Graft-versus-leukemia reactions after bone marrow transplantation.  
17 *Blood* (1990) **75**:555–562.
- 18 6. Masuda K, Hiraki A, Fujii N, Watanabe T, Tanaka M, Matsue K, Ogama Y, Ouchida M,  
19 Shimizu K, Ikeda K, et al. Loss or down-regulation of HLA class I expression at the allelic  
20 level in freshly isolated leukemic blasts. *Cancer Sci* (2007) **98**:102–108.  
21 doi:10.1111/j.1349-7006.2006.00356.x
- 22 7. Brouwer RE, van der Heiden P, Schreuder GMT, Mulder A, Datema G, Anholts JDH,  
23 Willemze R, Claas FHJ, Falkenburg JHF. Loss or downregulation of HLA class I expression  
24 at the allelic level in acute leukemia is infrequent but functionally relevant, and can be  
25 restored by interferon. *Hum Immunol* (2002) **63**:200–210.
- 26 8. Vago L, Perna SK, Zanussi M, Mazzi B, Barlassina C, Stanghellini MTL, Perrelli NF,  
27 Cosentino C, Torri F, Angius A, et al. Loss of mismatched HLA in leukemia after stem-cell  
28 transplantation. *N Engl J Med* (2009) **361**:478–488. doi:10.1056/NEJMoa0811036
- 29 9. Mazzi B, Clerici TD, Zanussi M, Lupo Stanghellini MT, Vago L, Sironi E, Peccatori J, Bernardi  
30 M, Carrera P, Palini A, et al. Genomic typing for patient-specific human leukocyte antigen-  
31 alleles is an efficient tool for relapse detection of high-risk hematopoietic malignancies  
32 after stem cell transplantation from alternative donors. *Leukemia* (2008) **22**:2119–2122.  
33 doi:10.1038/leu.2008.98
- 34 10. Makishima H, Maciejewski JP. Pathogenesis and consequences of uniparental disomy in  
35 cancer. *Clin Cancer Res* (2011) **17**:3913–3923. doi:10.1158/1078-0432.CCR-10-2900
- 36 11. O'Keefe C, McDevitt MA, Maciejewski JP. Copy neutral loss of heterozygosity: a novel  
37 chromosomal lesion in myeloid malignancies. *Blood* (2010) **115**:2731–2739.  
38 doi:10.1182/blood-2009-10-201848
- 39 12. Tuna M, Knuutila S, Mills GB. Uniparental disomy in cancer. *Trends in Molecular Medicine*  
40 (2009) **15**:120–128. doi:10.1016/j.molmed.2009.01.005



- 1 13. Villalobos IB, Takahashi Y, Akatsuka Y, Muramatsu H, Nishio N, Hama A, Yagasaki H, Saji H,  
2 Kato M, Ogawa S, et al. Relapse of leukemia with loss of mismatched HLA resulting from  
3 uniparental disomy after haploidentical hematopoietic stem cell transplantation. *Blood*  
4 (2010) **115**:3158–3161. doi:10.1182/blood-2009-11-254284
- 5 14. Kärre K, Ljunggren HG, Piontek G, Kiessling R. Selective rejection of H-2-deficient  
6 lymphoma variants suggests alternative immune defence strategy. *Nature* (1986)  
7 **319**:675–678. doi:10.1038/319675a0
- 8 15. Barrett J, Blazar BR. Genetic Trickery — Escape of Leukemia from Immune Attack. *New*  
9 *England Journal of Medicine* (2009) **361**:524–525. doi:10.1056/NEJMe0903177
- 10 16. Gupta M, Raghavan M, Gale RE, Chelala C, Allen C, Molloy G, Chaplin T, Linch DC, Cazier J-B,  
11 Young BD. Novel regions of acquired uniparental disomy discovered in acute myeloid  
12 leukemia. *Genes Chromosomes Cancer* (2008) **47**:729–739. doi:10.1002/gcc.20573
- 13 17. Dubois V, Sloan-Béna F, Cesbron A, Hepkema BG, Gagne K, Gimelli S, Heim D, Tichelli A,  
14 Delaunay J, Drouet M, et al. Pretransplant HLA mistyping in diagnostic samples of acute  
15 myeloid leukemia patients due to acquired uniparental disomy. *Leukemia* (2012)  
16 **26**:2079–2085. doi:10.1038/leu.2012.68
- 17 18. Pereira S, Vayntrub T, Hiraki DD, Cherry AM, Arai S, Dvorak CC, Grumet FC. Short tandem  
18 repeat and human leukocyte antigen mutations or losses confound engraftment and  
19 typing analysis in hematopoietic stem cell transplants. *Human Immunology* (2011)  
20 **72**:503–509. doi:10.1016/j.humimm.2011.03.003
- 21 19. Crucitti L, Crocchiolo R, Toffalori C, Mazzi B, Greco R, Signori A, Sizzano F, Chiesa L, Zino E,  
22 Lupo Stanghellini MT, et al. Incidence, risk factors and clinical outcome of leukemia  
23 relapses with loss of the mismatched HLA after partially incompatible hematopoietic  
24 stem cell transplantation. *Leukemia* (2015) **29**:1143–1152. doi:10.1038/leu.2014.314
- 25 20. McCurdy SR, Iglehart BS, Batista DA, Gocke CD, Ning Y, Knaus HA, Jackson AM, Leffell MS,  
26 Luznik L, Gojo I. Loss of the mismatched human leukocyte antigen haplotype in two acute  
27 myelogenous leukemia relapses after haploidentical bone marrow transplantation with  
28 post-transplantation cyclophosphamide. *Leukemia* (2016) **30**:2102–2106.  
29 doi:10.1038/leu.2016.144
- 30 21. Grosso D, Johnson E, Colombe B, Alpdogan O, Carabasi M, Filicko-O'Hara J, Gaballa S,  
31 Kasner M, Klumpp T, Martinez-Outschoorn U, et al. Acquired uniparental disomy in  
32 chromosome 6p as a feature of relapse after T-cell replete haploidentical hematopoietic  
33 stem cell transplantation using cyclophosphamide tolerization. *Bone Marrow Transplant*  
34 (2017) **52**:615–619. doi:10.1038/bmt.2016.324
- 35 22. Peccatori J, Forcina A, Clerici D, Crocchiolo R, Vago L, Stanghellini MTL, Noviello M,  
36 Messina C, Crotta A, Assanelli A, et al. Sirolimus-based graft-versus-host disease  
37 prophylaxis promotes the in vivo expansion of regulatory T cells and permits peripheral  
38 blood stem cell transplantation from haploidentical donors. *Leukemia* (2015) **29**:396–  
39 405. doi:10.1038/leu.2014.180
- 40 23. Cieri N, Greco R, Crucitti L, Morelli M, Giglio F, Levati G, Assanelli A, Carrabba MG, Bellio L,  
41 Milani R, et al. Post-transplantation Cyclophosphamide and Sirolimus after  
42 Haploidentical Hematopoietic Stem Cell Transplantation Using a Treosulfan-based

- 1 Myeloablative Conditioning and Peripheral Blood Stem Cells. *Biol Blood Marrow*  
2 *Transplant* (2015) **21**:1506–1514. doi:10.1016/j.bbmt.2015.04.025
- 3 24. Toffalori C, Cavattoni I, Deola S, Mastaglio S, Giglio F, Mazzi B, Assanelli A, Peccatori J,  
4 Bordignon C, Bonini C, et al. Genomic loss of patient-specific HLA in acute myeloid  
5 leukemia relapse after well-matched unrelated donor HSCT. *Blood* (2012) **119**:4813–  
6 4815. doi:10.1182/blood-2012-02-411686
- 7 25. Waterhouse M, Pfeifer D, Pantic M, Emmerich F, Bertz H, Finke J. Genome-wide profiling in  
8 AML patients relapsing after allogeneic hematopoietic cell transplantation. *Biol Blood*  
9 *Marrow Transplant* (2011) **17**:1450-1459.e1. doi:10.1016/j.bbmt.2011.07.012
- 10 26. Hamdi A, Cao K, Poon LM, Aung F, Kornblau S, Fernandez Vina MA, Champlin RE, Ciurea  
11 SO. Are changes in HLA Ags responsible for leukemia relapse after HLA-matched  
12 allogeneic hematopoietic SCT? *Bone Marrow Transplant* (2015) **50**:411–413.  
13 doi:10.1038/bmt.2014.285
- 14 27. Jan M, Leventhal MJ, Morgan EA, Wengrod JC, Nag A, Drinan SD, Wollison BM, Ducar MD,  
15 Thorner AR, Leppanen S, et al. Recurrent genetic HLA loss in AML relapsed after matched  
16 unrelated allogeneic hematopoietic cell transplantation. *Blood Adv* (2019) **3**:2199–2204.  
17 doi:10.1182/bloodadvances.2019000445
- 18 28. Tsirigotis P, Byrne M, Schmid C, Baron F, Ciceri F, Esteve J, Gorin NC, Giebel S, Mohty M,  
19 Savani BN, et al. Relapse of AML after hematopoietic stem cell transplantation: methods  
20 of monitoring and preventive strategies. A review from the ALWP of the EBMT. *Bone*  
21 *Marrow Transplantation* (2016) **51**:1431–1438. doi:10.1038/bmt.2016.167
- 22 29. Ahci M, Toffalori C, Bouwmans E, Crivello P, Brambati C, Pultrone C, Stempelmann K, Bost  
23 D, Mazzi B, Beelen DW, et al. A new tool for rapid and reliable diagnosis of HLA loss  
24 relapses after HSCT. *Blood* (2017) **130**:1270–1273. doi:10.1182/blood-2017-05-784306
- 25 30. Vago L, Ciceri F. Choosing the Alternative. *Biology of Blood and Marrow Transplantation*  
26 (2017) **23**:1813–1814. doi:10.1016/j.bbmt.2017.09.009
- 27 31. Imus PH, Blackford AL, Bettinotti M, Iglehart B, Dietrich A, Tucker N, Symons H, Cooke KR,  
28 Luznik L, Fuchs EJ, et al. Major Histocompatibility Mismatch and Donor Choice for Second  
29 Allogeneic Bone Marrow Transplantation. *Biol Blood Marrow Transplant* (2017)  
30 **23**:1887–1894. doi:10.1016/j.bbmt.2017.07.014
- 31 32. Toffalori C, Zito L, Gambacorta V, Riba M, Oliveira G, Bucci G, Barcella M, Spinelli O, Greco  
32 R, Crucitti L, et al. Immune signature drives leukemia escape and relapse after  
33 hematopoietic cell transplantation. *Nat Med* (2019) **25**:603–611. doi:10.1038/s41591-  
34 019-0400-z
- 35 33. Christopher MJ, Petti AA, Rettig MP, Miller CA, Chendamarai E, Duncavage EJ, Klco JM,  
36 Helton NM, O’Laughlin M, Fronick CC, et al. Immune Escape of Relapsed AML Cells after  
37 Allogeneic Transplantation. *N Engl J Med* (2018) **379**:2330–2341.  
38 doi:10.1056/NEJMoa1808777
- 39 34. Stevanović S, van Schie MLJ, Griffioen M, Falkenburg JH. HLA-class II disparity is necessary  
40 for effective T cell mediated Graft-versus-Leukemia effects in NOD/scid mice engrafted

- 1 with human acute lymphoblastic leukemia. *Leukemia* (2013) **27**:985–987.  
2 doi:10.1038/leu.2012.270
- 3 35. Ennishi D, Takata K, Béguelin W, Duns G, Mottok A, Farinha P, Bashashati A, Saberi S,  
4 Boyle M, Meissner B, et al. Molecular and Genetic Characterization of MHC Deficiency  
5 Identifies EZH2 as Therapeutic Target for Enhancing Immune Recognition. *Cancer Discov*  
6 (2019) **9**:546–563. doi:10.1158/2159-8290.CD-18-1090
- 7 36. Rimsza LM, Roberts RA, Miller TP, Unger JM, LeBlanc M, Braziel RM, Weisenberger DD,  
8 Chan WC, Muller-Hermelink HK, Jaffe ES, et al. Loss of MHC class II gene and protein  
9 expression in diffuse large B-cell lymphoma is related to decreased tumor  
10 immunosurveillance and poor patient survival regardless of other prognostic factors: a  
11 follow-up study from the Leukemia and Lymphoma Molecular Profiling Project. *Blood*  
12 (2004) **103**:4251–4258. doi:10.1182/blood-2003-07-2365
- 13 37. Løvig T, Andersen SN, Thorstensen L, Diep CB, Meling GI, Lothe RA, Rognum TO. Strong  
14 HLA-DR expression in microsatellite stable carcinomas of the large bowel is associated  
15 with good prognosis. *Br J Cancer* (2002) **87**:756–762. doi:10.1038/sj.bjc.6600507
- 16 38. Roemer MGM, Redd RA, Cader FZ, Pak CJ, Abdelrahman S, Ouyang J, Sasse S, Younes A,  
17 Fanale M, Santoro A, et al. Major Histocompatibility Complex Class II and Programmed  
18 Death Ligand 1 Expression Predict Outcome After Programmed Death 1 Blockade in  
19 Classic Hodgkin Lymphoma. *J Clin Oncol* (2018) **36**:942–950.  
20 doi:10.1200/JCO.2017.77.3994
- 21 39. Steidl C, Shah SP, Woolcock BW, Rui L, Kawahara M, Farinha P, Johnson NA, Zhao Y,  
22 Telenius A, Neriah SB, et al. MHC class II transactivator CIITA is a recurrent gene fusion  
23 partner in lymphoid cancers. *Nature* (2011) **471**:377–381. doi:10.1038/nature09754
- 24 40. Rimsza LM, Roberts RA, Campo E, Grogan TM, Bea S, Salaverria I, Zettl A, Rosenwald A, Ott  
25 G, Muller-Hermelink HK, et al. Loss of major histocompatibility class II expression in non-  
26 immune-privileged site diffuse large B-cell lymphoma is highly coordinated and not due  
27 to chromosomal deletions. *Blood* (2006) **107**:1101–1107. doi:10.1182/blood-2005-04-  
28 1510
- 29 41. Cycon KA, Mulvaney K, Rimsza LM, Persky D, Murphy SP. Histone deacetylase inhibitors  
30 activate CIITA and MHC class II antigen expression in diffuse large B-cell lymphoma.  
31 *Immunology* (2013) **140**:259–272. doi:10.1111/imm.12136
- 32 42. Tarafdar A, Hopcroft LEM, Gallipoli P, Pellicano F, Cassels J, Hair A, Korfi K, Jørgensen HG,  
33 Vetrie D, Holyoake TL, et al. CML cells actively evade host immune surveillance through  
34 cytokine-mediated downregulation of MHC-II expression. *Blood* (2017) **129**:199–208.  
35 doi:10.1182/blood-2016-09-742049
- 36 43. Naka K, Hoshii T, Muraguchi T, Tadokoro Y, Ooshio T, Kondo Y, Nakao S, Motoyama N,  
37 Hirao A. TGF-beta-FOXO signalling maintains leukaemia-initiating cells in chronic  
38 myeloid leukaemia. *Nature* (2010) **463**:676–680. doi:10.1038/nature08734
- 39 44. Lee YJ, Han Y, Lu HT, Nguyen V, Qin H, Howe PH, Hocevar BA, Boss JM, Ransohoff RM,  
40 Benveniste EN. TGF-beta suppresses IFN-gamma induction of class II MHC gene  
41 expression by inhibiting class II transactivator messenger RNA expression. *J Immunol*  
42 (1997) **158**:2065–2075.

- 1 45. Norde WJ, Maas F, Hobo W, Korman A, Quigley M, Kester MGD, Hebeda K, Falkenburg JHF,  
2 Schaap N, de Witte TM, et al. PD-1/PD-L1 interactions contribute to functional T-cell  
3 impairment in patients who relapse with cancer after allogeneic stem cell  
4 transplantation. *Cancer Res* (2011) **71**:5111–5122. doi:10.1158/0008-5472.CAN-11-  
5 0108
- 6 46. Green MR, Monti S, Rodig SJ, Juszczynski P, Currie T, O'Donnell E, Chapuy B, Takeyama K,  
7 Neuberg D, Golub TR, et al. Integrative analysis reveals selective 9p24.1 amplification,  
8 increased PD-1 ligand expression, and further induction via JAK2 in nodular sclerosing  
9 Hodgkin lymphoma and primary mediastinal large B-cell lymphoma. *Blood* (2010)  
10 **116**:3268–3277. doi:10.1182/blood-2010-05-282780
- 11 47. Prestipino A, Emhardt AJ, Aumann K, O'Sullivan D, Gorantla SP, Duquesne S, Melchinger W,  
12 Braun L, Vuckovic S, Boerries M, et al. Oncogenic JAK2V617F causes PD-L1 expression,  
13 mediating immune escape in myeloproliferative neoplasms. *Sci Transl Med* (2018) **10**:  
14 doi:10.1126/scitranslmed.aam7729
- 15 48. Shin DS, Zaretsky JM, Escuin-Ordinas H, Garcia-Diaz A, Hu-Lieskovan S, Kalbasi A, Grasso  
16 CS, Hugo W, Sandoval S, Torrejon DY, et al. Primary Resistance to PD-1 Blockade  
17 Mediated by JAK1/2 Mutations. *Cancer Discov* (2017) **7**:188–201. doi:10.1158/2159-  
18 8290.CD-16-1223
- 19 49. Zaretsky JM, Garcia-Diaz A, Shin DS, Escuin-Ordinas H, Hugo W, Hu-Lieskovan S, Torrejon  
20 DY, Abril-Rodriguez G, Sandoval S, Barthly L, et al. Mutations Associated with Acquired  
21 Resistance to PD-1 Blockade in Melanoma. *N Engl J Med* (2016) **375**:819–829.  
22 doi:10.1056/NEJMoa1604958
- 23 50. Sucker A, Zhao F, Pieper N, Heeke C, Maltaner R, Stadtler N, Real B, Bielefeld N, Howe S,  
24 Weide B, et al. Acquired IFN $\gamma$  resistance impairs anti-tumor immunity and gives rise to T-  
25 cell-resistant melanoma lesions. *Nat Commun* (2017) **8**:15440.  
26 doi:10.1038/ncomms15440
- 27 51. Casey SC, Tong L, Li Y, Do R, Walz S, Fitzgerald KN, Gouw AM, Baylot V, Gütgemann I, Eilers  
28 M, et al. MYC regulates the antitumor immune response through CD47 and PD-L1. *Science*  
29 (2016) **352**:227–231. doi:10.1126/science.aac9935
- 30 52. Wrangle J, Wang W, Koch A, Easwaran H, Mohammad HP, Vendetti F, Vancracking W,  
31 Demeyer T, Du Z, Parsana P, et al. Alterations of immune response of Non-Small Cell Lung  
32 Cancer with Azacytidine. *Oncotarget* (2013) **4**:2067–2079.  
33 doi:10.18632/oncotarget.1542
- 34 53. Wang X, Li J, Dong K, Lin F, Long M, Ouyang Y, Wei J, Chen X, Weng Y, He T, et al. Tumor  
35 suppressor miR-34a targets PD-L1 and functions as a potential immunotherapeutic  
36 target in acute myeloid leukemia. *Cell Signal* (2015) **27**:443–452.  
37 doi:10.1016/j.cellsig.2014.12.003
- 38 54. Li C-W, Lim S-O, Xia W, Lee H-H, Chan L-C, Kuo C-W, Khoo K-H, Chang S-S, Cha J-H, Kim T,  
39 et al. Glycosylation and stabilization of programmed death ligand-1 suppresses T-cell  
40 activity. *Nat Commun* (2016) **7**:12632. doi:10.1038/ncomms12632
- 41 55. Liu J, Hamrouni A, Wolowiec D, Coiteux V, Kuliczowski K, Hetuin D, Saudemont A,  
42 Quesnel B. Plasma cells from multiple myeloma patients express B7-H1 (PD-L1) and

- 1 increase expression after stimulation with IFN- $\gamma$  and TLR ligands via a MyD88-,  
2 TRAF6-, and MEK-dependent pathway. *Blood* (2007) **110**:296–304. doi:10.1182/blood-  
3 2006-10-051482
- 4 56. Noviello M, Manfredi F, Ruggiero E, Perini T, Oliveira G, Cortesi F, De Simone P, Toffalori C,  
5 Gambacorta V, Greco R, et al. Bone marrow central memory and memory stem T-cell  
6 exhaustion in AML patients relapsing after HSCT. *Nat Commun* (2019) **10**:1065.  
7 doi:10.1038/s41467-019-08871-1
- 8 57. Simonetta F, Pradier A, Bosshard C, Masouridi-Levrat S, Dantin C, Koutsi A, Tirefort Y,  
9 Roosnek E, Chalandon Y. Dynamics of Expression of Programmed Cell Death Protein-1  
10 (PD-1) on T Cells After Allogeneic Hematopoietic Stem Cell Transplantation. *Front*  
11 *Immunol* (2019) **10**:1034. doi:10.3389/fimmu.2019.01034
- 12 58. Hutten TJA, Norde WJ, Woestenenk R, Wang RC, Maas F, Kester M, Falkenburg JHF,  
13 Berglund S, Luznik L, Jansen JH, et al. Increased Coexpression of PD-1, TIGIT, and KLRG-1  
14 on Tumor-Reactive CD8+ T Cells During Relapse after Allogeneic Stem Cell  
15 Transplantation. *Biol Blood Marrow Transplant* (2018) **24**:666–677.  
16 doi:10.1016/j.bbmt.2017.11.027
- 17 59. Knaus HA, Berglund S, Hackl H, Blackford AL, Zeidner JF, Montiel-Esparza R,  
18 Mukhopadhyay R, Vanura K, Blazar BR, Karp JE, et al. Signatures of CD8+ T cell  
19 dysfunction in AML patients and their reversibility with response to chemotherapy. *JCI*  
20 *Insight* (2018) **3**: doi:10.1172/jci.insight.120974
- 21 60. Cloppenburg T, Stanulla M, Zimmermann M, Schrappe M, Welte K, Klein C.  
22 Immunosurveillance of childhood ALL: polymorphic interferon-gamma alleles are  
23 associated with age at diagnosis and clinical risk groups. *Leukemia* (2005) **19**:44–48.  
24 doi:10.1038/sj.leu.2403553
- 25 61. Colpitts SL, Stonier SW, Stoklasek TA, Root SH, Aguila HL, Schluns KS, Lefrançois L.  
26 Transcriptional regulation of IL-15 expression during hematopoiesis. *J Immunol* (2013)  
27 **191**:3017–3024. doi:10.4049/jimmunol.1301389
- 28 62. Cieri N, Camisa B, Cocchiarella F, Forcato M, Oliveira G, Provasi E, Bondanza A, Bordignon  
29 C, Peccatori J, Ciceri F, et al. IL-7 and IL-15 instruct the generation of human memory  
30 stem T cells from naive precursors. *Blood* (2013) **121**:573–584. doi:10.1182/blood-  
31 2012-05-431718
- 32 63. Thiant S, Yakoub-Agha I, Magro L, Trauet J, Coiteux V, Jouet J-P, Dessaint J-P, Labalette M.  
33 Plasma levels of IL-7 and IL-15 in the first month after myeloablative BMT are predictive  
34 biomarkers of both acute GVHD and relapse. *Bone Marrow Transplant* (2010) **45**:1546–  
35 1552. doi:10.1038/bmt.2010.13
- 36 64. Mathew NR, Baumgartner F, Braun L, O'Sullivan D, Thomas S, Waterhouse M, Müller TA,  
37 Hanke K, Taromi S, Apostolova P, et al. Sorafenib promotes graft-versus-leukemia  
38 activity in mice and humans through IL-15 production in FLT3-ITD-mutant leukemia  
39 cells. *Nat Med* (2018) **24**:282–291. doi:10.1038/nm.4484
- 40 65. Folgiero V, Goffredo BM, Filippini P, Masetti R, Bonanno G, Caruso R, Bertaina V,  
41 Mastronuzzi A, Gaspari S, Zecca M, et al. Indoleamine 2,3-dioxygenase 1 (IDO1) activity in

- 1 leukemia blasts correlates with poor outcome in childhood acute myeloid leukemia.  
2 *Oncotarget* (2014) **5**:2052–2064. doi:10.18632/oncotarget.1504
- 3 66. Munn DH, Sharma MD, Baban B, Harding HP, Zhang Y, Ron D, Mellor AL. GCN2 kinase in T  
4 cells mediates proliferative arrest and anergy induction in response to indoleamine 2,3-  
5 dioxygenase. *Immunity* (2005) **22**:633–642. doi:10.1016/j.immuni.2005.03.013
- 6 67. Mussai F, De Santo C, Abu-Dayyeh I, Booth S, Quek L, McEwen-Smith RM, Qureshi A, Dazzi  
7 F, Vyas P, Cerundolo V. Acute myeloid leukemia creates an arginase-dependent  
8 immunosuppressive microenvironment. *Blood* (2013) **122**:749–758. doi:10.1182/blood-  
9 2013-01-480129
- 10 68. Serra S, Horenstein AL, Vaisitti T, Brusa D, Rossi D, Laurenti L, D’Arena G, Coscia M,  
11 Tripodo C, Inghirami G, et al. CD73-generated extracellular adenosine in chronic  
12 lymphocytic leukemia creates local conditions counteracting drug-induced cell death.  
13 *Blood* (2011) **118**:6141–6152. doi:10.1182/blood-2011-08-374728
- 14 69. Dulphy N, Henry G, Hemon P, Khaznadar Z, Dombret H, Boissel N, Bensussan A, Toubert A.  
15 Contribution of CD39 to the immunosuppressive microenvironment of acute myeloid  
16 leukaemia at diagnosis. *Br J Haematol* (2014) **165**:722–725. doi:10.1111/bjh.12774
- 17 70. Vodnala SK, Eil R, Kishton RJ, Sukumar M, Yamamoto TN, Ha N-H, Lee P-H, Shin M, Patel SJ,  
18 Yu Z, et al. T cell stemness and dysfunction in tumors are triggered by a common  
19 mechanism. *Science* (2019) **363**: doi:10.1126/science.aau0135
- 20 71. Huang X-J, Liu D-H, Liu K-Y, Xu L-P, Chen H, Han W. Donor lymphocyte infusion for the  
21 treatment of leukemia relapse after HLA-mismatched/haploidentical T-cell-replete  
22 hematopoietic stem cell transplantation. *Haematologica* (2007) **92**:414–417.  
23 doi:10.3324/haematol.10570
- 24 72. Zeidan AM, Forde PM, Symons H, Chen A, Smith BD, Pratz K, Carraway H, Gladstone DE,  
25 Fuchs EJ, Luznik L, et al. HLA-haploidentical donor lymphocyte infusions for patients  
26 with relapsed hematologic malignancies after related HLA-haploidentical bone marrow  
27 transplantation. *Biol Blood Marrow Transplant* (2014) **20**:314–318.  
28 doi:10.1016/j.bbmt.2013.11.020
- 29 73. Ghiso A, Raiola AM, Gualandi F, Dominiotto A, Varaldo R, Van Lint MT, Bregante S, Di  
30 Grazia C, Lamparelli T, Galaverna F, et al. DLI after haploidentical BMT with post-  
31 transplant CY. *Bone Marrow Transplant* (2015) **50**:56–61. doi:10.1038/bmt.2014.217
- 32 74. Huang X-J, Liu D-H, Liu K-Y, Xu L-P, Chen Y-H, Wang Y, Han W, Chen H. Modified donor  
33 lymphocyte infusion after HLA-mismatched/haploidentical T cell-replete hematopoietic  
34 stem cell transplantation for prophylaxis of relapse of leukemia in patients with  
35 advanced leukemia. *J Clin Immunol* (2008) **28**:276–283. doi:10.1007/s10875-007-9166-  
36 z
- 37 75. Jedlickova Z, Schmid C, Koenecke C, Hertenstein B, Baurmann H, Schwerdtfeger R, Tischer  
38 J, Kolb H-J, Schleuning M. Long-term results of adjuvant donor lymphocyte transfusion in  
39 AML after allogeneic stem cell transplantation. *Bone Marrow Transplant* (2016) **51**:663–  
40 667. doi:10.1038/bmt.2015.234

- 1 76. Schmid C, Labopin M, Schaap N, Veelken H, Schleuning M, Stadler M, Finke J, Hurst E,  
2 Baron F, Ringden O, et al. Prophylactic donor lymphocyte infusion after allogeneic stem  
3 cell transplantation in acute leukaemia - a matched pair analysis by the Acute Leukaemia  
4 Working Party of EBMT. *Br J Haematol* (2019) **184**:782–787. doi:10.1111/bjh.15691
- 5 77. Rettinger E, Willasch AM, Kreyenberg H, Borkhardt A, Holter W, Kremens B, Strahm B,  
6 Woessmann W, Mauz-Koerholz C, Gruhn B, et al. Preemptive immunotherapy in  
7 childhood acute myeloid leukemia for patients showing evidence of mixed chimerism  
8 after allogeneic stem cell transplantation. *Blood* (2011) **118**:5681–5688.  
9 doi:10.1182/blood-2011-04-348805
- 10 78. Yan C-H, Liu D-H, Liu K-Y, Xu L-P, Liu Y-R, Chen H, Han W, Wang Y, Qin Y-Z, Huang X-J. Risk  
11 stratification-directed donor lymphocyte infusion could reduce relapse of standard-risk  
12 acute leukemia patients after allogeneic hematopoietic stem cell transplantation. *Blood*  
13 (2012) **119**:3256–3262. doi:10.1182/blood-2011-09-380386
- 14 79. Mo X-D, Zhang X-H, Xu L-P, Wang Y, Yan C-H, Chen H, Chen Y-H, Han W, Wang F-R, Wang J-  
15 Z, et al. Comparison of outcomes after donor lymphocyte infusion with or without prior  
16 chemotherapy for minimal residual disease in acute leukemia/myelodysplastic  
17 syndrome after allogeneic hematopoietic stem cell transplantation. *Ann Hematol* (2017)  
18 **96**:829–838. doi:10.1007/s00277-017-2960-7
- 19 80. Schmid C, Labopin M, Nagler A, Bornhäuser M, Finke J, Fassas A, Volin L, Gürman G,  
20 Maertens J, Bordigoni P, et al. Donor lymphocyte infusion in the treatment of first  
21 hematological relapse after allogeneic stem-cell transplantation in adults with acute  
22 myeloid leukemia: a retrospective risk factors analysis and comparison with other  
23 strategies by the EBMT Acute Leukemia Working Party. *J Clin Oncol* (2007) **25**:4938–  
24 4945. doi:10.1200/JCO.2007.11.6053
- 25 81. Roux C, Tifratene K, Socié G, Galambrun C, Bertrand Y, Rialland F, Jubert C, Pochon C,  
26 Paillard C, Sirvent A, et al. Outcome after failure of allogeneic hematopoietic stem cell  
27 transplantation in children with acute leukemia: a study by the société Francophone de  
28 greffe de moelle et de thérapie cellulaire (SFGM-TC). *Bone Marrow Transplant* (2017)  
29 **52**:678–682. doi:10.1038/bmt.2016.360
- 30 82. Miyamoto T, Fukuda T, Nakashima M, Henzan T, Kusakabe S, Kobayashi N, Sugita J, Mori T,  
31 Kurokawa M, Mori S-I. Donor Lymphocyte Infusion for Relapsed Hematological  
32 Malignancies after Unrelated Allogeneic Bone Marrow Transplantation Facilitated by the  
33 Japan Marrow Donor Program. *Biol Blood Marrow Transplant* (2017) **23**:938–944.  
34 doi:10.1016/j.bbmt.2017.02.012
- 35 83. Michallet M, Tanguy ML, Socié G, Thiébaud A, Belhabri A, Milpied N, Reiffers J, Kuentz M,  
36 Cahn JY, Blaise D, et al. Second allogeneic haematopoietic stem cell transplantation in  
37 relapsed acute and chronic leukaemias for patients who underwent a first allogeneic  
38 bone marrow transplantation: a survey of the Société Française de Greffe de moelle  
39 (SFGM). *Br J Haematol* (2000) **108**:400–407.
- 40 84. Radich JP, Sanders JE, Buckner CD, Martin PJ, Petersen FB, Bensinger W, McDonald GB,  
41 Mori M, Schoch G, Hansen JA. Second allogeneic marrow transplantation for patients with  
42 recurrent leukemia after initial transplant with total-body irradiation-containing  
43 regimens. *J Clin Oncol* (1993) **11**:304–313. doi:10.1200/JCO.1993.11.2.304

- 1 85. Ghosh A, Smith M, James SE, Davila ML, Velardi E, Argyropoulos KV, Gunset G, Perna F,  
2 Kreines FM, Levy ER, et al. Donor CD19 CAR T cells exert potent graft-versus-lymphoma  
3 activity with diminished graft-versus-host activity. *Nat Med* (2017) **23**:242–249.  
4 doi:10.1038/nm.4258
- 5 86. Smith M, Zakrzewski J, James S, Sadelain M. Posttransplant chimeric antigen receptor  
6 therapy. *Blood* (2018) **131**:1045–1052. doi:10.1182/blood-2017-08-752121
- 7 87. Porter DL, Levine BL, Kalos M, Bagg A, June CH. Chimeric antigen receptor-modified T cells  
8 in chronic lymphoid leukemia. *N Engl J Med* (2011) **365**:725–733.  
9 doi:10.1056/NEJMoa1103849
- 10 88. Kochenderfer JN, Dudley ME, Feldman SA, Wilson WH, Spaner DE, Maric I, Stetler-  
11 Stevenson M, Phan GQ, Hughes MS, Sherry RM, et al. B-cell depletion and remissions of  
12 malignancy along with cytokine-associated toxicity in a clinical trial of anti-CD19  
13 chimeric-antigen-receptor-transduced T cells. *Blood* (2012) **119**:2709–2720.  
14 doi:10.1182/blood-2011-10-384388
- 15 89. Grupp SA, Kalos M, Barrett D, Aplenc R, Porter DL, Rheingold SR, Teachey DT, Chew A,  
16 Hauck B, Wright JF, et al. Chimeric antigen receptor-modified T cells for acute lymphoid  
17 leukemia. *N Engl J Med* (2013) **368**:1509–1518. doi:10.1056/NEJMoa1215134
- 18 90. Schuster SJ, Svoboda J, Chong EA, Nasta SD, Mato AR, Anak Ö, Brogdon JL, Pruteanu-  
19 Malinici I, Bhoj V, Landsburg D, et al. Chimeric Antigen Receptor T Cells in Refractory B-  
20 Cell Lymphomas. *N Engl J Med* (2017) **377**:2545–2554. doi:10.1056/NEJMoa1708566
- 21 91. Schuster SJ, Bishop MR, Tam CS, Waller EK, Borchmann P, McGuirk JP, Jäger U, Jaglowski S,  
22 Andreadis C, Westin JR, et al. Tisagenlecleucel in Adult Relapsed or Refractory Diffuse  
23 Large B-Cell Lymphoma. *N Engl J Med* (2019) **380**:45–56. doi:10.1056/NEJMoa1804980
- 24 92. Park JH, Rivière I, Gonen M, Wang X, Sénéchal B, Curran KJ, Sauter C, Wang Y, Santomaso  
25 B, Mead E, et al. Long-Term Follow-up of CD19 CAR Therapy in Acute Lymphoblastic  
26 Leukemia. *N Engl J Med* (2018) **378**:449–459. doi:10.1056/NEJMoa1709919
- 27 93. Kochenderfer JN, Dudley ME, Carpenter RO, Kassim SH, Rose JJ, Telford WG, Hakim FT,  
28 Halverson DC, Fowler DH, Hardy NM, et al. Donor-derived CD19-targeted T cells cause  
29 regression of malignancy persisting after allogeneic hematopoietic stem cell  
30 transplantation. *Blood* (2013) **122**:4129–4139. doi:10.1182/blood-2013-08-519413
- 31 94. Brudno JN, Somerville RPT, Shi V, Rose JJ, Halverson DC, Fowler DH, Gea-Banacloche JC,  
32 Pavletic SZ, Hickstein DD, Lu TL, et al. Allogeneic T Cells That Express an Anti-CD19  
33 Chimeric Antigen Receptor Induce Remissions of B-Cell Malignancies That Progress After  
34 Allogeneic Hematopoietic Stem-Cell Transplantation Without Causing Graft-Versus-Host  
35 Disease. *J Clin Oncol* (2016) **34**:1112–1121. doi:10.1200/JCO.2015.64.5929
- 36 95. Kebriaei P, Singh H, Huls MH, Figliola MJ, Bassett R, Olivares S, Jena B, Dawson MJ,  
37 Kumaresan PR, Su S, et al. Phase I trials using Sleeping Beauty to generate CD19-specific  
38 CAR T cells. *J Clin Invest* (2016) **126**:3363–3376. doi:10.1172/JCI86721
- 39 96. Jia H, Wang Z, Wang Y, Liu Y, Dai H, Tong C, Guo Y, Guo B, Ti D, Han X, et al. Haploidentical  
40 CD19/CD22 bispecific CAR-T cells induced MRD-negative remission in a patient with



- 1 relapsed and refractory adult B-ALL after haploidentical hematopoietic stem cell  
2 transplantation. *J Hematol Oncol* (2019) **12**:57. doi:10.1186/s13045-019-0741-6
- 3 97. Hu Y, Wang J, Wei G, Yu J, Luo Y, Shi J, Wu W, Zhao K, Xiao L, Zhang Y, et al. A retrospective  
4 comparison of allogenic and autologous chimeric antigen receptor T cell therapy  
5 targeting CD19 in patients with relapsed/refractory acute lymphoblastic leukemia. *Bone*  
6 *Marrow Transplant* (2019) **54**:1208–1217. doi:10.1038/s41409-018-0403-2
- 7 98. Eyquem J, Mansilla-Soto J, Giavridis T, van der Stegen SJC, Hamieh M, Cunanan KM, Odak A,  
8 Gönen M, Sadelain M. Targeting a CAR to the TRAC locus with CRISPR/Cas9 enhances  
9 tumour rejection. *Nature* (2017) **543**:113–117. doi:10.1038/nature21405
- 10 99. Rotolo A, Caputo VS, Holubova M, Baxan N, Dubois O, Chaudhry MS, Xiao X, Goudevenou K,  
11 Pitcher DS, Petevi K, et al. Enhanced Anti-lymphoma Activity of CAR19-iNKT Cells  
12 Underpinned by Dual CD19 and CD1d Targeting. *Cancer Cell* (2018) **34**:596-610.e11.  
13 doi:10.1016/j.ccell.2018.08.017
- 14 100. Liu E, Tong Y, Dotti G, Shaim H, Savoldo B, Mukherjee M, Orange J, Wan X, Lu X, Reynolds  
15 A, et al. Cord blood NK cells engineered to express IL-15 and a CD19-targeted CAR show  
16 long-term persistence and potent antitumor activity. *Leukemia* (2018) **32**:520–531.  
17 doi:10.1038/leu.2017.226
- 18 101. Sebestyen Z, Prinz I, Déchanet-Merville J, Silva-Santos B, Kuball J. Translating  
19 gammadelta ( $\gamma\delta$ ) T cells and their receptors into cancer cell therapies. *Nat Rev Drug*  
20 *Discov* (2019) doi:10.1038/s41573-019-0038-z
- 21 102. Offner S, Hofmeister R, Romaniuk A, Kufer P, Baeuerle PA. Induction of regular cytolytic T  
22 cell synapses by bispecific single-chain antibody constructs on MHC class I-negative  
23 tumor cells. *Mol Immunol* (2006) **43**:763–771. doi:10.1016/j.molimm.2005.03.007
- 24 103. Zhukovsky EA, Morse RJ, Maus MV. Bispecific antibodies and CARs: generalized  
25 immunotherapeutics harnessing T cell redirection. *Curr Opin Immunol* (2016) **40**:24–35.  
26 doi:10.1016/j.coi.2016.02.006
- 27 104. Haas C, Krinner E, Brischwein K, Hoffmann P, Lutterbüse R, Schlereth B, Kufer P,  
28 Baeuerle PA. Mode of cytotoxic action of T cell-engaging BiTE antibody MT110.  
29 *Immunobiology* (2009) **214**:441–453. doi:10.1016/j.imbio.2008.11.014
- 30 105. Hornig N, Reinhardt K, Kermer V, Kontermann RE, Müller D. Evaluating combinations of  
31 costimulatory antibody-ligand fusion proteins for targeted cancer immunotherapy.  
32 *Cancer Immunol Immunother* (2013) **62**:1369–1380. doi:10.1007/s00262-013-1441-7
- 33 106. Hornig N, Kermer V, Frey K, Diebolder P, Kontermann RE, Müller D. Combination of a  
34 bispecific antibody and costimulatory antibody-ligand fusion proteins for targeted  
35 cancer immunotherapy. *J Immunother* (2012) **35**:418–429.  
36 doi:10.1097/CJI.0b013e3182594387
- 37 107. Arndt C, Feldmann A, von Bonin M, Cartellieri M, Ewen E-M, Koristka S, Michalk I,  
38 Stamova S, Berndt N, Gocht A, et al. Costimulation improves the killing capability of T  
39 cells redirected to tumor cells expressing low levels of CD33: description of a novel  
40 modular targeting system. *Leukemia* (2014) **28**:59–69. doi:10.1038/leu.2013.243

- 1 108. Köhnke T, Krupka C, Tischer J, Knösel T, Subklewe M. Increase of PD-L1 expressing B-  
2 precursor ALL cells in a patient resistant to the CD19/CD3-bispecific T cell engager  
3 antibody blinatumomab. *J Hematol Oncol* (2015) **8**:111. doi:10.1186/s13045-015-0213-6
- 4 109. Laszlo GS, Gudgeon CJ, Harrington KH, Walter RB. T-cell ligands modulate the cytolytic  
5 activity of the CD33/CD3 BiTE antibody construct, AMG 330. *Blood Cancer J* (2015)  
6 **5**:e340. doi:10.1038/bcj.2015.68
- 7 110. Yano H, Thakur A, Tomaszewski EN, Choi M, Deol A, Lum LG. Ipilimumab augments  
8 antitumor activity of bispecific antibody-armed T cells. *J Transl Med* (2014) **12**:191.  
9 doi:10.1186/1479-5876-12-191
- 10 111. Frikeche J, Clavert A, Delaunay J, Brissot E, Grégoire M, Gaugler B, Mohty M. Impact of the  
11 hypomethylating agent 5-azacytidine on dendritic cells function. *Exp Hematol* (2011)  
12 **39**:1056–1063. doi:10.1016/j.exphem.2011.08.004
- 13 112. Pinto A, Maio M, Attadia V, Zappacosta S, Cimino R. Modulation of HLA-DR antigens  
14 expression in human myeloid leukaemia cells by cytarabine and 5-aza-2'-deoxycytidine.  
15 *Lancet* (1984) **2**:867–868. doi:10.1016/s0140-6736(84)90900-0
- 16 113. Flotho C, Claus R, Batz C, Schneider M, Sandrock I, Ihde S, Plass C, Niemeyer CM, Lübbert  
17 M. The DNA methyltransferase inhibitors azacitidine, decitabine and zebularine exert  
18 differential effects on cancer gene expression in acute myeloid leukemia cells. *Leukemia*  
19 (2009) **23**:1019–1028. doi:10.1038/leu.2008.397
- 20 114. Atanackovic D, Luetkens T, Kloth B, Fuchs G, Cao Y, Hildebrandt Y, Meyer S, Bartels K,  
21 Reinhard H, Lajmi N, et al. Cancer-testis antigen expression and its epigenetic modulation  
22 in acute myeloid leukemia. *Am J Hematol* (2011) **86**:918–922. doi:10.1002/ajh.22141
- 23 115. Goodyear O, Agathangelou A, Novitzky-Basso I, Siddique S, McSkeane T, Ryan G, Vyas P,  
24 Cavenagh J, Stankovic T, Moss P, et al. Induction of a CD8+ T-cell response to the MAGE  
25 cancer testis antigen by combined treatment with azacitidine and sodium valproate in  
26 patients with acute myeloid leukemia and myelodysplasia. *Blood* (2010) **116**:1908–  
27 1918. doi:10.1182/blood-2009-11-249474
- 28 116. Goodyear OC, Dennis M, Jilani NY, Loke J, Siddique S, Ryan G, Nunnick J, Khanum R,  
29 Raghavan M, Cook M, et al. Azacitidine augments expansion of regulatory T cells after  
30 allogeneic stem cell transplantation in patients with acute myeloid leukemia (AML).  
31 *Blood* (2012) **119**:3361–3369. doi:10.1182/blood-2011-09-377044
- 32 117. Sánchez-Abarca LI, Gutierrez-Cosio S, Santamaría C, Caballero-Velazquez T, Blanco B,  
33 Herrero-Sánchez C, García JL, Carrancio S, Hernández-Campo P, González FJ, et al.  
34 Immunomodulatory effect of 5-azacytidine (5-azaC): potential role in the transplantation  
35 setting. *Blood* (2010) **115**:107–121. doi:10.1182/blood-2009-03-210393
- 36 118. Almstedt M, Blagitko-Dorfs N, Duque-Afonso J, Karbach J, Pfeifer D, Jäger E, Lübbert M.  
37 The DNA demethylating agent 5-aza-2'-deoxycytidine induces expression of NY-ESO-1  
38 and other cancer/testis antigens in myeloid leukemia cells. *Leuk Res* (2010) **34**:899–905.  
39 doi:10.1016/j.leukres.2010.02.004
- 40 119. Guo ZS, Hong JA, Irvine KR, Chen GA, Spiess PJ, Liu Y, Zeng G, Wunderlich JR, Nguyen DM,  
41 Restifo NP, et al. De novo induction of a cancer/testis antigen by 5-aza-2'-deoxycytidine

- 1       augments adoptive immunotherapy in a murine tumor model. *Cancer Res* (2006)  
2       **66**:1105–1113. doi:10.1158/0008-5472.CAN-05-3020
- 3   120. Weber J, Salgaller M, Samid D, Johnson B, Herlyn M, Lassam N, Treisman J, Rosenberg SA.  
4       Expression of the MAGE-1 tumor antigen is up-regulated by the demethylating agent 5-  
5       aza-2'-deoxycytidine. *Cancer Res* (1994) **54**:1766–1771.
- 6   121. Dubovsky JA, McNeel DG, Powers JJ, Gordon J, Sotomayor EM, Pinilla-Ibarz JA. Treatment  
7       of chronic lymphocytic leukemia with a hypomethylating agent induces expression of  
8       NXF2, an immunogenic cancer testis antigen. *Clin Cancer Res* (2009) **15**:3406–3415.  
9       doi:10.1158/1078-0432.CCR-08-2099
- 10  122. Fonsatti E, Nicolay HJM, Sigalotti L, Calabrò L, Pezzani L, Colizzi F, Altomonte M,  
11       Guidoboni M, Marincola FM, Maio M. Functional up-regulation of human leukocyte  
12       antigen class I antigens expression by 5-aza-2'-deoxycytidine in cutaneous melanoma:  
13       immunotherapeutic implications. *Clin Cancer Res* (2007) **13**:3333–3338.  
14       doi:10.1158/1078-0432.CCR-06-3091
- 15  123. Chiappinelli KB, Strissel PL, Desrichard A, Li H, Henke C, Akman B, Hein A, Rote NS, Cope  
16       LM, Snyder A, et al. Inhibiting DNA Methylation Causes an Interferon Response in Cancer  
17       via dsRNA Including Endogenous Retroviruses. *Cell* (2015) **162**:974–986.  
18       doi:10.1016/j.cell.2015.07.011
- 19  124. Roulois D, Loo Yau H, Singhania R, Wang Y, Danesh A, Shen SY, Han H, Liang G, Jones PA,  
20       Pugh TJ, et al. DNA-Demethylating Agents Target Colorectal Cancer Cells by Inducing  
21       Viral Mimicry by Endogenous Transcripts. *Cell* (2015) **162**:961–973.  
22       doi:10.1016/j.cell.2015.07.056
- 23  125. Parker BS, Rautela J, Hertzog PJ. Antitumour actions of interferons: implications for  
24       cancer therapy. *Nat Rev Cancer* (2016) **16**:131–144. doi:10.1038/nrc.2016.14
- 25  126. Yang H, Bueso-Ramos C, DiNardo C, Estecio MR, Davanlou M, Geng Q-R, Fang Z, Nguyen  
26       M, Pierce S, Wei Y, et al. Expression of PD-L1, PD-L2, PD-1 and CTLA4 in myelodysplastic  
27       syndromes is enhanced by treatment with hypomethylating agents. *Leukemia* (2014)  
28       **28**:1280–1288. doi:10.1038/leu.2013.355
- 29  127. Ørskov AD, Treppendahl MB, Skovbo A, Holm MS, Friis LS, Hokland M, Grønbaek K.  
30       Hypomethylation and up-regulation of PD-1 in T cells by azacytidine in MDS/AML  
31       patients: A rationale for combined targeting of PD-1 and DNA methylation. *Oncotarget*  
32       (2015) **6**:9612–9626. doi:10.18632/oncotarget.3324
- 33  128. Jabbour E, Giralt S, Kantarjian H, Garcia-Manero G, Jagasia M, Kebriaei P, de Padua L,  
34       Shpall EJ, Champlin R, de Lima M. Low-dose azacitidine after allogeneic stem cell  
35       transplantation for acute leukemia. *Cancer* (2009) **115**:1899–1905.  
36       doi:10.1002/cncr.24198
- 37  129. Schroeder T, Czibere A, Platzbecker U, Bug G, Uharek L, Luft T, Giagounidis A, Zohren F,  
38       Bruns I, Wolschke C, et al. Azacitidine and donor lymphocyte infusions as first salvage  
39       therapy for relapse of AML or MDS after allogeneic stem cell transplantation. *Leukemia*  
40       (2013) **27**:1229–1235. doi:10.1038/leu.2013.7

- 1 130. Schroeder T, Rachlis E, Bug G, Stelljes M, Klein S, Steckel NK, Wolf D, Ringhoffer M,  
2 Czibere A, Nachtkamp K, et al. Treatment of acute myeloid leukemia or myelodysplastic  
3 syndrome relapse after allogeneic stem cell transplantation with azacitidine and donor  
4 lymphocyte infusions--a retrospective multicenter analysis from the German Cooperative  
5 Transplant Study Group. *Biol Blood Marrow Transplant* (2015) **21**:653–660.  
6 doi:10.1016/j.bbmt.2014.12.016
- 7 131. Craddock C, Labopin M, Robin M, Finke J, Chevallier P, Yakoub-Agha I, Bourhis JH,  
8 Sengelov H, Blaise D, Luft T, et al. Clinical activity of azacitidine in patients who relapse  
9 after allogeneic stem cell transplantation for acute myeloid leukemia. *Haematologica*  
10 (2016) **101**:879–883. doi:10.3324/haematol.2015.140996
- 11 132. Ghobadi A, Choi J, Fiala MA, Fletcher T, Liu J, Eissenberg LG, Abboud C, Cashen A, Vij R,  
12 Schroeder MA, et al. Phase I study of azacitidine following donor lymphocyte infusion for  
13 relapsed acute myeloid leukemia post allogeneic stem cell transplantation. *Leuk Res*  
14 (2016) **49**:1–6. doi:10.1016/j.leukres.2016.07.010
- 15 133. Woo J, Deeg HJ, Storer B, Yeung C, Fang M, Mielcarek M, Scott BL. Factors Determining  
16 Responses to Azacitidine in Patients with Myelodysplastic Syndromes and Acute Myeloid  
17 Leukemia with Early Post-Transplantation Relapse: A Prospective Trial. *Biol Blood*  
18 *Marrow Transplant* (2017) **23**:176–179. doi:10.1016/j.bbmt.2016.10.016
- 19 134. Ward PS, Patel J, Wise DR, Abdel-Wahab O, Bennett BD, Collier HA, Cross JR, Fantin VR,  
20 Hedvat CV, Perl AE, et al. The common feature of leukemia-associated IDH1 and IDH2  
21 mutations is a neomorphic enzyme activity converting alpha-ketoglutarate to 2-  
22 hydroxyglutarate. *Cancer Cell* (2010) **17**:225–234. doi:10.1016/j.ccr.2010.01.020
- 23 135. Choi SW, Braun T, Chang L, Ferrara JLM, Pawarode A, Magenau JM, Hou G, Beumer JH,  
24 Levine JE, Goldstein S, et al. Vorinostat plus tacrolimus and mycophenolate to prevent  
25 graft-versus-host disease after related-donor reduced-intensity conditioning allogeneic  
26 haemopoietic stem-cell transplantation: a phase 1/2 trial. *Lancet Oncol* (2014) **15**:87–95.  
27 doi:10.1016/S1470-2045(13)70512-6
- 28 136. Choi SW, Gatzka E, Hou G, Sun Y, Whitfield J, Song Y, Oravec-Wilson K, Tawara I, Dinarello  
29 CA, Reddy P. Histone deacetylase inhibition regulates inflammation and enhances Tregs  
30 after allogeneic hematopoietic cell transplantation in humans. *Blood* (2015) **125**:815–  
31 819. doi:10.1182/blood-2014-10-605238
- 32 137. Bug G, Burchert A, Wagner E-M, Kröger N, Berg T, Güller S, Metzelder SK, Wolf A,  
33 Hünecke S, Bader P, et al. Phase I/II study of the deacetylase inhibitor panobinostat after  
34 allogeneic stem cell transplantation in patients with high-risk MDS or AML (PANOBEST  
35 trial). *Leukemia* (2017) **31**:2523–2525. doi:10.1038/leu.2017.242
- 36 138. Early Post-Transplant Epigenetic Therapy By Panobinostat and Decitabine Followed By  
37 Donor Lymphocyte Infusion (DLI): Interim Results of the HOVON-116 Phase I/II  
38 Feasibility Study in Poor-Risk AML Recipients of Allogeneic Stem Cell Transplantation  
39 (alloHS... | Blood Journal. Available at:  
40 <http://www.bloodjournal.org/content/128/22/832> [Accessed June 29, 2019]
- 41 139. Greil R, Hutterer E, Hartmann TN, Pleyer L. Reactivation of dormant anti-tumor  
42 immunity - a clinical perspective of therapeutic immune checkpoint modulation. *Cell*  
43 *Commun Signal* (2017) **15**:5. doi:10.1186/s12964-016-0155-9

- 1 140. Pardoll DM. The blockade of immune checkpoints in cancer immunotherapy. *Nat Rev*  
2 *Cancer* (2012) **12**:252–264. doi:10.1038/nrc3239
- 3 141. Chen L, Flies DB. Molecular mechanisms of T cell co-stimulation and co-inhibition. *Nat*  
4 *Rev Immunol* (2013) **13**:227–242. doi:10.1038/nri3405
- 5 142. Bashey A, Medina B, Corringham S, Pasek M, Carrier E, Vrooman L, Lowy I, Solomon SR,  
6 Morris LE, Holland HK, et al. CTLA4 blockade with ipilimumab to treat relapse of  
7 malignancy after allogeneic hematopoietic cell transplantation. *Blood* (2009) **113**:1581–  
8 1588. doi:10.1182/blood-2008-07-168468
- 9 143. Davids MS, Kim HT, Bachireddy P, Costello C, Liguori R, Savell A, Lukez AP, Avigan D,  
10 Chen Y-B, McSweeney P, et al. Ipilimumab for Patients with Relapse after Allogeneic  
11 Transplantation. *N Engl J Med* (2016) **375**:143–153. doi:10.1056/NEJMoa1601202
- 12 144. Albring JC, Inselmann S, Sauer T, Schliemann C, Altvater B, Kailayangiri S, Rössig C,  
13 Hartmann W, Knorrenschild JR, Sohlbach K, et al. PD-1 checkpoint blockade in patients  
14 with relapsed AML after allogeneic stem cell transplantation. *Bone Marrow Transplant*  
15 (2017) **52**:317–320. doi:10.1038/bmt.2016.274
- 16 145. McDuffee E, Aue G, Cook L, Ramos-Delgado C, Shalabi R, Worthy T, Vo P, Childs RW.  
17 Tumor regression concomitant with steroid-refractory GvHD highlights the pitfalls of PD-  
18 1 blockade following allogeneic hematopoietic stem cell transplantation. *Bone Marrow*  
19 *Transplant* (2017) **52**:759–761. doi:10.1038/bmt.2016.346
- 20 146. Onizuka M, Kojima M, Matsui K, Machida S, Toyosaki M, Aoyama Y, Kawai H, Amaki J,  
21 Hara R, Ichiki A, et al. Successful treatment with low-dose nivolumab in refractory  
22 Hodgkin lymphoma after allogeneic stem cell transplantation. *Int J Hematol* (2017)  
23 **106**:141–145. doi:10.1007/s12185-017-2181-9
- 24 147. Herbaux C, Gauthier J, Brice P, Drumez E, Ysebaert L, Doyen H, Fornecker L, Bouabdallah  
25 K, Manson G, Ghesquières H, et al. Efficacy and tolerability of nivolumab after allogeneic  
26 transplantation for relapsed Hodgkin lymphoma. *Blood* (2017) **129**:2471–2478.  
27 doi:10.1182/blood-2016-11-749556
- 28 148. Haverkos BM, Abbott D, Hamadani M, Armand P, Flowers ME, Merryman R, Kamdar M,  
29 Kanate AS, Saad A, Mehta A, et al. PD-1 blockade for relapsed lymphoma post-allogeneic  
30 hematopoietic cell transplant: high response rate but frequent GVHD. *Blood* (2017)  
31 **130**:221–228. doi:10.1182/blood-2017-01-761346
- 32 149. Wang L, Amoozgar Z, Huang J, Saleh MH, Xing D, Orsulic S, Goldberg MS. Decitabine  
33 Enhances Lymphocyte Migration and Function and Synergizes with CTLA-4 Blockade in a  
34 Murine Ovarian Cancer Model. *Cancer Immunol Res* (2015) **3**:1030–1041.  
35 doi:10.1158/2326-6066.CIR-15-0073
- 36 150. Daver N, Boddu P, Garcia-Manero G, Yadav SS, Sharma P, Allison J, Kantarjian H.  
37 Hypomethylating agents in combination with immune checkpoint inhibitors in acute  
38 myeloid leukemia and myelodysplastic syndromes. *Leukemia* (2018) **32**:1094–1105.  
39 doi:10.1038/s41375-018-0070-8
- 40 151. Dear AE. Epigenetic Modulators and the New Immunotherapies. *N Engl J Med* (2016)  
41 **374**:684–686. doi:10.1056/NEJMcibr1514673

- 1 152. Daver N, Garcia-Manero G, Basu S, Boddu PC, Alfayez M, Cortes JE, Konopleva M, Ravandi-  
2 Kashani F, Jabbour E, Kadia T, et al. Efficacy, Safety, and Biomarkers of Response to  
3 Azacitidine and Nivolumab in Relapsed/Refractory Acute Myeloid Leukemia: A  
4 Nonrandomized, Open-Label, Phase II Study. *Cancer Discov* (2019) **9**:370–383.  
5 doi:10.1158/2159-8290.CD-18-0774
- 6 153. Ettinghausen SE, Lipford EH, Mulé JJ, Rosenberg SA. Recombinant interleukin 2  
7 stimulates in vivo proliferation of adoptively transferred lymphokine-activated killer  
8 (LAK) cells. *J Immunol* (1985) **135**:3623–3635.
- 9 154. Alatrash G, Jakher H, Stafford PD, Mittendorf EA. Cancer immunotherapies, their safety  
10 and toxicity. *Expert Opin Drug Saf* (2013) **12**:631–645.  
11 doi:10.1517/14740338.2013.795944
- 12 155. Foa R, Guarini A, Gansbacher B. IL2 treatment for cancer: from biology to gene therapy.  
13 *Br J Cancer* (1992) **66**:992–998. doi:10.1038/bjc.1992.400
- 14 156. Buyse M, Squifflet P, Lange BJ, Alonzo TA, Larson RA, Kolitz JE, George SL, Bloomfield CD,  
15 Castaigne S, Chevret S, et al. Individual patient data meta-analysis of randomized trials  
16 evaluating IL-2 monotherapy as remission maintenance therapy in acute myeloid  
17 leukemia. *Blood* (2011) **117**:7007–7013. doi:10.1182/blood-2011-02-337725
- 18 157. Acuto O, Di Bartolo V, Michel F. Tailoring T-cell receptor signals by proximal negative  
19 feedback mechanisms. *Nat Rev Immunol* (2008) **8**:699–712. doi:10.1038/nri2397
- 20 158. Ustun C, Miller JS, Munn DH, Weisdorf DJ, Blazar BR. Regulatory T cells in acute  
21 myelogenous leukemia: is it time for immunomodulation? *Blood* (2011) **118**:5084–5095.  
22 doi:10.1182/blood-2011-07-365817
- 23 159. Kolitz JE, George SL, Benson DM, Maharry K, Marcucci G, Vij R, Powell BL, Allen SL,  
24 Deangelo DJ, Shea TC, et al. Recombinant interleukin-2 in patients aged younger than 60  
25 years with acute myeloid leukemia in first complete remission: results from Cancer and  
26 Leukemia Group B 19808. *Cancer* (2014) **120**:1010–1017. doi:10.1002/cncr.28516
- 27 160. Plataniias LC. Interferons and their antitumor properties. *J Interferon Cytokine Res* (2013)  
28 **33**:143–144. doi:10.1089/jir.2013.0019
- 29 161. Le Bon A, Tough DF. Type I interferon as a stimulus for cross-priming. *Cytokine Growth*  
30 *Factor Rev* (2008) **19**:33–40. doi:10.1016/j.cytogfr.2007.10.007
- 31 162. Papewalis C, Jacobs B, Wuttke M, Ullrich E, Baehring T, Fenk R, Willenberg HS, Schinner S,  
32 Cohnen M, Seissler J, et al. IFN-alpha skews monocytes into CD56+-expressing dendritic  
33 cells with potent functional activities in vitro and in vivo. *J Immunol* (2008) **180**:1462–  
34 1470. doi:10.4049/jimmunol.180.3.1462
- 35 163. Bekisz J, Sato Y, Johnson C, Husain SR, Puri RK, Zoon KC. Immunomodulatory effects of  
36 interferons in malignancies. *J Interferon Cytokine Res* (2013) **33**:154–161.  
37 doi:10.1089/jir.2012.0167
- 38 164. Anguille S, Lion E, Willemen Y, Van Tendeloo VFI, Berneman ZN, Smits ELJM. Interferon- $\alpha$   
39 in acute myeloid leukemia: an old drug revisited. *Leukemia* (2011) **25**:739–748.  
40 doi:10.1038/leu.2010.324

- 1 165. Colamonici OR, Domanski P, Platanius LC, Diaz MO. Correlation between interferon (IFN)  
2 alpha resistance and deletion of the IFN alpha/beta genes in acute leukemia cell lines  
3 suggests selection against the IFN system. *Blood* (1992) **80**:744–749.
- 4 166. Smits ELJM, Anguille S, Berneman ZN. Interferon  $\alpha$  may be back on track to treat acute  
5 myeloid leukemia. *Oncoimmunology* (2013) **2**:e23619. doi:10.4161/onci.23619
- 6 167. Robb RJ, Kreijveld E, Kuns RD, Wilson YA, Olver SD, Don ALJ, Raffelt NC, De Weerd NA,  
7 Lineburg KE, Varelias A, et al. Type I-IFNs control GVHD and GVL responses after  
8 transplantation. *Blood* (2011) **118**:3399–3409. doi:10.1182/blood-2010-12-325746
- 9 168. Steel JC, Waldmann TA, Morris JC. Interleukin-15 biology and its therapeutic implications  
10 in cancer. *Trends Pharmacol Sci* (2012) **33**:35–41. doi:10.1016/j.tips.2011.09.004
- 11 169. Conlon KC, Lugli E, Welles HC, Rosenberg SA, Fojo AT, Morris JC, Fleisher TA, Dubois SP,  
12 Perera LP, Stewart DM, et al. Redistribution, hyperproliferation, activation of natural  
13 killer cells and CD8 T cells, and cytokine production during first-in-human clinical trial of  
14 recombinant human interleukin-15 in patients with cancer. *J Clin Oncol* (2015) **33**:74–82.  
15 doi:10.1200/JCO.2014.57.3329
- 16 170. Klebanoff CA, Finkelstein SE, Surman DR, Lichtman MK, Gattinoni L, Theoret MR, Grewal  
17 N, Spiess PJ, Antony PA, Palmer DC, et al. IL-15 enhances the in vivo antitumor activity of  
18 tumor-reactive CD8+ T cells. *Proc Natl Acad Sci USA* (2004) **101**:1969–1974.  
19 doi:10.1073/pnas.0307298101
- 20 171. Cieri N, Oliveira G, Greco R, Forcato M, Taccioli C, Cianciotti B, Valtolina V, Noviello M,  
21 Vago L, Bondanza A, et al. Generation of human memory stem T cells after haploidentical  
22 T-replete hematopoietic stem cell transplantation. *Blood* (2015) **125**:2865–2874.  
23 doi:10.1182/blood-2014-11-608539
- 24 172. Ring AM, Lin J-X, Feng D, Mitra S, Rickert M, Bowman GR, Pande VS, Li P, Moraga I,  
25 Spolski R, et al. Mechanistic and structural insight into the functional dichotomy between  
26 IL-2 and IL-15. *Nat Immunol* (2012) **13**:1187–1195. doi:10.1038/ni.2449
- 27 173. Romee R, Cooley S, Berrien-Elliott MM, Westervelt P, Verneris MR, Wagner JE, Weisdorf  
28 DJ, Blazar BR, Ustun C, DeFor TE, et al. First-in-human phase 1 clinical study of the IL-15  
29 superagonist complex ALT-803 to treat relapse after transplantation. *Blood* (2018)  
30 **131**:2515–2527. doi:10.1182/blood-2017-12-823757
- 31 174. Escobar G, Barbarossa L, Barbiera G, Norelli M, Genua M, Ranghetti A, Plati T, Camisa B,  
32 Brombin C, Cittaro D, et al. Interferon gene therapy reprograms the leukemia  
33 microenvironment inducing protective immunity to multiple tumor antigens. *Nat*  
34 *Commun* (2018) **9**:2896. doi:10.1038/s41467-018-05315-0
- 35 175. Pastor F, Berraondo P, Etxeberria I, Frederick J, Sahin U, Gilboa E, Melero I. An RNA  
36 toolbox for cancer immunotherapy. *Nat Rev Drug Discov* (2018) **17**:751–767.  
37 doi:10.1038/nrd.2018.132
- 38 176. Olavarria E, Siddique S, Griffiths MJ, Avery S, Byrne JL, Piper KP, Lennard AL, Pallan L,  
39 Arrazi JM, Perz JB, et al. Posttransplantation imatinib as a strategy to postpone the  
40 requirement for immunotherapy in patients undergoing reduced-intensity allografts for

- 1 chronic myeloid leukemia. *Blood* (2007) **110**:4614–4617. doi:10.1182/blood-2007-04-  
2 082990
- 3 177. Ribera J-M, Oriol A, González M, Vidriales B, Brunet S, Esteve J, Del Potro E, Rivas C,  
4 Moreno M-J, Tormo M, et al. Concurrent intensive chemotherapy and imatinib before and  
5 after stem cell transplantation in newly diagnosed Philadelphia chromosome-positive  
6 acute lymphoblastic leukemia. Final results of the CSTIBES02 trial. *Haematologica*  
7 (2010) **95**:87–95. doi:10.3324/haematol.2009.011221
- 8 178. Shin JY, Hu W, Naramura M, Park CY. High c-Kit expression identifies hematopoietic stem  
9 cells with impaired self-renewal and megakaryocytic bias. *J Exp Med* (2014) **211**:217–  
10 231. doi:10.1084/jem.20131128
- 11 179. Bodine DM, Seidel NE, Zsebo KM, Orlic D. In vivo administration of stem cell factor to  
12 mice increases the absolute number of pluripotent hematopoietic stem cells. *Blood*  
13 (1993) **82**:445–455.
- 14 180. Thorén LA, Liuba K, Bryder D, Nygren JM, Jensen CT, Qian H, Antonchuk J, Jacobsen S-EW.  
15 Kit regulates maintenance of quiescent hematopoietic stem cells. *J Immunol* (2008)  
16 **180**:2045–2053. doi:10.4049/jimmunol.180.4.2045
- 17 181. Zitvogel L, Rusakiewicz S, Routy B, Ayyoub M, Kroemer G. Immunological off-target  
18 effects of imatinib. *Nat Rev Clin Oncol* (2016) **13**:431–446.  
19 doi:10.1038/nrclinonc.2016.41
- 20 182. Appel S, Rupf A, Weck MM, Schoor O, Brümmendorf TH, Weinschenk T, Grünebach F,  
21 Brossart P. Effects of imatinib on monocyte-derived dendritic cells are mediated by  
22 inhibition of nuclear factor-kappaB and Akt signaling pathways. *Clin Cancer Res* (2005)  
23 **11**:1928–1940. doi:10.1158/1078-0432.CCR-04-1713
- 24 183. Appel S, Boehmler AM, Grünebach F, Müller MR, Rupf A, Weck MM, Hartmann U,  
25 Reichardt VL, Kanz L, Brümmendorf TH, et al. Imatinib mesylate affects the development  
26 and function of dendritic cells generated from CD34+ peripheral blood progenitor cells.  
27 *Blood* (2004) **103**:538–544. doi:10.1182/blood-2003-03-0975
- 28 184. Taïeb J, Maruyama K, Borg C, Terme M, Zitvogel L. Imatinib mesylate impairs Flt3L-  
29 mediated dendritic cell expansion and antitumor effects in vivo. *Blood* (2004) **103**:1966–  
30 1967; author reply 1967. doi:10.1182/blood-2003-10-3475
- 31 185. Boissel N, Rousselot P, Raffoux E, Cayuela J-M, Maarek O, Charron D, Degos L, Dombret H,  
32 Toubert A, Rea D. Defective blood dendritic cells in chronic myeloid leukemia correlate  
33 with high plasmatic VEGF and are not normalized by imatinib mesylate. *Leukemia* (2004)  
34 **18**:1656–1661. doi:10.1038/sj.leu.2403474
- 35 186. van Dongen M, Savage ND, Jordanova ES, Briaire-de Bruijn IH, Walburg KV, Ottenhoff  
36 THM, Hogendoorn PCW, van der Burg SH, Gelderblom H, van Hall T. Anti-inflammatory  
37 M2 type macrophages characterize metastasized and tyrosine kinase inhibitor-treated  
38 gastrointestinal stromal tumors. *Int J Cancer* (2010) **127**:899–909.  
39 doi:10.1002/ijc.25113

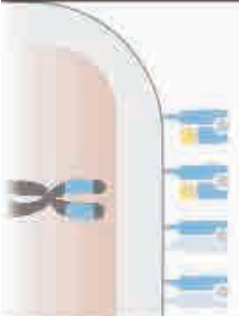

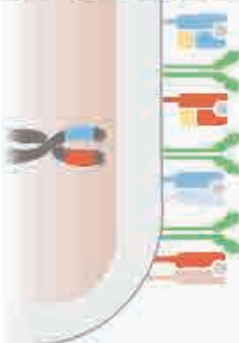


- 1 187. Cavnar MJ, Zeng S, Kim TS, Sorenson EC, Ocuin LM, Balachandran VP, Seifert AM, Greer  
2 JB, Popow R, Crawley MH, et al. KIT oncogene inhibition drives intratumoral macrophage  
3 M2 polarization. *J Exp Med* (2013) **210**:2873–2886. doi:10.1084/jem.20130875
- 4 188. Seggewiss R, Loré K, Greiner E, Magnusson MK, Price DA, Douek DC, Dunbar CE, Wiestner  
5 A. Imatinib inhibits T-cell receptor-mediated T-cell proliferation and activation in a dose-  
6 dependent manner. *Blood* (2005) **105**:2473–2479. doi:10.1182/blood-2004-07-2527
- 7 189. Gao H, Lee B-N, Talpaz M, Donato NJ, Cortes JE, Kantarjian HM, Reuben JM. Imatinib  
8 mesylate suppresses cytokine synthesis by activated CD4 T cells of patients with chronic  
9 myelogenous leukemia. *Leukemia* (2005) **19**:1905–1911. doi:10.1038/sj.leu.2403933
- 10 190. de Lavallade H, Khoder A, Hart M, Sarvaria A, Sekine T, Alsuliman A, Mielke S, Bazeos A,  
11 Stringaris K, Ali S, et al. Tyrosine kinase inhibitors impair B-cell immune responses in  
12 CML through off-target inhibition of kinases important for cell signaling. *Blood* (2013)  
13 **122**:227–238. doi:10.1182/blood-2012-11-465039
- 14 191. Steegmann JL, Moreno G, Aláez C, Osorio S, Granda A, de la Cámara R, Arranz E, Reino FG,  
15 Salvanés FR, Fernández-Rañada JM, et al. Chronic myeloid leukemia patients resistant to  
16 or intolerant of interferon alpha and subsequently treated with imatinib show reduced  
17 immunoglobulin levels and hypogammaglobulinemia. *Haematologica* (2003) **88**:762–  
18 768.
- 19 192. Carulli G, Cannizzo E, Ottaviano V, Cervetti G, Buda G, Galimberti S, Baratè C, Marini A,  
20 Petrini M. Abnormal phenotype of bone marrow plasma cells in patients with chronic  
21 myeloid leukemia undergoing therapy with Imatinib. *Leuk Res* (2010) **34**:1336–1339.  
22 doi:10.1016/j.leukres.2010.01.012
- 23 193. Balachandran VP, Cavnar MJ, Zeng S, Bamboat ZM, Ocuin LM, Obaid H, Sorenson EC,  
24 Popow R, Ariyan C, Rossi F, et al. Imatinib potentiates antitumor T cell responses in  
25 gastrointestinal stromal tumor through the inhibition of Ido. *Nat Med* (2011) **17**:1094–  
26 1100. doi:10.1038/nm.2438
- 27 194. Larmonier N, Janikashvili N, LaCasse CJ, Larmonier CB, Cantrell J, Situ E, Lundeen T,  
28 Bonnotte B, Katsanis E. Imatinib mesylate inhibits CD4+ CD25+ regulatory T cell activity  
29 and enhances active immunotherapy against BCR-ABL- tumors. *J Immunol* (2008)  
30 **181**:6955–6963. doi:10.4049/jimmunol.181.10.6955
- 31 195. Giallongo C, Parrinello N, Tibullo D, La Cava P, Romano A, Chiarenza A, Barbagallo I,  
32 Palumbo GA, Stagno F, Vigneri P, et al. Myeloid derived suppressor cells (MDSCs) are  
33 increased and exert immunosuppressive activity together with polymorphonuclear  
34 leukocytes (PMNs) in chronic myeloid leukemia patients. *PLoS ONE* (2014) **9**:e101848.  
35 doi:10.1371/journal.pone.0101848
- 36 196. Christiansson L, Söderlund S, Mangsbo S, Hjorth-Hansen H, Höglund M, Markevärn B,  
37 Richter J, Stenke L, Mustjoki S, Loskog A, et al. The tyrosine kinase inhibitors imatinib and  
38 dasatinib reduce myeloid suppressor cells and release effector lymphocyte responses.  
39 *Mol Cancer Ther* (2015) **14**:1181–1191. doi:10.1158/1535-7163.MCT-14-0849
- 40 197. Christiansson L, Söderlund S, Svensson E, Mustjoki S, Bengtsson M, Simonsson B, Olsson-  
41 Strömberg U, Loskog ASI. Increased level of myeloid-derived suppressor cells,  
42 programmed death receptor ligand 1/programmed death receptor 1, and soluble CD25

- 1 in Sokal high risk chronic myeloid leukemia. *PLoS ONE* (2013) **8**:e55818.  
2 doi:10.1371/journal.pone.0055818
- 3 198. Legros L, Bourcier C, Jacquel A, Mahon F-X, Cassuto J-P, Auberger P, Pagès G. Imatinib  
4 mesylate (STI571) decreases the vascular endothelial growth factor plasma  
5 concentration in patients with chronic myeloid leukemia. *Blood* (2004) **104**:495–501.  
6 doi:10.1182/blood-2003-08-2695
- 7 199. Legros L, Guilhot J, Huault S, Mahon FX, Preudhomme C, Guilhot F, Hueber AO, French  
8 CML Group (FI-LMC). Interferon decreases VEGF levels in patients with chronic myeloid  
9 leukemia treated with imatinib. *Leuk Res* (2014) **38**:662–665.  
10 doi:10.1016/j.leukres.2014.01.010
- 11 200. Chen CI-U, Maecker HT, Lee PP. Development and dynamics of robust T-cell responses to  
12 CML under imatinib treatment. *Blood* (2008) **111**:5342–5349. doi:10.1182/blood-2007-  
13 12-128397
- 14 201. Riva G, Luppi M, Barozzi P, Quadrelli C, Basso S, Vallerini D, Zanetti E, Morselli M,  
15 Forghieri F, Maccaferri M, et al. Emergence of BCR-ABL-specific cytotoxic T cells in the  
16 bone marrow of patients with Ph+ acute lymphoblastic leukemia during long-term  
17 imatinib mesylate treatment. *Blood* (2010) **115**:1512–1518. doi:10.1182/blood-2009-  
18 06-230391
- 19 202. Riva G, Luppi M, Lagreca I, Barozzi P, Quadrelli C, Vallerini D, Zanetti E, Basso S, Forghieri  
20 F, Morselli M, et al. Long-term molecular remission with persistence of BCR-ABL1-  
21 specific cytotoxic T cells following imatinib withdrawal in an elderly patient with  
22 Philadelphia-positive ALL. *Br J Haematol* (2014) **164**:299–302. doi:10.1111/bjh.12612
- 23 203. Ohyashiki K, Katagiri S, Tauchi T, Ohyashiki JH, Maeda Y, Matsumura I, Kyo T. Increased  
24 natural killer cells and decreased CD3(+)CD8(+)CD62L(+) T cells in CML patients who  
25 sustained complete molecular remission after discontinuation of imatinib. *Br J Haematol*  
26 (2012) **157**:254–256. doi:10.1111/j.1365-2141.2011.08939.x
- 27

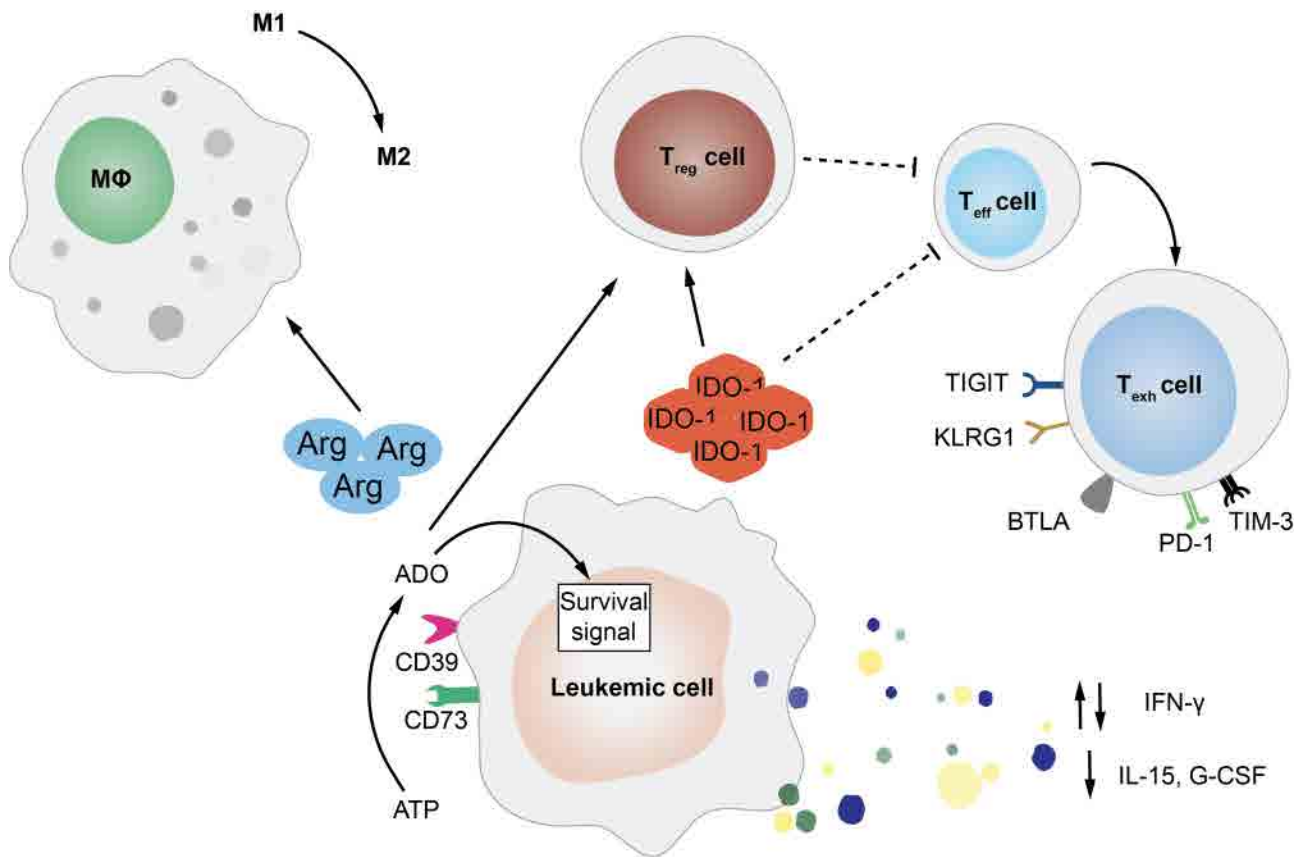
1 **FIGURES**

2  
 3 **Figure 1.** Tumor-Intrinsic Mechanisms of Immune Evasion and Relapse  
 4

	<b>Alteration</b>	<b>Molecules involved</b>	<b>Therapy</b>
	Genomic HLA loss (CN-LOH)	Incompatible HLAs (both class I and II)	Second transplantation or non HLA-restricted immunotherapies
	Epigenetic downregulation of HLA class II	Compatible and Incompatible class II HLAs	Induction of IFN- $\gamma$ release (leukemia cross-recognition, inflammatory microenvironment)
	Epigenetic upregulation of inhibitory molecules	PD-L1, B7-H3, PVR, PVRL2	Immune checkpoint blockade

5  
 6

1 **Figure 2.** Tumor-Extrinsic Mechanisms of Immune Evasion and Relapse  
2



3

**Chapter 7.**

**Integrated Epigenetic Profiling Identifies EZH2 as a Therapeutic Target to Re-Establish Immune Recognition of Leukemia Relapses with Loss of HLA Class II Expression**

Gambacorta V, Gnani D, Zito L, Beretta S, Zanotti L, Oliveira G, Cittaro D, Merelli I, Ciceri F, Di Micco R\* and Vago L\*

*In preparation*

## **Integrated Epigenetic Profiling Identifies EZH2 as a Therapeutic Target To Re-Establish Immune Recognition of Leukemia Relapses with Loss of HLA Class II Expression**

Gambacorta V<sup>1,2,3</sup>, Gnani D<sup>2</sup>, Zito L<sup>1</sup>, Beretta S<sup>4</sup>, Zanotti L<sup>1</sup>, Oliveira G<sup>1</sup>, Cittaro D<sup>5</sup>, Merelli I<sup>4</sup>, Ciceri F<sup>6,7</sup>, Di Micco R<sup>2,¶</sup> and Vago L<sup>1,6,¶</sup>

<sup>1</sup> Unit of Immunogenetics, Leukemia Genomics and Immunobiology, Division of Immunology, Transplantation and Infectious Disease, IRCCS San Raffaele Scientific Institute, Milano, Italy; <sup>2</sup> Unit of Senescence in Stem Cell Aging, Differentiation and Cancer, San Raffaele Telethon Institute for Gene Therapy (SR-TIGET), IRCCS San Raffaele Scientific Institute, Milano, Italy; <sup>3</sup> University of Milano Bicocca, Milano, Italy; <sup>4</sup> Institute for Biomedical Technologies, National Research Council, Segrate, Italy; <sup>6</sup> Hematology and Bone Marrow Transplantation Unit, IRCCS San Raffaele Scientific Institute, Milano, Italy; <sup>7</sup> San Raffaele Vita-Salute University, Milano, Italy.

¶ These authors contributed equally to this work

RUNNING TITLE: Epigenetic Control of Immune Evasion and Relapse after allo-HCT

ABSTRACT/TEXT WORD COUNT: 308/5299

FIGURES/TABLES/REFERENCES: 3/0/21

Correspondence should be addressed to Dr. Raffaella Di Micco, Unit of Senescence in Stem Cell Aging, Differentiation and Cancer, IRCCS San Raffaele Scientific Institute, Milano, Italy via Olgettina 60, Milano, Italy. Phone: +390226435024. E-mail: dimicco.raffaella@hsr.it; or to Dr. Luca Vago, Unit of Immunogenetics, Leukemia Genomics and Immunobiology, IRCCS San Raffaele Scientific Institute, Milano, Italy, via Olgettina 60, Milano, Italy. Phone: +390226434341. E-mail: vago.luca@hsr.it

1 **Abstract**

2 Allogeneic hematopoietic cell transplantation (allo-HCT) can cure acute myeloid leukemia  
3 (AML), but relapses remain frequent. Recently, it has been described that in up to 40% of post-  
4 transplantation AML relapses the malignant cells evade immune elimination by losing the surface  
5 expression of HLA class II molecules. Since genomic studies failed to identify mutations  
6 responsible for this phenotype, here we aim to decipher epigenetic alterations responsible for  
7 transcriptional downregulation of HLA class II expression in AML post-transplantation relapse.  
8 We generated PDXs from paired diagnosis and relapse AML samples with this relapse modality  
9 and performed cutting-edge NGS technologies coupled with integrative bioinformatic approaches  
10 to characterize changes in gene expression, DNA methylation, histone modifications and  
11 chromatin accessibility. This integrated analysis evidenced that the differences between diagnosis  
12 and relapse mostly rely in chromatin accessibility and histone modification changes and were  
13 largely unrelated to changes in DNA methylation. We documented that epigenetically  
14 deregulated genes match known targets of EZH2, the enzymatic subunit of the PRC2 chromatin  
15 repressor complex. These computational analyses were supported by the evidence of a relapse-  
16 specific closed chromatin status of HLA class II genes and their regulators. To revert these  
17 epigenetic changes, we employed a panel of chemical inhibitors targeting different subunits of  
18 the polycomb repressive complex 2 (PRC2) in AML relapses with downregulated expression of  
19 HLA class II. PRC2 inhibition reduced the levels of the repressor mark H3K27me3, increased the  
20 surface expression of HLA class II molecules and ultimately improved leukemia recognition by  
21 CD4<sup>+</sup> T cells. Notably, these effects were even more pronounced when EZH2 inhibition was  
22 combined with IFN- $\gamma$  treatment, suggesting synergism between this epigenetic compound and  
23 cytokines released by immune cells upon target recognition.

1 Our results provide mechanistic insights into epigenetic regulation of HLA class II negative  
2 leukemia and pave the way for the development of new strategies for the treatment of AML post-  
3 transplantation immune evasion and relapse.

4



1 **Introduction**

2 In the last few decades, major breakthroughs have improved the feasibility and safety of  
3 allogeneic hematopoietic cell transplantation (allo-HCT) to cure patients affected by acute  
4 myeloid leukemia (AML). Still, post-transplantation relapses remain a major unsolved issue,  
5 occurring in up to 50% of transplanted patients. It is becoming increasingly recognized that  
6 evasion from immune control represents one of the main drivers of AML relapse after  
7 transplantation<sup>1</sup>. Among the immune escape mechanisms described so far, alteration in the  
8 expression of HLA class II genes represents one of the most frequent relapse modality,  
9 accounting for up to 40% of post-transplantation relapses<sup>2,3</sup>. The central role of the interaction  
10 between CD4<sup>+</sup> T cells and HLA class II molecules in driving the graft versus tumor effect of allo-  
11 HCT has been suggested by both pre-clinical<sup>4</sup> and clinical studies<sup>5</sup>, and the observation that loss  
12 of HLA class can be sufficient to prompt clinical relapse is another strong evidence in this  
13 direction.

14 Noticeably, genomic characterization of relapses with downregulation of HLA class molecules  
15 did not identify any specific genomic lesions in the coding sequence of HLA genes or their  
16 known regulators<sup>3</sup>, suggesting that the molecular foundation of this immune evasion modality  
17 might lie in the poorly investigated field of epigenome regulation. This hypothesis is further  
18 supported by recent data demonstrating that relapse-specific epigenetic heterogeneity can evolve  
19 independently from the genetic background<sup>6</sup>.

20 Given these premises, this paper aims to better understand the molecular mechanisms that govern  
21 non-genomic loss of HLA class II molecule in AML post-transplantation relapses, investigating  
22 the links between epigenetic changes and immune evasion, with the final goal of providing the  
23 rationale for novel therapeutic interventions.

24

25

1 **Materials and Methods**

2 ***Patient and sample characteristics***

3 We selected one patient diagnosed with *de novo* AML who experienced disease relapse after allo-  
4 HCT, characterized by non-genomic loss of HLA class II expression and for whom paired pre-  
5 and post-transplantation viable leukemic samples had been collected. The patient gave specific  
6 informed consent to the San Raffaele Leukemia Biobank (Protocol “ALLO-RELAPSE” approved  
7 by the San Raffaele Ethic Committee on 11/03/17 and Protocol “Banca Neoplasie Ematologiche”  
8 approved by the San Raffaele Ethic Committee on 10/05/10, latest amendment on 06/14/12) in  
9 agreement with the Declaration of Helsinki.

10

11 ***Processing of biological samples***

12 Primary samples were thawed and kept for 20 minutes at 37 °C in fetal bovine serum (FBS,  
13 Euroclone, MI, Italy) supplemented with 25 units/mL of Benzonase® Nuclease (Sigma-Aldrich®,  
14 Prod. No. E1014) at a concentration of 1-2x10<sup>6</sup> cells/mL. Leukemia blasts were labelled in 100 µl  
15 of Gartner’s medium for 20 min at 4 °C using fluorescent antibodies according to their leukemia  
16 associated immunophenotype (LAIP), using CD45-PE-Cy7 (Clone HI30, Cat. No. 304016, Lot  
17 N°B229089), CD3-FITC (Clone SK7, Catalog. N° 344804, Lot N°B231398) both from  
18 BioLegend, San Diego, CA, USA CD33-APC (Clone WM53, Catalog. N° 551378, Lot  
19 N°9008623) from BD Biosciences, Franklin Lakes, NJ, USA) and CD14-APC-Cy7 (Clone  
20 M5E2, Catalog. N°301820, Lot N°B251038) (BioLegend, San Diego, CA, USA), 2µL each.  
21 Leukemia samples were washed with 10 mL of Gartner’s medium, filtered with a cell strainer  
22 and then FACS-purified using a MoFlo™ XDP (Beckman Coulter, Brea, CA, USA) cell sorter.  
23 Patient derived xenograft (PDX) samples were retrieved by collecting and processing mice  
24 spleens. For all the experiments, mouse cells were depleted by column selection (Miltenyi Biotec

1 GmbH, Bergisch Gladbach, Germany) taking advantage of the mouse CD45 microbeads  
2 (Miltenyi Biotec GmbH, Bergisch Gladbach, Germany; 130-045-801).

3 Genomic DNA for Reduced Representation Bisulfite Sequencing (RRBS) was extracted by  
4 taking advantage of the Wizard SV Genomic DNA purification system (Promega, Madison,  
5 Wisconsin, USA; Product ID: A2361), following manufacturer's instruction plus a step of protein  
6 lysis by adding 1 µg/µL of Proteinase K (New England Biolabs, Ipswich, Massachusetts, USA;  
7 Cat. No. P8102S). The integrity of genomic DNA was assessed by running samples on agarose  
8 gel 1%.

9 Genomic DNA after chromatin immunoprecipitation was extracted by using QIAquick® PCR  
10 Purification Kit (Cat. No. 28106) and transposed DNA by MinElute® Reaction Cleanup Kit (Cat.  
11 No. 28204) both from (Quiagen, Hilden, Germany).

12 Total RNA was extracted by using the RNeasy® Plus Mini or Micro Kits (Qiagen, Hilden,  
13 Germany, used for samples analyzed by both RT-PCR and RNA-seq; Cat. N° 74134 and 74034),  
14 following the manufacturers' indications.

15 The concentration of nucleic acid was calculated using Invitrogen's Qubit™ dsDNA or RNA high  
16 sensitivity assay kits (Thermo Fisher Scientific, Waltham, MA, USA), and quality control were  
17 performed using the Agilent Bioanalyzer technology or the RNA Screen Tape System (both from  
18 Agilent, Santa Clara, CA, USA; Cat. N°5067-5592).

19

### 20 ***Generation of Patient Derived Xenografts (PDXs)***

21 All *in vivo* experiments were performed upon approval by the San Raffaele Institutional Animal  
22 Care and Use Committee (IACUC, protocol number 651), by the San Raffaele Ethic Committee  
23 (protocol AML-PDX, approved on 11/03/17) and by the Italian Ministry of Health (Authorization  
24 number 97/2015-PR on 02/18/15).

1 FACS-sorted blasts were engrafted into four-week old, non-irradiated NOD-SCID  $\gamma$ -chain null  
2 mice by tail vein infusion of about  $5 \times 10^6$  cells. Engraftment were monitored weekly on 50  $\mu$ L of  
3 peripheral blood by flow cytometry. Samples were stained in 100 $\mu$ L of 1X PBS, 2% FBS plus the  
4 relevant mixture of antibodies for 10 min at room temperature (RT), using human CD45-PE-Cy7  
5 (Clone HI30, Cat. No. 304016, Lot N°B264588), CD3-FITC (Clone SK7, Catalog. N° 344804,  
6 Lot N°B231398) from BioLegend, San Diego, CA, USA, CD33-APC (Clone WM53, Catalog.  
7 N° 551378, Lot N°9008623) from BD Biosciences, Franklin Lakes, NJ, USA) and CD14-APC-  
8 Cy7 (Clone M5E2, Catalog. N°301820, Lot N°B251038) (BioLegend, San Diego, CA, USA),  
9 2 $\mu$ L each. After the incubation time, the erythrocytes were eliminated (3 mL ammonium chloride  
10 potassium lysis buffer for 5 min at RT) and samples washed by centrifugation (1600 rpm for 5  
11 min).

12 For flow cytometry analysis, a first gate was set to discriminate between mouse or human CD45  
13 cells and the absolute counts of leukemia blasts were quantified upon gating on leukemia specific  
14 marker CD33 within the gate of human CD45-positive cells. We determined the absolute count  
15 (cells/ $\mu$ L) by addition of count beads into each sample (Beckman Coulter, Brea, CA, USA). Each  
16 experiment included at least 5 mice per group.

17

### 18 ***Multiparametric Flow Cytometry***

19 For immunophenotypic analysis a maximum of  $0.5 \times 10^6$  cells per tube were stained in 100  $\mu$ L of  
20 1X PBS, 2% FBS plus the mixture of antibodies. Staining was performed at RT for 15 min,  
21 followed by washing with 2 ml of 1X PBS, 2% FBS before the analysis. Here, the complete list  
22 of antibodies: mouse CD45 PerCP-Cy5.5 (Clone HB15e, Catalog. N° 305320, Lot B165130),  
23 human CD45 PE-Cy7 (Clone HI30, Catalog. N° 304016, Lot N°B264588), CD33 BV510 (Clone  
24 WM53, Catalog. N° 303422, Lot N°B244960), CD34 BV605 (Clone 581, Catalog. N° 343529,  
25 Lot N°B256713), CD14 APC-Cy7 (Clone HI30, Catalog. N° 304016, Lot N°B229089), CD3

1 Alexa700 (Clone HI30, Catalog. N° 304016, Lot N°B229089), HLA-ABC Pacific Blue (Clone  
2 W6/32, Catalog. N° 311418, Lot N°B191431), HLA-DR FITC (Clone L243, Catalog. N°  
3 307604, Lot N°B275368), PD-L1 PE (Clone 29E2A3, Catalog. N° 329706, Lot N°B282353) and  
4 B7-H3 APC (Clone 85504, Catalog. N° FAB1027A, Lot N°AAPJ0213061), all from Thermo  
5 Fisher Scientific (Waltham, MA, USA).

6 All antibodies were tested on cell lines reported to be positive for the markers of interest and  
7 titrated for optimal on target/off target activity. For data analysis, a first logical gate was based on  
8 side scatter and CD45 intensity, followed by a second gate on the leukemia-specific marker  
9 CD33. HLA-DR expression was assessed within the CD33 positive gate. At least 200.000 events  
10 in the live cells gate were acquired per sample. Analysis of human samples was performed using  
11 LSR Fortessa flow cytometer equipped with 355nm, 405nm, 488nm, 561nm and 640nm lasers  
12 and BD FACS Symphony A5 Sorp flow cytometer equipped with 488 nm, 561 nm, 637 nm, 405  
13 nm, 355 nm lasers (both instruments were from BD Biosciences, Franklin Lakes, NJ, USA).  
14 Analysis of PDX samples was performed using a Gallios flow cytometer equipped with 488nm,  
15 638nm and 405nm lasers (Beckman Coulter, Brea, CA, USA). Each acquisition was calibrated  
16 using Rainbow Calibration Particles (Spherotech, Lake Forest, IL, USA; Cat No. RCP-30-5A) to  
17 correct for day-to-day laser intensity variations. Data were processed using FlowJo version 10.5.2  
18 (Tree Star, Ashland, OR, USA) or Kaluza (Beckman Coulter, Brea, CA, USA).

19

## 20 ***RNA-Seq***

21 Library preparation was performed by starting from 300 ng of total RNA and using the TruSeq  
22 Stranded mRNA library preparation kit (Illumina, San Diego, California, USA; Cat. N° 2002-  
23 0594) in accordance with low-throughput protocol. After PCR enrichment (15 cycles) and  
24 purification of adapter-ligated fragments, the concentration and length of DNA fragments were

1 measured. Then, RNA-seq libraries were sequenced using the Illumina Next-Seq 500 high  
2 platform in order to obtain a minimum of  $30 \times 10^6$  paired-end reads per sample.

3

#### 4 **Assay for Transposase-Accessible Chromatin using Sequencing (ATAC-Seq)**

5 A total of  $50 \times 10^5$  cells from FACS-sorted AML samples will be simultaneously lysed with  
6 digitonin (Promega, Madison, WI, USA; Cat N° G944A) and tagmented with an engineered Tn5  
7 transposase (Illumina, San Diego, California, USA Cat N°15027865) at 37°C for 20 minutes,  
8 following a protocol optimized for blood cells<sup>7</sup>. Then, all the tagmented DNA was purified (see  
9 processing of biological sample section) and amplified with 10 cycles of PCR. Before the  
10 sequencing, fragments with a size ranging from 1000 and 5000 base pairs were removed by  
11 magnetic separation with AMPure XP beads (Beckman Coulter, Brea, CA, USA; Cat. N°  
12 A63881). Libraries were then sequenced on Illumina Next-seq 500 high platform in order to  
13 obtain 40 million of paired-end reads per sample.

14

#### 15 ***Chromatin Immunoprecipitation followed by Sequencing (ChIP-Seq)***

16 Chromatin isolated from primary and PDX samples was subjected to ChIP-Seq procedure as  
17 reported<sup>8</sup> with some modifications. Briefly, a minimum of  $2 \times 10^6$  cells per ChIP were crosslinked  
18 with 1% formaldehyde and the reaction quenched with the addition of glycine (0.25%).  
19 Cytoplasmic membranes and nuclei were then lysed and chromatin fragmented by sonication (15  
20 cycles, 30sec On/Off) using the Bioruptor® Pico (Diagenode, Denville, NJ, USA). Chromatin was  
21 then subjected to ChIP for H3K4me3 (Rabbit, Cat N° ab8580, Lot N°GR273043-6) and  
22 H3K27ac (Rabbit, Cat N°ab4729, Lot N°GR3187597-1) (all from Abcam, Cambridge, UK).

23 ChIP-Seq libraries were generated using Accel-NGS® 2S DNA Library Kit (Swift Biosciences™,  
24 Ann Arbor, MI, USA; Cat. No. 21024), following the protocol instructions for low input material.  
25 Then, ChIP-Seq libraries were sequenced using the Illumina Next-Seq 500 high platform in order

1 to obtain a minimum of  $10 \times 10^6$  (for H3K4me3) or  $20 \times 10^6$  (for H3K27me3) paired-end reads per  
2 sample.

3

#### 4 ***Reduced Representation Bisulfite Sequencing (RRBS)***

5 A total of 50 ng of purified DNA was used per sample and processed as previously described<sup>9</sup>.  
6 Briefly, genomic DNA was digested using methylation-insensitive restriction enzymes to  
7 generate short fragments enriched for CpG dinucleotides at the extremities. After end-repair, A-  
8 tailing and ligation to methylated adapters, the CpG-rich DNA fragments were subjected to size  
9 selection, bisulfite conversion, PCR amplification and sequencing.

10

#### 11 ***Bioinformatic Analyses***

12 RNA-Seq. In order to quantify gene expression levels, read tags were pseudoaligned to gencode  
13 v28 transcripts using kallisto v 0.44.0 (parameters: -t 8 --single --rf-stranded -l 200 -s 20).  
14 Abundancies were summarized to genes using txImport package and analyzed using edgeR with  
15 a design matrix including sample identity, disease condition and coordinates of the first two  
16 components of multidimensional scaling of the count matrix (~sample\_id + condition + X + Y).  
17 Fold change was then calculated on the “condition” covariate.

18 ATAC-Seq. Reads were aligned to the hg38 human genome assembly using BWA software and  
19 peaks calling was performed using MAC2 software. Annotations was done by proximity with  
20 TSS of nearest expressed gene.

21 ChIP-Seq. Sequencing reads were aligned by BWA software using Bowtie to the hg38 human  
22 genome. We used the MACS2 peak finding algorithm, to identify regions of enrichment, and for  
23 generating normalized read density files for visualization on the IGV browser.

24

25

1 ***Mixed lymphocyte culture (MLC)***

2 Briefly, CD4<sup>+</sup> T cells were selected from peripheral blood mononuclear cells of HLA-disparate  
3 healthy individuals following two steps of magnetic bead separation. We firstly used the Pan T  
4 Cell Isolation Kit (Miltenyi Biotec GmbH, Bergisch Gladbach, Germany; Cat. No. 130-096-535)  
5 to obtain pure, untouched T cells. Then, CD4<sup>+</sup> T cells were obtained by further depleting CD8<sup>+</sup>  
6 T cells, taking advantage of the human CD8 microbeads (Miltenyi Biotec GmbH, Bergisch  
7 Gladbach, Germany; Cat. No. 130-045-201). Purified T cells were stimulated with leukemic  
8 blasts at diagnosis at an effector:target ratio of 1:2. Cells were cultured in Iscove's Modified  
9 Dulbecco's Media supplemented with 1% glutamine (G), 1% penicillin/streptomycin (P/S), 10%  
10 HS (Euroclone, MI, Italy; Cat No. ECS0219D) and IL-2 (Novartis, Basel, Switzerland; Cat. No.  
11 027131010) at a final concentration of 150 UI/ml. IL-2 was replaced every 3–4 days and  
12 responders were re-stimulated every 7 days for a total of 14 days. After the second round of  
13 stimulation, CD4<sup>+</sup> T cell activation from MLCs was tested for activation as reported below.

14

15 ***Epigenetic treatment of leukemic blasts in vitro***

16 Leukemic blasts (0.5x10<sup>6</sup> cells/well) were co-cultured with supportive mesenchymal stromal cells  
17 (MS-5) for one week in Gartner's medium in presence or absence of Tazemetostat/EPZ-6438  
18 (Selleckchem, Houston, Tx, USA Cat. N°. S7128), GSK126, GSK343, PF067263, EI1, GSK503,  
19 EPZ011989, CPI169, UNC1999, EEDi 1, EED226, JIB-04 all used at 10 μM all purchased from  
20 MedChemExpress, NJ, USA, IFN-γ (10 ng/μl) (Peprotech, London, UK, Cat. N° 300-02),  
21 Vidaza®/Azacytidine (Celgene, Summit, NJ, USA) and combinations. DMSO at the same  
22 concentration or water were used as negative controls. All the compounds were added twice (at  
23 day 0 and at day 3). At the end of treatments, part of the sample was used to assess the cell  
24 surface expression of HLA-ABC, HLA-DR and -PD-L1 analyzed as described above and the rest  
25 employed for functional *in vitro* experiments.



1 ***Functional assays for T cell recognition of target cells***

2 Activation of CD4<sup>+</sup> T cells was tested by measuring cytokine release through IFN- $\gamma$  ELISpot  
3 assay. Briefly, responder T cells from the MLR were re-challenged for 24h at 37 °C in 5% CO<sup>2</sup>  
4 with target cells pre-treated or not with the epigenetic compounds in 200  $\mu$ l of Iscove's Modified  
5 Dulbecco's Media supplemented with 1% glutamine (G), 1% penicillin/streptomycin (P/S), 10%  
6 HS (Effector:target ratio 1:1). Spots were counted by a KS Elispot Reader (Zeiss, Oberkochen,  
7 Germany).

8  
9 ***Immunofluorescence analysis***

10 Immunofluorescence was performed on relapsed samples treated with Tazemetostat or DMSO. A  
11 maximum of  $1 \times 10^5$  cells were seeded on 10 mm round coverslips pre-coated with 1 mg/mL of  
12 poly-L-lysine solution (Sigma-Aldrich®, St Louis, Missouri, USA; Prod. N° 25988-63-0) for 20  
13 min. Cells were fixed with 4% paraformaldehyde (Santa Cruz Biotechnology, Dallas, TX, USA)  
14 for 20 min at RT and then permeabilized with 0.3% Triton-X 100 in PBS for 10 min. After  
15 washing, coverslips were blocked in PBG (0.2% cold water fish gelatin, 0.5% bovine serum  
16 albumin, in PBS) for 30 min and stained for 1 hour at RT with primary monoclonal antibody  
17 targeting H3K27me3 (Mouse, Cat. N° ab6002, Lot N°GR275911-4) purchased from Abcam,  
18 Cambridge, UK. Alexa488 goat anti-rabbit secondary antibody was then added to probe primary  
19 antibody followed by DAPI staining and slides were mounted with Aqua-Poly-mount®  
20 (Polysciences, Inc, Warrington, PA, USA; Cat No. 18606). Images were obtained with Leica  
21 TCS SP5 confocal laser microscope and visualized with Leica application suite software (Leica  
22 Microsystems, Wetzlar, Germany).

23

24

25

1 **Western Blot**

2 Leukemic cells were harvested in lysis buffer (125 mM Tris pH 6.8, 4% SDS and 20% glycerol).  
3 After the addition of 4X Laemmli sample buffer, 20 µg of proteins were boiled and resolved on  
4 15% Tris-glycine SDS-PAGE gel and transferred to nitrocellulose membranes (Amersham,  
5 Little Chalfont, UK) for 1 hr at 400 mA. Membranes were blocked for 1 hr with 5% nonfat milk  
6 and probed with primary antibodies for 1h at RT (K3K27me3 from Abcam; tubulin from sigma).  
7 Membranes were incubated with horseradish-peroxidase-conjugated secondary antibodies for 1  
8 hr before revealing with peroxidase-conjugated secondary antibodies for 1 hr before revealing  
9 with enhanced chemiluminescence plus western blotting detection kit.

10

11 **qPCR quantification of gene transcripts**

12 qPCR assays and primers for the quantification of HLA-A, HLA-C, HLA-DRB, HLA-DPB1, and  
13 CIITA transcripts were developed in house as reported<sup>2</sup>. For all reactions, 30 ng of total RNA  
14 were retro-transcribed with the iScript cDNA synthesis kit (Biorad, Hercules, CA, USA; Cat No.  
15 1708891), according to the manufacturer's instructions. The synthesized cDNA was then pre-  
16 amplified using TaqMan PreAmp Master Mix (Thermo Fisher Scientific, Massachusetts, USA;  
17 Cat. No. 4488593). Gene expression levels were measured by real-time quantitative PCR (RT-  
18 qPCR) on a Vii7 Real-Time PCR System (Applied Biosystems, Foster City, CA, USA) using  
19 the Fast Sybr<sup>®</sup>Green chemistry (Thermo Fisher Scientific, Massachusetts, USA; Cat. No.  
20 4385618). The relative expression of each target gene was first normalized to RNaseP or GUSB  
21 reference genes ( $\Delta C_T$ ) and then as fold changes ( $\Delta\Delta C_T$ ) relative to the indicated control  
22 conditions.

23

24

25

1 **Results**

2 ***Patient derived xenografts (PDXs) mirror primary relapse-specific epigenetic alterations***

3 To deeply characterize the epigenetic changes responsible for HLA class II downregulation  
4 occurring in acute myeloid leukemia (AML) blasts post-HCT, we first performed comparative  
5 analyses of primary samples and patient-derived xenografts (PDXs), widely used models  
6 instrumental to expand the leukemic blasts in order to have enough material for our  
7 comprehensive molecular analysis. Diagnosis and post-HCT relapse samples from the same  
8 patient were subjected to FACS-sorting in order to purify leukemic blasts before the infusion into  
9 immunodeficient mice (3 mice per condition). Upon expansion into mice, hematopoietic cells of  
10 murine origin were removed, and human blasts were processed for epigenetic analyses (**Fig. 1A**).  
11 Specifically, we employed RNA-Seq to account for differences in gene expression profile and  
12 reduced representation bisulfite sequencing (RRBS) to assess possible alterations in DNA  
13 methylation patterns. To evaluate changes in chromatin compaction, we employed assay for  
14 transposase-accessible chromatin using sequencing (ATAC-Seq) to characterize open/closed  
15 chromatin regions and chromatin immunoprecipitation followed by sequencing (ChIP-Seq) for  
16 gene promoters (by H3K4me3 ChIP) or regulatory elements/active enhancers (by H3K27ac  
17 ChIP) (**Fig. 1A**).

18 We first verified if PDXs recapitulated the immune-related differences between diagnosis and  
19 post-transplantation relapse, including the relapse-specific loss of HLA class II expression. As  
20 reported in **Fig. 1B**, immunophenotypic analysis showed that HLA class II level of expression  
21 (represented by HLA-DR signal) was similar in primary and corresponding PDXs and was  
22 consistent among replicates. To globally evaluate the validity of PDXs in recapitulating the  
23 transcriptional and epigenetic profiles of the primary original samples, we performed the  
24 principal component analysis (PCA) on data retrieved from each technique. We observed that the  
25 first component (PC1), defined the clear segregation of the diagnosis and relapse samples and

1 this was consistent for all the techniques (mean variance 69.2%, range 41-90%) (in **Fig. 1C**, PCA  
2 from RNA-Seq and ATAC-Seq data are reported). Importantly, transcriptional deregulation  
3 revealed by RNA-Seq and changes in chromatin architecture detected by ATAC-Seq, exhibited  
4 significant positive correlation ( $R^2 = 0.34$ ;  $P < 0.0001$ ) (**Fig. 1D**). Our observations indicate that  
5 PDXs recapitulate the epigenetic composition of primary AML samples, allowing us to employ  
6 them in combination with the original primary samples, to dive into the epigenetic  
7 characterization of post-transplantation relapses characterized by the non-genomic loss of  
8 expression of HLA class II molecules.

9

10 ***Integrative bioinformatic analysis highlights relapse-specific chromatin conformational***  
11 ***changes in immune related genes***

12 In order to analyze all the data obtained from the different epigenetic technologies in an  
13 integrative and unsupervised way, we applied a new bioinformatic tool called Multi Omics Factor  
14 Analysis (MOFA)<sup>10</sup>. This computational method is able to extract the major factors of variability  
15 (called latent factors, LFs) from all the different epigenetic data given in input, concomitantly  
16 taking into account all the biological and technical layers of variability of the samples analyzed,  
17 in terms of cell of origin (primary or PDX) and condition (diagnosis and relapse).

18 The results obtained by MOFA documented that the differences between diagnosis and relapse  
19 mostly relied into chromatin accessibility ( $R^2 = 0.79$ ) and histone modification changes ( $R^2 =$   
20  $0.92$  for H3K27ac and  $R^2 = 0.61$  for H3K4me3), with a minor contribution of DNA methylation  
21 ( $R^2 = 33$ ) (**Fig. 2A**). Specifically, gene set enrichment analysis (GSEA) performed on the  
22 information obtained from the major factor of variability (latent factor 1, LF1), confirmed a  
23 significant matching with the immune-related relapse signature (**Fig. 2B**). Accordingly, we  
24 documented a significant and relapse-specific transcriptional downregulation of HLA class II  
25 genes (represented by HLA-DPB1) and their regulators (CIITA) documented by RNA-Seq,

1 which is mirrored and explained by a decrease in chromatin accessibility at the level of their  
2 promoters as assessed by ATAC-Seq signals (**Fig. 2C**).

3  
4 ***Polycomb Repressive Complex 2 (PRC2) emerges as a potential player in triggering immune***  
5 ***evasion of HLA class II negative post-transplantation relapse***

6 To gain more insight into the identification of epigenetic actors involved in transcriptional  
7 regulation of HLA class II negative relapses, we assessed the semantic distance between the  
8 significant deregulated biological processes emerged from the GSEA analysis performed on data  
9 from LF1. This approach allowed us to group GSEA categories into deregulated clusters and to  
10 identify one cluster encompassing genes target of polycomb repressive complex 2 (PRC2) (NES  
11 = 1.89, qvalue = 0.0004). This multiprotein complex acts as a chromatin repressor, by catalyzing  
12 the reaction of trimethylation at the level of lysine 27 of histone 3 (H3K27me3), thus inducing  
13 transcriptional repression at its target loci. The reported biological functions of PRC2, together  
14 with our evidence that the promoters of HLA class II genes and regulators appeared in a closed  
15 conformational status (**Fig. 2C**) and that computational analyses highlighted PRC2 target genes  
16 as one of the main gene category deregulated in our sample sets, led us to the hypothesis that  
17 PRC2 may act as a potential player driving immune evasion of HLA class II negative leukemia  
18 post-transplantation relapses.

19  
20 ***Pharmacological inhibition of Enhancer of Zeste Homologue 2 (EZH2) rescues the HLA class***  
21 ***II expression of post-transplantation relapses***

22 To experimentally test the involvement of PRC2 in maintaining the transcriptional repression of  
23 HLA class II loci, we examined the effect of a panel of inhibitors targeting the catalytic domain  
24 of PRC2, EZH2 (Tazemetostat/EPZ-6438, GSK126, GSK34, PF06726, EI1, GSK503,  
25 EPZ01198, CPI169, UNC1999), and other subunits relevant for PRC2 correct assembly and

1 function, EED (EEDi 1 and EED226) and JARID2 (JIB-04). In accordance with the previously  
2 reported data<sup>11</sup>, we found that all PRC2 chemical inhibitors tested restore the HLA class II  
3 expression to a similar extent (expression after DMSO treatment = 2.01%; Mean of all the PRC2  
4 inhibitors tested = 8.7%; range 4.2-13.8%). (**Fig. 3A**). Among the EZH2 inhibitors tested,  
5 Tazemetostat is in early stage clinical trials for the treatment of a variety of hematological  
6 malignancies including lymphoma. Thus, we decided to use this specific inhibitor for all  
7 subsequent experiments.

8 Tazemetostat was effective in reducing H3K27me3 levels in Jurkat cell line and in our case of  
9 HLA class II negative relapse (**Fig. 3B-C**). Next, we performed ex vivo treatment with  
10 Tazemetostat of two AML relapses with non-genomic loss of HLA class II expression. Of note,  
11 chemical inhibition of EZH2 through the use of the small molecule Tazemetostat significantly  
12 increased both transcriptional and surface expression of HLA class II genes (**Fig. 3D-E**). To  
13 further enhance the degree of transcriptional induction of HLA class II genes, we tested the effect  
14 of Tazemetostat in presence of IFN- $\gamma$ , a well-established positive regulator of HLA class II  
15 expression via CIITA promoter activation. In line with other works reporting that PRC2  
16 inhibition can potentiate the transcriptional response to IFN- $\gamma$  of HLA class I genes<sup>12</sup>, the  
17 suppression of PRC2 enzymatic activity amplified the IFN- $\gamma$ -induced HLA class II upregulation  
18 in both the HLA class II negative relapse tested and this is consistent for all the PRC2 inhibitors  
19 employed (**Fig. 3F**). Interestingly and consistent with our bioinformatic analysis showing no  
20 involvement of DNA methylation changes in the regulation of post-transplantation immune  
21 evasion of HLA class II negative relapse (**Fig. 2A**), the treatment with the hypomethylating agent  
22 azacytidine had no effect on the expression of HLA class II genes even in combination with IFN-  
23  $\gamma$  treatment. These observations showed that PRC2-dependent changes, and not DNA  
24 methylation, contribute to the transcriptional repression of HLA class II genes and its inhibition  
25 renders these genes more prone to respond to IFN- $\gamma$  stimulation.

1 ***EZH2i-mediated upregulation of HLA class II expression enhances T cell recognition of***  
2 ***relapsed leukemia***

3 To evaluate whether PRC2 inhibition rescues T-cell mediated recognition of AML blasts, we  
4 collected CD4<sup>+</sup> T cells from an HLA-disparate individuals and co-cultured them with leukemia  
5 blasts at the time of diagnosis to enriched for tumor-specific T cells. After two rounds of  
6 stimulation, we tested primed CD4<sup>+</sup> T cells against leukemia at diagnosis and at post-  
7 transplantation relapse upon treatment with EPZ-6438, IFN- $\gamma$  and combination of the two  
8 treatments.

9 The level of cytotoxicity was measured by IFN- $\gamma$  ELISpot assay. As expected, we found full T  
10 cell recognition of patient leukemia at diagnosis and a lack of response of the same T cells  
11 against leukemia blasts post-transplantation (Mean N° = 51.7). Importantly, we detected, as  
12 expected, T cell activation against leukemic blasts at diagnosis (the number of spot reached the  
13 saturation point, we thus reported N° = 1000 as a convention), no recognition of relapse blasts  
14 pre-treated with DMSO (Mean N° = 51.7), a slight increase of spot number in Tazemetostat  
15 condition (Mean N° = 72), a recovery of T cell recognition when the blasts were pre-treated with  
16 IFN-  $\gamma$  (Mean N° = 113.5) and the maximum T cell activation against relapsed blasts pre-treated  
17 with both Tazemetostat and IFN- $\gamma$  that maximally induced HLA class II expression (Mean N° =  
18 222.5) (**Fig. 3G**). Our results suggest that PRC2 inhibition unlocks the repression of HLA class II  
19 genes and further primes blasts to respond to IFN- $\gamma$  treatment for efficient CD4<sup>+</sup> T cell activation  
20 and leukemia eradication.

21

22 **Discussion**

23 In the context of allo-HCT for AML, the main mediators of immunotherapeutic effects are the  
24 donor CD4<sup>+</sup> and CD8<sup>+</sup> T cells transferred to the host as part of the graft. Indeed, alloreactivity  
25 against mismatched HLA molecules accounts for a significant fraction of to the graft versus

1 leukemia (GvL) effect. This strong and prolonged donor T cell function can eventually lead to the  
2 selection of immune-resistant clones, able to evade immune control and eventually leading to  
3 clinical relapse<sup>13,14</sup>. A common way for tumor cells to achieve the invisibility from cytotoxic T  
4 cells is, for obvious immunological reasons, the deregulation of HLAs and other molecules  
5 belonging to the antigen processing and presentation machinery<sup>13,14</sup>. Genomic loss of  
6 incompatible HLA molecules is one frequent and well-established mechanism of AML immune  
7 evasion and post-transplantation relapse, accounting for up to one third of relapses after allo-HCT  
8 from partially-incompatible family donors<sup>15,16,17</sup>. However, both in leukemia and in solid tumors  
9 not all alterations in the antigen processing and presentation pathway can be explained by genetic  
10 mutations, and there is growing evidence that silencing of HLA molecules and regulators could  
11 be linked to epigenetic changes.

12 Our group and others recently described that transcriptional silencing of HLA class II genes  
13 accounts for more than the 40% of all the immune-evasion mechanisms occurring after allo-  
14 HCT<sup>18,2</sup>. The failure to detect somatic mutations in HLA genes and their known regulators  
15 pointed to the epigenetic nature of this phenomenon, but the molecular alterations at its basis  
16 remained elusive, providing the rationale for the present study, which aims to extensively  
17 characterize the epigenetic alterations driving the non-genomic loss of HLA class II expression in  
18 leukemia post-transplantation AML relapses.

19 For this purpose, we selected an exemplary case of relapse with non-genomic loss of expression  
20 of HLA class II and analyzed in detail the changes in gene expression, DNA methylation and  
21 chromatin architecture that occurred in leukemic cells during disease history. Confirming the  
22 immune-related origin of this relapse case, gene expression profiling confirmed the deregulation  
23 of genes belonging to the transcriptional signature identified in our previous work<sup>2</sup>. Intriguingly,  
24 these transcriptional changes correlated with alterations in the chromatin architecture, supporting  
25 our driver hypothesis that immune-related alteration may be consequence of epigenetic



1 remodeling enacted by leukemic relapsed blasts to counteract donor immune system recognition  
2 and killing.

3 The two main ways by which epigenetic regulators can silence gene expression are DNA  
4 methylation and chromatin compaction driven by modifications of histone tails. Which one of  
5 these two routes, and the main targets of their action, remained to be investigated in order to  
6 understand this phenomenon. CIITA, the master regulator of HLA class II gene expression, has  
7 been found downregulated in the majority of cases with HLA class II deficiency, and its  
8 downregulation positively correlates with suppression of HLA class II. CIITA silencing has been  
9 linked to increased methylation of its promoter region, and Christopher and colleagues, recently  
10 reported a modest increase in DNA methylation in the region of the CIITA promoter/intron 1 in  
11 two cases with HLA class II downregulation<sup>18</sup>; however, in contrast with this evidence, our  
12 comprehensive analysis performed by MOFA showed that in our case, the differences between  
13 diagnosis and relapse samples mainly relied on chromatin conformational changes. Moreover, at  
14 the functional level, we never observed efficacy of the hypomethylating agent azacytidine in  
15 restoring HLA class II expression.

16 Several emerging evidences reported a role for polycomb repressive complex 2 (PRC2) in  
17 regulating expression of HLA molecules. Specifically, it has been reported that HLA deficiency  
18 in diffuse large B-cell lymphomas is due to mutations hitting the catalytic subunit of the  
19 epigenetic repressor PRC2<sup>11</sup> and, more recently, another study demonstrated that the  
20 transcriptional downregulation of HLA class I genes and regulators can be explained by aberrant  
21 functions of the same complex<sup>12</sup>. On the same line, we found that the chromatin in proximity of  
22 the promoters of HLA class II genes and the master regulator of their transcription CIITA, is in a  
23 closed conformational status, suggesting the presence of a repressor occupying that region. To  
24 gain more insights into this phenomenon, we screened a number of epigenetic compounds  
25 targeting some of the PRC2 subunits including the catalytic domain EZH2 and the accessory

1 molecules EED and JARID2. In accordance with our omics data, we found that all tested PRC2  
2 inhibitors restored HLA class II expression and that the combinatorial treatment with IFN- $\gamma$   
3 further enhanced this rescue.

4 Although the direct PRC2 dependent regulation of immune-related gene signatures requires  
5 further characterizations, including the identification of PRC2 binding sites or the specific  
6 localization of its associated repressive histone mark (H3K27me3), our functional analyses gave  
7 us confidence that PRC2 regulates directly or through the orchestrated interaction with other  
8 epigenetic factors or pathways, HLA class II genes and regulators in these specific cases of post-  
9 transplantation disease relapse.

10 Among the EZH2 inhibitors tested, GSK126 and Tazemetostat/EPZ-6438 are the ones in the  
11 most advanced stage of clinical testing for the treatment of a variety of hematological  
12 malignancies including lymphoma, possibly speeding up their eventual testing in the setting of  
13 AML post-transplantation relapse. Of notice, besides their intended antiproliferative effects and  
14 their role in restoring HLA class I and II expression, recently published preclinical data  
15 highlighted the role of EZH2 inhibitors in enhancing antitumor immunity by altering the ratio  
16 between the effector and regulatory T cells in favor of the first population<sup>19</sup>. Moreover, the  
17 effects of epigenetic therapies in inducing endogenous retroviral (ERV) transcripts triggering the  
18 series of immune-activation cascades bringing to antitumor efficacy are well known<sup>20,21</sup>. Thus,  
19 we can speculate that EZH2 inhibitor-induced antitumor effects can as well be linked to ERVs  
20 reactivations, further suggesting that they may well apply to the setting of allo-HCT.

21 However, by targeting the catalytic subunit of PRC2, EZH2, we obtained just the partial rescue of  
22 HLA class II expression. It is well established that EZH2 paralogue, EZH1, can as well become  
23 part of the complex by associating with EED and SUZ12. Thus, EZH1 activity may compensate  
24 for the inhibition of EZH2, maintaining the HLA class II genes still suppressed. Indeed,

1 inhibitors that effectively target both EZH1 and EZH2 or the other component of the complex  
2 have to be tested to prove this model.

3 The molecular insights described here provide a detailed understanding of how AML post-  
4 transplantation relapse blasts suppress HLA class II genes to evade immune surveillance. This  
5 also support the hypothesis that the resistance to immune pressure, arising very frequently in the  
6 context of allo-HCT, may occur not only through genomic alterations<sup>15,16,17</sup>, but also through  
7 non-genomic mechanisms that exploit the activity of repressive chromatin complexes such as  
8 PRC2. Lastly, our experimental evidence paves the way for future therapeutic strategies aiming at  
9 incorporating PRC2 inhibition into immunotherapeutic protocols to avoid post-transplantation  
10 immune evasion and relapse.

11

## 12 **Acknowledgments**

13 This work was supported by a San Raffaele Pilot Grant awarded to R.D.M. and L.V., by the  
14 Italian Ministry of Health (RF-2011-02351998 to F.C. and L.V., RF-2011-02348034 to L.V.,  
15 GR-2018-12367860 and TRANSCAN HLALOSS to L.V.), by the Associazione Italiana per la  
16 Ricerca sul Cancro (Start-Up Grant #14162 and IG #22197to L.V.), by Telethon (TIGET grant  
17 E5 to R.D.M.), by a Career Development Award from Human Frontier Science Program (HFSP  
18 to R.D.M.), by an Advanced Research Grant from the European Hematology Association (EHA  
19 to R.D.M.), by a Hollis Brownstein Research Grant from Leukemia Research Foundation (LRF  
20 to R.D.M.) and by the Interstellar Initiative on Healthy Longevity from NYAS and AMED (to  
21 R.D.M.).

22

## 23 **Author contributions**

24 V.G. designed experiments, performed experimental work, analyzed the data and wrote  
25 manuscript. V.G., D.G., L.Zi. and L.Za. performed the *ex vivo* and *in vitro* experiments. V.G. and

1 G.O. performed the *in vivo* experiments. S.B., I.M. and D.C. performed all bioinformatic  
2 analyses. L.V. and F.C. collected and analyzed patient samples and clinical data. R.D.M. and  
3 L.V. conceived the study, interpreted data, supervised research and wrote the manuscript.

4

5 **Competing interests**

6 L.V. received research support from GenDx and Moderna Therapeutics. None of the other  
7 authors has any relevant conflicts of interest to disclose.

1 **References**

- 2 1. Zeiser, R. & Vago, L. Mechanisms of immune escape after allogeneic hematopoietic cell  
3 transplantation. *Blood* **133**, 1290–1297 (2019).
- 4 2. Toffalori, C. et al. Immune signature drives leukemia escape and relapse after  
5 hematopoietic cell transplantation. *Nat. Med.* **25**, 603–611 (2019).
- 6 3. Christopher, M. J. et al. Immune Escape of Relapsed AML Cells after Allogeneic  
7 Transplantation. *N. Engl. J. Med.* **379**, 2330–2341 (2018).
- 8 4. Stevanović, S., van Schie, M. L. J., Griffioen, M. & Falkenburg, J. H. HLA-class II  
9 disparity is necessary for effective T cell mediated Graft-versus-Leukemia effects in NOD/scid  
10 mice engrafted with human acute lymphoblastic leukemia. *Leukemia* **27**, 985–987 (2013).
- 11 5. Fleischhauer, K. & Shaw, B. E. HLA-DP in unrelated hematopoietic cell transplantation  
12 revisited: challenges and opportunities. *Blood* **130**, 1089–1096 (2017).
- 13 6. Li, S. et al. Distinct evolution and dynamics of epigenetic and genetic heterogeneity in  
14 acute myeloid leukemia. *Nat. Med.* **22**, 792–799 (2016).
- 15 7. Corces, M. R. et al. Lineage-specific and single cell chromatin accessibility charts human  
16 hematopoiesis and leukemia evolution. *Nat Genet* **48**, 1193–1203 (2016).
- 17 8. Ntziachristos, P. et al. Genetic inactivation of the polycomb repressive complex 2 in T  
18 cell acute lymphoblastic leukemia. *Nat. Med.* **18**, 298–301 (2012).
- 19 9. Gu, H. et al. Preparation of reduced representation bisulfite sequencing libraries for  
20 genome-scale DNA methylation profiling. *Nat Protoc* **6**, 468–481 (2011).
- 21 10. Argelaguet, R. et al. Multi-Omics Factor Analysis—a framework for unsupervised  
22 integration of multi-omics data sets. *Mol. Syst. Biol.* **14**, e8124 (2018).
- 23 11. Ennishi, D. et al. Molecular and Genetic Characterization of MHC Deficiency Identifies  
24 EZH2 as Therapeutic Target for Enhancing Immune Recognition. *Cancer Discov* **9**, 546–563  
25 (2019).

- 1 12. Burr, M. L. et al. An Evolutionarily Conserved Function of Polycomb Silences the MHC  
2 Class I Antigen Presentation Pathway and Enables Immune Evasion in Cancer. *Cancer Cell*  
3 (2019) doi:10.1016/j.ccell.2019.08.008.
- 4 13. Garrido, F., Aptsiauri, N., Doorduijn, E. M., Garcia Lora, A. M. & van Hall, T. The  
5 urgent need to recover MHC class I in cancers for effective immunotherapy. *Current Opinion in*  
6 *Immunology* **39**, 44–51 (2016).
- 7 14. Leone, P. et al. MHC Class I Antigen Processing and Presenting Machinery:  
8 Organization, Function, and Defects in Tumor Cells. *JNCI Journal of the National Cancer*  
9 *Institute* **105**, 1172–1187 (2013).
- 10 15. Vago, L. et al. Loss of mismatched HLA in leukemia after stem-cell transplantation. *N.*  
11 *Engl. J. Med.* **361**, 478–488 (2009).
- 12 16. Crucitti, L. et al. Incidence, risk factors and clinical outcome of leukemia relapses with  
13 loss of the mismatched HLA after partially incompatible hematopoietic stem cell transplantation.  
14 *Leukemia* **29**, 1143–1152 (2015).
- 15 17. Vago, L., Toffalori, C., Ciceri, F. & Fleischhauer, K. Genomic loss of mismatched human  
16 leukocyte antigen and leukemia immune escape from haploidentical graft-versus-leukemia.  
17 *Semin. Oncol.* **39**, 707–715 (2012).
- 18 18. Christopher, M. J. et al. Immune Escape of Relapsed AML Cells after Allogeneic  
19 Transplantation. *N. Engl. J. Med.* **379**, 2330–2341 (2018).
- 20 19. Wang, D. et al. Targeting EZH2 Reprograms Intratumoral Regulatory T Cells to Enhance  
21 Cancer Immunity. *Cell Reports* **23**, 3262–3274 (2018).
- 22 20. Chiappinelli, K. B. et al. Inhibiting DNA Methylation Causes an Interferon Response in  
23 Cancer via dsRNA Including Endogenous Retroviruses. *Cell* **162**, 974–986 (2015).
- 24 21. Roulois, D. et al. DNA-Demethylating Agents Target Colorectal Cancer Cells by  
25 Inducing Viral Mimicry by Endogenous Transcripts. *Cell* **162**, 961–973 (2015).

1 **Figure legends**

2 **Figure 1.** Patient-Derived Xenografts Recapitulate the Immune-Related and Epigenetic Features  
3 of Primary Post-Transplantation Relapses. (a) Experimental sample sets including diagnosis  
4 (blue) and relapse (red) primary and patient derived xenografts (PDXs) (b) Representative FACS  
5 analysis and percentage of HLA-DR surface expression of primary (stars) and PDX (shapes)  
6 diagnosis (red) and relapse (blue) samples. (c) Principal Component Analysis (PCA) showing the  
7 clear separation of diagnosis and relapse samples by RNA-Seq (left panel) and ATAC-Seq (right  
8 panel). D. Correlation between transcript deregulation detected by RNA-Seq and differential  
9 chromatin accessibility detected by ATAC-Seq.

10 **Figure 2.** HLA class II downregulation at relapse is associated to chromatin compaction and  
11 activity of the PRC2 repressor complex. (a) Integrative epigenomics analysis by MOFA  
12 indicating the relative contribution of each technique in explaining the technical and biological  
13 variability between diagnosis and relapse samples. (b) Gene set enrichment analysis (GSEA)  
14 performed on latent factor 1 from MOFA matched with the relapse immune signature (c) GSEA  
15 performed on latent factor 1 from MOFA matched with EZH2 target gene list (d) IGV  
16 visualization of RNA-Seq and ATAC-Seq tracks from UPN#03 primary and PDX representative  
17 samples. Shown are the coordinates where HLA-DPB1 (left panel) and CIITA (right panel) are  
18 located to the genome.

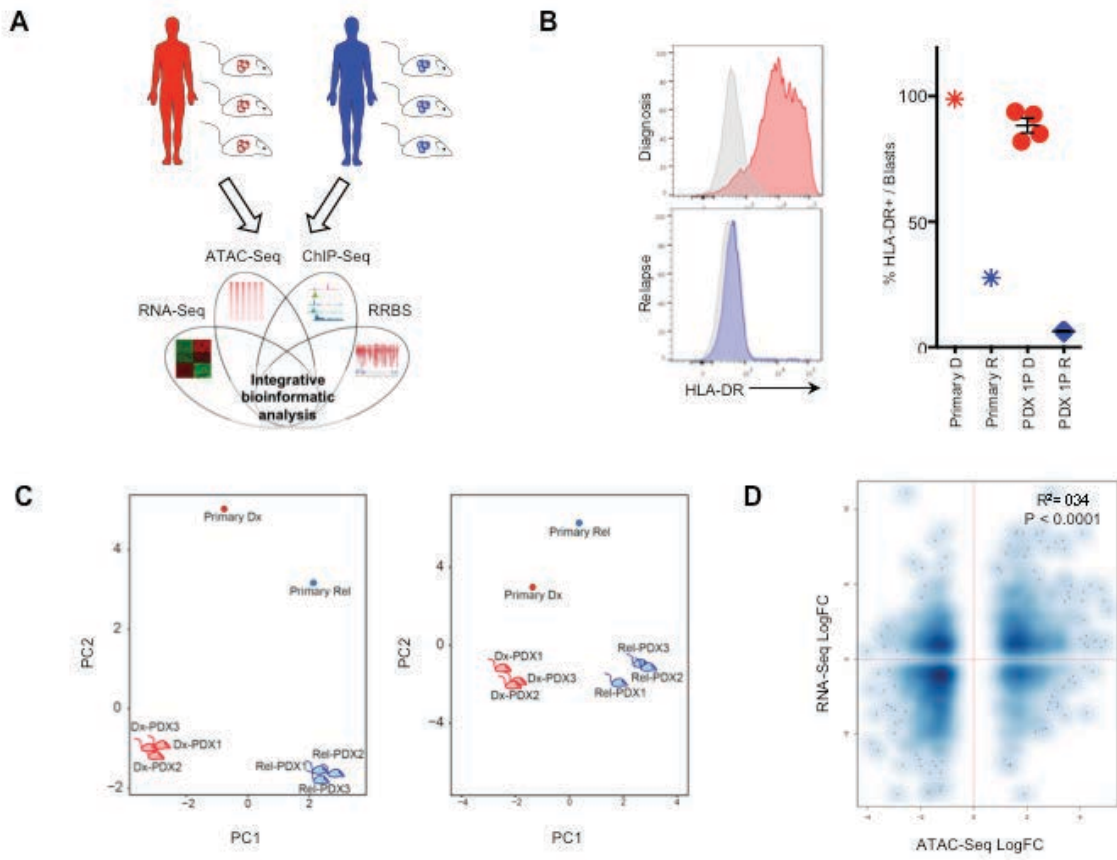
19 **Figure 3.** Inhibition of PRC2 and its subunit EZH2 leads to recovery of HLA class II expression  
20 on relapsed leukemia. (a) Surface expression of HLA-DR molecule after the treatment with a list  
21 of PRC2 inhibitors. The results on one experiment performed on UPN#03 are shown. The  
22 different shades of grey indicates that the compounds differ according to the PRC2 subunit they  
23 target. (b) Western blot for H3K27me3 performed on Jurkat cell line indicates that the histone  
24 methyltransferase inhibitor EPZ6438 is able to inhibit EZH2 activity (reduction of H3K27me3)  
25 already at day3 after the treatment in a dose-dependent manner. Tubulin was used as a loading

1 control. (c) Immunofluorescence analysis for H3K27me3 (in green) and DAPI (blue) of a  
2 primary AML relapse sample co-cultured for 7 days with supportive MS-5 cells in presence or  
3 absence of EPZ-6438. (d) Gene expression analysis of CIITA, and some HLA class II genes  
4 measured by qPCR of UPN#03 (top panel) and UPN#10 (bottom panel) (e) Representative plots  
5 showing the immunophenotypic analysis of HLA-DR cell surface expression of UPN#03 (left  
6 panel) and summary of 6 experiments performed on the same sample (right panel). For all  
7 comparisons paired t test was used (\*\*P < 0.01, \*\*\*P < 0.005). (f) Surface expression of HLA-  
8 DR molecule after the treatment with a list of PRC2 inhibitors in combination with IFN- $\gamma$ . (g)  
9 ELISpot assay showing the CD4<sup>+</sup> T cell activation against AML samples at diagnosis and relapse  
10 alone or after treatments.

11

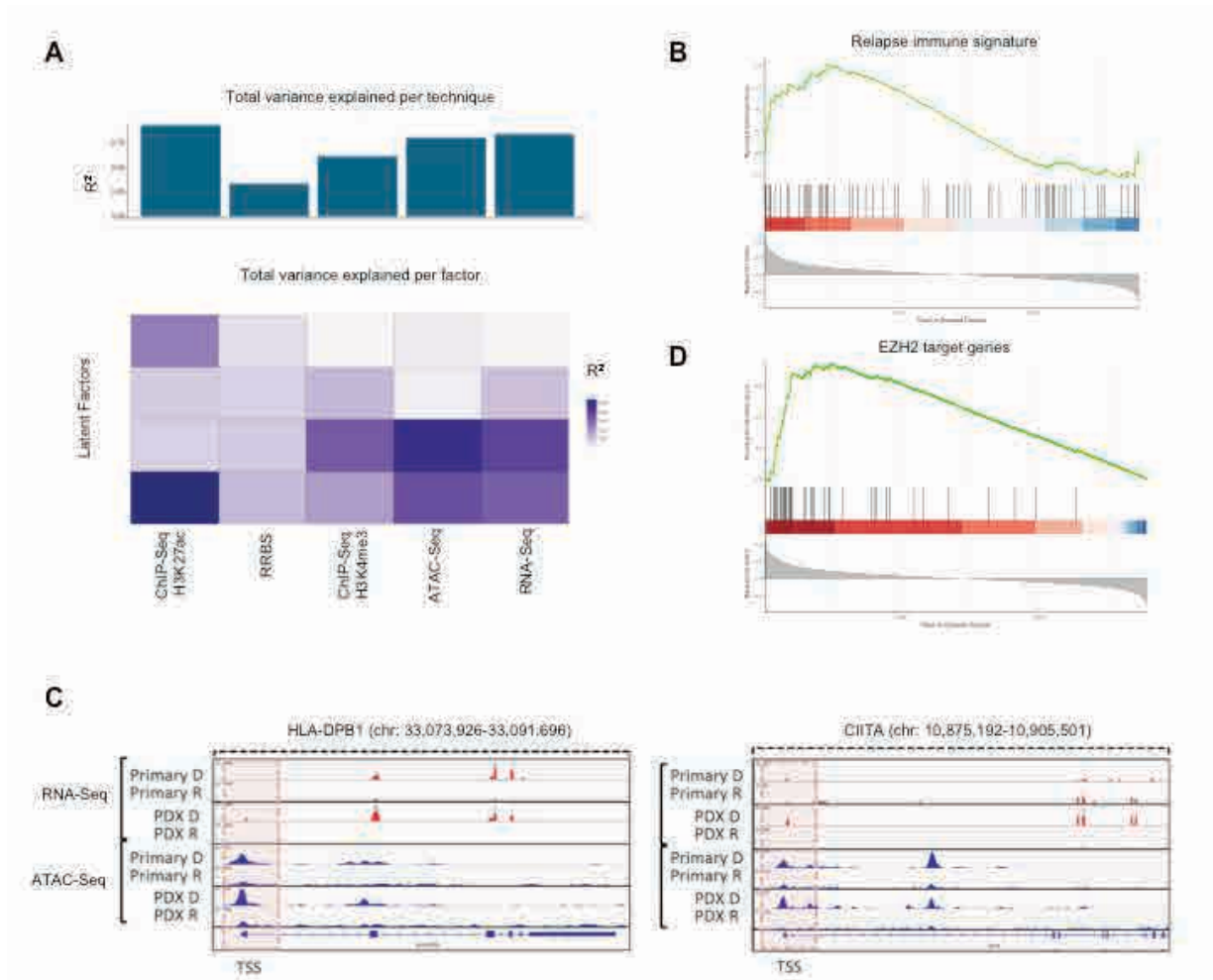


1 **Figure 1**



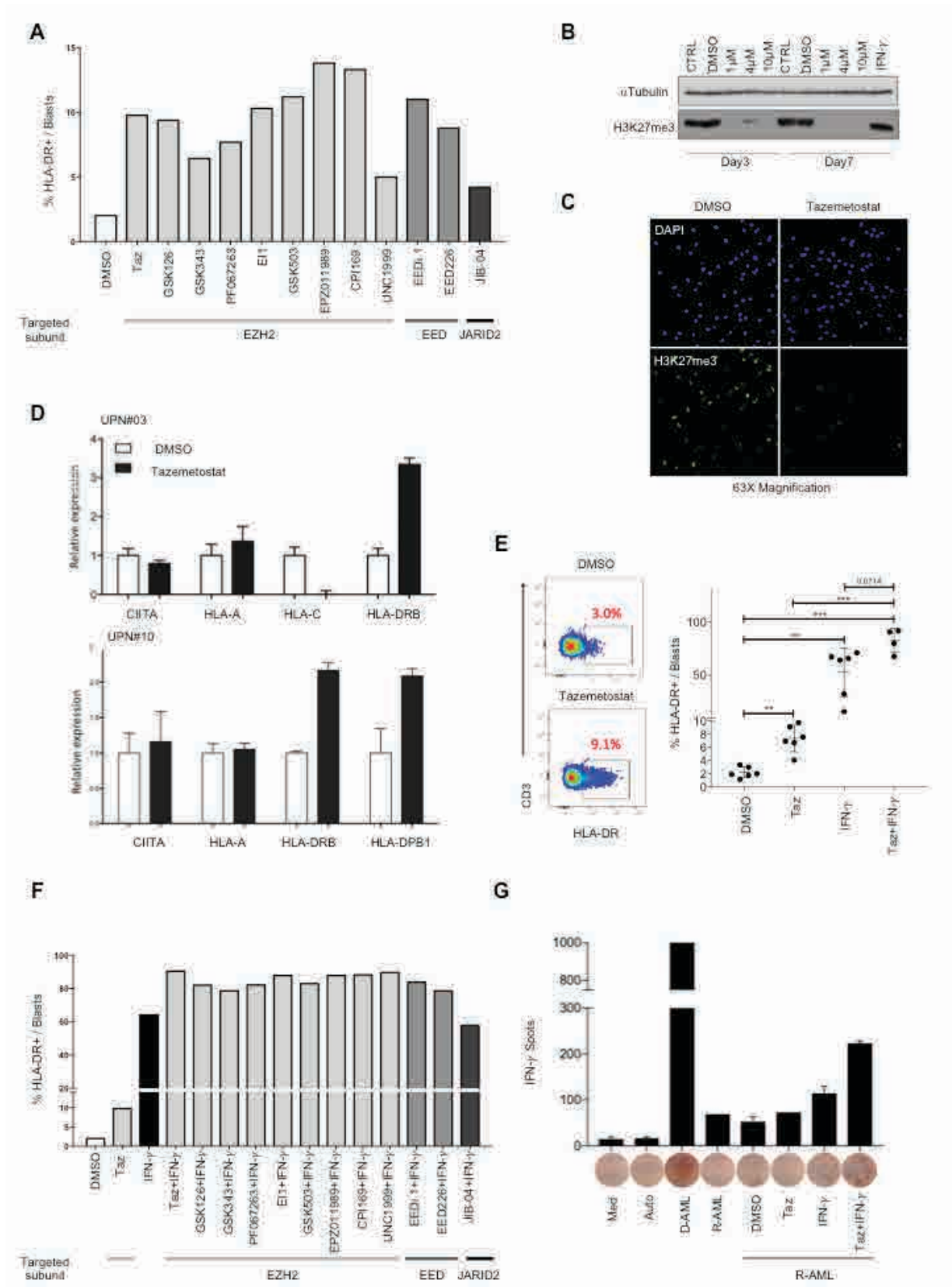
2

1 **Figure 2**



2

1 **Figure 3**



2



**Chapter 8.**

**Epigenetic Therapies for Acute Myeloid Leukemia and Their Immune-Related Effects**

Gambacorta V, Gnani D, Vago L, Di Micco R

*Published in Frontiers in Cell and Developmental Biology (2019)*



# Epigenetic Therapies for Acute Myeloid Leukemia and Their Immune-Related Effects

Valentina Gambacorta<sup>1,2,3</sup>, Daniela Gnani<sup>1</sup>, Luca Vago<sup>2,4</sup> and Raffaella Di Micco<sup>1\*</sup>

<sup>1</sup> Unit of Senescence in Stem Cell Aging, Differentiation and Cancer, San Raffaele Telethon Institute for Gene Therapy (SR-TIGET), IRCCS San Raffaele Scientific Institute, Milan, Italy, <sup>2</sup> Unit of Immunogenetics, Leukemia Genomics and Immunobiology, IRCCS San Raffaele Scientific Institute, Milan, Italy, <sup>3</sup> Milano-Bicocca University, Milan, Italy, <sup>4</sup> Unit of Hematology and Bone Marrow Transplantation, IRCCS San Raffaele Scientific Institute, Milan, Italy

## OPEN ACCESS

### Edited by:

Chiara Lanzuolo,  
Institute of Cell Biology  
and Neurobiology (CNR), Italy

### Reviewed by:

Antonius Plagge,  
University of Liverpool,  
United Kingdom  
Ivana Gojo,  
Johns Hopkins University,  
United States

### \*Correspondence:

Raffaella Di Micco  
dimicco.raffaella@hsr.it

### Specialty section:

This article was submitted to  
Epigenomics and Epigenetics,  
a section of the journal  
Frontiers in Cell and Developmental  
Biology

Received: 23 May 2019

Accepted: 11 September 2019

Published: 11 October 2019

### Citation:

Gambacorta V, Gnani D, Vago L  
and Di Micco R (2019) Epigenetic  
Therapies for Acute Myeloid Leukemia  
and Their Immune-Related Effects.  
*Front. Cell Dev. Biol.* 7:207.  
doi: 10.3389/fcell.2019.00207

Over the past decades, our molecular understanding of acute myeloid leukemia (AML) pathogenesis dramatically increased, thanks also to the advent of next-generation sequencing (NGS) technologies. Many of these findings, however, have not yet translated into new prognostic markers or rationales for treatments. We now know that AML is a highly heterogeneous disease characterized by a very low mutational burden. Interestingly, the few mutations identified mainly reside in epigenetic regulators, which shape and define leukemic cell identity. In the light of these discoveries and given the increasing number of drugs targeting epigenetic regulators in clinical development and testing, great interest is emerging for the use of small molecules targeting leukemia epigenome. Together with their effects on leukemia cell-intrinsic properties, such as proliferation and survival, epigenetic drugs may affect the way leukemic cells communicate with the surrounding components of the tumor and immune microenvironment. Here, we review current knowledge on alterations in the AML epigenetic landscape and discuss the promises of epigenetic therapies for AML treatment. Finally, we summarize emerging molecular studies elucidating how epigenetic rewiring in cancer cells may as well exert immune-modulatory functions, boost the immune system, and potentially contribute to better patient outcomes.

**Keywords:** acute myeloid leukemia, epigenetics, therapy, immune activation, chromatin

## INTRODUCTION

Acute myeloid leukemia (AML) is an aggressive blood cancer, characterized by the uncontrolled proliferation of poorly differentiated hematopoietic stem and progenitor cells. Even if disease prognosis has improved over the last decades, mainly thanks to decreased treatment-related mortality and wider use of allogeneic hematopoietic cell transplantation (allo-HCT) as consolidation therapy, prognostic classification of AML patients remains inaccurate and therapeutic options for high-risk patient are largely unsatisfactory (Dohner et al., 2015).

Moreover, even if AML is often initially sensitive to chemotherapy, relapse events remain frequent either due to the emergence of chemotherapy-resistant clones (Lokody, 2014) or post-transplantation immune-escape mechanisms enacted by leukemic cells to evade donor immune system control (Vago et al., 2009; Toffalori et al., 2012; Christopher et al., 2018; Toffalori et al., 2019; Zeiser and Vago, 2019). Therefore, more effective combinatorial or alternative therapies are needed for AML patients.

In spite of being one of the tumors with the lowest mutational load, AML is a highly heterogeneous disease in terms of genetic background and clinical manifestation. Interestingly, although very few, mutations frequently hit genes encoding for proteins that regulate DNA methylation (such as DNMT3A, TET2, IDH1, and IDH2), affect post-translational modifications on histone tails (such as EZH2, ASXL1, and others), and drive three-dimensional chromatin conformation of cancer cells (such as CTCF and cohesin complex). In addition to mutations in epigenetic regulators, some of the fusion proteins that are known to drive abnormal transcriptional programs in AML act through aberrant expression or redirected specificity of epigenetic regulators. More broadly, global alterations in DNA methylation patterns and enhancer deregulation were recently linked to AML clonal expansion, further supporting the notion that epigenetic heterogeneity better explains leukemia identity compared to the genetic background (Corces et al., 2016; Li S. et al., 2016). The AML epigenome has therefore emerged as a new exciting target for drug discovery. Epigenetic modifications regulate chromatin states and gene expression changes without altering DNA sequences through distinct mechanisms including, among others, DNA methylation and post-translational modifications on histone tails. Our genome encodes for several enzymes that are able to deposit or remove chemical marks within specialized domains (writers and erasers, respectively) and to bind and recognize them (readers). The coordinated action of epigenetic writers, erasers, and readers are important for tight regulation of gene expression through downstream molecular effectors, thus contributing to both cancer development and progression. Unlike genetic alterations, epigenetic changes are dynamic and reversible, and the past decades have seen a dramatic increase of discoveries and clinical applications of small molecules targeting epigenetic modifiers with the final goal to restore normal epigenetic patterns in cancer cells. Compared to other targeted approaches, epigenetic therapies may potentially reduce the emergence of molecular resistance and clinical recurrence by simultaneously impacting on distinct cellular pathways. In addition, besides the aforementioned cell autonomous mechanisms of action, epigenetic therapies may have immunomodulatory properties and further enhance the sensitivity of cancer cells to immune therapies. In this Review, we provide an overview of epigenomic changes involved in AML pathogenesis and describe the mechanisms of action of epigenetic drugs currently in use or under investigation for AML treatment. **Table 1** summarizes the status of epigenetic therapies for AML from preclinical testing to clinical approval. Finally, we discuss emerging concepts and promising new therapeutic approaches based

on the interplay between epigenetic therapies and immune system modulation.

## EPIGENOME DEREGULATION AND EPIGENETIC THERAPIES FOR AML TREATMENT

### Epigenome Writers

The enzymes able to catalyze modifications on DNA or histone proteins are named “epigenetic writers” and can be classified into enzymes impacting on DNA methylation, histone methyltransferases (HMTs), and histone acetyltransferases (HATs). The first category includes all the proteins that directly contribute to the regulation of DNA methylation (DNA methyltransferases; DNMTs). The HMT category comprises lysine methyltransferases (KMTs) and arginine methyltransferases (PRMTs). Methylation of histone tails promotes both gene activation and repression depending on the modified histone residue. In detail, methylation of H3K4, H3K36, H3K79, and H4R3 is generally associated to transcriptional activation, while methylation of H3K9, H3K27, and H4K20 induces transcriptional repression. Finally, HATs are epigenetic writers responsible for acetylation of lysine residues on nucleosomes, which is associated to open chromatin and activation of gene expression.

### DNA Methylation

#### *DNMTs*

DNA methylation is a heritable epigenetic mark mainly contributing to gene repression. Specifically, DNA methylation levels are under the control of enzymes able to modulate the addition (by DNA methyl transferases; DNMTs) or the removal (by the indirect action of TET and IDH1/2 proteins) of methyl groups to cytosine or adenine residues. Besides the essential physiological functions, alterations in DNA methylation pattern have been extensively described in different cancer types including AML. Importantly, it has been reported that genetic alleles and epialleles (as assessed by genome-wide DNA methylation profile) can evolve independently from each other during AML progression and that the DNA methylation patterns can be used to stratify patients and predict clinical outcome (Li S. et al., 2016; Figueroa et al., 2010b). Interestingly, these changes are mostly determined by DNA methylation of non-promoter regulatory regions rather than at the level of gene promoters. Indeed, different methylation patterns of enhancer elements can also precisely distinguish normal blood cell from leukemic cells in different disease stages (Figueroa et al., 2010b; Qu et al., 2017). Moreover, in AML cells, aberrantly methylated sites, mainly residing in gene bodies and enhancer elements, often display features associated with aged blood cells including, among the others, chromatin changes in immune and cell-adhesion genes (Glass et al., 2017; Adelman et al., 2019). One possible driver of the epigenetic reprogramming of AML blasts can be the presence of somatic mutations affecting DNMTs. DNMT3A, a *de novo* methyltransferase, is mutated in 20–25% of AML patients (Thol et al., 2011a; Cancer Genome Atlas Research et al., 2013;

**TABLE 1 |** Epigenetic therapies in AML.

Epigenetic regulator	Function	Frequency in AML	Compound	Target	Pre Clinical Studies	Clinical Trials	Approved
DNMT	DNA methylation	20–25%	Azacitidine (5-azacytidine)	RNA (60–80%) and DNA (20%)	█	█	█
			Decitabine (5-aza-2'-deoxycytidine)	DNA	█	█	█
			Guadecitabine (SGI-110)	DNA	█	█	█
TET	Regulation of DNA methylation	8–10%	Vitamin C	TET2 mut	█	█	█
			2-hydroxyglutarate	TET2 mut	█	█	█
IDH1/2	Regulation of DNA methylation	6–13%	AGI-5197	IDH1 mut	█	█	█
			HMS-101	IDH1 mut	█	█	█
			Ivosidenib (AG-120)	IDH1 mut	█	█	█
			AGI-6780	IDH2 mut	█	█	█
			Enasidenib (AG-221)	IDH2 mut	█	█	█
MLL	Histone lysine methyltransferase	5–10%	MI-401	MLL-WDR5	█	█	█
			MIV-6R	MLL-Menin	█	█	█
			MI-463	MLL-Menin	█	█	█
			MI-503	MLL-Menin	█	█	█
			EPZ-04777	DOT1L	█	█	█
			SGC-0946	DOT1L	█	█	█
			Pinometostat (EPZ-5676)	DOT1L	█	█	█
			EPZ-040414	SETD2	█	█	█
SETD2	Histone lysine methyltransferase	>20% of MLL-Rearranged leukemias	Pinometostat (EPZ-5676)	DOT1L	█	█	█
			JIB-04	KDM4A	█	█	█
PoG	Histone lysine methyltransferase	Rare (2%)	Tazemetostat (EPZ-6438)	EZH2	█	█	█
			GSK126	EZH2	█	█	█
			UNC1999	EZH1/2	█	█	█
			MAK683	EED	█	█	█
			UNC0638	G9a	█	█	█
G9a	Histone lysine methyltransferase	None	UNC0642	G9a	█	█	█
			A366	G9a	█	█	█
			AMI-408	G9a	█	█	█
PRMT	Histone arginine methyltransferase	None	PRMT1	PRMT1	█	█	█
			EPZ015655	PRMT5	█	█	█
HAT	Histone acetyltransferase	Rare	C646	p300	█	█	█
			L002	p300	█	█	█

(Continued)



TABLE 1 | Continued

Epigenetic regulator	Function	Frequency in AML	Compound	Target	Pre Clinical Studies	Clinical Trials	Approved
KDM1 (LSD1)	Histone lysine demethylase	Rare	Tranylcypromine (TCP)	KDM1	█	█	█
			NCD25	KDM1	█	█	█
			NCD28	KDM1	█	█	█
			SP2509	KDM1	█	█	█
			GSK2879552	KDM1	█	█	█
			IMG-7289	KDM1	█	█	█
HDAC	Histone deacetylase	Rare	Varinostat	HDAC class I/II	█	█	█
			Panobinostat (LBH589)	HDAC class I/II	█	█	█
			Valproic acid (VPA)	HDAC class I	█	█	█
			Romidepsine/depsipeptide	HDAC class I	█	█	█
			Mocetinostat	HDAC class I	█	█	█
			Entinostat	HDAC class I	█	█	█
			BET	Reader of acetyl groups on lysine residues	None	JQ1	BET proteins
I-BET151	BET proteins	█				█	█
OTX015	BET proteins	█				█	█
TEN-010	BET proteins	█				█	█
CPI-0610	BET proteins	█				█	█
GSK525762	BET proteins	█				█	█
EP11313	BET proteins	█				█	█
EP11336	BET proteins	█				█	█
BI-894999	BET proteins	█				█	█

Papaemmanuil et al., 2016) and linked by several studies to decreased overall survival (Thol et al., 2011a; Ribeiro et al., 2012). Notably, the majority of somatic DNMT3A mutations occurs at arginine (R) 882 and lead to decreased catalytic activity and DNA binding affinity. However, the molecular mechanisms by which DNMT3A mutations favor leukemia occurrence are still unclear. It has been originally reported that mutant DNMT3A alters the expression of genes involved in key cellular pathways including apoptosis and hematopoietic stem cell (HSC) self-renewal (Tadokoro et al., 2007; Thol et al., 2011a,b). Deletion of DNMT3A in mice was shown to impair HSC differentiation and to increase the number of phenotypically defined HSCs although no signs of overt malignancy were observed upon transplantation of DNMT3A-deleted HSCs, suggesting that additional alterations may be required for leukemia development (Challen et al., 2011).

Given the pivotal role of DNA methylation in remodeling AML epigenome at both promoters and distal regulatory elements, DNMTs emerged as attractive therapeutic targets to restore normal DNA methylation patterns in leukemic blasts. Two nucleosidic epigenetic compounds inhibiting DNMT activity, azacytidine (5-azacytidine) and decitabine (5-aza-2'-deoxycytidine) (DNMTi), are currently in clinical use for myeloid malignancies. Azacytidine, upon conversion to decitabine, incorporates into newly synthesized DNA, thwarting the binding of DNMTs. Of notice, azacytidine is predominantly incorporated into RNA with a more evident effect on gene translation (Navada et al., 2014). Chemical DNMT inhibition significantly alters DNA methylation patterns with consequent induction of cell cycle arrest, DNA damage accumulation, apoptosis, differentiation, and immune cell activation (Wouters and Delwel, 2016). Both azacytidine and decitabine initially entered standard clinical practice for the treatment of myelodysplastic syndrome (MDS) and AML patients with low blast count. In a subsequent phase II clinical trial, decitabine showed acceptable tolerability and efficacy also in AML patients older than 60 with >30% of blasts and not eligible for intensive chemotherapy (Cashen et al., 2010). Moreover, a phase III trial in older or unfit AML patients reported higher response rate and survival advantage in patients treated with decitabine compared with current standard of care (low-dose cytarabine or supportive care) (Kantarjian et al., 2012). More recently, next-generation DNMT inhibitors with improved stability such as guadecitabine (SGI-110) have been developed and tested in clinical trials with promising results (Issa et al., 2015; Stein and Tallman, 2016; Garcia-Manero et al., 2019). However, to date, the efficacy of DNMTi as single agents for AML treatment is limited, possibly due to the fact that targeting a single layer of epigenetic deregulation (e.g., DNA methylation) cannot be sufficient to reach a complete rescue of the epigenetic landscape of leukemic blasts. On this purpose, several studies reported promising preliminary results from combinatorial treatments of DNMTi with other epigenetic drugs including HDAC inhibitors (HDACi; discussed below), or with agents commonly in use for AML patients such as FLT3 inhibitors, lenalidomide, and antibody-drug conjugates (Gardin and Dombret, 2017). To date, the most promising combination for AML treatment is the one with azacytidine or decitabine and venetoclax (ABT-199), an inhibitor of the anti-apoptotic

protein BCL-2. Mechanistically, venetoclax in combination with hypomethylating agents leads to a metabolic rewiring that suppresses oxidative phosphorylation and selectively triggers apoptosis in leukemic stem cells (Pollyea et al., 2018). From a clinical standpoint, the combinatorial treatment of venetoclax plus DNMTi was effective and well tolerated in elderly AML patients not eligible for intensive chemotherapy (DiNardo et al., 2019).

### TET

Another layer of epigenetic regulation of DNA is the oxidation of 5mC (5hmC), which indirectly prevents the addition of methyl groups on cytosine by DNMTs. This modification is catalyzed by the Ten-Eleven-Translocation (TET) enzymes and depends on the action of isocitrate dehydrogenase 1/2 (IDH1/2) proteins, which in turn produce  $\alpha$ -ketoglutarate ( $\alpha$ -KG) to stimulate TET activity. Somatic mutations in both these classes of enzymes cause aberrant DNA hypermethylation mainly occurring at gene promoters. Specifically, TET2 mutations affect 8–10% of patients with *de novo* AML (Thol et al., 2011a; Cancer Genome Atlas Research et al., 2013; Papaemmanuil et al., 2016) and are associated to a global reduction of 5hmC. This deregulation leads to alterations in several biological processes including differentiation and proliferation (Figueroa et al., 2010a; Moran-Crusio et al., 2011; Quivoron et al., 2011). As previously reported for DNMTs, TET2 activity is not only limited to promoter regions. In fact, genome-wide mapping of TET2 binding sites revealed the presence of this protein also in regulatory regions such as enhancers where it is fundamental for the recruitment of hematopoietic transcription factors including IRE, CEBP, GATA, and HOX proteins (Rasmussen et al., 2015). Also, TET2 loss-of-function mutations have been very recently reported to be important for immune cell activation and for leukemic blast differentiation. Thus, drugs acting on TET2 function (including vitamin C and 2-hydroxyglutarate) can both halt leukemia progression and induce antitumor immune cell-mediated response (Tyrakis et al., 2016; Cimmino et al., 2017; Fraietta et al., 2018).

### IDH1/2

Present in around 6 to 13% of AML patients (Ward et al., 2010), IDH1/2 mutations lead to the production of 2-hydroxyglutarate (2-HG), are mutually exclusive with TET2 alterations and trigger a hypermethylation signature almost completely overlapping to the one characteristic of TET2 mutant cells. Given the relatively high frequency of IDH mutations in AML, over recent years, several small molecules targeting mutated IDH1/2 have been developed, and, upon successful testing in clinical trials, some of them have already been approved by the Food and Drug Administration.

AGI-5198 was the first potent inhibitor of mutant IDH1, initially described in the context of glioma cells. Blockade of IDH1/IDH2 mutant forms reduces 2-HG production and H3K9me3 levels, thus inducing cancer cell differentiation (Rohle et al., 2013). Another IDH1 inhibitor, ivosidenib (AG-120), showed similar ability to promote differentiation of mutated

leukemia cells and received FDA approval last year thanks to the very high response rate in relapse/refractory AML patients (DiNardo et al., 2018). Furthermore, a computational drug screening identified another selective inhibitor of mutant IDH1 (HMS-101), which was also effective in inhibiting leukemia growth *in vitro* (Chaturvedi et al., 2013).

Regarding inhibitors of IDH2, AGI-6780 and enasidenib (AG-221) showed high selectivity for the mutant form of IDH2 sparing the wild-type isoform and have been shown to induce differentiation in AML cells both *in vitro* and in xenograft models of AML (Wang et al., 2013; Yen et al., 2017). The efficacy of enasidenib was also confirmed in relapse/refractory AML patients carrying IDH2 mutation, leading to its recent clinical approval (Stein et al., 2017, 2019).

## Histone Methylation

### MLL

Part of the *Drosophila* Trithorax family of proteins, the lysine methyltransferase MLL (or KMT2A) is involved in the methylation of H3K4 residue (H3K4me1/2/3), a transcriptional activation mark. MLL translocations with multiple factors as well as MLL partial tandem duplications (MLL-PTD) are observed with frequencies ranging from 5 to 10% in AML patients, and are associated with poor prognosis (Schichman et al., 1994; Caligiuri et al., 1998; Dohner et al., 2002; Milne et al., 2002). To date, more than 80 different MLL fusion partners have been identified. MLL translocations result in fusion oncoproteins, which lack the C-terminal SET domain of MLL (responsible for the H3K4 methylation activity) and gain domains from the different fusion partners. Several small molecules inhibiting MLL complexes and cofactors have been developed, and some of them are currently in clinical trials for the treatment of MLL-rearranged leukemias. MM-401 blocks the MLL-WDR5 fusion gene, leading to proliferation arrest and myeloid differentiation of leukemia cells while sparing normal hematopoietic stem/progenitor cells (Cao et al., 2014). Through high-throughput screening and structure-based chemical development, other small molecules targeting the MLL-cofactor interactions were discovered and optimized to target MLL-Menin oncoprotein. Specifically, MIV-6R, MI-463 and MI-503 efficiently and selectively suppressed MLL-rearranged leukemia growth both *in vitro* and *in vivo* (Grembecka et al., 2012; He et al., 2014; Borkin et al., 2015). In the last years, some studies also revealed that in order to drive tumorigenesis, MLL fusion proteins require DOT1L, a unique HMT that specifically catalyzes H3K79 methylation (Okada et al., 2005; Bernt et al., 2011; Jo et al., 2011; Nguyen et al., 2011). Upon DOT1L blockade, levels of H3K79 methylation drop, and this in turn blocks the expression of MLL fusion proteins target genes including HOXA9 and MEIS2 and trigger selective death in MLL-rearranged cell lines harboring DOT1L-recruiting fusion partners (Daigle et al., 2011, 2013; Chen et al., 2013). Based on these findings, the DOT1L inhibitor EPZ-5676 is currently being tested in several early phase clinical trials for MLL-rearranged leukemias. Published results from a phase I trial revealed an acceptable safety profile and an interesting overall response rate in patients with advanced hematological cancers with MLL rearrangements

(Stein et al., 2018). Moreover, the potential therapeutic effect of DOT1L inhibitors has been described in other genetically defined AML subgroups such as the ones bearing partial tandem duplications within the MLL gene (MLL-PTD). Indeed, the MLL-PTD leukemias share critical biological features with MLL-rearranged leukemia, including the requirement of DOT1L for their oncogenic activity and high expression levels of HOXA-cluster genes. Given these similarities, MLL-PTD positive leukemias showed high sensitivity to EPZ-5676 in both *in vitro* and *in vivo* models (Kuhn et al., 2015) and were therefore also included in the phase I clinical trial mentioned above (Stein et al., 2018).

### SETD2

SETD2 is a lysine methyltransferase responsible for trimethylation of the transcriptional elongation mark H3K36 that has been found to be mutated in different tumor types, including hematological malignancies (Mar et al., 2014; Zhu et al., 2014; Moffitt et al., 2017; Lin et al., 2018). Mutations in SETD2 result in global reduction of H3K36me3 in tumor cells, which in turn exhibit impaired DNA damage signaling and fail to activate the tumor suppressor p53 (Carvalho et al., 2014). Interestingly, SETD2 loss-of-function mutations have been identified in more than 20% of leukemia patients with MLL gene rearrangement (Bu et al., 2018), contributing to both initiation and leukemia progression by enhancing the self-renewal potential of leukemic stem cells. According to some studies, SETD2 appears to be required for sustaining the functionality and the correct differentiation of HSCs (Zhang et al., 2018; Zhou et al., 2018). Initially considered as a tumor suppressor, recent data suggest that SETD2 may as well act as an oncogene. In fact, if partial SETD2 loss accelerates leukemogenesis and induces drug resistance, complete SETD2 loss delays leukemia progression. This opposite behavior of SETD2 may rely on independent H3K36me3 functions that need to be further investigated (Skucha et al., 2019). Interestingly, the DOT1L inhibitor EPZ-5676 induced differentiation and cell death in a MLL-rearranged leukemia model bearing SETD2 mutation (Bu et al., 2018). Interestingly, a recent study showed that the treatment with JIB-04, an inhibitor of the lysine demethylase KDM4A, was able to restore H3K36 methylation levels and chemotherapy sensitivity to SETD2-mutant leukemias (Mar et al., 2017).

### Polycomb Proteins

First discovered in *Drosophila*, Polycomb group (PcG) proteins are constituents of two chromatin-remodeling complexes (PRC1 and PRC2) that act as transcriptional repressors, regulating key biological processes including cell proliferation, differentiation, and stem cell plasticity (Margueron and Reinberg, 2011; Morey et al., 2015). PRC1 composition is variable, with two core components, RING1A and RING1B (Margueron and Reinberg, 2011), and several accessory components. The PRC1 complex acts through mono-ubiquitination of histone H2A lysine 119. One of the accessory PRC1 components, BMI1, has been shown to have a role in controlling the self-renewal of normal and leukemic stem cells in AML (Lessard and Sauvageau, 2003).

Based on the role of BMI1 in HSC homeostasis, overexpression of this protein is frequently found in patients with hematologic disorders (Mihara et al., 2006; Chowdhury et al., 2007; Rizo et al., 2009).

PRC2 is a multi-subunit complex consisting in four core constituents: drosophila enhancer of zeste homolog 2 (EZH2), embryonic ectoderm development (EED), suppressor of zeste 12 homolog (SUZ12), and human retinoblastoma binding protein 4 (RBBP4). Furthermore, accessory molecules favoring PRC2 recruitment and stabilization include JARID2 and YY1. EZH2 is the catalytic subunit of the PRC2 complex and is involved in mono, di, and tri-methylation of H3 lysine 27 (H3K27me1/2/3), leading to chromatin compaction and transcriptional repression of target genes. Acting both as oncogene and tumor suppressor, EZH2 plays contrasting roles in AML pathogenesis (Basheer et al., 2019). Frequently overexpressed in solid tumors, lymphomas (Morin et al., 2010) and in myeloid malignancies, EZH2 has a dual role: in fact, it can potentially act as a tumor suppressor, as suggested by a number of identified loss-of-function mutations (Nikoloski et al., 2010), or promote tumorigenesis and be linked to inferior patient outcome when overexpressed (Grubach et al., 2008; Nikoloski et al., 2010; Xu et al., 2011). Consistent with the oncogenic role of EZH2, inhibition of EZH2 in a mouse model of leukemia resulted in reduced number of leukemic stem cells and impaired leukemia growth (Fujita et al., 2018). Accordingly, the differentiation and growth inhibitory effects of the EZH2 silencing on AML cells further corroborate the oncogenic function of EZH2 in AML (Tanaka et al., 2012). Besides EZH2, deregulation of other members of PRC2 components including ASXL1, JARID2, EED, and SUZ12 has been implicated in the development and propagation of hematological malignancies, including AML (Boulton et al., 2010; Chou et al., 2010; Metzeler et al., 2011; Beekman et al., 2012; Puda et al., 2012; Schnittger et al., 2013; Micol et al., 2014; Paschka et al., 2015; Qi et al., 2017).

Given this evidence, several small molecules inhibiting PRC2 complex and its components have been developed and tested in preclinical and clinical settings. Both GSK126 and EPZ-6438 (tazemetostat) are currently in early stage clinical trials for a variety of hematological malignancies including lymphoma. Recent studies show that PRC2 acts in parallel with MLL rearrangements to sustain leukemia growth (Neff et al., 2012; Shi et al., 2013). Based on this, UNC1999, an EZH1/EZH2 dual inhibitor, showed its efficacy in suppressing AML growth in both *in vitro* and *in vivo* experiments in MLL-rearranged AML models reverting the repressed PRC2 target gene signatures to an active status (Xu et al., 2015). In addition to inhibitors of the PRC2 enzymatic domain, small molecules targeting other components of the complex have been developed. By directly binding H3K27, EED is essential for the HMT activity of PRC2. The small molecule MAK683 disrupts EED-EZH2 protein-protein interaction, preventing H3K27 trimethylation. This has been associated with decreased tumor cell proliferation in diffuse large B-cell lymphoma (DLBCL) cell lines and to tumor regression in a mouse lymphoma xenograft model (Qi et al., 2017). While a clinical trial is testing MAK683 in

lymphoma patients (NCT02900651), the clinical potential of PRC inhibitors in AML patients remains to be determined. Recently, the emergence of resistance to EZH2 inhibition has been reported in preclinical models of lymphoma. Interestingly, the majority of the pathways involved in the establishment of resistance mechanisms to epigenetic therapies are in common between different drugs and tumor types. This is the case of inhibitors of EZH2 and BET proteins (discussed below). Indeed, in response to each treatment, inhibitor-resistant cells showed the constitutive activation of the phosphoinositide-3-kinase (PI3K) pathway (Kurimchak et al., 2016; Bissierier and Wajapeyee, 2018). Other works described that the acquisition of genetic mutations in EZH2 gene confers resistance to EZH2 inhibition in the same diffuse large B-cell lymphoma cell lines (Baker et al., 2015; Gibaja et al., 2016).

### G9a

G9a is a lysine methyltransferase belonging to the Su(var)3-9 family, which catalyzes the reaction of mono/di-methylation at H3K9 (H3K9me1/2) triggering gene repression (Shankar et al., 2013). Even if there are no mutations in AML targeting the G9a gene, recent studies reported that loss of this protein suppressed leukemogenesis in a mouse model of leukemia induced by HOXA9, an oncoprotein overexpressed in 50–70% of AML patients and for which there are no currently available inhibitors (Lehnertz et al., 2014). Two G9a inhibitors, UNC0638 and UNC0642, the latter displaying an improved pharmacokinetics, showed remarkable cytotoxicity against AML cell lines (Vedadi et al., 2011; Liu et al., 2013). A-366, a recently developed peptide-competitive inhibitor of G9a, displayed a reduced toxicity profile compared to UNC0638 and UNC0642 in human prostate cancer cell lines (Sweis et al., 2014). The role of G9a inhibitors in AML patients remains to be tested.

### PRMT

Arginine residues within histone tails (H3 and H4) can be regulated through methylation by protein arginine methyltransferases (PRMTs). Protein arginine methylation is an abundant post-translational modification, which regulates a plethora of pathways including signal transduction, gene transcription, DNA repair, and mRNA splicing. Crosstalk occurring between PRMT and KMT is necessary to establish appropriate patterns of histone methylation (Hyllus et al., 2007; Iberg et al., 2008). Among PRMT targets, there are also non-histone substrates, including AML1 and ASH2L, suggesting that alterations in the activity of PRMTs may have widespread effects. Even if no mutations have been found in PRMT genes, overexpression of these proteins is often present in various cancer types including leukemia rendering these enzymes particularly intriguing as therapeutic targets. Within the PRMT family, PRMT1 catalyzes asymmetric di-methylation of arginine 3 of H4 (H4R3me2) that results in transcriptional activation, by promoting p300-mediated acetylation of K8 and K12 on H4 (Wang et al., 2001; An et al., 2004). In normal hematopoiesis, PRMT1-mediated methylation of the transcription factor AML1 enhances its ability to activate the transcription of several target genes during hematopoietic differentiation



(Zhao et al., 2008). Moreover, PRMT1 has also been found to methylate ASH2L, which has been suggested to act as an oncoprotein (Butler et al., 2011).

The interest in targeting PRMTs for AML therapy comes from several studies reporting specific requirement of PRMT1 for leukemogenesis in some genetic subsets of AML, including those with AML1-ETO and MLL rearrangements. In particular, PRMT1 has been found to be required for leukemia initiation by the fusion proteins MLL-GAS7 and MOZ-TIF2 and its silencing was able to block leukemia transformation (Cheung et al., 2016). Moreover, PRMT1 methylates the AE9a isoform of the AML1-ETO leukemogenic fusion protein and activates AE9a target genes, enhancing proliferation of hematopoietic progenitor cells. Accordingly, knockdown of PRMT1 suppresses the self-renewal capability of AE9a-positive cells, suggesting a role of PRMT1 in regulating leukemogenesis (Shia et al., 2012). Along these lines, preclinical studies reported that small molecules inhibiting PRMT1 (AMI-408) suppressed the growth of both human AML cell lines and leukemia mouse models (Dillon et al., 2012; Cheung et al., 2016). Similar cytotoxic effects were reported in lymphoma models overexpressing PRMT5 upon treatment with the PRMT5 specific inhibitor EPZ015666 both *in vitro* and *in vivo* (Chan-Penebre et al., 2015). ERZ015666 was also recently reported to rescue the differentiation block of human leukemic cells *in vitro* and in a mouse model of MLL-rearranged leukemia (Kaushik et al., 2018).

## HISTONE ACETYLATION

Although poorly described so far, alterations of enzymes belonging to HAT family have been detected in AML. In particular, several translocations involving HAT proteins as fusion partners have been described, including t(8;16) (p11;p13) and t(8;22) (p11;p13). These rearrangements generate the MOZ-CBP and the MOZ-P300 fusion proteins respectively and both have been shown to contribute to leukemogenesis (Borrow et al., 1996; Kitabayashi et al., 2001). Inhibitors targeting components of this family of enzymes have been developed and tested in preclinical models. In particular, the P300 inhibitors C646 and L002 showed great selectivity in inducing proliferation arrest of leukemia and lymphoma cell lines (Gao et al., 2013; Yang et al., 2013).

## Epigenetic Erasers

Enzymes able to remove epigenetic marks are identified as “epigenetic erasers.” There are two main groups of proteins belonging to this class: histone demethylases (HDMs) and histone deacetylases (HDACs).

### HDM

The first group of proteins can be, in turn, classified into two other big families: amino oxidase homolog lysine demethylase 1 (KDM1) and JMJC domain containing HDMs. Mutations of genes belonging to the latter family are rare in AML and mainly limited to the ones occurring in lysine demethylase 6A (KDMT6A) (Cancer Genome Atlas Research et al., 2013). The

lysine demethylase KDM1 (also known as LSD1) demethylates di- and mono-methylated K4 on histone H3, reducing the levels of H3K4me3, normally associated with active gene transcription. LSD1 has been shown to affect a wide range of transcriptional programs, acting either as a transcriptional repressor or as an activator depending on the cellular context (Maiques-Diaz and Somervaille, 2016). Pharmacological inhibition or genetic depletion of LSD1 induces differentiation of MLL-driven AML stem cells and of other genetically defined AML subtypes (Maiques-Diaz et al., 2018). A recent study showed that the LSD1 inhibitor tranylcypromine (TCP) induced the expression of myeloid differentiation genes in AML cells and that combination of TCP with ATRA exerted a potent anti-leukemic effect (Schenk et al., 2012). Recently, two novel LSD1 inhibitors, NCD25 and NCD38, were identified for their ability to halt leukemia growth and induce myeloid differentiation. In particular, NCD38 was shown to reactivate clusters of enhancer elements (e.g., super-enhancers) that control hematopoietic genes and that are abnormally silenced by LSD1 during leukemia progression (Sugino et al., 2017). If the treatment with the LSD1 inhibitor SP2509 demonstrated high efficacy in blocking leukemia growth, the co-treatment with a specific histone deacetylase (HDAC) inhibitor, panobinostat, was synergistically lethal against both primary and leukemia cell lines (Fiskus et al., 2014). The LSD1 inhibitors GSK2879552 and IMG-7289, alone or in combination with all-trans retinoic acid therapy (ATRA), showed promising activity against AML *in vitro* (Smitheman et al., 2019), leading to two ongoing phase I trials for patients with relapsed/refractory AML (NCT0217782, NCT02842827) and to a phase I/II trial for MDS patients (NCT02929498).

### HDAC

Given the importance of histone acetylation in regulating the expression of many genes, it is not surprising that enzymes able to regulate this modification are frequently hit by alterations in different tumor types including hematological malignancies. Thus, HDAC alterations can be linked to both silencing of tumor suppressor genes and activation of oncogenic processes altering the cell cycle progression, activation of the DNA damage response (DDR) pathway, apoptosis, and many others. Although HDAC somatic mutations have been identified so far in several solid tumors with a relatively high frequency (Stark and Hayward, 2007; Taylor et al., 2011), they are rare in AML patients. However, the contribution of HDAC to AML pathogenesis has been linked to aberrant recruitment of these enzymes by myeloid oncoproteins such as AML1-ETO, PML-RARA, and EVI1 (Izutsu et al., 2001; Senyuk et al., 2002; Hug and Lazar, 2004; Falkenberg and Johnstone, 2014).

In the last years, several clinical trials have been conducted with HDACi in patients with MDS and AML. The HDACi vorinostat and panobinostat are among the earliest approved by FDA for treatment of cutaneous T cell lymphoma and multiple myeloma, given their capacity to induce cancer cell differentiation. Second-generation HDACi are currently in use in several clinical trials for different tumors, including relapsed AML (Finazzi et al., 2013; Li Y. et al., 2016). In the past years, several studies addressed the molecular effects

of HDAC inhibition in cancer cells. Microarray analyses revealed transcriptional changes of a large number of genes (approximately 10–20% of the genome), including proapoptotic inducers and genes involved in cell cycle arrest in leukemic cell lines after exposure to different HDACi (Peart et al., 2005). According to the literature, HDACi exert their anti-proliferative effects via induction of apoptosis, regulation of different signaling pathways (Bali et al., 2005; Insinga et al., 2005; Nebbioso et al., 2005; Xu et al., 2006), and activation of the DDR pathway in oncogene-expressing cells (Di Micco et al., 2011). Of note, it has also been reported that HDAC inhibition in normal and leukemic cells induces DDR activation in the absence of physical DNA lesions. Specifically, chromatin remodeling induced by these inhibitors may directly activate DDR through the increased phosphorylation of the histone H2AX ( $\gamma$ H2AX) and/or through ROS production (Gaymes et al., 2006; Petruccioli et al., 2011).

Valproic acid (VPA) is a short-chain fatty acid acting as a powerful HDACi that causes hyperacetylation of the N-terminal tails of H3 and H4 histones by inhibiting the catalytic activity of class I HDACs (Gottlicher et al., 2001). VPA has a wide range of effects on leukemic cells. By analyzing the effects of VPA treatment on AML patient blasts (Rucker et al., 2016) identified a signature enriched for pathways implicated in cell cycle arrest, apoptosis, and DNA repair. However, indirect effects of VPA on the reactivation of antitumor immune response may also be considered. In addition to VPA, other HDACi including romidepsin/depsipeptide, mocetinostat, and entinostat, have been tested in phase I/2 studies for leukemia treatment. However, HDACi have shown better results when used in combination with other agents with known anti-leukemia activity (Garcia-Manero et al., 2012; Gojo et al., 2013; Kirschbaum et al., 2014). Panobinostat, already approved for the treatment of multiple myeloma, is now under clinical investigation for AML patients. As a single agent, panobinostat showed modest anti-leukemic activity in clinical trials for myeloid malignancies (Giles et al., 2006; DeAngelo et al., 2013; Schlenk et al., 2018). On the other hand, *in vitro* studies showed that combinations of panobinostat with other treatments or epigenetic drugs could have synergistically lethal effects on AML cells (Fiskus et al., 2014). However, results from a recent clinical trial of panobinostat in combination with intensive chemotherapy did not show any clinical improvement and was accompanied by increased toxicities in treated AML patients (Schlenk et al., 2018). Overall, as HDACs also deacetylate numerous non-histone proteins, the widespread effects on the whole cellular proteome should be better investigated and taken into consideration to fine-tune successful therapies.

## Epigenetic Readers

The group of proteins able to recognize and bind post-translational modifications are called “epigenetic readers.” These proteins have specialized domains able to recognize a variety of nucleosome modifications acting directly on the transcription or indirectly by serving as scaffold for the recruitment of other epigenetic regulators. The cooperation between these proteins and the chromatin-modifying enzymes is therefore fundamental

for gene expression patterns and deregulation of chromatin readers has been frequently reported in cancer.

## BET

Bromodomain and extra-terminal domain (BET) proteins are a class of chromatin readers that act by binding histone and non-histone acetyl groups at lysine residues (Wu and Chiang, 2007). Among these, BRD4 has emerged as a key regulator of transcriptional networks in development and cellular differentiation (Di Micco et al., 2014; Dey et al., 2019) as well as a key player in driving aberrant transcriptional programs in cancer cells (Asangani et al., 2014; Filippakopoulos and Knapp, 2014; Shu et al., 2016; Fontanals-Cirera et al., 2017). In the context of AML, BRD4 sustains the expression of c-MYC to promote aberrant self-renewal (Zuber et al., 2011). More recently, it has been reported that BRD4 binds and recognizes specialized regions of H3K27 acetylation called “super-enhancers,” which control several lineage-specific genes and can be hijacked by tumor cells to express critical oncogenes (Loven et al., 2013). In addition to its originally described chromatin reader activity, BRD4 was recently shown to have HAT activity that results in chromatin relaxation and is conserved across species (Devaiah et al., 2016). Based on these findings, and on the detrimental effects of BRD4 depletion on AML proliferation, many inhibitors targeting BET proteins have been designed and tested against several tumor types, including leukemia (Perez-Salvia and Esteller, 2017). Among these, the small molecules JQ1 and the I-BET151 have been shown to be highly effective in inducing cell cycle arrest and apoptosis of MLL-rearranged leukemia cells both *in vitro* and *in vivo*. These inhibitors act by displacing BRD4 from regulatory elements and blocking the RNA Pol II mediated transcriptional elongation at the level of specific oncogenes including c-MYC, BCL2, and CDK6 (Dawson et al., 2011; Zuber et al., 2011). Similarly, the BET inhibitor OTX015 showed the ability to induce apoptosis in a variety of leukemic cell types (Coude et al., 2015). Several clinical trials testing BET inhibitors are currently ongoing; the small molecule RO6870810/TEN-010 (a more stable derivate of JQ1) has been tested in a recently completed phase I trial for the treatment of refractory AML and MDS (NCT02308761), and a phase II trial testing the BET inhibitor CPI-0610 in combination with ruxolitinib is open for patients with myelofibrosis (NCT02158858). On the same line, the BRD4 inhibitor GSK525762 entered early phase clinical trials for patients with relapsed refractory hematological malignancies. Importantly, a recent work by Gerlach et al. (2018) identified a novel BET inhibitor (BI-894999) belonging to the family of [1,2,4]triazolo[4,3-a]pyrazines. Distinct in structure compared to other BET inhibitors, BI-894999, although regulating the same genes as JQ1, showed a higher efficacy in killing AML cells derived from primary samples and xenograft models. In addition, the combination with an inhibitor of CDK9, a component of the transcriptional elongation complex, strongly enhanced its antitumor effects (Gerlach et al., 2018). Even if the interest in targeting BET proteins for cancer treatment keeps growing, there is still a lack of valuable BET transgenic animal models to elucidate the toxic effects and the mechanisms of action of BET inhibitors. Of note, an inducible BRD4 RNA interference

animal model showed that BRD4 depletion causes toxicity in several organs and induces intestinal stem cell depletion (Bolden et al., 2014). Furthermore, even though still largely unexplored, one of the best-characterized mechanisms of tumor resistance to epigenetic therapy includes resistance to BET inhibitors. In particular, it has been reported in a MLL-AF9;Nras(G12D) AML mouse model that resistance to BET inhibition involves chromatin remodeling that in turn activates the WNT signaling pathway (Rathert et al., 2015). In addition, elevated levels of ERK/PI3K activity were shown to mediate BET inhibitor resistance (Kurimchak et al., 2016) providing a rationale for combinatorial strategies that simultaneously target BET proteins and receptor tyrosine kinases (RTKs) (Wyce et al., 2018) or the PI3K pathway (Stratikopoulos et al., 2015).

## ENHANCER DEREGULATION IN AML

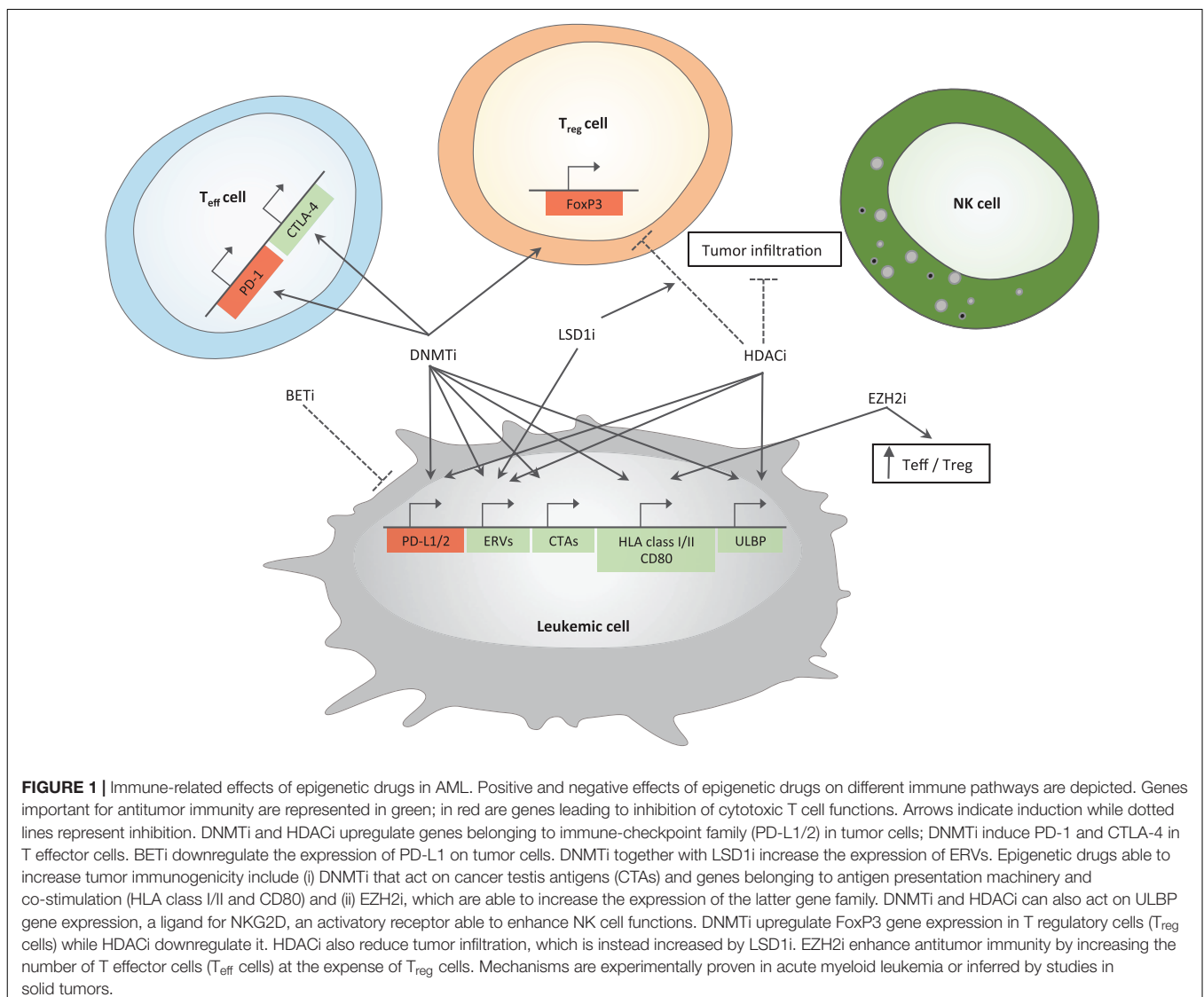
The systematic characterization of regulatory regions in normal and AML blasts led to the identification of clusters of transcriptionally active chromatin domains with putative or proven enhancer activity for expression of leukemic genes (defined as “active enhancers” or “super-enhancers”). Enhancer elements present in normal blood cells may accumulate mutations that generate new binding sites for transcription factors and establish new enhancers driving leukemia oncogene expression (Mansour et al., 2014). Similarly, pre-existing enhancers may be inverted, translocated, or even undergo duplications to drive the aberrant upregulation of oncogenes or to suppress the expression of tumor suppressor genes. In addition, mutations in CTCF, a key player in driving the 3D chromatin organization (Zuin et al., 2014), may favor novel promoter/enhancer interactions to sustain leukemic cell proliferation. Recently, it was reported that a blood enhancer cluster (BENC) known to regulate the expression of c-MYC in normal HSCs can be hijacked by leukemic stem cells in mouse models of leukemia and displays an accessible chromatin profile even in primary AML samples (Bahr et al., 2018). Furthermore, charting the enhancer landscape by chromatin accessibility in single AML cells revealed a peculiar “regulome” profile that paralleled the developmental stage of disease, with the acquisition of a closed chromatin conformation at the level of HOXA genes, which have been suggested to be important in the first step of leukemogenesis (Corces et al., 2016).

## EPIGENETIC THERAPIES AND IMMUNE RESPONSE

To date, most of the studies on epigenetic drugs focused on understanding the direct effects of epigenetic therapy on tumor cells. However, interest is now extending to decipher whether epigenome rewiring may as well contribute to cancer cell eradication by triggering changes in the tumor microenvironment and in particular in the interplay between cancer cells and the immune system. In fact, the accumulation of epigenetic alterations during tumorigenesis contributes to

profound changes in a plethora of transcriptional signatures including genes regulating antitumor immunity (Figure 1). As described earlier, there has been a substantial body of research showing that hypomethylating agents (such as DNMTi) act on tumor cells by counteracting hypermethylation in tumor suppressors, differentiation genes, and pathways involved in cell cycle progression. More recently, studies have highlighted a series of both positive and negative effects of epigenetic drugs on immune cells. An indirect way to unleash the immune system against AML cells is to upregulate the expression of developmental antigens in order to increase tumor antigenicity. These proteins are often regulated at the level of promoter methylation and are expressed in cancer cells due to epigenetic changes. In AML cell lines, the use of azacytidine and decitabine resulted in increased expression of the tumor-associated antigens NY-ESO-1 and WT1 and of the MAGE cancer testis antigen, with consequent activation of cytotoxic T cells (Almstedt et al., 2010; Goodyear et al., 2010). In some tumor types, including AML, the treatment with epigenetic drugs, including high doses of DNMT and HDACi, induces the reactivation of human endogenous retroviral transcripts (ERVs) (Conti et al., 2016; Daskalakis et al., 2018). ERVs are epigenetically repressed in normal somatic cells and their reactivation has been originally associated to increased genomic instability or aberrant expression of oncogenes in several cancers (Bannert et al., 2018). However, recent pieces of evidence support a role for ERV reactivation in fighting cancer in response to epigenetic therapies. Indeed, cancer cell treatment with azacytidine and decitabine leads to the cytosolic accumulation of ERV nucleic acids that in turn (i) trigger the interferon-induced viral defense pathways, (ii) boost antitumor innate and adaptive immune responses, and (iii) potentiate the effects of immune checkpoint therapies (Chiappinelli et al., 2015; Roulois et al., 2015). Similarly, gene expression analyses of transposable elements in a panel of cancer cell lines treated or not with epigenetic drugs revealed increased levels of ERVs also in response to the HDACi SB939, with an even stronger ERV reactivation observed when treating cancer cells with a combination of SB939 and decitabine (Daskalakis et al., 2018). In agreement with this observation, HDACi have been shown to induce cryptic transcription start sites encoded in long terminal repeats (Brocks et al., 2017). Whether or not HDACi exert their anticancer activity also via immune-mediated recognition of ERV nucleic acids remains to be further investigated. Finally, chemical inhibition of LSD1 was shown to concomitantly increase ERV transcription and their accumulation through reduced stability of the RNA-induced silencing complex (RISC). As a consequence, LSD1 inhibition triggers viral mimicry interferon responses, increases the infiltration of effector T cells in the tumor microenvironment, and, in preclinical models of melanoma, synergizes with the anticancer activities of immune checkpoint blockade (Sheng et al., 2018). Despite the abovementioned promising antitumor effects, further studies need to elucidate the potential impact of epigenetic therapy-mediated transposable element reactivation on cancer cell genomic instability and tumor aggressiveness.

In addition to CTAs and ERVs, genes involved in antigen presentation, both via HLA class I and class II, have been



shown to be under the control of DNA methylation (Coral et al., 1999, 2013; Campoli and Ferrone, 2008). Moreover, the expression of CD80, a key co-stimulatory molecule normally absent in cancer cells, can be increased by hypomethylating agents resulting in enhanced antitumor immunity (Goodyear et al., 2010). In addition, hypomethylating agents can act also by enhancing the susceptibility of AML cells to NK cell action. In fact, azacytidine in combination with other differentiation-promoting drugs resulted in enhanced NK cell-mediated antitumor activity through the up-regulation on tumor cells of ligands for the NK cell activating receptor NKG2D (Rohner et al., 2007). Besides these positive effects on immune system activation against cancer cells, treatment of AML and MDS patients with azacytidine also led to elevated expression of a series of immune-checkpoint molecules on T cells including CTLA-4, PD-1 and its ligands (PD-L1 and PD-L2) (Yang et al., 2014). However, other studies showed that DNMT inhibitors may avoid the onset of exhaustion of cytotoxic T

lymphocytes and reprogram exhausted cells into effector cells (Ghoneim et al., 2017).

Whereas it might be difficult to leverage on these immune-related effects in patients that are treatment-naïve or exposed to a tight schedule of cycles of intensive chemotherapy, boosting an anti-leukemic immune response might be highly desirable in the maintenance setting, especially after allo-HCT. It is in fact well established that most of the therapeutic effect of allo-HCT relies on the transfer from the donor to the patient of a healthy immune system, capable of recognizing and eliminating residual cancer cells. Boosting this “graft-versus-leukemia” effect, possibly without unleashing severe graft-versus-host disease, has indeed over the last decades represented the “holy grail” of transplanters. For instance, the ability of DNMT inhibitors to concomitantly prime T cell-mediated anti-leukemic responses and induce T regulatory cells (Tregs) has attracted considerable interest in the allo-HCT setting (Kim and Leonard, 2007; Polansky et al., 2008; Lal et al., 2009; Feng et al., 2014). Supporting this hypothesis, in



murine models of allo-HCT, the use of hypomethylating agents suppresses T cell proliferation and cytokine production, resulting in reduced graft versus host disease without any effect on graft versus leukemia (Choi et al., 2010; Sanchez-Abarca et al., 2010). Similar results were also reported in AML patients, where post-transplantation treatment with azacytidine was associated with an increase in the number of Tregs (Goodyear et al., 2012). Indeed, trials testing azacytidine in the prophylactic (de Lima et al., 2010; Craddock et al., 2016a) and pre-emptive (Platzbecker et al., 2012) settings have reported encouraging results in terms of both overall survival and donor chimerism stabilization.

Interestingly, azacytidine, either alone or in combination with donor lymphocyte infusions (DLIs), has shown interesting results also in the more challenging setting of the treatment of AML patients with frank hematological relapse. To date, data on more than 600 patients have been collected, reporting very variable results in terms of clinical outcomes (Lubbert et al., 2010; Schroeder et al., 2013, 2015; Steinmann et al., 2015; Ghobadi et al., 2016; Craddock et al., 2016b). Starting from these heterogeneous results and lack of consent on treatment schedules, two retrospective surveys have been performed in more homogeneous cohorts of patients, with the aim of identifying prognostic factors for treatment response and long-term survival. These studies reported that patients with the highest benefit from azacytidine + DLI combination were those transplanted in complete remission, who presented with low disease burden at the time of relapse (molecular relapse or blasts <20% in bone marrow) and that experienced a longer remission time from HCT to overt relapse (Schroeder et al., 2015; Craddock et al., 2016a). Even if not so well substantiated, studies reporting the efficacy of decitabine after allo-HCT showed similar results (Han et al., 2015; Pusic et al., 2015; Schroeder et al., 2018).

Like DNMT inhibitors, small molecules targeting HDAC activity are able to induce positive and negative immunomodulatory effects; in fact, they can increase cancer immunogenicity through the expression of HLA class I genes and tumor antigens and/or block T cell response by the upregulation of ligand for checkpoint inhibitor receptors as well as by reducing the number of Tregs (Setiadi et al., 2007; Shen et al., 2012; Woods et al., 2015).

As a result of the evidence that both DNMT and HDACi can contribute to T cell exhaustion, a number of clinical studies are currently testing the combination of these epigenetic drugs with immune checkpoint inhibitors (Daver et al., 2019).

With these immune-related effects in mind, HDACi alone or in combination with azacytidine and DLI have been tested in a post-transplantation setting. Results on phase I/II trials testing the combinatorial treatment as maintenance therapy after transplantation reported a 2-year rate overall survival and a relapse free survival rate of 81 and 75%, respectively, (Bug et al., 2017).

Besides their reported effect in suppressing tumor cell proliferation, recently published preclinical studies highlighted the role of EZH2 inhibitors in enhancing antitumor immunity by altering the ratio between effector and regulatory T cells in favor of the first population (Wang et al., 2018). Another interesting property of these drugs is the ability to restore HLA

class I and II expression in EZH2-mutated cases of DLBCL (Ennishi et al., 2019), rendering them promising candidates to be tested in the post-transplantation setting.

## DISCUSSION

AML is a highly heterogeneous cancer type often associated with bad prognosis, with the minority of patients being cured without allo-HCT and for which new therapeutic approaches are urgently needed. Here, we provide a comprehensive overview of studies documenting the effects of epigenetic aberrations in AML pathogenesis and summarized the most recent clinical efforts reporting safety and efficacy of epigenetic compounds for AML treatment. By targeting multiple pathways simultaneously, epigenetic drugs hold great therapeutic promise, although several challenges need to be faced to see in the clinics the full success of such a therapy. One of the most clinically relevant issue still limiting the full implementation of epigenetic therapies in the treatment algorithms for AML patient relates to our incomplete understanding of their interactions with chemo- and immunotherapies. Understanding synergistic and antagonistic effects of epigenetic drugs with current therapeutic paradigms will be fundamental to design new trials incorporating epigenetic therapies based on a specific biological rationale, possibly associated to ancillary studies aimed at determining their effects on leukemic cells and the immune system. For this purpose, it will be necessary to develop new models to test epigenetic therapies, possibly employing actual primary patient samples instead of cell lines and mouse models, that poorly recapitulate the complexity of such a heterogeneous disease. Very recently, the group of Melnick developed a platform to systematically study long-term effects of epigenetic drugs as monotherapy and in combination on a large number of *ex vivo* cultured primary AML (Duy et al., 2019). Other suitable models known to better mirror AML complexity are next-generation patient-derived xenograft (PDX) models and humanized niche xenograft models (Antonelli et al., 2016; Reinisch et al., 2016; Abarrategi et al., 2017). Although the stability of the epigenetic landscape of primary AML samples in these models remains to be experimentally tested, they can provide a valid alternative to monitor the long-term biological consequences of epigenetic treatments and study their impact on tumor cells as well as on several components of the tumor microenvironment. Given the abovementioned impact of epigenetic therapies in modulating antitumor immunity, the same preclinical *ex vivo* and *in vivo* models will be instrumental to also test epigenetic drugs in combinations with immunotherapy to further enhance their antitumor efficacy. Of note, most epigenetic regulators will have an impact on transcriptional programs fundamental also for normal cell fitness, posing the risk for increased toxicity. Accurate selection of patients that will benefit from a given epigenetic therapy is thus needed to guide a proper choice of epigenetic therapies in AML patients. Additionally, the concomitant presence of distinct leukemia subclones may further challenge the success of epigenetic therapies for AML treatment. The advent of NGS technologies mapping all the different

layers of epigenetic regulation at a single-cell level together with transcriptomic and genomic analysis will help to better address these questions in the setting of AML. Altogether, we believe that the application of innovative technologies and more suitable preclinical models that take into consideration the interplay between cancer cells and the immune system will, in the near future, better elucidate biological processes on the basis of tumor response to epigenetic therapy and contribute to move one step forward toward personalized medicine for cancer treatment.

## AUTHOR CONTRIBUTIONS

All authors contributed to writing the review and discussed its contents.

## ACKNOWLEDGMENTS

The authors would like to acknowledge support from a “Pilot and Seed Grant 2015” from the San Raffaele Hospital

awarded to LV and RDM. Work in LV lab is supported by the Italian Ministry of Health (RF-2011-02351998, RF-2011-02348034, and TRANSCAN HLALOSS), the Associazione Italiana per la Ricerca sul Cancro (Start-Up Grant #14162 and IG #22197), and the DKMS Mechtild Harf Foundation (DKMS Mechtild Harf Research Grant 2015). Work in RDM lab is supported by Telethon (TIGET grant E5), a Career Development Award from Human Frontier Science Program (HFSP), an Advanced Research Grant from the European Hematology Association (EHA), a Hollis Brownstein Research Grant from Leukemia Research Foundation (LRF) and the Interstellar Initiative on “Healthy Longevity” from New York Academy of sciences (NYAS) and the Japan Agency for Medical Research and Development (AMED). VG conducted this study as partial fulfillment of her Ph.D. in Translational and Molecular Medicine—DIMET, Bicocca University. DG was supported by a postdoctoral fellowship from the IBSA Foundation. The authors apologize with all authors that were not quoted in this Review article because of space constraints.

## REFERENCES

- Abarrategi, A., Foster, K., Hamilton, A., Mian, S. A., Passaro, D., Gribben, J., et al. (2017). Versatile humanized niche model enables study of normal and malignant human hematopoiesis. *J. Clin. Invest.* 127, 543–548. doi: 10.1172/JCI89364
- Adelman, E. R., Huang, H. T., Roisman, A., Olsson, A., Colaprico, A., Qin, T., et al. (2019). Aging human hematopoietic stem cells manifest profound epigenetic reprogramming of enhancers that may predispose to leukemia. *Cancer Discov.* doi: 10.1158/2159-8290.CD-18-1474
- Almstedt, M., Blagitko-Dorfs, N., Duque-Afonso, J., Karbach, J., Pfeifer, D., Jager, E., et al. (2010). The DNA demethylating agent 5-aza-2'-deoxycytidine induces expression of NY-ESO-1 and other cancer/testis antigens in myeloid leukemia cells. *Leuk. Res.* 34, 899–905. doi: 10.1016/j.leukres.2010.02.004
- An, W., Kim, J., and Roeder, R. G. (2004). Ordered cooperative functions of PRMT1, p300, and CARM1 in transcriptional activation by p53. *Cell* 117, 735–748. doi: 10.1016/j.cell.2004.05.009
- Antonelli, A., Noort, W. A., Jaques, J., de Boer, B., de Jong-Korlaar, R., Brouwers-Vos, A. Z., et al. (2016). Establishing human leukemia xenograft mouse models by implanting human bone marrow-like scaffold-based niches. *Blood* 128, 2949–2959. doi: 10.1182/blood-2016-05-719021
- Asangani, I. A., Dommetti, V. L., Wang, X., Malik, R., Cieslik, M., Yang, R., et al. (2014). Therapeutic targeting of BET bromodomain proteins in castration-resistant prostate cancer. *Nature* 510, 278–282. doi: 10.1038/nature13229
- Bahr, C., von Paleske, L., Uslu, V. V., Remeseiro, S., Takayama, N., Ng, S. W., et al. (2018). A Myc enhancer cluster regulates normal and leukaemic haematopoietic stem cell hierarchies. *Nature* 553, 515–520. doi: 10.1038/nature25193.
- Baker, T., Nerle, S., Pritchard, J., Zhao, B., Rivera, V. M., Garner, A., et al. (2015). Acquisition of a single EZH2 D1 domain mutation confers acquired resistance to EZH2-targeted inhibitors. *Oncotarget* 6, 32646–32655. doi: 10.18632/oncotarget.5066
- Bali, P., Pranpat, M., Bradner, J., Balasis, M., Fiskus, W., Guo, F., et al. (2005). Inhibition of histone deacetylase 6 acetylates and disrupts the chaperone function of heat shock protein 90: a novel basis for antileukemia activity of histone deacetylase inhibitors. *J. Biol. Chem.* 280, 26729–26734. doi: 10.1074/jbc.C500186200
- Bannert, N., Hofmann, H., Block, A., and Hohn, O. (2018). HERVs new role in cancer: from accused perpetrators to cheerful protectors. *Front. Microbiol.* 9:178. doi: 10.3389/fmicb.2018.00178
- Basheer, F., Giotopoulos, G., Meduri, E., Yun, H., Mazan, M., Sasca, D., et al. (2019). Contrasting requirements during disease evolution identify EZH2 as a therapeutic target in AML. *J. Exp. Med.* 216, 966–981. doi: 10.1084/jem.20181276
- Beekman, R., Valkhof, M. G., Sanders, M. A., van Strien, P. M., Haanstra, J. R., Broeders, L., et al. (2012). Sequential gain of mutations in severe congenital neutropenia progressing to acute myeloid leukemia. *Blood* 119, 5071–5077. doi: 10.1182/blood-2012-01-406116
- Bernt, K. M., Zhu, N., Sinha, A. U., Vempati, S., Faber, J., Krivtsov, A. V., et al. (2011). MLL-rearranged leukemia is dependent on aberrant H3K79 methylation by DOT1L. *Cancer Cell* 20, 66–78. doi: 10.1016/j.ccr.2011.06.010
- Bisserier, M., and Wajapeyee, N. (2018). Mechanisms of resistance to EZH2 inhibitors in diffuse large B-cell lymphomas. *Blood* 131, 2125–2137. doi: 10.1182/blood-2017-08-804344
- Bolden, J. E., Tasdemir, N., Dow, L. E., van Es, J. H., Wilkinson, J. E., Zhao, Z., et al. (2014). Inducible in vivo silencing of Brd4 identifies potential toxicities of sustained BET protein inhibition. *Cell Rep* 8, 1919–1929. doi: 10.1016/j.celrep.2014.08.025
- Borkin, D., He, S., Miao, H., Kempinska, K., Pollock, J., Chase, J., et al. (2015). Pharmacologic inhibition of the Menin-MLL interaction blocks progression of MLL leukemia in vivo. *Cancer Cell* 27, 589–602. doi: 10.1016/j.ccell.2015.02.016
- Borrow, J., Stanton, V. P., Jr., Andresen, J. M., Becher, R., Behm, F. G., et al. (1996). The translocation t(8;16)(p11;p13) of acute myeloid leukaemia fuses a putative acetyltransferase to the CREB-binding protein. *Nat. Genet.* 14, 33–41. doi: 10.1038/ng0996-33
- Boultonwood, J., Perry, J., Pellagatti, A., Fernandez-Mercado, M., Fernandez-Santamaria, C., Calasanz, M. J., et al. (2010). Frequent mutation of the polycomb-associated gene ASXL1 in the myelodysplastic syndromes and in acute myeloid leukemia. *Leukemia* 24, 1062–1065. doi: 10.1038/leu.2010.20
- Brocks, D., Schmidt, C. R., Daskalakis, M., Jang, H. S., Shah, N. M., Li, D., et al. (2017). DNMT and HDAC inhibitors induce cryptic transcription start sites encoded in long terminal repeats. *Nat. Genet.* 49, 1052–1060. doi: 10.1038/ng.3889
- Bu, J., Chen, A., Yan, X., He, F., Dong, Y., Zhou, Y., et al. (2018). SETD2-mediated crosstalk between H3K36me3 and H3K79me2 in MLL-rearranged leukemia. *Leukemia* 32, 890–899. doi: 10.1038/leu.2017.339
- Bug, G., Burchert, A., Wagner, E. M., Kroger, N., Berg, T., Guller, S., et al. (2017). Phase I/II study of the deacetylase inhibitor panobinostat after allogeneic stem cell transplantation in patients with high-risk MDS or AML (PANOBEST trial). *Leukemia* 31, 2523–2525. doi: 10.1038/leu.2017.242
- Butler, J. S., Zurita-Lopez, C. I., Clarke, S. G., Bedford, M. T., and Dent, S. Y. (2011). Protein-arginine methyltransferase 1 (PRMT1) methylates Ash2L, a shared component of mammalian histone H3K4 methyltransferase complexes. *J. Biol. Chem.* 286, 12234–12244. doi: 10.1074/jbc.M110.202416

- Caligiuri, M. A., Strout, M. P., Lawrence, D., Arthur, D. C., Baer, M. R., Yu, F., et al. (1998). Rearrangement of ALL1 (MLL) in acute myeloid leukemia with normal cytogenetics. *Cancer Res.* 58, 55–59.
- Campoli, M., and Ferrone, S. (2008). HLA antigen changes in malignant cells: epigenetic mechanisms and biologic significance. *Oncogene* 27, 5869–5885. doi: 10.1038/onc.2008.273
- Cancer Genome Atlas Research, N., Ley, T. J., Miller, C., Ding, L., Raphael, B. J., Mungall, A. J., et al. (2013). Genomic and epigenomic landscapes of adult de novo acute myeloid leukemia. *N. Engl. J. Med.* 368, 2059–2074. doi: 10.1056/NEJMoa1301689
- Cao, F., Townsend, E. C., Karatas, H., Xu, J., Li, L., Lee, S., et al. (2014). Targeting MLL1 H3K4 methyltransferase activity in mixed-lineage leukemia. *Mol. Cell.* 53, 247–261. doi: 10.1016/j.molcel.2013.12.001
- Carvalho, S., Vitor, A. C., Sridhara, S. C., Martins, F. B., Raposo, A. C., Desterro, J. M., et al. (2014). SETD2 is required for DNA double-strand break repair and activation of the p53-mediated checkpoint. *eLife* 3:e02482. doi: 10.7554/eLife.02482
- Cashen, A. F., Schiller, G. J., O'Donnell, M. R., and DiPersio, J. F. (2010). Multicenter, phase II study of decitabine for the first-line treatment of older patients with acute myeloid leukemia. *J. Clin. Oncol.* 28, 556–561. doi: 10.1200/JCO.2009.23.9178
- Challen, G. A., Sun, D., Jeong, M., Luo, M., Jelinek, J., Berg, J. S., et al. (2011). Dnmt3a is essential for hematopoietic stem cell differentiation. *Nat. Genet.* 44, 23–31. doi: 10.1038/ng.1009
- Chan-Penebre, E., Kuplast, K. G., Majer, C. R., Boriack-Sjodin, P. A., Wigle, T. J., Johnston, L. D., et al. (2015). A selective inhibitor of PRMT5 with *in vivo* and *in vitro* potency in MCL models. *Nat. Chem. Biol.* 11, 432–437. doi: 10.1038/nchembio.1810
- Chaturvedi, A., Araujo Cruz, M. M., Jyotsana, N., Sharma, A., Yun, H., Gorlich, K., et al. (2013). Mutant IDH1 promotes leukemogenesis *in vivo* and can be specifically targeted in human AML. *Blood* 122, 2877–2887. doi: 10.1182/blood-2013-03-491571
- Chen, L., Deshpande, A. J., Banka, D., Bernt, K. M., Dias, S., Buske, C., et al. (2013). Abrogation of MLL-AF10 and CALM-AF10-mediated transformation through genetic inactivation or pharmacological inhibition of the H3K79 methyltransferase Dot1l. *Leukemia* 27, 813–822. doi: 10.1038/leu.2012.327
- Cheung, N., Fung, T. K., Zeisig, B. B., Holmes, K., Rane, J. K., Mowen, K. A., et al. (2016). Targeting aberrant epigenetic networks mediated by PRMT1 and KDM4C in acute myeloid leukemia. *Cancer Cell* 29, 32–48. doi: 10.1016/j.ccell.2015.12.007
- Chiappinelli, K. B., Strissel, P. L., Desrichard, A., Li, H., Henke, C., Akman, B., et al. (2015). Inhibiting DNA methylation causes an interferon response in cancer via dsRNA including endogenous retroviruses. *Cell* 162, 974–986. doi: 10.1016/j.cell.2015.07.011
- Choi, J., Ritchey, J., Prior, J.L., Holt, M., Shannon, W.D., Deych, E., et al. (2010). *In vivo* administration of hypomethylating agents mitigate graft-versus-host disease without sacrificing graft-versus-leukemia. *Blood* 116, 129–139. doi: 10.1182/blood-2009-12-257253
- Chou, W. C., Huang, H. H., Hou, H. A., Chen, C. Y., Tang, J. L., Yao, M., et al. (2010). Distinct clinical and biological features of de novo acute myeloid leukemia with additional sex comb-like 1 (ASXL1) mutations. *Blood* 116, 4086–4094. doi: 10.1182/blood-2010-05-283291
- Chowdhury, M., Mihara, K., Yasunaga, S., Ohtaki, M., Takihara, Y., and Kimura, A. (2007). Expression of polycomb-group (PcG) protein BMI-1 predicts prognosis in patients with acute myeloid leukemia. *Leukemia* 21, 1116–1122. doi: 10.1038/sj.leu.2404623
- Christopher, M. J., Petti, A. A., Rettig, M. P., Miller, C. A., Chendamalai, E., Duncavage, E. J., et al. (2018). Immune escape of relapsed AML cells after allogeneic transplantation. *N. Engl. J. Med.* 379, 2330–2341. doi: 10.1056/NEJMoa1808777
- Cimmino, L., Dolgalev, I., Wang, Y., Yoshimi, A., Martin, G. H., Wang, J., et al. (2017). Restoration of TET2 function blocks aberrant self-renewal and leukemia progression. *Cell* 170:1079–1095.e20. doi: 10.1016/j.cell.2017.07.032
- Conti, A., Rota, F., Ragni, E., Favero, C., Motta, V., Lazzari, L., et al. (2016). Hydroquinone induces DNA hypomethylation-independent overexpression of retroelements in human leukemia and hematopoietic stem cells. *Biochem. Biophys. Res. Commun.* 474, 691–695. doi: 10.1016/j.bbrc.2016.05.010
- Coral, S., Parisi, G., Nicolay, H. J., Colizzi, F., Danielli, R., Fratta, E., et al. (2013). Immunomodulatory activity of SGI-110, a 5-aza-2'-deoxycytidine-containing demethylating dinucleotide. *Cancer Immunol. Immunother.* 62, 605–614. doi: 10.1007/s00262-012-1365-1367
- Coral, S., Sigalotti, L., Gasparollo, A., Cattarossi, I., Visintin, A., Cattelan, A., et al. (1999). Prolonged upregulation of the expression of HLA class I antigens and costimulatory molecules on melanoma cells treated with 5-aza-2'-deoxycytidine (5-AZA-CdR). *J. Immunother.* 22, 16–24. doi: 10.1097/00002371-199901000-00003
- Corces, M. R., Buenrostro, J. D., Wu, B., Greenside, P. G., Chan, S. M., Koenig, J. L., et al. (2016). Lineage-specific and single-cell chromatin accessibility charts human hematopoiesis and leukemia evolution. *Nat. Genet.* 48, 1193–1203. doi: 10.1038/ng.3646
- Coude, M. M., Braun, T., Berrou, J., Dupont, M., Bertrand, S., Masse, A., et al. (2015). BET inhibitor OTX015 targets BRD2 and BRD4 and decreases c-MYC in acute leukemia cells. *Oncotarget* 6, 17698–17712. doi: 10.18632/oncotarget.4131
- Craddock, C., Jilani, N., Siddique, S., Yap, C., Khan, J., Nagra, S., et al. (2016a). Tolerability and clinical activity of post-transplantation azacitidine in patients allografted for acute myeloid leukemia treated on the RICAZA trial. *Biol. Blood Marrow Transplant.* 22, 385–390. doi: 10.1016/j.bbmt.2015.09.004
- Craddock, C., Labopin, M., Robin, M., Finke, J., Chevallier, P., Yakoub-Agha, I., et al. (2016b). Clinical activity of azacitidine in patients who relapse after allogeneic stem cell transplantation for acute myeloid leukemia. *Haematologica* 101, 879–883. doi: 10.3324/haematol.2015.140996
- Daigle, S. R., Olhava, E. J., Therkelsen, C. A., Basavapathruni, A., Jin, L., Boriack-Sjodin, P. A., et al. (2013). Potent inhibition of DOT1L as treatment of MLL-fusion leukemia. *Blood* 122, 1017–1025. doi: 10.1182/blood-2013-04-497644
- Daigle, S. R., Olhava, E. J., Therkelsen, C. A., Majer, C. R., Sneeringer, C. J., Song, J., et al. (2011). Selective killing of mixed lineage leukemia cells by a potent small-molecule DOT1L inhibitor. *Cancer Cell* 20, 53–65. doi: 10.1016/j.ccr.2011.06.009
- Daskalakis, M., Brocks, D., Sheng, Y. H., Islam, M. S., Ressenrova, A., Assenov, Y., et al. (2018). Reactivation of endogenous retroviral elements via treatment with DNMT- and HDAC-inhibitors. *Cell Cycle* 17, 811–822. doi: 10.1080/15384101.2018.1442623
- Daver, N., Garcia-Manero, G., Basu, S., Boddur, P. C., Alfayez, M., Cortes, J. E., et al. (2019). Efficacy, safety, and biomarkers of response to azacitidine and nivolumab in relapsed/refractory acute myeloid leukemia: a nonrandomized, open-label, phase II study. *Cancer Discov.* 9, 370–383. doi: 10.1158/2159-8290.CD-18-0774
- Dawson, M. A., Prinjha, R. K., Dittmann, A., Giotopoulos, G., Bantscheff, M., Chan, W. I., et al. (2011). Inhibition of BET recruitment to chromatin as an effective treatment for MLL-fusion leukaemia. *Nature* 478, 529–533. doi: 10.1038/nature10509
- de Lima, M., Giral, S., Thall, P. F., de Padua Silva, L., Jones, R. B., Komanduri, K., et al. (2010). Maintenance therapy with low-dose azacitidine after allogeneic hematopoietic stem cell transplantation for recurrent acute myelogenous leukemia or myelodysplastic syndrome: a dose and schedule finding study. *Cancer* 116, 5420–5431. doi: 10.1002/cncr.25500
- DeAngelo, D. J., Spencer, A., Bhalla, K. N., Prince, H. M., Fischer, T., Kindler, T., et al. (2013). Phase Ia/II, two-arm, open-label, dose-escalation study of oral panobinostat administered via two dosing schedules in patients with advanced hematologic malignancies. *Leukemia* 27, 1628–1636. doi: 10.1038/leu.2013.38
- Devaiah, B. N., Case-Borden, C., Geggion, A., Hsu, C. H., Chen, Q., Meerzaman, D., et al. (2016). BRD4 is a histone acetyltransferase that evicts nucleosomes from chromatin. *Nat. Struct. Mol. Biol.* 23, 540–548. doi: 10.1038/nsmb.3228
- Dey, A., Yang, W., Geggion, A., Nishiyama, A., Pan, R., Yagi, R., et al. (2019). BRD4 directs hematopoietic stem cell development and modulates macrophage inflammatory responses. *EMBO J.* 38:e100293. doi: 10.15252/embj.2018100293
- Di Micco, R., Fontanals-Cirera, B., Low, V., Ntziachristos, P., Yuen, S. K., Lovell, C. D., et al. (2014). Control of embryonic stem cell identity by BRD4-dependent transcriptional elongation of super-enhancer-associated pluripotency genes. *Cell Rep.* 9, 234–247. doi: 10.1016/j.celrep.2014.08.055
- Di Micco, R., Sulli, G., Dobrova, M., Liontos, M., Botrugno, O. A., Gargiulo, G., et al. (2011). Interplay between oncogene-induced DNA damage response



- and heterochromatin in senescence and cancer. *Nat. Cell Biol.* 13, 292–302. doi: 10.1038/ncb2170
- Dillon, M. B., Bachovchin, D. A., Brown, S. J., Finn, M. G., Rosen, H., Cravatt, B. F., et al. (2012). Novel inhibitors for PRMT1 discovered by high-throughput screening using activity-based fluorescence polarization. *ACS Chem Biol* 7, 1198–1204. doi: 10.1021/cb300024c
- DiNardo, C. D., Pratz, K., Pullarkat, V., Jonas, B. A., Arellano, M., Becker, P. S., et al. (2019). Venetoclax combined with decitabine or azacitidine in treatment-naïve, elderly patients with acute myeloid leukemia. *Blood* 133, 7–17. doi: 10.1182/blood-2018-08-868752
- DiNardo, C. D., Stein, E. M., de Botton, S., Roboz, G. J., Altman, J. K., Mims, A. S., et al. (2018). Durable remissions with ivosidenib in IDH1-mutated relapsed or refractory AML. *N. Engl. J. Med.* 378, 2386–2398. doi: 10.1056/NEJMoa1716984
- Dohner, H., Weisdorf, D. J., and Bloomfield, C. D. (2015). Acute myeloid leukemia. *N. Engl. J. Med.* 373, 1136–1152. doi: 10.1056/NEJMra1406184
- Dohner, K., Tobis, K., Ulrich, R., Frohling, S., Benner, A., Schlenk, R. F., et al. (2002). Prognostic significance of partial tandem duplications of the MLL gene in adult patients 16 to 60 years old with acute myeloid leukemia and normal cytogenetics: a study of the acute myeloid leukemia study group ulm. *J. Clin. Oncol.* 20, 3254–3261. doi: 10.1200/JCO.2002.09.088
- Duy, C., Teater, M., Garrett-Bakelman, F. E., Lee, T. C., Meydan, C., Glass, J. L., et al. (2019). Rational targeting of cooperating layers of the epigenome yields enhanced therapeutic efficacy against AML. *Cancer Discov.* 9, 872–889
- Ennishi, D., Takata, K., Beguelin, W., Duns, G., Mottok, A., Farinha, P., et al. (2019). Molecular and genetic characterization of MHC deficiency identifies EZH2 as therapeutic target for enhancing immune recognition. *Cancer Discov.* 9:CD-18-1090. doi: 10.1158/2159-8290.CD-18-1090
- Falkenberg, K. J., and Johnstone, R. W. (2014). Histone deacetylases and their inhibitors in cancer, neurological diseases and immune disorders. *Nat. Rev. Drug Discov.* 13, 673–691. doi: 10.1038/nrd4360
- Feng, Y., Arvey, A., Chinen, T., van der Veen, J., Gasteiger, G., and Rudensky, A. Y. (2014). Control of the inheritance of regulatory T cell identity by a cis element in the Foxp3 locus. *Cell* 158, 749–763. doi: 10.1016/j.cell.2014.07.031
- Figueroa, M. E., Abdel-Wahab, O., Lu, C., Ward, P. S., Patel, J., Shih, A., et al. (2010a). Leukemic IDH1 and IDH2 mutations result in a hypermethylation phenotype, disrupt TET2 function, and impair hematopoietic differentiation. *Cancer Cell* 18, 553–567. doi: 10.1016/j.ccr.2010.11.015
- Figueroa, M. E., Lugthart, S., Li, Y., Erpelinck-Verschuere, C., Deng, X., Christos, P. J., et al. (2010b). DNA methylation signatures identify biologically distinct subtypes in acute myeloid leukemia. *Cancer Cell* 17, 13–27. doi: 10.1016/j.ccr.2009.11.020
- Filippakopoulos, P., and Knapp, S. (2014). Targeting bromodomains: epigenetic readers of lysine acetylation. *Nat. Rev. Drug Discov.* 13, 337–356. doi: 10.1038/nrd4286
- Finazzi, G., Vannucchi, A. M., Martinelli, V., Ruggeri, M., Nobile, F., Specchia, G., et al. (2013). A phase II study of Givinostat in combination with hydroxycarbamide in patients with polycythaemia vera unresponsive to hydroxycarbamide monotherapy. *Br. J. Haematol.* 161, 688–694. doi: 10.1111/bjh.12332
- Fiskus, W., Sharma, S., Shah, B., Portier, B. P., Devaraj, S. G., Liu, K., et al. (2014). Highly effective combination of LSD1 (KDM1A) antagonist and pan-histone deacetylase inhibitor against human AML cells. *Leukemia* 28, 2155–2164. doi: 10.1038/leu.2014.119
- Fontanals-Cirera, B., Hasson, D., Vardabasso, C., Di Micco, R., Agrawal, P., Chowdhury, A., et al. (2017). Harnessing BET inhibitor sensitivity reveals AMIGO2 as a melanoma survival gene. *Mol. Cell.* 68:31-744.e9. doi: 10.1016/j.molcel.2017.11.004
- Fraietta, J. A., Nobles, C. L., Sammons, M. A., Lundh, S., Carty, S. A., Reich, T. J., et al. (2018). Disruption of TET2 promotes the therapeutic efficacy of CD19-targeted T cells. *Nature* 558, 307–312. doi: 10.1038/s41586-018-0178-z
- Fujita, S., Honma, D., Adachi, N., Araki, K., Takamatsu, E., Katsumoto, T., et al. (2018). Dual inhibition of EZH1/2 breaks the quiescence of leukemia stem cells in acute myeloid leukemia. *Leukemia* 32, 855–864. doi: 10.1038/leu.2017.300
- Gao, X. N., Lin, J., Ning, Q. Y., Gao, L., Yao, Y. S., Zhou, J. H., et al. (2013). A histone acetyltransferase p300 inhibitor C646 induces cell cycle arrest and apoptosis selectively in AML1-ETO-positive AML cells. *PLoS One* 8:e55481. doi: 10.1371/journal.pone.0055481
- Garcia-Manero, G., Roboz, G., Walsh, K., Kantarjian, H., Ritchie, E., Kropf, P., et al. (2019). Guadecitabine (SGI-110) in patients with intermediate or high-risk myelodysplastic syndromes: phase 2 results from a multicentre, open-label, randomised, phase 1/2 trial. *Lancet Haematol.* 6, e317–e327. doi: 10.1016/S2352-3026(19)30029-30028
- Garcia-Manero, G., Tambaro, F. P., Bekele, N. B., Yang, H., Ravandi, F., Jabbour, E., et al. (2012). Phase II trial of vorinostat with idarubicin and cytarabine for patients with newly diagnosed acute myelogenous leukemia or myelodysplastic syndrome. *J. Clin. Oncol.* 30, 2204–2210. doi: 10.1200/JCO.2011.38.3265
- Gardin, C., and Dombret, H. (2017). Hypomethylating agents as a therapy for AML. *Curr. Hematol. Malig. Rep.* 12, 1–10. doi: 10.1007/s11899-017-0363-364
- Gaymes, T. J., Padua, R. A., Pla, M., Orr, S., Omidvar, N., Chomienne, C., et al. (2006). Histone deacetylase inhibitors (HDI) cause DNA damage in leukemia cells: a mechanism for leukemia-specific HDI-dependent apoptosis? *Mol. Cancer Res.* 4, 563–573. doi: 10.1158/1541-7786.MCR-06-0111
- Gerlach, D., Tontsch-Grunt, U., Baum, A., Popow, J., Scharn, D., Hofmann, M. H., et al. (2018). The novel BET bromodomain inhibitor BI 894999 represses super-enhancer-associated transcription and synergizes with CDK9 inhibition in AML. *Oncogene* 37, 2687–2701. doi: 10.1038/s41388-018-0150-152
- Ghobadi, A., Choi, J., Fiala, M. A., Fletcher, T., Liu, J., Eissenberg, L. G., et al. (2016). Phase I study of azacitidine following donor lymphocyte infusion for relapsed acute myeloid leukemia post allogeneic stem cell transplantation. *Leuk. Res.* 49, 1–6. doi: 10.1016/j.leukres.2016.07.010
- Ghoneim, H. E., Fan, Y., Moustaki, A., Abdelsamed, H. A., Dash, P., Dogra, P., et al. (2017). De novo epigenetic programs inhibit PD-1 blockade-mediated T cell rejuvenation. *Cell* 170:142-157.e19. doi: 10.1016/j.cell.2017.06.007
- Gibaja, V., Shen, F., Harari, J., Korn, J., Ruddy, D., Saenz-Vash, V., et al. (2016). Development of secondary mutations in wild-type and mutant EZH2 alleles cooperates to confer resistance to EZH2 inhibitors. *Oncogene* 35, 558–566. doi: 10.1038/onc.2015.114
- Giles, F., Fischer, T., Cortes, J., Garcia-Manero, G., Beck, J., Ravandi, F., et al. (2006). A phase I study of intravenous LBH589, a novel cinnamic hydroxamic acid analogue histone deacetylase inhibitor, in patients with refractory hematologic malignancies. *Clin. Cancer Res.* 12, 4628–4635. doi: 10.1158/1078-0432.CCR-06-0511
- Glass, J. L., Hassane, D., Wouters, B. J., Kunimoto, H., Avellino, R., Garrett-Bakelman, F. E., et al. (2017). Epigenetic identity in AML depends on disruption of nonpromoter regulatory elements and is affected by antagonistic effects of mutations in epigenetic modifiers. *Cancer Discov.* 7, 868–883. doi: 10.1158/2159-8290.CD-16-1032
- Gojo, I., Tan, M., Fang, H. B., Sadowska, M., Lapidus, R., Baer, M. R., et al. (2013). Translational phase I trial of vorinostat (suberoylanilide hydroxamic acid) combined with cytarabine and etoposide in patients with relapsed, refractory, or high-risk acute myeloid leukemia. *Clin. Cancer Res.* 19, 1838–1851. doi: 10.1158/1078-0432.CCR-12-3165
- Goodyear, O., Agathangelou, A., Novitzky-Basso, I., Siddique, S., McSkeane, T., Ryan, G., et al. (2010). Induction of a CD8+ T-cell response to the MAGE cancer testis antigen by combined treatment with azacitidine and sodium valproate in patients with acute myeloid leukemia and myelodysplasia. *Blood* 116, 1908–1918. doi: 10.1182/blood-2009-11-249474
- Goodyear, O. C., Dennis, M., Jilani, N. Y., Loke, J., Siddique, S., Ryan, G., et al. (2012). Azacitidine augments expansion of regulatory T cells after allogeneic stem cell transplantation in patients with acute myeloid leukemia (AML). *Blood* 119, 3361–3369. doi: 10.1182/blood-2011-09-377044
- Gottlicher, M., Minucci, S., Zhu, P., Kramer, O. H., Schimpf, A., Giavara, S., et al. (2001). Valproic acid defines a novel class of HDAC inhibitors inducing differentiation of transformed cells. *EMBO J.* 20, 6969–6978. doi: 10.1093/emboj/20.24.6969
- Grembecka, J., He, S., Shi, A., Purohit, T., Muntean, A. G., Sorenson, R. J., et al. (2012). Menin-MLL inhibitors reverse oncogenic activity of MLL fusion proteins in leukemia. *Nat. Chem. Biol.* 8, 277–284. doi: 10.1038/nchembio.773
- Grubich, L., Juhl-Christensen, C., Rethmeier, A., Olesen, L. H., Aggerholm, A., Hokland, P., et al. (2008). Gene expression profiling of polycomb, hox and meis genes in patients with acute myeloid leukaemia. *Eur. J. Haematol.* 81, 112–122. doi: 10.1111/j.1600-0609.2008.01083.x
- Han, S., Kim, Y. J., Lee, J., Jeon, S., Hong, T., Park, G. J., et al. (2015). Model-based adaptive phase I trial design of post-transplant decitabine maintenance

- in myelodysplastic syndrome. *J. Hematol. Oncol.* 8:118. doi: 10.1186/s13045-015-0208-203
- He, S., Senter, T. J., Pollock, J., Han, C., Upadhyay, S. K., Purohit, T., et al. (2014). High-affinity small-molecule inhibitors of the menin-mixed lineage leukemia (MLL) interaction closely mimic a natural protein-protein interaction. *J. Med. Chem.* 57, 1543–1556. doi: 10.1021/jm401868d
- Hug, B. A., and Lazar, M. A. (2004). ETO interacting proteins. *Oncogene* 23, 4270–4274. doi: 10.1038/sj.onc.1207674
- Hyllus, D., Stein, C., Schnabel, K., Schiltz, E., Imhof, A., Dou, Y., et al. (2007). PRMT6-mediated methylation of R2 in histone H3 antagonizes H3 K4 trimethylation. *Genes Dev.* 21, 3369–3380. doi: 10.1101/gad.447007
- Iberg, A. N., Espejo, A., Cheng, D., Kim, D., Michaud-Levesque, J., Richard, S., et al. (2008). Arginine methylation of the histone H3 tail impedes effector binding. *J. Biol. Chem.* 283, 3006–3010. doi: 10.1074/jbc.C700192200
- Insinga, A., Monestiroli, S., Ronzoni, S., Gelmetti, V., Marchesi, F., Viale, A., et al. (2005). Inhibitors of histone deacetylases induce tumor-selective apoptosis through activation of the death receptor pathway. *Nat. Med.* 11, 71–76. doi: 10.1038/nm1160
- Issa, J. J., Roboz, G., Rizzieri, D., Jabbour, E., Stock, W., O'Connell, C., et al. (2015). Safety and tolerability of guadecitabine (SGI-110) in patients with myelodysplastic syndrome and acute myeloid leukaemia: a multicentre, randomised, dose-escalation phase 1 study. *Lancet Oncol.* 16, 1099–1110. doi: 10.1016/S1470-2045(15)00038-38
- Izutsu, K., Kurokawa, M., Imai, Y., Maki, K., Mitani, K., and Hirai, H. (2001). The corepressor CtBP interacts with Evi-1 to repress transforming growth factor beta signaling. *Blood* 97, 2815–2822.
- Jo, S. Y., Granowicz, E. M., Maillard, I., Thomas, D., and Hess, J. L. (2011). Requirement for Dot1l in murine postnatal hematopoiesis and leukemogenesis by MLL translocation. *Blood* 117, 4759–4768. doi: 10.1182/blood-2010-12-327668
- Kantarjian, H. M., Thomas, X. G., Dmoszynska, A., Wierzbowska, A., Mazur, G., Mayer, J., et al. (2012). Multicenter, randomized, open-label, phase III trial of decitabine versus patient choice, with physician advice, of either supportive care or low-dose cytarabine for the treatment of older patients with newly diagnosed acute myeloid leukemia. *J. Clin. Oncol.* 30, 2670–2677. doi: 10.1200/JCO.2011.38.9429
- Kaushik, S., Liu, F., Veazey, K. J., Gao, G., Das, P., Neves, L. F., et al. (2018). Genetic deletion or small-molecule inhibition of the arginine methyltransferase PRMT5 exhibit anti-tumoral activity in mouse models of MLL-rearranged AML. *Leukemia* 32, 499–509. doi: 10.1038/leu.2017.206
- Kim, H. P., and Leonard, W. J. (2007). CREB/ATF-dependent T cell receptor-induced FoxP3 gene expression: a role for DNA methylation. *J. Exp. Med.* 204, 1543–1551. doi: 10.1084/jem.20070109
- Kirschbaum, M., Gojo, I., Goldberg, S. L., Bredeson, C., Kujawski, L. A., Yang, A., et al. (2014). A phase 1 clinical trial of vorinostat in combination with decitabine in patients with acute myeloid leukaemia or myelodysplastic syndrome. *Br. J. Haematol.* 167, 185–193. doi: 10.1111/bjh.13016
- Kitabayashi, I., Aikawa, Y., Yokoyama, A., Hosoda, F., Nagai, M., Kakazu, N., et al. (2001). Fusion of MOZ and p300 histone acetyltransferases in acute monocytic leukemia with a t(8;22)(p11;q13) chromosome translocation. *Leukemia* 15, 89–94. doi: 10.1038/sj.leu.2401983
- Kuhn, M. W., Hadler, M. J., Daigle, S. R., Koche, R. P., Krivtsov, A. V., Olhava, E. J., et al. (2015). MLL partial tandem duplication leukemia cells are sensitive to small molecule DOT1L inhibition. *Haematologica* 100, e190–193. doi: 10.3324/haematol.2014.115337
- Kurimchak, A. M., Shelton, C., Duncan, K. E., Johnson, K. J., Brown, J., O'Brien, S., et al. (2016). Resistance to BET bromodomain inhibitors is mediated by kinome reprogramming in ovarian cancer. *Cell Rep.* 16, 1273–1286. doi: 10.1016/j.celrep.2016.06.091
- Lal, G., Zhang, N., van der Touw, W., Ding, Y., Ju, W., Bottinger, E. P., et al. (2009). Epigenetic regulation of Foxp3 expression in regulatory T cells by DNA methylation. *J. Immunol.* 182, 259–273. doi: 10.4049/jimmunol.182.1.259
- Lehnertz, B., Pabst, C., Su, L., Miller, M., Liu, F., Yi, L., et al. (2014). The methyltransferase G9a regulates HoxA9-dependent transcription in AML. *Genes Dev.* 28, 317–327. doi: 10.1101/gad.236794.113
- Lessard, J., and Sauvageau, G. (2003). Polycomb group genes as epigenetic regulators of normal and leukemic hemopoiesis. *Exp. Hematol.* 31, 567–585. doi: 10.1016/s0301-472x(03)00081-x
- Li, S., Garrett-Bakelman, F. E., Chung, S. S., Sanders, M. A., Hricik, T., Rapaport, F., et al. (2016). Distinct evolution and dynamics of epigenetic and genetic heterogeneity in acute myeloid leukemia. *Nat. Med.* 22, 792–799. doi: 10.1038/nm.4125
- Li, Y., Zhao, K., Yao, C., Kahwash, S., Tang, Y., Zhang, G., et al. (2016). Givinostat, a type II histone deacetylase inhibitor, induces potent caspase-dependent apoptosis in human lymphoblastic leukemia. *Genes Cancer* 7, 292–300. doi: 10.18632/genesandcancer.117
- Lin, C. H., Wong, S. H., Kurzer, J. H., Schneidawind, C., Wei, M. C., Duque-Afonso, J., et al. (2018). SETDB2 links E2A-PBX1 to cell-cycle dysregulation in acute leukemia through CDKN2C repression. *Cell Rep.* 23, 1166–1177. doi: 10.1016/j.celrep.2018.03.124
- Liu, F., Barsyte-Lovejoy, D., Li, F., Xiong, Y., Korboukh, V., Huang, X. P., et al. (2013). Discovery of an in vivo chemical probe of the lysine methyltransferases G9a and GLP. *J. Med. Chem.* 56, 8931–8942. doi: 10.1021/jm401480r
- Lokody, I. (2014). Drug resistance: overcoming resistance in acute myeloid leukaemia treatment. *Nat. Rev. Cancer* 14, 452–453. doi: 10.1038/nrc3776
- Loven, J., Hoke, H. A., Lin, C. Y., Lau, A., Orlando, D. A., Vakoc, C. R., et al. (2013). Selective inhibition of tumor oncogenes by disruption of super-enhancers. *Cell* 153, 320–334. doi: 10.1016/j.cell.2013.03.036
- Lubbert, M., Bertz, H., Wasch, R., Marks, R., Ruter, B., Claus, R., et al. (2010). Efficacy of a 3-day, low-dose treatment with 5-azacytidine followed by donor lymphocyte infusions in older patients with acute myeloid leukemia or chronic myelomonocytic leukemia relapsed after allografting. *Bone Marrow Transplant.* 45, 627–632. doi: 10.1038/bmt.2009.222
- Maiques-Diaz, A., Lynch, J. T., Spencer, G. J., and Somervaille, T. C. P. (2018). LSD1 inhibitors disrupt the GF11 transcription repressor complex. *Mol. Cell Oncol.* 5:e1481813. doi: 10.1080/23723556.2018.1481813
- Maiques-Diaz, A., and Somervaille, T. C. (2016). LSD1: biologic roles and therapeutic targeting. *Epigenomics* 8, 1103–1116. doi: 10.2217/epi-2016-2019
- Mansour, M. R., Abraham, B. J., Anders, L., Berezovskaya, A., Gutierrez, A., Durbin, A. D., et al. (2014). Oncogene regulation. an oncogenic super-enhancer formed through somatic mutation of a noncoding intergenic element. *Science* 346, 1373–1377. doi: 10.1126/science.1259037
- Mar, B. G., Bullinger, L. B., McLean, K. M., Grauman, P. V., Harris, M. H., Stevenson, K., et al. (2014). Mutations in epigenetic regulators including SETD2 are gained during relapse in paediatric acute lymphoblastic leukaemia. *Nat. Commun.* 5:3469. doi: 10.1038/ncomms4469
- Mar, B. G., Chu, S. H., Kahn, J. D., Krivtsov, A. V., Koche, R., Castellano, C. A., et al. (2017). SETD2 alterations impair DNA damage recognition and lead to resistance to chemotherapy in leukemia. *Blood* 130, 2631–2641. doi: 10.1182/blood-2017-03-775569
- Margueron, R., and Reinberg, D. (2011). The polycomb complex PRC2 and its mark in life. *Nature* 469, 343–349. doi: 10.1038/nature09784
- Metzeler, K. H., Becker, H., Maharry, K., Radmacher, M. D., Kohlschmidt, J., Mrozek, K., et al. (2011). ASXL1 mutations identify a high-risk subgroup of older patients with primary cytogenetically normal AML within the ELN favorable genetic category. *Blood* 118, 6920–6929. doi: 10.1182/blood-2011-08-368225
- Micol, J. B., Duployez, N., Boissel, N., Petit, A., Geffroy, S., Nibourel, O., et al. (2014). Frequent ASXL2 mutations in acute myeloid leukemia patients with t(8;21)/RUNX1-RUNX1T1 chromosomal translocations. *Blood* 124, 1445–1449. doi: 10.1182/blood-2014-04-571018
- Mihara, K., Chowdhury, M., Nakaju, N., Hidani, S., Ihara, A., Hyodo, H., et al. (2006). Bmi-1 is useful as a novel molecular marker for predicting progression of myelodysplastic syndrome and patient prognosis. *Blood* 107, 305–308. doi: 10.1182/blood-2005-06-2393
- Milne, T. A., Briggs, S. D., Brock, H. W., Martin, M. E., Gibbs, D., Allis, C. D., et al. (2002). MLL targets SET domain methyltransferase activity to Hox gene promoters. *Mol. Cell.* 10, 1107–1117. doi: 10.1016/s1097-2765(02)00741-4
- Moffitt, A. B., Ondrejka, S. L., McKinney, M., Rempel, R. E., Goodlad, J. R., Teh, C. H., et al. (2017). Enteropathy-associated T cell lymphoma subtypes are characterized by loss of function of SETD2. *J. Exp. Med.* 214, 1371–1386. doi: 10.1084/jem.20160894
- Moran-Crusio, K., Reavie, L., Shih, A., Abdel-Wahab, O., Ndiaye-Lobry, D., Lobry, C., et al. (2011). Tet2 loss leads to increased hematopoietic stem cell self-renewal and myeloid transformation. *Cancer Cell* 20, 11–24. doi: 10.1016/j.ccr.2011.06.001

- Morey, L., Santanach, A., Blanco, E., Aloia, L., Nora, E. P., Bruneau, B. G., et al. (2015). Polycomb regulates mesoderm cell fate-specification in embryonic stem cells through activation and repression mechanisms. *Cell Stem Cell* 17, 300–315. doi: 10.1016/j.stem.2015.08.009
- Morin, R. D., Johnson, N. A., Severson, T. M., Mungall, A. J., An, J., Goya, R., et al. (2010). Somatic mutations altering EZH2 (Tyr641) in follicular and diffuse large B-cell lymphomas of germinal-center origin. *Nat. Genet.* 42, 181–185. doi: 10.1038/ng.518
- Navada, S. C., Steinmann, J., Lubbert, M., and Silverman, L. R. (2014). Clinical development of demethylating agents in hematology. *J. Clin. Invest.* 124, 40–46. doi: 10.1172/JCI69739
- Nebbioso, A., Clarke, N., Voltz, E., Germain, E., Ambrosino, C., Bontempo, P., et al. (2005). Tumor-selective action of HDAC inhibitors involves TRAIL induction in acute myeloid leukemia cells. *Nat. Med.* 11, 77–84. doi: 10.1038/nm1161
- Neff, T., Sinha, A. U., Kluk, M. J., Zhu, N., Khattab, M. H., Stein, L., et al. (2012). Polycomb repressive complex 2 is required for MLL-AF9 leukemia. *Proc. Natl. Acad. Sci. U.S.A.* 109, 5028–5033. doi: 10.1073/pnas.1202258109
- Nguyen, A. T., Taranova, O., He, J., and Zhang, Y. (2011). DOT1L, the H3K79 methyltransferase, is required for MLL-AF9-mediated leukemogenesis. *Blood* 117, 6912–6922. doi: 10.1182/blood-2011-02-334359
- Nikoloski, G., Langemeijer, S. M., Kuiper, R. P., Knops, R., Massop, M., Tonnissen, E. R., et al. (2010). Somatic mutations of the histone methyltransferase gene EZH2 in myelodysplastic syndromes. *Nat. Genet.* 42, 665–667. doi: 10.1038/ng.620
- Okada, Y., Feng, Q., Lin, Y., Jiang, Q., Li, Y., Coffield, V. M., et al. (2005). hDOT1L links histone methylation to leukemogenesis. *Cell* 121, 167–178. doi: 10.1016/j.cell.2005.02.020
- Papaemmanuil, E., Gerstung, M., Bullinger, L., Gaidzik, V. I., Paschka, P., Roberts, N. D., et al. (2016). Genomic classification and prognosis in acute myeloid leukemia. *N. Engl. J. Med.* 374, 2209–2221. doi: 10.1056/NEJMoa1516192
- Paschka, P., Schlenk, R. F., Gaidzik, V. I., Herzig, J. K., Aulitzky, T., Bullinger, L., et al. (2015). ASXL1 mutations in younger adult patients with acute myeloid leukemia: a study by the german—austrian acute myeloid leukemia study group. *Haematologica* 100, 324–330. doi: 10.3324/haematol.2014.114157
- Peart, M. J., Smyth, G. K., van Laar, R. K., Bowtell, D. D., Richon, V. M., Marks, P. A., et al. (2005). Identification and functional significance of genes regulated by structurally different histone deacetylase inhibitors. *Proc. Natl. Acad. Sci. U.S.A.* 102, 3697–3702. doi: 10.1073/pnas.0500369102
- Perez-Salvia, M., and Esteller, M. (2017). Bromodomain inhibitors and cancer therapy: from structures to applications. *Epigenetics* 12, 323–339. doi: 10.1080/15592294.2016.1265710
- Petrucelli, L. A., Dupere-Richer, D., Petterson, F., Retrouvey, H., and Skoulikas, S. M. (2011). Vorinostat induces reactive oxygen species and DNA damage in acute myeloid leukemia cells. *PLoS One* 6:e20987. doi: 10.1371/journal.pone.0020987
- Platzbecker, U., Wermke, M., Radke, J., Oelschlaegel, U., Seltmann, F., Kiani, A., et al. (2012). Azacitidine for treatment of imminent relapse in MDS or AML patients after allogeneic HSCT: results of the RELAZA trial. *Leukemia* 26, 381–389. doi: 10.1038/leu.2011.234
- Polansky, J. K., Kretschmer, K., Freyer, J., Floess, S., Garbe, A., Baron, U., et al. (2008). DNA methylation controls Foxp3 gene expression. *Eur. J. Immunol.* 38, 1654–1663. doi: 10.1002/eji.200838105
- Pollyea, D. A., Stevens, B. M., Jones, C. L., Winters, A., Pei, S., Minhajuddin, M., et al. (2018). Venetoclax with azacitidine disrupts energy metabolism and targets leukemia stem cells in patients with acute myeloid leukemia. *Nat. Med.* 24, 1859–1866. doi: 10.1038/s41591-018-0233-231
- Puda, A., Milosevic, J. D., Berg, T., Klampfl, T., Harutyunyan, A. S., Gisslinger, B., et al. (2012). Frequent deletions of JARID2 in leukemic transformation of chronic myeloid malignancies. *Am. J. Hematol.* 87, 245–250. doi: 10.1002/ajh.22257
- Pusic, I., Choi, J., Fiala, M. A., Gao, F., Holt, M., Cashen, A. F., et al. (2015). Maintenance therapy with decitabine after allogeneic stem cell transplantation for acute myelogenous leukemia and myelodysplastic syndrome. *Biol. Blood Marrow Transplant.* 21, 1761–1769. doi: 10.1016/j.bbmt.2015.05.026
- Qi, W., Zhao, K., Gu, J., Huang, Y., Wang, Y., Zhang, H., et al. (2017). An allosteric PRC2 inhibitor targeting the H3K27me3 binding pocket of EED. *Nat. Chem. Biol.* 13, 381–388. doi: 10.1038/nchembio.2304
- Qu, Y., Siggins, L., Cordeddu, L., Gaidzik, V. I., Karlsson, K., Bullinger, L., et al. (2017). Cancer-specific changes in DNA methylation reveal aberrant silencing and activation of enhancers in leukemia. *Blood* 129, e13–e25. doi: 10.1182/blood-2016-07-726877
- Quivoron, C., Couronne, L., Della Valle, V., Lopez, C. K., Plo, I., Wagner-Ballon, O., et al. (2011). TET2 inactivation results in pleiotropic hematopoietic abnormalities in mouse and is a recurrent event during human lymphomagenesis. *Cancer Cell* 20, 25–38. doi: 10.1016/j.ccr.2011.06.003
- Rasmussen, K. D., Jia, G., Johansen, J. V., Pedersen, M. T., Rapin, N., Bagger, F. O., et al. (2015). Loss of TET2 in hematopoietic cells leads to DNA hypermethylation of active enhancers and induction of leukemogenesis. *Genes Dev.* 29, 910–922. doi: 10.1101/gad.26017.4.115
- Rathert, P., Roth, M., Neumann, T., Muerdter, F., Roe, J. S., Muhar, M., et al. (2015). Transcriptional plasticity promotes primary and acquired resistance to BET inhibition. *Nature* 525, 543–547. doi: 10.1038/nature14898
- Reinisch, A., Thomas, D., Corces, M. R., Zhang, X., Gratzinger, D., Hong, W. J., et al. (2016). A humanized bone marrow ossicle xenotransplantation model enables improved engraftment of healthy and leukemic human hematopoietic cells. *Nat. Med.* 22, 812–821. doi: 10.1038/nm.4103
- Ribeiro, A. F., Pratorcorona, M., Erpelinck-Verschuere, C., Rockova, V., Sanders, M., Abbas, S., et al. (2012). Mutant DNMT3A: a marker of poor prognosis in acute myeloid leukemia. *Blood* 119, 5824–5831. doi: 10.1182/blood-2011-07-367961.
- Rizo, A., Olthof, S., Han, L., Vellenga, E., de Haan, G., and Schuringa, J. J. (2009). Repression of BMI1 in normal and leukemic human CD34(+) cells impairs self-renewal and induces apoptosis. *Blood* 114, 1498–1505. doi: 10.1182/blood-2009-03-209734
- Rohle, D., Popovici-Muller, J., Palaskas, N., Turcan, S., Grommes, C., Campos, C., et al. (2013). An inhibitor of mutant IDH1 delays growth and promotes differentiation of glioma cells. *Science* 340, 626–630. doi: 10.1126/science.1236062
- Rohner, A., Langenkamp, U., Siegler, U., Kalberer, C. P., and Wodnar-Filipowicz, A. (2007). Differentiation-promoting drugs up-regulate NKG2D ligand expression and enhance the susceptibility of acute myeloid leukemia cells to natural killer cell-mediated lysis. *Leuk. Res.* 31, 1393–1402. doi: 10.1016/j.leukres.2007.02.020
- Roulois, D., Loo Yau, H., Singhanian, R., Wang, Y., Danesh, A., Shen, S. Y., et al. (2015). DNA-demethylating agents target colorectal cancer cells by inducing viral mimicry by endogenous transcripts. *Cell* 162, 961–973. doi: 10.1016/j.cell.2015.07.056
- Rucker, F. G., Lang, K. M., Futterer, M., Komarica, V., Schmid, M., Dohner, H., et al. (2016). Molecular dissection of valproic acid effects in acute myeloid leukemia identifies predictive networks. *Epigenetics* 11, 517–525. doi: 10.1080/15592294.2016.1187350
- Sanchez-Abarca, L. I., Gutierrez-Cosio, S., Santamaria, C., Caballero-Velazquez, T., Blanco, B., Herrero-Sanchez, C., et al. (2010). Immunomodulatory effect of 5-azacytidine (5-azaC): potential role in the transplantation setting. *Blood* 115, 107–121. doi: 10.1182/blood-2009-03-210393
- Schenk, T., Chen, W. C., Gollner, S., Howell, L., Jin, L., Hebestreit, K., et al. (2012). Inhibition of the LSD1 (KDM1A) demethylase reactivates the all-trans-retinoic acid differentiation pathway in acute myeloid leukemia. *Nat. Med.* 18, 605–611. doi: 10.1038/nm.2661
- Schichman, S. A., Caligiuri, M. A., Gu, Y., Strout, M. P., Canaani, E., Bloomfield, C. D., et al. (1994). ALL-1 partial duplication in acute leukemia. *Proc. Natl. Acad. Sci. U.S.A.* 91, 6236–6239. doi: 10.1073/pnas.91.13.6236
- Schlenk, R. F., Krauter, J., Raffoux, E., Kreuzer, K. A., Schaich, M., Noens, L., et al. (2018). Panobinostat monotherapy and combination therapy in patients with acute myeloid leukemia: results from two clinical trials. *Haematologica* 103, e25–e28. doi: 10.3324/haematol.2017.172411
- Schnittger, S., Eder, C., Jeromin, S., Alpermann, T., Fasan, A., Grossmann, V., et al. (2013). ASXL1 exon 12 mutations are frequent in AML with intermediate risk karyotype and are independently associated with an adverse outcome. *Leukemia* 27, 82–91. doi: 10.1038/leu.2012.262
- Schroeder, T., Czibere, A., Platzbecker, U., Bug, G., Uharek, L., Luft, T., et al. (2013). Azacitidine and donor lymphocyte infusions as first salvage therapy for relapse of AML or MDS after allogeneic stem cell transplantation. *Leukemia* 27, 1229–1235. doi: 10.1038/leu.2013.7



- Schroeder, T., Rachlis, E., Bug, G., Stelljes, M., Klein, S., Steckel, N. K., et al. (2015). Treatment of acute myeloid leukemia or myelodysplastic syndrome relapse after allogeneic stem cell transplantation with azacitidine and donor lymphocyte infusions—a retrospective multicenter analysis from the German cooperative transplant study group. *Biol. Blood Marrow Transplant.* 21, 653–660. doi: 10.1016/j.bbmt.2014.12.016
- Schroeder, T., Rautenberg, C., Kruger, W., Platzbecker, U., Bug, G., Steinmann, J., et al. (2018). Treatment of relapsed AML and MDS after allogeneic stem cell transplantation with decitabine and DLI—a retrospective multicenter analysis on behalf of the German cooperative transplant study group. *Ann. Hematol.* 97, 335–342. doi: 10.1007/s00277-017-3185-3185
- Senyuk, V., Chakraborty, S., Mikhail, F. M., Zhao, R., Chi, Y., and Nucifora, G. (2002). The leukemia-associated transcription repressor AML1/MDS1/EV11 requires CtBP to induce abnormal growth and differentiation of murine hematopoietic cells. *Oncogene* 21, 3232–3240. doi: 10.1038/sj.onc.1205436
- Setiadi, A. F., David, M. D., Seipp, R. P., Hartikainen, J. A., Gopaul, R., and Jefferies, W. A. (2007). Epigenetic control of the immune escape mechanisms in malignant carcinomas. *Mol. Cell. Biol.* 27, 7886–7894. doi: 10.1128/MCB.01547-1547
- Shankar, S. R., Bahirvani, A. G., Rao, V. K., Bharathy, N., Ow, J. R., and Taneja, R. (2013). G9a, a multipotent regulator of gene expression. *Epigenetics* 8, 16–22. doi: 10.4161/epi.23331
- Shen, L., Ciesielski, M., Ramakrishnan, S., Miles, K. M., Ellis, L., Sotomayor, P., et al. (2012). Class I histone deacetylase inhibitor entinostat suppresses regulatory T cells and enhances immunotherapies in renal and prostate cancer models. *PLoS One* 7:e30815. doi: 10.1371/journal.pone.0030815
- Sheng, W., LaFleur, M. W., Nguyen, T. H., Chen, S., Chakravarthy, A., Conway, J. R., et al. (2018). LSD1 ablation stimulates anti-tumor immunity and enables checkpoint blockade. *Cell* 174, 549–563 e519. doi: 10.1016/j.cell.2018.05.052
- Shi, J., Wang, E., Zuber, J., Rappaport, A., Taylor, M., Johns, C., et al. (2013). The polycomb complex PRC2 supports aberrant self-renewal in a mouse model of MLL-AF9;Nras(G12D) acute myeloid leukemia. *Oncogene* 32, 930–938. doi: 10.1038/onc.2012.110
- Shia, W. J., Okumura, A. J., Yan, M., Sarkeshik, A., Lo, M. C., Matsuura, S., et al. (2012). PRMT1 interacts with AML1-ETO to promote its transcriptional activation and progenitor cell proliferative potential. *Blood* 119, 4953–4962. doi: 10.1182/blood-2011-04-347476
- Shu, S., Lin, C. Y., He, H. H., Witwicki, R. M., Tabassum, D. P., Roberts, J. M., et al. (2016). Response and resistance to BET bromodomain inhibitors in triple-negative breast cancer. *Nature* 529, 413–417. doi: 10.1038/nature16508
- Skucha, A., Ebner, J., and Grebien, F. (2019). Roles of SETD2 in leukemia-transcription, DNA-damage, and beyond. *Int. J. Mol. Sci.* 20:1029. doi: 10.3390/ijms20051029
- Smitheman, K. N., Severson, T. M., Rajapurkar, S. R., McCabe, M. T., Karpnich, N., Foley, J., et al. (2019). Lysine specific demethylase 1 inactivation enhances differentiation and promotes cytotoxic response when combined with all-trans retinoic acid in acute myeloid leukemia across subtypes. *Haematologica* 104, 1156–1167. doi: 10.3324/haematol.2018.199190
- Stark, M., and Hayward, N. (2007). Genome-wide loss of heterozygosity and copy number analysis in melanoma using high-density single-nucleotide polymorphism arrays. *Cancer Res.* 67, 2632–2642. doi: 10.1158/0008-5472.CAN-06-4152
- Stein, E. M., DiNardo, C. D., Fathi, A. T., Pollyea, D. A., Stone, R. M., Altman, J. K., et al. (2019). Molecular remission and response patterns in patients with mutant-IDH2 acute myeloid leukemia treated with enasidenib. *Blood* 133, 676–687. doi: 10.1182/blood-2018-08-869008
- Stein, E. M., DiNardo, C. D., Pollyea, D. A., Fathi, A. T., Roboz, G. J., Altman, J. K., et al. (2017). Enasidenib in mutant IDH2 relapsed or refractory acute myeloid leukemia. *Blood* 130, 722–731. doi: 10.1182/blood-2017-04-779405
- Stein, E. M., Garcia-Manero, G., Rizzieri, D. A., Tibes, R., Berdeja, J. G., Savona, M. R., et al. (2018). The DOT1L inhibitor pinometostat reduces H3K79 methylation and has modest clinical activity in adult acute leukemia. *Blood* 131, 2661–2669. doi: 10.1182/blood-2017-12-818948
- Stein, E. M., and Tallman, M. S. (2016). Emerging therapeutic drugs for AML. *Blood* 127, 71–78. doi: 10.1182/blood-2015-07-604538
- Steinmann, J., Bertz, H., Wasch, R., Marks, R., Zeiser, R., Bogatyreva, L., et al. (2015). 5-Azacytidine and DLI can induce long-term remissions in AML patients relapsed after allograft. *Bone Marrow Transplant.* 50, 690–695. doi: 10.1038/bmt.2015.10
- Stratikopoulos, E. E., Dendy, M., Szabolcs, M., Khaykin, A. J., Lefebvre, C., Zhou, M. M., et al. (2015). Kinase and BET inhibitors together clamp inhibition of PI3K signaling and overcome resistance to therapy. *Cancer Cell* 27, 837–851. doi: 10.1016/j.ccr.2015.05.006
- Sugino, N., Kawahara, M., Tatsumi, G., Kanai, A., Matsui, H., Yamamoto, R., et al. (2017). A novel LSD1 inhibitor NCD38 ameliorates MDS-related leukemia with complex karyotype by attenuating leukemia programs via activating super-enhancers. *Leukemia* 31, 2303–2314. doi: 10.1038/leu.2017.59
- Sweis, R. F., Pliushchev, M., Brown, P. J., Guo, J., Li, F., Maag, D., et al. (2014). Discovery and development of potent and selective inhibitors of histone methyltransferase G9a. *ACS Med. Chem. Lett.* 5, 205–209. doi: 10.1021/ml400496h
- Tadokoro, Y., Ema, H., Okano, M., Li, E., and Nakauchi, H. (2007). De novo DNA methyltransferase is essential for self-renewal, but not for differentiation, in hematopoietic stem cells. *J. Exp. Med.* 204, 715–722. doi: 10.1084/jem.20060750
- Tanaka, S., Miyagi, S., Sashida, G., Chiba, T., Yuan, J., Mochizuki-Kashio, M., et al. (2012). Ezh2 augments leukemogenicity by reinforcing differentiation blockage in acute myeloid leukemia. *Blood* 120, 1107–1117. doi: 10.1182/blood-2011-11-394932
- Taylor, B. S., DeCarolis, P. L., Angeles, C. V., Brenet, F., Schultz, N., Antonescu, C. R., et al. (2011). Frequent alterations and epigenetic silencing of differentiation pathway genes in structurally rearranged liposarcomas. *Cancer Discov.* 1, 587–597. doi: 10.1158/2159-8290.CD-11-0181
- Thol, F., Damm, F., Ludeking, A., Winschel, C., Wagner, K., Morgan, M., et al. (2011a). Incidence and prognostic influence of DNMT3A mutations in acute myeloid leukemia. *J. Clin. Oncol.* 29, 2889–2896. doi: 10.1200/JCO.2011.35.4894
- Thol, F., Winschel, C., Ludeking, A., Yun, H., Friesen, I., Damm, F., et al. (2011b). Rare occurrence of DNMT3A mutations in myelodysplastic syndromes. *Haematologica* 96, 1870–1873. doi: 10.3324/haematol.2011.045559
- Toffalori, C., Cavattoni, I., Deola, S., Mastaglio, S., Giglio, F., Mazzi, B., et al. (2012). Genomic loss of patient-specific HLA in acute myeloid leukemia relapse after well-matched unrelated donor HSCT. *Blood* 119, 4813–4815. doi: 10.1182/blood-2012-02-411686
- Toffalori, C., Zito, L., Gambacorta, V., Riba, M., Oliveira, G., Bucci, G., et al. (2019). Immune signature drives leukemia escape and relapse after hematopoietic cell transplantation. *Nat. Med.* 25, 603–611. doi: 10.1038/s41591-019-0400-z
- Tyrakis, P. A., Palazon, A., Macias, D., Lee, K. L., Phan, A. T., Velica, P., et al. (2016). S-2-hydroxyglutarate regulates CD8(+) T-lymphocyte fate. *Nature* 540, 236–241. doi: 10.1038/nature20165
- Vago, L., Perna, S. K., Zanussi, M., Mazzi, B., Barlassina, C., Stanghellini, M. T., et al. (2009). Loss of mismatched HLA in leukemia after stem-cell transplantation. *N. Engl. J. Med.* 361, 478–488. doi: 10.1056/NEJMoa0811036
- Vedadi, M., Baryte-Lovejoy, D., Liu, F., Rival-Gervier, S., Allali-Hassani, A., Labrie, V., et al. (2011). A chemical probe selectively inhibits G9a and GLP methyltransferase activity in cells. *Nat. Chem. Biol.* 7, 566–574. doi: 10.1038/nchembio.599
- Wang, D., Quiros, J., Mahuron, K., Pai, C. C., Ranzani, V., Young, A., et al. (2018). Targeting EZH2 reprograms intratumoral regulatory T cells to enhance cancer immunity. *Cell Rep.* 23, 3262–3274. doi: 10.1016/j.celrep.2018.05.050
- Wang, F., Travins, J., DeLaBarre, B., Penard-Lacronique, V., Schalm, S., Hansen, E., et al. (2013). Targeted inhibition of mutant IDH2 in leukemia cells induces cellular differentiation. *Science* 340, 622–626. doi: 10.1126/science.1234769
- Wang, H., Huang, Z. Q., Xia, L., Feng, Q., Erdjument-Bromage, H., Strahl, B. D., et al. (2001). Methylation of histone H4 at arginine 3 facilitating transcriptional activation by nuclear hormone receptor. *Science* 293, 853–857. doi: 10.1126/science.1060781
- Ward, P. S., Patel, J., Wise, D. R., Abdel-Wahab, O., Bennett, B. D., Collier, H. A., et al. (2010). The common feature of leukemia-associated IDH1 and IDH2 mutations is a neomorphic enzyme activity converting alpha-ketoglutarate to 2-hydroxyglutarate. *Cancer Cell* 17, 225–234. doi: 10.1016/j.ccr.2010.01.020

- Woods, D. M., Sodre, A. L., Villagra, A., Sarnaik, A., Sotomayor, E. M., and Weber, J. (2015). HDAC inhibition upregulates PD-1 ligands in melanoma and augments immunotherapy with PD-1 Blockade. *Cancer Immunol. Res.* 3, 1375–1385. doi: 10.1158/2326-6066.CIR-15-0077-T
- Wouters, B. J., and Delwel, R. (2016). Epigenetics and approaches to targeted epigenetic therapy in acute myeloid leukemia. *Blood* 127, 42–52. doi: 10.1182/blood-2015-07-604512
- Wu, S. Y., and Chiang, C. M. (2007). The double bromodomain-containing chromatin adaptor Brd4 and transcriptional regulation. *J. Biol. Chem.* 282, 13141–13145. doi: 10.1074/jbc.R70001200
- Wyce, A., Matteo, J. J., Foley, S. W., Felitsky, D. J., Rajapurkar, S. R., Zhang, X. P., et al. (2018). MEK inhibitors overcome resistance to BET inhibition across a number of solid and hematologic cancers. *Oncogenesis* 7:35. doi: 10.1038/s41389-018-0043-49
- Xu, B., On, D. M., Ma, A., Parton, T., Konze, K. D., Pattenden, S. G., et al. (2015). Selective inhibition of EZH2 and EZH1 enzymatic activity by a small molecule suppresses MLL-rearranged leukemia. *Blood* 125, 346–357. doi: 10.1182/blood-2014-06-581082
- Xu, F., Li, X., Wu, L., Zhang, Q., Yang, R., Yang, Y., et al. (2011). Overexpression of the EZH2, RING1 and BMI1 genes is common in myelodysplastic syndromes: relation to adverse epigenetic alteration and poor prognostic scoring. *Ann. Hematol.* 90, 643–653. doi: 10.1007/s00277-010-1128-1125
- Xu, W., Ngo, L., Perez, G., Dokmanovic, M., and Marks, P. A. (2006). Intrinsic apoptotic and thioredoxin pathways in human prostate cancer cell response to histone deacetylase inhibitor. *Proc. Natl. Acad. Sci. U.S.A.* 103, 15540–15545. doi: 10.1073/pnas.0607518103
- Yang, H., Bueso-Ramos, C., DiNardo, C., Estecio, M. R., Davanlou, M., Geng, Q. R., et al. (2014). Expression of PD-L1, PD-L2, PD-1 and CTLA4 in myelodysplastic syndromes is enhanced by treatment with hypomethylating agents. *Leukemia* 28, 1280–1288. doi: 10.1038/leu.2013.355
- Yang, H., Pinello, C. E., Luo, J., Li, D., Wang, Y., Zhao, L. Y., et al. (2013). Small-molecule inhibitors of acetyltransferase p300 identified by high-throughput screening are potent anticancer agents. *Mol. Cancer Ther.* 12, 610–620. doi: 10.1158/1535-7163.MCT-12-0930
- Yen, K., Travins, J., Wang, F., David, M. D., Artin, E., Straley, K., et al. (2017). AG-221, a first-in-class therapy targeting acute myeloid leukemia harboring oncogenic IDH2 mutations. *Cancer Discov.* 7, 478–493. doi: 10.1158/2159-8290.CD-16-1034
- Zeiser, R., and Vago, L. (2019). Mechanisms of immune escape after allogeneic hematopoietic cell transplantation. *Blood* 133, 1290–1297. doi: 10.1182/blood-2018-10-846824
- Zhang, Y. L., Sun, J. W., Xie, Y. Y., Zhou, Y., Liu, P., Song, J. C., et al. (2018). Setd2 deficiency impairs hematopoietic stem cell self-renewal and causes malignant transformation. *Cell Res.* 28, 476–490. doi: 10.1038/s41422-018-0015-19
- Zhao, X., Jankovic, V., Gural, A., Huang, G., Pardnani, A., Menendez, S., et al. (2008). Methylation of RUNX1 by PRMT1 abrogates SIN3A binding and potentiates its transcriptional activity. *Genes Dev.* 22, 640–653. doi: 10.1101/gad.1632608
- Zhou, Y., Yan, X., Feng, X., Bu, J., Dong, Y., Lin, P., et al. (2018). Setd2 regulates quiescence and differentiation of adult hematopoietic stem cells by restricting RNA polymerase II elongation. *Haematologica* 103, 1110–1123. doi: 10.3324/haematol.2018.187708
- Zhu, X., He, F., Zeng, H., Ling, S., Chen, A., Wang, Y., et al. (2014). Identification of functional cooperative mutations of SETD2 in human acute leukemia. *Nat. Genet.* 46, 287–293. doi: 10.1038/ng.2894
- Zuber, J., Shi, J., Wang, E., Rappaport, A. R., Herrmann, H., Sison, E. A., et al. (2011). RNAi screen identifies Brd4 as a therapeutic target in acute myeloid leukaemia. *Nature* 478, 524–528. doi: 10.1038/nature10334
- Zuin, J., Dixon, J. R., van der Reijden, M. I., Ye, Z., Kolovos, P., Brouwer, R. W., et al. (2014). Cohesin and CTCF differentially affect chromatin architecture and gene expression in human cells. *Proc. Natl. Acad. Sci. U.S.A.* 111, 996–1001. doi: 10.1073/pnas.1317788111

**Conflict of Interest:** The authors declare that the research was conducted in the absence of any commercial or financial relationships that could be construed as a potential conflict of interest.

The reviewer IG declared a past co-authorship with one of the authors LV to the handling Editor.

Copyright © 2019 Gambacorta, Gnani, Vago and Di Micco. This is an open-access article distributed under the terms of the Creative Commons Attribution License (CC BY). The use, distribution or reproduction in other forums is permitted, provided the original author(s) and the copyright owner(s) are credited and that the original publication in this journal is cited, in accordance with accepted academic practice. No use, distribution or reproduction is permitted which does not comply with these terms.



## **Chapter 9. Summary, Conclusions and Future Perspectives**

### **9.1 Summary**

The number of acute myeloid leukemia (AML) patients cured by allogeneic hematopoietic cell transplantation (allo-HCT) is constantly increasing. The therapeutic effectiveness of this procedure mainly relies on the transfer from the donor to the patient of immune cells, capable of recognizing and eliminating residual tumor cells. Still, up to 50% of transplanted AML patients still experience relapse, and the prognosis of these patients remains extremely poor.

Thus, aim of my thesis work was to improve current understanding on the immunobiology of post-transplantation relapse by investigating i) how therapies and underlying disease affect immune reconstitution, ii) how to refine detection of leukemia reappearance at the stage minimal residual disease (MRD), and iii) the molecular mechanisms at the basis of leukemia immune evasion and strategies to circumvent them.

In particular, I first presented the results of a prospective study that showed the superiority of monitoring patient-specific chimerism using peripheral blood rather than bone marrow specimens, for the early detection of leukemia relapses after transplantation.

Next I reported the results of two studies on NK and T cell recovery dynamics after allo-HCT. Both studies aim at understanding the determinants of donor immune system failure in controlling AML disease recurrence with the potential implications of using the

identified features as biomarkers to predict post-transplantation relapse.

In the last sections I presented published and unpublished data on the biological mechanisms underlying post-transplantation disease relapse, reporting how this knowledge can be easily translated in novel therapeutic rationales to combat disease recurrence.

Included in these sections are two recent reviews I authored, focused, respectively, on the immunobiology of post-transplantation relapse, and on the state-of-the art regarding epigenetic therapies for AML and their effects on the immune system.

## 9.2 Conclusions and Future Perspectives

To date, one of the greatest challenges for the HCT field is to anticipate relapse detection in order to treat the disease at the minimal residual disease stage (MRD) and, as a consequence, to identify the best markers and methodologies for post-transplantation follow-up monitoring. The advantages in the use of assays designed to detect disease specific markers, such as recurrent gene mutations, are several. Being disease specific, these mutations are not detectable in stromal or healthy hematopoietic cells and thus the obtained results show high specificity. However, given the genetic heterogeneity and clonal plasticity of acute myeloid leukemia (AML), the identification of frequent and stable-over-time mutations remains challenging. Another possibility is to follow a surrogate marker of leukemia persistence, represented by host-specific chimerism. The gold standard method to discriminate between host- and donor-derived hematopoiesis is represented by STR-PCR, commonly utilizing bone marrow (BM) samples. Our study provides new evidence that the high sensitivity of quantitative PCR (qPCR) allows peripheral blood (PB) monitoring, and that in turn this renders possible a tighter follow up of high-risk patients (**Chapter 2**). Unfortunately, a sizable fraction of individuals who relapse after myeloablative HCT develop recurrence very early after transplantation, thus making it difficult to understand whether detection of disease markers indicates a still ongoing process of disease eradication or if it is conversely a sign of impending relapse. Tighter monitoring and use of more accurate techniques, such as

digital PCR, might help to better understand disease kinetics in the very first weeks after allo-HCT, possibly guiding early immune interventions.

Studying the immune reconstitution after allo-HCT represents a unique opportunity not only to understand how immune cell dynamics can be influenced by therapies and by the underlying disease, but may also lead to the identification of novel and clinically relevant biomarkers. In our work, reported in **Chapter 3**, we observed that mature NK cells from the donor, infused as part of the graft, encountered a cytokine rich microenvironment, which prompted them to proliferate, rendering them target for cyclophosphamide action. This observation, if from one hand evidence a gap in the NK cell-mediated immune-therapeutic potential of allo-HCT, on the other hand, suggests that there is a temporal window (immediately after cyclophosphamide treatment) with a cytokine milieu favorable to the adoptive infusion of mature donor NK cells. Together with the anti-proliferative effects of post-transplantation cyclophosphamide on NK cells, other pharmacological treatments used for this GvHD prophylaxis can negatively affect NK cell functions<sup>1,2</sup>. Thus, new agents able to improve NK cell mediated antileukemic response, such as Trike constructs<sup>3</sup>, have to be investigated.

Focusing on T cells, the main actors of both GvHD and GvT effect in allo-HCT settings, I discussed the results of the recently published work reported in **Chapter 4**. Our work documented that bone marrow CD8<sup>+</sup> T cells exhibited a unique exhaustion signature in

patients relapsing after allo-HCT and that these cells were the ones with specificity for relapsing cells. Consistent with this evidence, in **Chapter 5**, we reported that one of the mechanisms enacted by leukemic cells to evade donor T cell control is the upregulation of ligands for inhibitory receptors. Our results suggest that selected patients could benefit from immune checkpoint-blocking agents in order to restore the GvT effect, and may help to spare the risk of exposing all other patients to a significant risk of severe GvHD.

Currently, no consensus is available regarding the best therapy for leukemia relapse. Indeed, most of the strategies currently adopted, such as the infusion of donor lymphocytes, salvage chemotherapy, second transplantation, have yielded very limited results.

The potential reason of these failures could rely in the poor understanding of the mechanisms at the basis of AML immune evasion and relapse, which we contributed to uncover in **Chapter 4**. For example, in relapses with downregulation of the surface expression of HLA class II molecules, the sole infusion of donor lymphocyte might not be sufficient to trigger cross-recognition and effectively eradicate leukemic blasts. We thus proposed in **Chapter 7** the use of epigenetic agents, and specifically EZH2 inhibitors, to recover the expression of HLA class II molecule on leukemic cells and re-establish recognition from donor-derived T cells.

In this particular type of relapse, being the recognition through the HLA impaired, the use of new engineered cellular product should be explored. Chimeric antigen receptor (CAR) T cells are capable of binding the surface antigen of choice without the need of TCR-HLA

interactions, thus representing a promising therapeutic option for patient relapsing with HLA genomic loss or downregulation.

Considering all the complexity linked to allo-HCT transplantation setting and the plethora of interactions between the immune system and tumor cells, it should be considered that only the an accurate definition of patient-specific relapse modalities and possibly the use of combinatorial therapies may tackle the still unsolved issue of post-transplantation relapse, further improving the effectiveness of allo-HCT.

## **References**

1. Derniame, S. *et al.* Differential effects of mycophenolate mofetil and cyclosporine A on peripheral blood and cord blood natural killer cells activated with interleukin-2. *Cytotherapy* **16**, 1409–1418 (2014).
2. Ohata, K., Espinoza, J. L., Lu, X., Kondo, Y. & Nakao, S. Mycophenolic acid inhibits natural killer cell proliferation and cytotoxic function: a possible disadvantage of including mycophenolate mofetil in the graft-versus-host disease prophylaxis regimen. *Biol. Blood Marrow Transplant.* **17**, 205–213 (2011).
3. Vallera, D. A. *et al.* IL15 Trispecific Killer Engagers (TriKE) Make Natural Killer Cells Specific to CD33+ Targets While Also Inducing Persistence, In Vivo Expansion, and Enhanced Function. *Clin. Cancer Res.* **22**, 3440–3450 (2016).

## **Acknowledgments**

*Ed eccomi qui, a due giorni dalla consegna della mia tesi di dottorato... ho ancora mille cose da fare e come sempre sono indietro, alla tv danno Bake-off ed io penso.... Non avrò nemmeno il tempo di farmi le unghie....*

*Si, chi mi conosce lo sa che le cose importanti non le dimentico mai! E una di queste sono i ringraziamenti. Allora scelgo, con grande difficoltà di mettermi a scriverli, mettendo in secondo piano le unghie. A parte gli scherzi, voglio scriverli di getto e non starò ad elencare uno per uno le persone che hanno contribuito a rendere speciale questo percorso. Già una cosa l'ho detta: è stato speciale... speciale perché ho desiderato di poter entrare in questo mondo fin da quando ho cominciato a studiare, senza capire bene di cosa si trattasse, ma sapevo di volerlo fare. Mi affascinava e mi affascina tutt'ora la continua possibilità di conoscere, sapere e scoprire, consapevole che più si sa e più passi si possono fare per aiutare una persona in difficoltà.*

*Inutile dire che la mia famiglia, tutta, ha contribuito ad alimentare questa mia passione che poi è diventato un lavoro, accompagnandomi in questo percorso difficile e che ti mette sempre nella posizione di dubitare delle tue capacità. Il loro appoggio è stato fondamentale per non abbattermi, per vedere sempre il bicchiere mezzo pieno e per credere in me stessa. La consapevolezza che qualunque cosa fosse accaduta, qualunque insuccesso avessi affrontato, qualunque città avessi scelto per vivere, che se non fossi*



*stata felice avrei sempre avuto un luogo sicuro in cui andare, è stata essenziale... La mia famiglia è il mio Posto Sicuro.*

*Ma se è vero che non sarei come sono se non fosse stato per loro, non sarei arrivata a questo punto senza qualcuno che fidandosi solo del proprio istinto ha creduto in me, dandomi non solo un'opportunità ma guidandomi verso una continua crescita e che spero continuerà a farlo anche quando prenderò strade diverse. Parlo di Luca, che sempre e dico Sempre, ha creduto in me, spronandomi, facendomi incazzare, piangere, disperare ma sempre facendomi sentire all'altezza di appartenere a questo mondo, il Suo.*

*Per fortuna la mia guida non è stata solo un uomo (le ragioni biologiche del "per fortuna" le conosciamo tutti), ma anche grazie a Luca, devo dire, ho conosciuto Raffaella. Un esempio di come una Donna capace e tenace Può e Deve arrivare dove vuole. Lei non è stata solo un mentore scientifico, ma ha saputo comprendere il mio caratteraccio, cercando sempre di farmi tirare fuori gli aspetti migliori, spronandomi a fare sempre meglio e a scacciare la mia negatività, che c'è ancora eh, ma ci stiamo lavorando. Una persona che ha messo su un gruppo fantastico, unito e competitivo e senza il quale il mio percorso non sarebbe stato lo stesso. Non sarebbe stato stupendo. Ci siamo confrontati, scontrati, divertiti e sempre nel rispetto dell'altro e sempre uniti da una passione comune, la scienza. Come tutte le regole, per essere confermate, serve un'eccezione: Lu. Io e lei di passioni comuni ne abbiamo, ma sono la moda e l'amore per il trash (anche la scienza dai). Perché nascondere, siamo anche questo. Ci siamo "scoperte" da poco ma da quel momento siamo*

*state inseparabili, così diverse ma così uguali. Credo di non poterne più fare a meno e spero che continueremo a vivere i nostri momenti di serietà e leggerezza per molto altro tempo ancora.*

*Ringrazio la persona che oltre ad una guida è diventata un'Amica, che mi ha insegnato ad affrontare il lavoro e la vita serenamente, a limare il mio lato duro e sempre ansioso e a trasformarlo in qualcosa di positivo. Ad affrontare le difficoltà "una alla volta" senza mai perdermi d'animo. Che non mi ha mai giudicata per non sapere ma mi ha insegnato con pazienza e mai con arroganza. Una persona che spero non perderò mai, Daniela.*

*Come posso non nominare le persone che hanno vissuto con me questi anni di laboratorio da quando sono arrivata, sopportando tutti i miei difetti, arrabbiate, malumori e mille mila domande, dubbi e insicurezze. Laura e Cristina, i pilastri del lab Vago, ma anche tutti i componenti passati e presenti che ogni giorno con le loro personalità uniche hanno caratterizzato e caratterizzano questo percorso speciale.*

*Non posso concludere senza dire che sicuramente in questi 4 anni ci sono state tantissime altre persone e che ringrazio tutte infinitamente per essere state importanti anche per un minuto, un'ora, un anno (Arnolda, Elisabetta, Giacomo, TUTTI).*

*Direi che i ringraziamenti sono venuti più lunghi della tesi e qui, ho detto tutto.*

**GRAZIE**